DSIS 89-01124 (U) PROCEEDINGS OF THE SIXTH SHIP CONTROL SYSTEMS
UNCLASS. UNLTD. SYMPOSIUM HELD AT OTTAWA, ONTARIO, CANADA, ... 1 OF 6

AD-A
211128

M 85-0003

PROCEEDINGS

SIXTH SHIP CONTROL SYSTEMS SYMPOSIUM

26 - 30 OCTOBER 1981

VOLUME 2

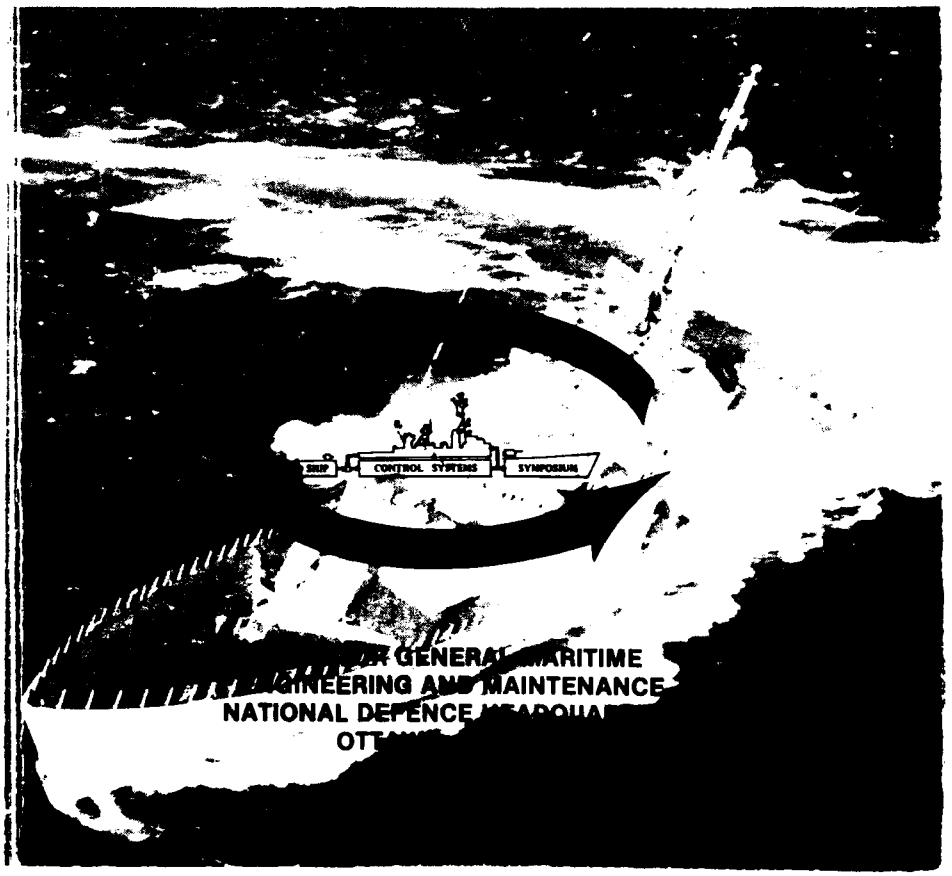

- PUBLICATION INFORMATION -

THESE PAPERS WERE PRINTED JUST AS RECEIVED FROM THE AUTHORS IN ORDER TO ASSURE THEIR AVAILABILITY FOR THE SYMPOSIUM.

STATEMENTS AND OPINIONS CONTAINED THEREIN ARE THOSE OF THE AUTHORS AND ARE NOT TO BE CONSTRUED AS OFFICIAL OR REFLECTING THE VIEWS OF THE CANADIAN DEPARTMENT OF NATIONAL DEFENCE.

ANY PAPER INVOLVED WITH COPYRIGHTING IS PROMINENTLY MARKED WITH THE COPYRIGHT SYMBOL AND WAS RELEASED FOR PUBLICATION IN THESE PROCEEDINGS.

REQUESTS FOR INFORMATION REGARDING THE PROCEEDINGS, THE SYMPOSIUM, OR THE SPONSOR - DIRECTOR GENERAL MARITIME ENGINEERING AND MAINTENANCE - SHOULD BE ADDRESSED TO NATIONAL DEFENCE HEADQUARTERS, 101 COLONEL BY DRIVE, OTTAWA ONTARIO, CANADA, K1A 0K2, ATTENTION: DMEE 7.

FOREWORD

The Director General Maritime Engineering and Maintenance (DGMEM) is pleased to present the Proceedings of the Sixth Ship Control System Symposium held at the Chateau Laurier/National Conference Centre complex in Ottawa, Canada, 26-30 October 1981. This is the sixth in a series of symposia on ship control systems. The First Ship Control Systems Symposium was convened in 1966.

The technical papers presented at the Symposium and published in these proceedings cover the entire spectrum of ship control systems and provide an insight into technological developments which are continuously offering the ship control system designer new options in addressing the complex man/machine operation. The microprocessor and its apparently unlimited development potential in future digital, distributed control systems appears ready to reshape the conventional concepts now so familiar in control system designs. There are many concerns that the advantages of the new technologies will be negated by the inability of training systems to graduate technicians who can adequately cope with these new systems.

The response to "Call For Papers" was outstanding and the papers selection committee constrained by the time available for presentations, was hard pressed to make their final selections from the many fine abstracts submitted. The final papers represent a unique international flavour which includes authors from every facet of the ship control system community. The final program is a balance of both theoretical and practical control system papers.

These Proceedings constitute the major record of the Sixth Ship Control Systems Symposium. The contents indicate the success of the Symposium and provide some insight into the effort that was required to ensure this success. The Symposium organizing committee, advisory groups, publications branch, authors, session chairmen, international coordinators, clerical and administrative personnel, and management all provided positive and cooperative support to the many tasks that had to be performed in organizing and presenting the Symposium.

This Symposium has continued to explore and present a number of specific aspects of ship control systems and undoubtly the next symposium will include new concepts and ideas which were unavailable for this Symposium. As in the past, we hope these Proceedings become a source document on ship control along with the previous proceedings. It is our hope that the Symposium has provided stimulation to those who will continue to advance this technical field.

Bruce H. Baxter
General Chairman

Philip V. Penny
Technical Chairman

VOLUME 2

CONTENTS

VOLUME 2

CONTENTS

VOLUME 2

CONTENTS

VOLUME 2

CONTENTS

STANDARDIZATION AND AUTOMATION IN ENGINEERING OPERATING SYSTEMS: HUMAN FACTORS ENGINEERING INPUTS

By Russell A. Benel and Thomas B. Malone
Essex Corporation

ABSTRACT

In surveys of human factors engineering (HFE) problems on ships, problems with engineering spaces are usually cited as most critical. A recent survey of ship propulsion engineering systems indicated a general absence of HFE consideration in system equipment design. These problems directly affected ship readiness, propulsion system availability, and personnel safety. Documented in the survey were specific problem areas where HFE criteria were ignored, with the result that the systems were unsafe and difficult to maintain, required extensive time to repair, and had experienced less than acceptable availability.

Similar results have been recorded in a number of other studies addressing the adequacy of the application of HFE technology to ship engineering systems. The DOD Task Force on Test and Evaluation stated in 1974 that it had discovered "a surprisingly large number of instances in which designs lacked adequate human factors considerations and, notable from a test and evaluation point of view, many in which development testing did not lead to early awareness of the problems." Apparently, more attention must be given to human factors in the initial design of propulsion engineering systems, and during modification and update of systems equipment. In addition, test and evaluation should be planned and conducted so as to ensure that human factors requirements have been adequately considered during design.

The implications of this problem are becoming more serious and also more obvious with the extensive application of automation to propulsion engineering systems on new ships. One major problem is that HFE principles are ignored when the decision is made to automate a system. Man is not superfluous to the operation of an automated system; on the contrary, he must perform such functions as monitoring, supervising, decisionmaking, managing, and intervening to take control from the automatic system.

Overlaying the console standardization process on these problems proves a difficult operational problem. This problem is multifaceted, including the cost of retrofitting existing ships, revision of training programs and manuals, type of standardization, and the degree to which a single standardization concept can apply equally to different ships, ship types, and types of propulsion systems. A related problem is acceptability of standardization by operators, designers and the industry. Thus, there is a great need for HFE inputs to ship propulsion engineering systems in general. Specifically, urgent inputs will be needed to ensure that as standardization and automation are implemented, HFE guidelines are applied.

The paper to be presented will outline an adaptation of Essex's man-systems integration approach. This approach is germane to these problems, has proven successful when applied to other equally complex systems, increases system safety, and meets with operator approval. The essence of the approach is twofold: the human operator is a critical element in the system, to be integrated with other elements such as hardware, software, and information; and design is dependent upon the comprehensive identification, analysis, and integration of requirements. Emphasis on the human operator makes this primarily an HFE approach and emphasis on requirements makes it a systems approach.

INTRODUCTION

In the Fifth Ships Control Systems Symposium a number of papers were addressed to the issue of automation in shipboard systems and apparently this trend has continued in the current symposium. Many of these papers are concerned with engineering issues in the implementation of automated control, but there have been discussions on the desirability of automation as a control procedure, particularly for propulsion systems. Holland and Fitzpatrick (1) succinctly reviewed the development of automation as a concept within the U.S. Navy. They noted a study was under way to insure that designs being introduced into the fleet were not overly complex or overdesigned. Two of the newest surface combatant classes (FFG 7 and DD 963) already have highly automated propulsion control systems. These ships' propulsion control systems will be operated in essentially the current configuration throughout their life cycle, probably in excess of two decades. Therefore, any approach to problems in automation must address designing retrofits for existing systems, as well as, inputs for emerging or planned systems.

The desirability of automation can be seen through analysis of life cycle costs wherein savings can easily approach and probably exceed one million dollars if one three- man watch station is eliminated for the assumed 20-year life of the ship (2). This is made all the more attractive when estimates of 80 percent of the annual operating cost are attached to the personnel factor and this factor represents perhaps half of the life cycle costs (perhaps more when salary inflation is accounted for). Not surprisingly, very similar conclusions have been reached by researchers looking at the British Royal Navy (3).

Recently this basic rationale for automation has been called into question. Propulsion plant manning may not be reduced by automation. Reasons for this include lack of operator trust in the system, failure of the system to perform in the automatic mode, lack of skilled operators, and ingrained conservatism (1). The increased requirement for on-the-job training of underskilled operators exacerbates the manning requirement by placing trainers and trainees in various stations to learn the system. Unskilled personnel must be accompanied by skilled personnel, thereby increasing substantially the actual manning of the system.

It may be reasonable to assume that the physical properties of the system can be improved to overcome the problem of mechanically and electronically unreliable equipment. This in turn may alleviate the lack of operator trust. Similarly, attrition may remove the vestiges of conservatism. The problem of skilled operator availability is likely to be a constant for the foreseeable future. Training resources have been constrained and the manpower pool is thought to provide a resource of dubious quality. Efforts to standardize consoles are designed to improve this situation by reducing training time for new operators. Console standardization can reduce fleet-wide training time because each shift to a new ship within or across classes is facilitated by the commonality among control systems.

The problems associated with engineering control station standardization are many and multifaceted. For one, there is the operational problem, the problems encountered in the fleet which form the basis for the requirements for standardization. A second set of problems involves the implementation of console standardization. The third problem area is the problem of standardization acceptance.

The operational problem which comprises the basis for a requirement for standardization itself has a number of facets. As they make transitions from ship to ship and from a training situation to the fleet, operators are faced with the need to adapt to completely individualized console designs, even though (as pointed out by the Maritime Administration Guide for a Standardized Engine Room Propulsion Control Console) the commonality observed for a range of different machinery designs was on the order of 80 to 90 percent (4). The MarAd Guide goes on to note that this high degree of similarity has not been achieved in the design of the associated propulsion systems consoles. Each designer has considered his propulsion system to be unique, and a variety of console designs has followed. The results of this proliferation of individual console designs are numerous: increased likelihood of

operator error; increased chances of confusion, leading to greater time to perform activities; individualized system-specific training courses and low-fidelity generalized training; system-specific documentation, procedures, and manuals; and ship installation requirements specific for each ship and system configuration.

Reversing the existing trend of individualism in control station design is highly desirable. French and Dorrian (5) listed two major benefits to early identification of ship propulsion control components. First, better decisions could be made on the proposed ship based on this information and, secondly, it would shorten development time. In their article, they provided guidance on stating the proper functional requirements for controls within the context of probable or likely ships within a given range. This strategy implies maximum standardization of system component parts. A critical requirement for this to be successful is an ability to foresee future ship configurations and make provisions for the most demanding case. As well stated as their case was for defining functional requirements, the actual system components for the man-machine interface (MMI) and their arrangement are a non trivial problem which is not solved directly by defining functional requirements.

Thus, another important aspect of the problem of the absence of standardization in existing engineering consoles has to do with the degree to which human factors engineering criteria and principles are included in the design of these consoles. The MarAd Guide on engineering console standardization states that one of the most important aspects of the console standardization process was the systematic attention to both engineering and human factors considerations with the objective of developing an integrated system that consists of optimum combinations of physical and human components. With the wide variety of engineering consoles currently in the fleet, it can be expected that they differ over a wide range in terms of human engineering. One of the objectives of a console standardization process would be to standardize the design concept which is optimal across all applications from a human factors engineering point of view. Under the standardized console concept, all console configurations would have been provided a uniform and high degree of human factors engineering input.

Another difficult operational problem to be addressed in the standardization of engineering consoles is that the console design must reflect the degree of automation implemented in the engineering control system. The automation of the propulsion engineering control system has been a problem with recent ship acquisitions. One major reason for this problem is the fact that, in deciding to automate a control system, human engineering principles are ignored. The thinking goes that since the system is to be automated, man is designed out of the system. In an automated process, however, man serves a role which is as important as that for a manual system. He must perform such functions as monitoring, supervising, decisionmaking, managing, and intervening to take control from the automatic system. The question of degree of automation, as well as the issue of man's role in intervening and assuming control in a backup mode, must be addressed before console design issues can be faced. The question of system automation thus becomes one of the important issues in the console standardization process.

The standardization implementation problem is also multifaceted. The cost of replacing EOS consoles on existing ships in the fleet will be considerable. Such changes will require the concurrence and cooperation of ship commanders and type commanders. Existing training courses and manuals will have to be revised. Currently trained operators would have to be retrained. A major problem in implementation of console standardization is how much standardization is required; to what degree components and arrangement of components must be standardized within a single console; and to what degree a single standardization concept can apply equally to different ships, ship types, and types of propulsion systems. The approach used by MarAd in developing a standardized propulsion engineering console was to develop a standard design with optional modular features to accommodate variations in power plant designs.

The acceptance problem in console standardization refers to acceptance of standardization as such, and acceptance of a specific standardized console design concept by

operators, designers, and the industry. The MarAd Guide to Console Standardization cites pitfalls of standardization which include inflexibility of design, limitation of innovative design, industry acceptance, and personal pride of design authorship.

These are the problems that must be addressed in developing a standardized engineering console design for automated (or even unautomated) systems. Therefore, there is an urgent need to establish systematic programs for insuring that HFE principles are considered. These programs will allow existing systems to fulfill their potential for saving manpower. HFE inputs to future systems should reduce manpower and training costs through proper design for operability (and concomitantly maintainability).

APPROACH TO HFE INPUTS — DEVELOPING SYSTEMS

In the United States Department of Defense, acquisitions of major systems are governed by a variety of directives, regulations, standards, and handbooks. MIL-H-46855, "Human Engineering Requirements for Military Systems, Equipments and Facilities," is directed specifically at the role of HFE in the acquisition process. This specification states that human factors program requirements are to include:

- Defining and allocating system functions. Human Factors Engineering principles and criteria are to be applied to allocate system functions to
  - automatic operations/maintenance
  - manual operation/maintenance or
  - a combination of manual/automatic operation/maintenance

- Information flow and processing analysis

- Estimates of potential operator/maintainer processing capabilities. Roles to be identified for humans such as
  - operator
  - maintainer
  - programmer
  - decisionmaker
  - communicator
  - monitor

  are required. Estimates concerning load, accuracy, rate, etc., are also to be identified

- Equipment identification. HFE principles and criteria are to be incorporated into the identification or selection of equipment which are to be operated/controlled/maintained by man.

- Task analysis. To be conducted and applied to design decision, analysis of manning levels, equipment procedures, etc.

- Analysis of critical tasks. Task analysis (above) extended to analysis of critical tasks to identify, for example:
  - information required by man
  - information available to man
  - information evaluation process
  - decision reached
  - action taken
  - body movements
  - tool required
  - job performance aids (JPA) required

- Loading analysis. Crew/individual workload analysis is to be applied and compared to performance criteria.

- o Preliminary system and subsystem design. HFE principles and data are to be applied to system/subsystem design. MIL-STD-1472 is to be complied with.

- o Detailed design. As above.

- o Studies, experiments, laboratory tests. Research is to be conducted to resolve man/machine trade-off problem areas and other HFE and life support problems.

- o Mock-ups and models. Mock-ups (3-D) to be constructed as an HFE design evaluation tool.

- o Dynamic simulation (as required for HFE design).

- o Design drawings.

- o Workspace environment. This would include
  - atmospheric conditions
  - weather and climate
  - bodily acceleration
  - noise
  - safety (handholds, etc.)

- o Test and evaluation. Planning, implementation and failure analysis.

The overall Essex approach is depicted in Figure 1. This figure indicates the specific steps to be taken in proceeding from program inputs to outputs. The program is segmented into two distinct phases. The outputs of Phase I, Concept Development, would include selected console standardization concept descriptions and functional specifications, and a set of concept evaluation criteria. The outputs of Phase II, Concept Evaluation, which are also the outputs of the overall program, include the standardized concept(s), criteria for console interfaces, console mockup(s), and results of comparisons of the standardized approach with existing console configuration. The following sections discuss the activities to be accomplished in each phase.

Phase I — Concept Development

The initial step in the program is a review of existing systems. This is accomplished through visits to ships selected on the basis of propulsion engineering systems similar to that under design. The first activity then is to identify the specific systems to which the standardization effort will apply. The review of existing systems encompasses observation of ongoing operations, interviews with operators and engineering officers, measurement of physical, environmental, and operational parameters, and review of documentation, drawings, specifications, procedures, manuals, engineering data, and operational experience data. These system reviews provide an operational and design data base from which improvements in the developing system can be made and measured; further it fasilitates identifying design problem areas so that they can be avoided in current system development.

For each propulsion system by ship type in the classification scheme, a mission analysis is performed. This analysis identifies the primary functions to be performed and enables determination of the different conditions under which functions are performed. For each function, task requirements are identified. Task requirements include tasks performed by the operator as well as those performed by automated control systems. Task requirements also include such task characteristics as sequential dependencies, frequency, duration constraints, initiating and terminating events, decisions and decision rules which are part of the task, feedback required to verify task completion, and task criticality.

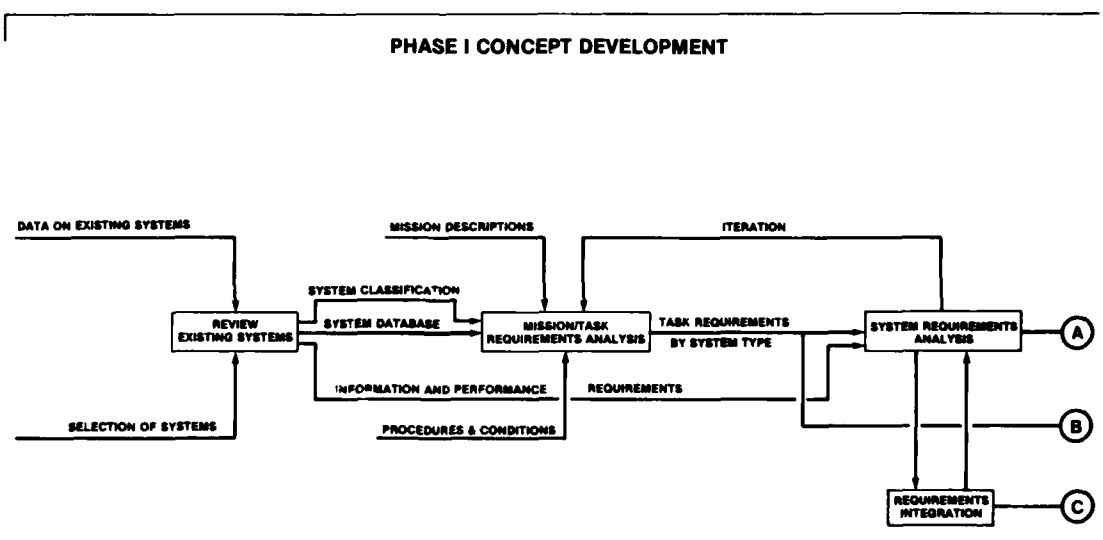

FIGURE 1 WORK STEPS TO BE PERFORMED IN THE DEVELOPMENT OF A STANDARDIZED ENGINEERING CONSOLE CONCEPT

PHASE I CONCEPT DEVELOPMENT (CONT)

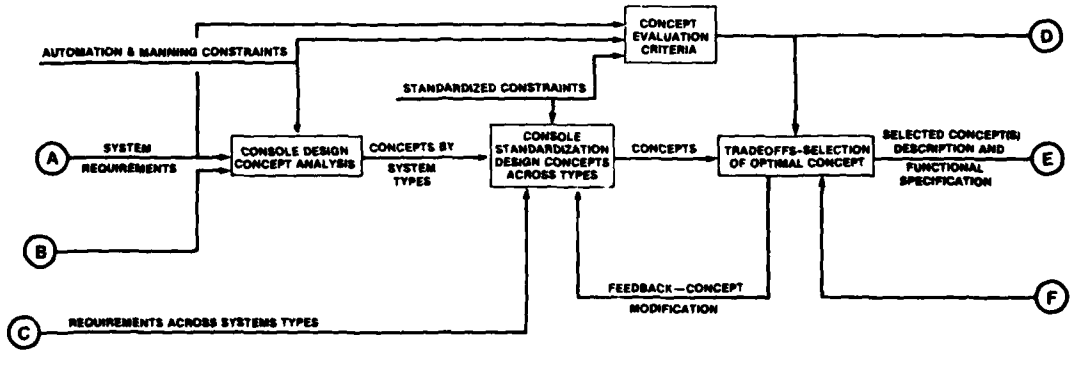

PHASE II CONCEPT DEVELOPMENT

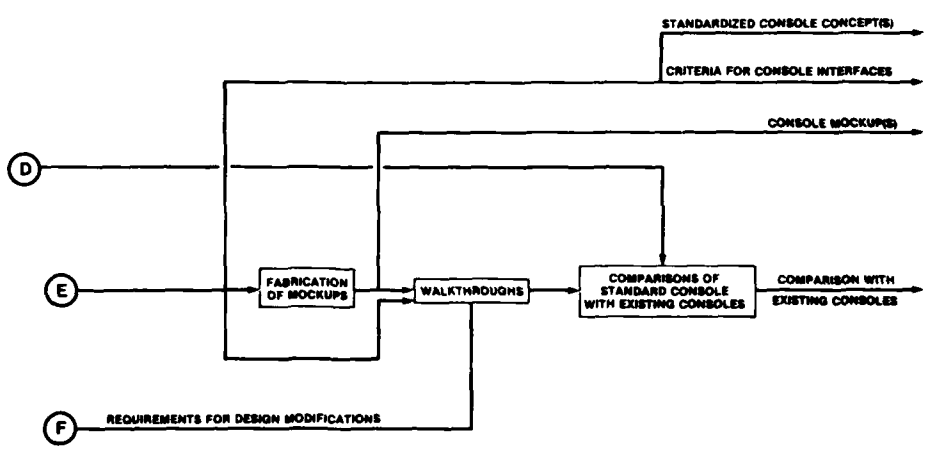

Task requirements are developed for emergency procedures as well as normal operating procedures, since one of the most critical functions of the control system is to diagnose abnormal conditions and return the system to normal.

For each task identified in the task analysis and especially for those tasks designated as critical, a systems requirements analysis are performed. This analysis identifies systems requirements of the following types:

- Information requirements — what the system needs to know to complete the task, to make decisions, and to verify that the task was completed successfully
- Performance requirements — standards of performance for each task, such as time, errors, probability of success, control precision, fuel expended, amount completed, etc.
- Decision requirements — decisions, decision rules, options, and effects of incorrect selection of options
- Support requirements — support required from ship elements external to the engineering control system
- Interface requirements — links with other ship elements, including data links, communication links, feedback links, command links, alarm links, and advisory links.

While requirements are being identified, they are analyzed through iterations of the mission/task analysis. The requirements are then integrated by establishing dependencies among them and by identifying inconsistencies and incompatabilities among different requirements. The final step in the integration process enables the prioritization of requirements which input to the resolution of conflicts among sets of requirements. After requirements integration, the requirements analysis process should produce a compatible set of prioritized requirements which serve as drivers of the concept development effort.

The initial step in the concept development step is to investigate different allocations of function for different sequences of tasks. Alternate allocation choices are: completely automated; automated control with manual information processing and process initiation; manual control with automated information processing; and completely manual. Alternate allocation schemes are developed for each system and ship type and are played against automation and manning constraints to determine the feasibility of the scheme.

The next step in the development of console design concepts is to develop man-machine interface concepts for each allocation based on system requirements. Concepts are developed for the following:

- Station work space
- Station equipment arrangement
- Visibility of machinery from the station
- Console arrangement within the station
- Station ingress and egress
- Console layout
- Control and display general arrangements

- o Station habitability
- o Console lighting
- o Console manning requirements.

As design concepts for system and ship types are developed, methods are implemented for integrating these concepts to produce a minimum number of standardized console design concepts. Standardized concepts address completely standard approaches as well as design alternatives based on a general standard with options for individual system and/or ship types.

Based on the system requirements, automation and manning constraints, standardization constraints, and other inputs, a set of concept evaluation criteria are developed. These address such issues as the following:

- o Concept operability
  - number of people
  - skill levels
  - special training required
  - operator performance limits
  - likelihood of error
  - ease of transition to backup modes
  - operator workload
  - time to detect problems
  - time to diagnose
- o Concept complexity/reliability
  - special engineering features (vs. off the shelf)
  - mean time to fail
  - effects of failures
- o Concept utility/support
  - growth potential
  - flexibility for new missions
  - computer programming required
  - space requirements
  - special support requirements, e.g., power
- o Concept generalizability
  - missions, systems, and ships served
  - application for critical tasks
  - application for high priority requirements
- o Concept safety
  - ship safety
  - engineering personnel safety
- o Concept cost
  - development costs
  - validation costs
  - support costs
  - life cycle costs
- o Concept effectiveness
  - likelihood of mission success
  - likelihood of system readiness.

Evaluation criteria are then be used to evaluate alternate concepts. While the trade-offs are proceeding, changes are made to candidate concepts demonstrated to perform less than adequately on some of the criteria. In this manner, a final set of concepts are fashioned which can be evaluated by means of the trade-off criteria. One approach is selected as optimal. A description of this concept is generated, and a functional specification is developed including a panel drawing and a description of human operator roles and responsibilities in the control system. These items comprise the outputs of Phase I.

Phase II — Concept Evaluation

The initial step in Phase II the fabrication of a mockup or mockups of the selected concept. Several mockup additions may be required if the selected concept incorporates optional panels. These mockups are used for operator walk-throughs of procedures for selected functions. On the basis of the walk-throughs it is expected that requirements for design modifications can be identified. The major objective of the walk-throughs is to obtain data on the performance of specific critical tasks using the standard console mockup. These data can then be compared with similar data obtained on existing consoles, and a comparison can be made of the standard console vs. existing consoles in terms of human performance capability. A comparison of the standard console and existing consoles can also be made in terms of the concept evaluation criteria developed in Phase I.

APPROACH TO HFE INPUTS—EXISTING SYSTEMS

Although the nature of the problem is changed slightly when HFE considerations are applied to existing systems, many of the constraints and procedures are similar. There may be two distinct instances when HFE is considered during a systems operational life cycle. The first is during updating or modernization of a working system. The second instance is somewhat more problematic, a fielded system that is found to be inoperable (or suboptimally operable) by the existing personnel. The ultimate objective in each case remains the same, i.e., fielding an operable system which performs as required. However, the impetus and immediacy may differ dramatically.

Modernization

During updating or modernization the systems operating characteristics are known and the modified systems' characteristics should have been sufficiently defined. Thus, the old system configuration provides a baseline against which the new might be measured. The nature of the constraints are much more apparent with an updated system. The equipment has generally existed and been operated in a tangible form for some period of time. Many of the constraints that were (or should have been) applied to the baseline system must be considered again. The functional requirements, however, do not provide the limiting factor. Training factors, although they are an important consideration, are also not the preeiminent factor. The most critical issues are the tied factors of space, time and cost. The physical dimensions have been established by the baseline system. This problem is particularly obvious in aircraft cockpits, but the ships propulsion areas, although larger, are space limited. Time is a constraint that is with all system development and modification programs. The final factor of cost runs through all system development phases and considerations. Thus, even if it were possible to dramatically rearrange the shape and size of available spaces, the time and cost would be exorbitant.

Although these constraints do impact the application of HFE principles and guidelines to system modifications, the basic approach is quite similar to that for new systems. Certainly this is true because new systems have generally been developed in a more or less evolutionary fashion from older systems. Also, there is an element of planned effort in both development and modernization.

Problem-solving

On the other hand, a system whose development has been so bereft of HFE inputs that it is basically inoperable or widely misses the performance objectives provides a serious challenge to the Human Factors Engineer. There is a question of immediacy if the system is already in the fleet. A number of possibilities exist for immediate attention to a poorly design man-machine interface.

For control/display problems, it is possible to improve operability subtantially through application of one or more of the following techniques:

- o enhanced labelling
- o functional demarcation
- o symbology
- o equipment replacement.

Enhanced labelling may be as simple as increasing the size of or rewording existing labels. This may make the relationships among system elements move immediately apparent. Functional demarcation may be accomplished through colored tape. Basically, it is a procedure which groups related items to aid in their identification. Operability is enhanced because scanning of control consoles is reduced. The use of symbology may reduce interpretation time for control/display labels which have been abbreviated. One serious drawback to this procedure is a current lack of standardized symbols. A somewhat more expensive, but often necessary step is equipment replacement. In many cases a different but functionally equivalent item will enhance operability.

If these simple expedients don't enhance operations sufficiently, there would be no choice but to redesign the man-machine interface. This would be extremely costly and perhaps difficult to justify. However, the penalty for not accomplishing a redesign can be quite severe, easily ranging to total equipment failure and loss of life.

PROBABLE PROBLEM AREAS

In a different but related context, (aircraft flight-deck automation) Wiener and Curry (6) delineated what they felt were general problem areas related to automation. Many of these issues cannot be eliminated by standardization of display/control equipment and, in some cases, HFE solutions are not presently available in a fully validated form. The problems included:

- o Automation of control tasks
- o Skill acquisition/retention
- o System complexity
- o Alerting/warning systems
- o Psychosocial aspects of automation

Automation of control tasks

This area has been the subject of considerable attention in the past. Automation reduces the role of man from an active control element to monitor or supervisor. The control task is generally performed satisfactorily by the automatic system. A great deal of research effort has been and is being devoted to man's ability to perform the monitoring functions. Research has addressed such issues as: (1) the failure detection ability of the

passive monitor compared to the active controller; (2) the transition from monitor to controller and the effect of "warmup delay;" (3) the nature of the interaction between system and man, i.e., who initiates changes, whether man is informed of changes; and (4) equipment reliability effects on operator performance.

The longest history of research into these problems probably resides in the area of vigilance and decrement in monitoring performance across time. Generally, man probably does not attend continuously to an automated system any better than he does to a CRT display of radar targets. This knowledge led Paul Fitts to declare that machines should monitor men and not vice versa. There is ample evidence to suggest that the manual takeover of a previously automatic operation is quite difficult. This relationship is confounded by the poor detection performance leading to delayed takeover decisions. Although these problems are related to limitations in the inherent capabilities of man, a properly designed system architecture can reduce, although probably not eliminate, the effects of these limitations on overall system performance. The optimal form of interaction between the operator and the automated system is not well-defined. If man is to be monitored by the machine, then it seems likely that man should initiate changes on system configuration. If not, the role of man in the decisionmaking process is that of a supervisor who must be informed of the impending change. The probability of the operator detecting failures would apparently be a function of the equipment reliability. Wiener and Curry had suggested an interesting corollary to increased machine reliability. Namely, the insidious effects of reliability assumed to exist at a higher level than the actual reliability. Overall system reliability might not be maximal with that level of machine reliability (assuming it is less than unity) because the operator might tend toward complacency in monitoring. Thus, the operator would actually detect failures less well with increased reliability. This might also be viewed as being a function of having had less experience with failures in general. These latter two topics require aditional research efforts to determine the appropriate HFE considerations for equipment design.

Skill Acquisition/retention

The two sides of training problems associated with automated systems involve the level of skill necessary to operate such systems and the retention of such levels under automated operation. Manual skilled performance will surely decline in the absence of practice through operation. The previously mentioned "warm-up" effect suggests with good supporting evidence that the manual performance level returns rapidly to asymptote. More problematic would be loss of procedural and sequential task skills. The issues relevant to acquisition and retention include:

- o Role of automation in acquisition
- o Initial required skill level
- o Rate of skill loss
- o Required frequency of prophylactic practice
- o Alternative practice
- o Checks for skill maintenance

Although these issues need not impact on equipment design for automated systems, it seems likely that some form of imbedded training and purposefully operated semi-automatic and fully manual (or other degraded) modes of operation will be required. Automation of system parts may speed acquisition. The full impact of part task training is still unknown. A more critical issue of training concerns the initial skill level required for operators. Extremely reliable equipment may not require over-trained operators. There is a risk in having operators unfamiliar with degraded modes of operation. Unless the equipment is designed to provide a great deal of cueing and other help there is the possibility that no

operator would have the requisite skills to operate the equipment when the automatic mode is not functioning.

Imbedded training and other than automatic operating modes may be needed to insure skill retention, on-the-job training opportunities, and checks for skill retention. This increased flexibility and operational capability comes at an initial system cost outlay above a baseline system. The HFE considerations for such configurations are not vastly different. However, the level of HFE inputs to a system which will be operated by marginally trained individuals becomes somewhat more important. In these circumstances, sufficient training is not possible to overcome an inadequate man-machine interface.

System complexity

Complexity of the underlying system does not make operation inherently difficult. Indeed, refrigerators are reasonable complex systems operated in wholly automatic modes by grossly undertrained operators with little, if any, problems. Complexity in that case is not particularly evident. Nuclear power plants are exceedingly complex and generally provide a bewildering array of displays and controls. HFE considerations are critical for these latter systems.

A general rule of thumb is to design in only as much complexity as is required to perform the function. The man-machine interface can be (and should be) designed on several levels. Such a hierarchical arrangement provides for primary displays and controls required for normal operation and those associated displays and controls needed for degraded modes. In fact, there is probably greater potential in automated systems for fault detection and diagnosis because of the trend toward inclusion of microprocessor-based control systems.

Alerting/warning systems

There are general HFE considerations which are applicable the design of alerting/warning systems. An ideal warning system is probably unattainable. There are a number of emerging technologies in voice output for which validated HFE guidelines do not exist. A research data base is accumulating for these technologies and there should be tentative guidelines available in the near future.

Problem areas in alerting/warning systems tend to center around the reaction of the human operator to the physical alarms. Operators may habituate to the alarms and not heed (hear or see) them. They may choose to ignore an alarm. The alarm was always false before, like the boy who cried wolf. This relates to problems in unacceptably high false alarm rates. Operators may or may not check the validity of alarms. Consequently, they troubleshoot false alarms or ignore real alarms. Operators may depend on alarm systems rather instrument scanning for normal operation.

The biggest challenge to HFE for alarm systems comes in the area of smart alarm systems. This would include the application of artificial intelligence to prevent "obvious" false alarms and prioritize alarms. Decisions for developing those systems will be important. Correct prioritization will be essential. Determining the validity of alarm indications must be possible.

Psychosocial aspects of automation

The basic attitudes of operators may influence their operation of the equipment. Conversely, the equipment may influence the attitudes of the operators. Apparently, automation can influence job satisfaction. One frequent complaint among fleet personnel is the operability of equipment. Perhaps, a proper design for operability including increased automation would lead to enhanced system operation and, in turn, proper operating characteristics may lead to job satisfaction. Equipment that is unreliable and difficult to

Automation is traditionally viewed as somehow undesirable to the worker reducing his role as a skilled operator. However, for the foreseeable future skilled operators will be a vital part of the man-machine system. For the satisfaction of attitudinal factors the man-machine interface design must satisfy both the operability criterion of the system designer and the relatively intangible characteristics deemed desirable by operational personnel. Many of the HFE steps outlined previously can serve to insure that these goals are satisfied mutually to the fullest extent.

SUMMARY

Human Factors Engineering is a critical part of the automation/standardization design process. Failure to follow HFE guidelines for the development of the man-machine interface will result in systems which have lower than optimal performance. As systems become automated the number of personnel should be reduced; however, the importance of the remaining personnel to the performance effectiveness of ship systems will increase. Personnel will continue to be responsible for functions such as decisionmaking, monitoring and managing. The number of functions in which people are employed may diminish, but the remaining functions will be of significantly increased importance.

When systems are not being operated properly by the available personnel, one possible response by managers is that the level of training in those personnel is inadequate. Therefore, what we have is a "well-designed" system with unskilled and untrained operators. The solution to this problem is enhanced training. This is likely to be true in some cases; however, a large number of systems have been founded to be seriously deficient in design for operability. One commonly proposed solution during development is that training will overcome any residual deficiencies in design.

The implications of this strategy are shown in Figures 2 and 3. In Figure 2 an hypothetical relationship between operability and training and operability and HFE application is shown. This simplified depiction is intended to show that within broad limits it is possible trade-off HFE dollars for training dollars. (Of Course, this ignores the fact that a modicum of each is absolutely necessary under nearly all circumstances.) Under various combinations of training and HFE outlays a given level of operability is possible (thus, the iso-operability curves). This may have no differential input to fielding a system because the dollar outlay would be constant for the initial operation.

The implications for life cycle cost are presented in Figure 3. HFE dollars expenditures are maximal during development (and planned modernizations). Thus, there is a point at which HFE expenditures do not increase cumulatively. However, training costs are high during development and remain at a moderate level throughout the life cycle. Likewise, any modernization would cause an increase in training costs for new instructional technologies. The critical factor is that training costs increase cumulatively throughout the life cycle. Each case of attrition is an example of training dollars lost. Thus, there is a required constant input of dollars to compensate the lost training dollars. Proper application of HFE can be an effective cost-avoidance strategy.

REFERENCES

(1) Holland, G.E. and Fitzpatrick, E. "Automation-Salvation or Delusion," Proceedings, Fifth Ship Control Systems Symposium," 1978.

(2) Rodman, R.R. "Personnel Trade-off Studies Influencing Design of Ship Control Automation," Proceedings, Third Ship Control Systems Symposium, 1972.

(3) Reeves, P. and Spencer, J.B. "Ship Automation in the Royal Navy," Proceedings, Fifth Ship Control Systems Symposium," 1978.

(4) Bullock, W.G. and Yonika, F. "Maritime administration guide for a standardized engine room propulsion control console,"

(4) Bullock, W.G. and Yonika, F. "Maritime administration guide for a standardized engine room propulsion control console,"

(5) French, C. and Dorrian, A.M. "Future propulsion control systems functional requirements," Proceedings. Fifth Ship Control Systems Symposium, 1978.

(6) Wiener, E.L. and Curry, R.E. "Flight-deck automation: Promises and problems," Moffett Field, CA: NASA TM 81206, 1981.

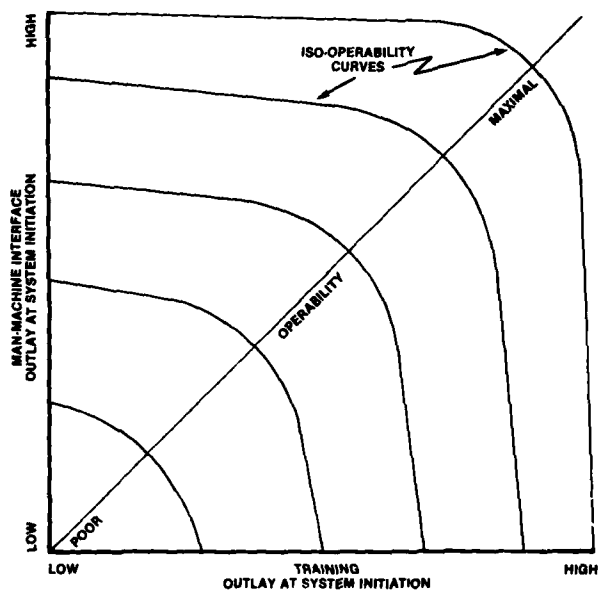

Figure 2. Hypothetical trade-off of training vs. HFE dollars prior to system initiation

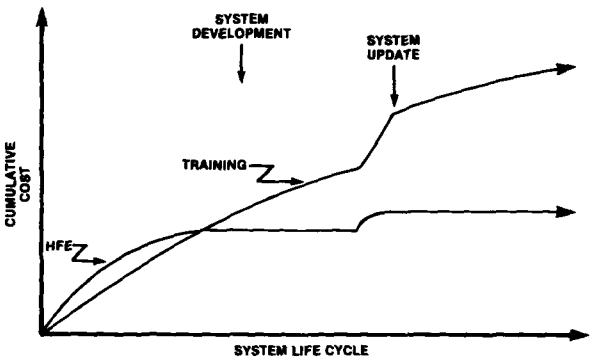

Figure 3. Cumulative Cost as a function system life cycle for HFE and training dollars

BRIDGE DESIGN - A HUMAN ENGINEERING APPROACH IN CANADA

by D. Beevis
Defence and Civil Institute of Environmental Medicine, Toronto

ABSTRACT

Under the sponsorship of the Directorate of Maritime Equipment Engineering of the Canadian Forces, DCIEM is conducting an analysis of human engineering factors in bridge design. Following from previous human engineering studies, the analysis is not intended to produce one, preferred, design. Instead the analysis emphasises, in human engineering terms, the various design issues and the trade-offs that must be made by those responsible for bridge design. It is hoped that the results of the analysis will, in this way, be generalisable, and useable as a design/evaluation guide.

Several existing bridge designs are compared to identify those design features where designers differ in approach to operability. From that basis the analysis breaks down the design of the bridge into a number of design factors, sub-factors, and design issues. The individual design issues are then analysed in detail. Wherever possible the design issues are analysed as trade-offs. For example, the impact of the fore-aft depth of the bridge can be assessed in terms of its effect on the field-of-view of the OOW, and on the space available for equipment and gangways.

In many cases, however, the design issues require human engineering guidelines rather than trade-offs, and in other cases the issues are choices between two or more options which cannot readily be expressed in operational or cost terms.

In general it has been found easier to provide trade-off data for issues of design principle, for example the preferred ranges of environmental parameters, than for design policy, for example personnel complement or bridge functions. The study has highlighted areas where current knowledge of bridge system operations is insufficient. Examples of such problems are given. It is hoped that the current study will set a framework within which some of these problems can be studied in a more systematic manner.

INTRODUCTION

It is a self evident fact that there is considerable variety in the designs of the bridges of modern warships, not only between the ships of different classes, but also between ships in comparable classes. Differences are evident in bridge architecture and equipment, and to a less obvious and less well documented extent, in the manning schedules and operating practices. This variety may be ascribed to two major causes.

Firstly it is a reflection of the fact that a bridge system is a compromise between a number of interrelated design factors. Different designs then reflect the different weightings given to individual factors by different design authorities. Secondly, it is a reflection of the comparatively recent development of the enclosed bridge and electronic navigation and communications equipment. This, coupled with the long in-service life of warships, has resulted in a relatively slow evolution of bridge designs in comparison with other techniques. A 'standard'

design of bridge has not therefore evolved.

Faced with this situation, the Directorate of Maritime Equipment Engineering in the Canadian Forces sponsored a human engineering review of bridge design. The study, which is being conducted by DCIEM, Toronto, has two main objectives:

- to establish the factors inherent in good bridge design, and the mutual effects of these factors and the trade-offs which result;

- to assist the C.F. bridge design authority in translating these factors into an acceptable bridge design.

The involvement of DCIEM in bridge design studies pre-dates the first Ship Control Symposium. At that time the emphasis of the majority of our human engineering studies was on developing a complete design package for specific projects. During the past ten years that emphasis has shifted to specifying or regulating for design by others. At the same time, in common with several other human engineering authorities, we have become increasingly concerned with finding the most effective way of integrating the results of our work into the project design/production cycle. The emphasis in the objectives of our tasking is therefore a direct outcome of our current concerns. It is based on the recognised need to make human engineering data directly available to those responsible for major project design decisions.

HUMAN ENGINEERING DATA

The first stage in the study was to review what data and guidelines were available which were relevant to the human engineering of ships' bridges. To do this it was necessary to draw from four overlapping sets of information:

i - operational data - details of current bridge designs, bridge operating practices, manning policies etc.

ii - critical incident data - details of the deficiences of current bridge systems, particularly the factors and circumstances which lead to near accidents;

iii - technology data - details of what equipment and systems are available to support the functions identified for the bridge systems;

iv - human engineering data - details of the performance capabilities of humans and the effects on those capabilities of the man/machine interface and the working environment.

At the time of writing, the data in all sets are considered incomplete. For the first three sets in particular, comparatively little information is available, and efforts are being initiated to increase our knowledge in each area. More information is required on how well (or how badly) existing systems operate. Work is also required to provide a better understanding of how humans perform the various ship control, navigation, collision avoidance and communications tasks. In the fourth information set, few human engineering design guides exist which deal specifically with shipboard systems. Three such sources have been identified at the time of writing (refs. 8, 20, 21). Only one of those guides is intended specifically for naval systems, and, because it caters to the design of all shipboard equipment, it does not discuss bridge design problems *per se*. The other two design guides were intended for the design of merchant ships' bridges. They were published as general guides, within which any bridge could be designed, depending on the role of the bridge system and the constraints applying to it. Both of these design guides are excellent sources of data for the detailed human engineering of bridges. They do not, however, fully meet the requirements of our study, of identifying the mutual trade-offs of the various bridge design factors.

Other sources of human engineering data are, of course available in the more general guidelines and text books. In North America the most frequently specified document is U.S. MIL-STD 1472, which, as a tri-service guide has replaced older, specifically naval texts. Besides those design guides, more qualitative human engineering data are available from a number of studies which have been carried out in Canada, The Netherlands, the United Kingdom and the U.S.A., some of which have been reported at previous Ship Control Symposia. The experience gained from those projects has been incorporated into the current study wherever possible. As those projects were reviewed the need became increasingly apparent for an overall design philosophy. A paradigm was required, which would rationalise the different approaches evident in the trade-off of design factors, and which would provide a referential framework for the increasing number of human engineering studies in this area. One of the most promising techniques for achieving these aims is, in our opinion, the Design Option Decision Tree.

DESIGN OPTION DECISION TREES

The essence of the Design Option Decision Tree approach is that the major system design decisions are identified and charted, as a series of branching options, the whole design process thereby being represented as a tree. The sequence of increasingly detailed decisions is then represented as progress along a particular branch of the tree. Once the tree has been developed it can be used to evaluate various options. It can also be used to study the impact of human engineering factors on each design decision. Information on the advantages and disadvantages of different design options can thereby be presented to the design authority for consideration during the design process. The information can also be presented to potential users to evaluate proposed designs. The emphasis on trade-off studies has been developed and used in human engineering design studies at DCIEM (e.g. ref. 3), although the term has been adopted from similar approaches in the U.S.A. (ref. 1). It is not particularly new; it can be traced back to the Matrix Evaluation techniques developed in the U.S.A. in the late 1950s (refs. 9, 16), but it does not seem to have been widely adopted. The approach differs from the more usual human engineering 'design package' approach in four significant aspects:

i - it developes an on-going design philosophy which can be refined through successive projects, rather than being applicable to one specific project;

ii - it is intended to foster an integrated design study involving all the relevant engineering disciplines, rather than being one of several independent design studies;

iii - it permits the development of a range of designs, rather than one recommended design which may be rejected in total if one specific design feature is unacceptable, or if the project requirements change;

iv - it presents the advantages and disadvantages of a number of options available to the design authority, in human engineering terms, so that the operational implications of each option can be assessed.

The approach is thus equivalent to other human engineering 'systems analysis' techniques in its emphasis on the effects of the individual components of human performance on the overall performance of the system.

The first step towards producing the decision tree was to identify those features wherein current bridge designs reflect different emphases in the compromise of the various design factors. As indicated in Table 1, a sample of five modern bridge designs reveals a number of features in which they differ significantly. If these eleven features were independent dichotomous choices available to the de-

TABLE 1. Comparative Features of Five Modern Bridges.

Ship / Bridge design feature	TRIBAL Canada	SPRUANCE USA	NITEROI Brazil	KORTENAER Netherlands	OLIVER HAZARD PERRY USA
Size	large	large	medium	medium	small
Shape	octagonal	rectangular	semi-circular	hexagonal	pentagonal
OOW position	fore-end, stbd, bulkhead console	fore-end no console	amidships at pelorus and forward centre-line, island console close to bulkhead	fore-end, stbd, bulkhead console	fore-end, port of centreline, bulkhead console
Command position	fore-end, port, bulkhead console	fore-end, port, chair	fore-end, stbd, island console close to bulk-head	fore-end, port, bulkhead console	unknown
Helmsman's posn.	fore-end, cen-treline, between OOW & Command	amidships	fore-end, port of OOW console	fore-end, cen-treline, between OOW & Command	fore-end, stbd, adjacent OOW
Radars	1, stbd, island	1, port, adja-cent chart table	1, port, adja-cent chart table	1, stbd, adja-cent OOW console	1, stbd, adja-cent chart table
Chart table	amidships, facing port	mid-length, port, facing forward	aft bulkhead, port, facing aft	mid-length, stbd, facing forward	aft bulkhead, stbd, facing aft
Pelorii	1 port, 1 stbd, 1 each bridge wing	1 fore-end, centreline, 1 each bridge wing	1 amidships, 1 each bridge wing	1 port, 1 stbd, 1 each bridge wing	1 amidships, 1 each bridge wing
Tactical display	1, mid-length, stbd	1, mid-length, stbd			
Seating	all, sit-stand, 2 levels	captain, sit-stand, tacti-cal display operator only	all, sit-stand or sit	all, sit-stand	OOW & ship con-trol operator, sit

signer, then the total of possible bridge designs would be 2048. Fortunately not all possible combinations of design features are viable, and it is because of this that it is possible to develop a design option tree, rather than an option matrix. The different features were grouped into a hierarchy of design factors as follows:

- bridge system functions - the starting point for any human engineering analysis, this factor includes topics such as the inclusion or deletion of navigation and combat system functions, the functions of the bridge complement, and the question of integrated versus conventional personnel functions;

- layout - topics such as the priority and usefulness of different bridge areas, gangway layout, the effect of interpersonnel communications on layout, OOW position, pelorus location etc.;

- architecture - topics such as the size and shape of the bridge, bridge wings and flag deck, window size etc.;

- individual workstation design - topics such as the information and instrumentation required for each bridge function, the integration of equipment, duplication of equipment, standard console designs, seating etc.;

- environment - added to reflect the effects on human performance of the working environment, this factor includes topics such as the acceptable values of noise, lighting, vibration etc., and the design requirements association with those factors, such as designing for ship motion.

From this list of major design factors an initial decision tree was drawn up (Fig. 1). Each design factor was then broken down into sub-factors, and the sub-factors broken down into specific design issues. One of the limitations of the technique is that it rapidly becomes very large, with many branches, if all interactions are represented. For example, at the system function level, the trade-offs involve the allocation of functions to either personnel, or to equipment, depending on the level of automation economically available and the reliability and work capacity of the bridge personnel. The functions allocated to the personnel in turn affect their information requirements and thus the individual workstation design factor. The personnel functions also affect the level of interpersonnel communication which, in turn, affects the bridge layout, and the design of the individual workstations. In view of this complexity the approach taken was to investigate each design issue in turn, and establish its interaction with others. When such interactions were identified they were analysed and cross-referenced.

Each design issue was evaluated in terms of its impact on four categories of operator behavior:

- information sensing, or detection;
- analysing and decision making;
- controlling;
- communicating.

The first three categories are frequently used in human engineering studies. They are the three basic functions dealing with Input Processes, Central Processes, and Output Processes, see, for example, ref. 17. The fourth category was added because a bridge system is a multi-operator system. Thus although interpersonnel communication and personnel movement are, strictly, covered by "sensing" and "controlling", their importance justifies a separate performance category. The final list of categories is essentially identical to a list of "processes" developed to quantify performance in a simulated environment (ref. 12).

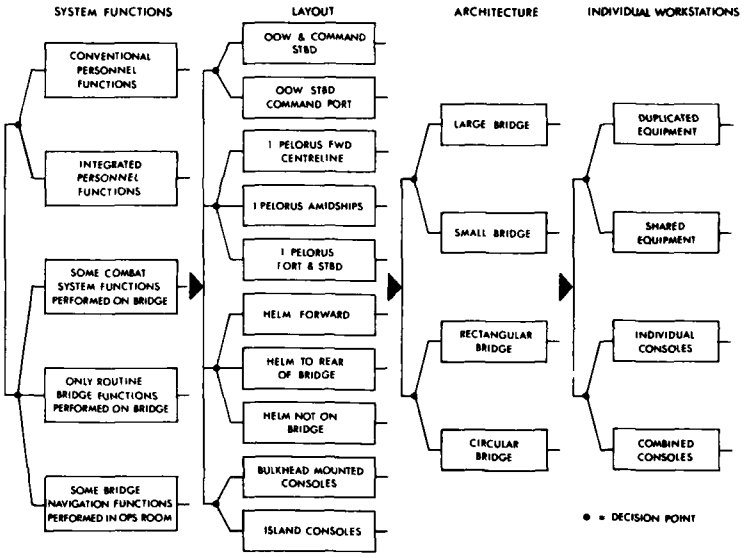

FIG. 1. Initial Design Option Decision Tree.

From the outset it was not anticipated that all the issues in the design of a bridge system could be expressed as simple trade-offs. Decisions in the early stages of a design clearly have implications for many subsequent options, resulting, as others have pointed out, in very complex analyses (ref. 9). Furthermore not all design issues can be expressed in simple quantitative terms. As the analysis proceeded it also became clear that not all design issues involved trade-offs. Some issues could, instead, be resolved with human engineering guidelines. Because it is hoped that the analysis will eventually be produced as a design guide it was necessary, in some cases, to provide guidelines in terms of the information that should be used in the design decision, or the constraints applying to the decision. The constraints were expressed, wherever possible, in terms of the acceptable ranges of human engineering factors.

Three types of design issue were therefore established:

i design issues for which guidelines could be established;

ii design issues for which quantitative trade-offs could be established;

iii design issues involving trade-offs which could not be expressed in simple quantitative terms.

GUIDELINE DESIGN ISSUES

At the time of writing, twenty-four design issues have been identified for which guidelines can be established (Table 2). A simple example of such an issue

TABLE 2. Guideline Design Issues.

Layout	Architecture
- factors affecting layout	- bridge architectural functions
- priority and importance of bridge areas	- requirement for panoramic vision
- personnel movements	- requirement for vision from bridge wings
- OOW location	- vision in the vertical plane
- night vision constraints on layout	- window size
Workstation Design	- bridge complement and bridge size
- common requirements for information	- constraints on fore-aft bridge length
- standard console designs	Environment
- console height	- noise
- seating	- lighting
- command position	- colour
- centreline conning position	- vibration
- ship control position	- heating/ventilation
- navigation position	
- communication position	
- Bosun's Mate's position	

is the question of the constraints on minimum fore-aft bridge depth. Based on previous bridge design studies, and on realistic allowances for consoles and gangways, limits can be set for the minimum practicable fore-aft depth of the bridge. The depth depends on the number of rows of consoles and gangways which are necessary, as shown in part in Fig. 2. As an example of the utility of such guidelines the data can be used to establish the length of the smallest practicable bridge, with, for example, two rows of consoles. By comparison, a layout with a bulkhead mounted pelorus, and a gangway running along the fore end, which is strongly favoured by

(a) Forward mounted console, overhead pelorus depth 5 metres (16 ft)

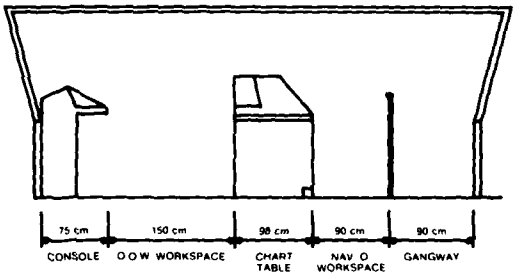

(b) As (a), with rearwards facing chart table: depth 5 metres (16 ft)

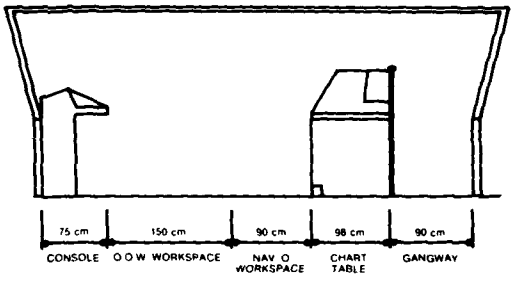

(c) Consoles back from front bulkhead, pelorus mounted forward: depth 6.3 metres (20.5 ft)

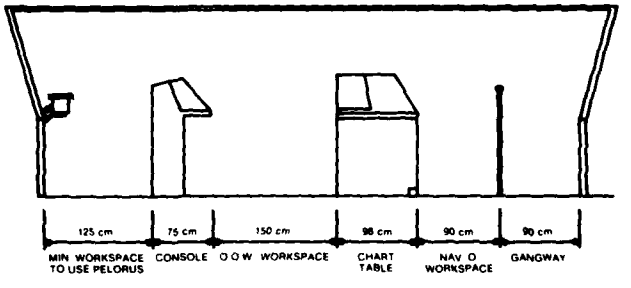

FIG. 2. Constraints on Minimum Fore-Aft Depth of Bridge.

some operators, increases the fore-aft depth by a significant extent (26%). In contrast a pelorus mounted in the main gangway used by the OOW would increase the depth of that space by some 500 mm, an increase of 10% in the overall bridge depth. Bridge size can then be related to other factors, such as visibility, as described below. The impact of the forward gangway on bridge size is reflected in the report that during the development of a ship which allowed only a limited bridge depth (5 m fore-aft), the layout was changed from one having island consoles at the fore end to a layout with bulkhead mounted consoles (ref. 7).

In analysing such constraints the aim was always to permit the designer as much freedom as possible. An example is provided by the analysis of console design constraints. A review of the relevant human engineering literature reveals a variety of recommended console designs. Although these designs are similar in overall profile, they differ significantly in detail. Such differences can be expected from the implementation of different equipment such as that based on the British Versatile Console System (refs. 2, 21 Ch. 4), or the European DIN standard for panel sizes. It does not seem appropriate, then, to legislate the use of one particular design of console, such as that recommended in MIL STD 1472. As an alternative approach, the design item discussing console design recommends that the console design conform with a specific reach envelope, which has a datum on the console edge (ref. 9).

Some of the issues are currently expressed as guidelines due to a lack of data. It is hoped that some of those issues will be expressed as trade-offs when more data are available. For example, under the issue of Ship Conning Information the analysis recommends the provision of rate-of-turn information. This follows from the demonstrated need for rate information when conning using radar, or, by extrapolation, in any conditions where an outside-world view is not available (ref. 14). Rate-of-turn information can be provided by dedicated instruments, or by gyro-compasses fitted with verniers, or it can be extracted from the conventional tape gyro-repeater. Although the dedicated rate-of-turn indicator is much more sensitive than the other two displays, and has been shown to contribute significantly to the control of large ships (ref. 19), the relative effectiveness of the three types of display for conning destroyer-sized ships is unknown. The need for rate-of-turn information is therefore provided as a guideline, and if comparative performance data become available, they will be included.

QUANTITATIVE TRADE-OFFS

Six design issues have been identified for which trade-offs can be expressed in quantitative terms (Table 3). These issues are mostly associated with architectural parameters such as bridge size, which can be expressed as a continuous variable. An example is given by the analysis of the trade-offs which determine the

TABLE 3. Quantitative Trade-offs.

Layout	Architecture
- effect of speaker-to-speaker distance on voice communication - pelorus location	- window slope to reduce reflections - bridge size and visibility - bridge fore-aft length and panoramic vision - bridge shape and visibility

shape of the bridge. When the effects of bridge shape are evaluated against the performance categories of sensing, analysing, controlling and communicating, it is seen that it has most effect on the first and last categories. Specifically, the shape of the bridge affects vision from within, and it affects the patterns of

movement of the different bridge personnel. The ideal bridge is a circular structure within which the OOW does not move. As others have shown (ref. 8) in the case of merchant ships, a hexagonal bridge can provide visibility which approaches that of a circular one. In warships the ratio of window to mullion is typically much less than in merchant ships. The effect of bridge shape on vision may not therefore be the same. The results of a comparison of the differences in total field of view in the forward quarters afforded by a circular planform and an octagonal planform bridge are shown in Fig. 3a. As can be seen, the difference between the two designs is comparatively small, particularly if the OOW stands well forward. It will be appreciated that the magnitude of these differences changes with bridge size and that the number of windows in a straight line is also critical to visibility. From analyses of the cumulative effects of wooding on visibility, as shown in Fig. 3b, it is clear that no more than five windows should lie in the same plane.

Two principles thus emerge from the analysis. The bridge should be nearly circular in planform, and no side have more than five windows in line. Many modern bridges conform with these requirements. Many others, however, do not, and the extent to which visibility is impaired from within the bridge can be assessed from the above analyses.

A second example of a design issue for which a quantitative trade-off can be established is the effect of background noise on the distance at which speech is intelligible. This relationship has been well established by psycho-acoustical research. Briefly there is a logarithmic relationship between the distance of the speech path and the ambient noise level (the A-weighted ambient sound pressure level) which will interfere with speech communication. These levels are specified in Table 4. To place the problem in context, the noise levels on the bridge of a typical gas turbine powered frigate are about 65 dBA, which will permit 'satisfactory

TABLE 4. Voice Level and Distance between Speaker and Listener for Satisfactory Face-to-Face Communication, as Limited by Ambient Noise Level (dBA).

(after Webster, 1969.)

Distance in feet between speaker and listener	Normal voice	Expected voice level (1)	Limit for unaided face-to-face speech communication (2)
	A weighted ambient sound pressure *level* (3)		
0.5	82 dBA	94 dBA	117 dBA
1	76 dBA	85 dBA	111 dBA
2	70 dBA	77 dBA	103 dBA
3	66 dBA	72 dBA	101 dBA
4	64 dBA	69 dBA	99 dBA
6	62 dBA	62 dBA	95 dBA
8	60 dBA	61 dBA	93 dBA
10	56 dBA	57 dBA	91 dBA
12	54 dBA	54 dBA	89 dBA

(1) The expected voice level is that to which normal-hearing persons would be expected to increase their vocal efforts to overcome masking efffects of ambient noise upon their auditory feedback. This increase in vocal effort is about 3 dB for each 10 dB increase in ambient noise level, at a level starting at about 50 dB. There is no guarantee that they will do so, however.

(2) Limited by maximum vocal effort.

(3) dB levels relative to .0002 dynes/sq. cm.

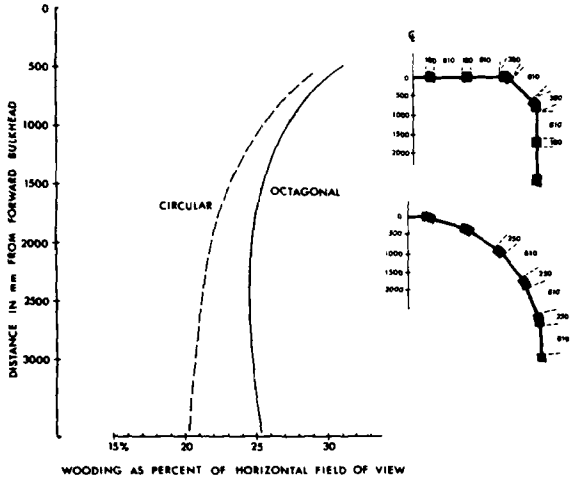

FIG. 3a. Percent of Wooding in Forward 180° Field of View for Octagonal and Circular Bridges.

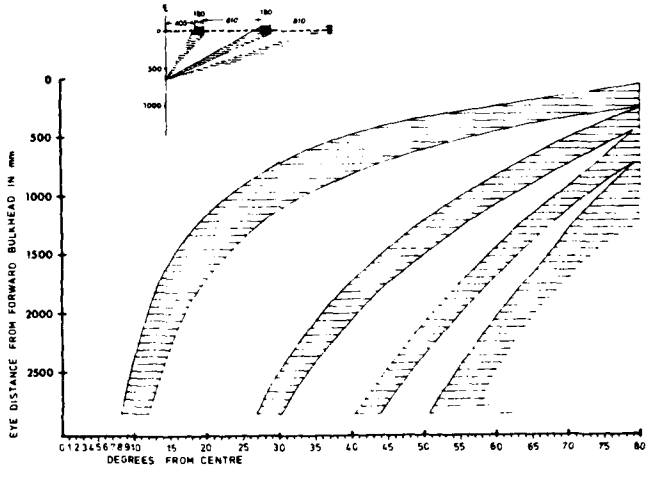

FIG. 3b. Effect of Wooding on Horizontal Field of View with Increasing Distance from Window.

voice communication among bridge personnel at expected levels up to about six feet' (ref. 6). If the design of the bridge system is such that personnel must speak over longer distances, or if the noise level is higher than specified for the distance, then there is a risk that orders or information will be misunderstood.

QUALITATIVE TRADE-OFFS

Eleven of the design trade-offs do not lend themselves so readily to quantification (Table 5). For those issues, the advantages and disadvantages of candidate

TABLE 5. Qualitative Trade-offs.

Functions	Layout
- bridge system functions - location of bridge functions - bridge complement and bridge functions - integrated vs. conventional personnel functions	- OOW / Captain location - helmsman location - pelorus location - gangways and passageways - bulkhead vs. island consoles

options have been presented in the form of a table, summarising the problem. A typical example is the still contentious issue of bulkhead versus island consoles. The various aspects of this issue are summarised in the trade-off Table 6. The issue is typical of the qualitative trade-offs; it is multi-parametric, and the parameters are, for the most part, non-quantifiable. This is not, of course, a novel situation for the ship designer, as the history of ship development attests (ref. 4). The complexity and the pace of development of technology are such, however, as to preclude solving such problems by trial and error.

Comparing the qualitative design issues with the quantitative issues, and the guideline issues, it can be seen that they tend to apply to different levels of the design decision tree. Guidelines are associated with the low level decisions; in contrast the qualitative trade-offs tend to be associated with high level decisions. The three categories of design option tend therefore to follow the hierarchy of design factors. At the top of the hierarchy are matters of policy, such as the functions of the bridge system, or the level of manning. At successively lower design levels, the design issues become increasingly concerned with matters of design principle. In general they are questions of how best to design the equipment and the working environment, once the system functions, tasks and manning have been decided. As indicated above, issues of design policy are difficult to quantify, in contrast with issues of principle.

Taking as an example the issue of integrated crew functions, the lack of hard performance data for different options makes it difficult to resolve. Evaluation of competing design concepts by simulation, either a physical, real-time simulation or a mathematical model would help resolve the issue. At the present time, however, such exercises tend to be limited in scope and to be both complex and costly. They are not likely to be undertaken as a routine design activity. Lacking such an approach system designers must either evaluate competing design concepts using conceptual criteria such as utility, reliability and likely cost, or they must base the design on precursors. Either approach is subject to strong bias on the part of both the designer and the ultimate user, and design issues which are subjected to this type of evaluation are likely to become extremely contentious.

TABLE 6. Example of Qualitative Trade-off.

Design Issue 4.4.7: Bulkhead vs. Island consoles.

	Bulkhead Mounted Consoles	Island or Free-standing Consoles
Advantages	- better control of speed and track possible than with island consoles - OOW has good vision (± 90° horizontally) through forward window, standing at console, and fair panoramic vision - OOW can readily refer to console mounted displays and controls, while maintaining a good lookout - suitable for a high level of equipment fit where much information is displayed - minimises bridge size	- OOW can stand right against all forward windows, maximising his forward view (± 90°) - OOW can stand forward of console lights at night, avoiding interference with night vision - minimal sunlight 'washout' problems on displays - effect of rain on windows minimised by standing close to them - good maintenance access to consoles.
Disadvantages	- field of view through forward windows less than maximum (± 80° vice ± 90°) - console instruments must be carefully illuminated to avoid interference with night vision - console design requires shielding to avoid display washout in direct sunlight - effects of rain on windows more severe than with island consoles - requires careful design to minimise interference of maintenance tasks on routine bridge activities.	- control of speed and track likely to be inferior to bulkhead console layouts - limited panoramic field of view unless OOW moves aft of consoles - OOW cannot readily refer to console mounted displays or controls; he must physically move to do so, which interferes with performance - unsuitable for bridge system with high level of information display - fore-aft depth significantly greater than minimum.

CRITERIA SELECTION PROBLEMS

It is possible that qualitative design issues may be resolved by analysing their impact on the lower-level design decisions, and thus on the overall performance of the system. For example, the question of bulkhead consoles could be resolved by working through the implications of the different options on successive design issues. As noted above, a large number of trade-offs are involved. The question of console location involves bridge size, personnel movement, ship conning performance, night vision, maintenance and console design. If it is assumed that competing designs can be produced which maintain the same level of night vision, then console cost and bridge size can be estimated, and, by simulation, personnel movement patterns established. Some indication of the differences in ship conning

performance can be obtained from the results of experiments such as those of Schuffel et al. (ref. 14), which showed that speed and planned track are maintained more accurately with bulkhead mounted consoles than with an island console layout. The question of ease of maintenance must be addressed either by making both designs equally easy to maintain, or by trading-off maintainability against ship handling.

Two problems emerge from this approach. The first is the problem of making multi-parametric analyses and identifying the most effective design. Such analyses require not only that the criteria be quantifiable in some way, but that the relative weightings of separate criteria can be established, for example maintainability versus ship handling. At present there appears to be no more satisfactory technique for doing this than using subjective opinion. Utiles - subjective estimates of utility - such as those used by Underwood and Buell in the bridge design study reported to the Fourth Ship Control Symposium (ref. 18), can be used to collapse all weightings into one rating of the utility of a particular design. This is useful for comparing different designs, but not for studying the impact of different design issues on overall utility. The technique of Criterion Function Synthesis developed by Ofstrofsky (ref. 11) permits the effects of individual parameters to be investigated in more detail, by manipulating non-independent parameters which are expressed in quantitative terms. However, the technique still requires the subjective assessment of the weightings of individual parameters, and of their first and second order interactions. To behavioral scientists, who are particularly sensitive to the unreliability of opinion, it appears basically unsatisfactory to have only shifted the point in the design process at which subjective evaluations become important, instead of eliminating it.

In this attitude we may be unduly reserved; it has been argued that almost every decision in system development and evaluation rests ultimately on the subjective interpretation of qualitative and quantitative data. At least the techniques such as Criterion Function Synthesis permit the importance of subjective opinions to be appreciated more readily, particularly if the subjective ratings are submitted to sensitivity analysis. Possibly more important than the use of subjective data is the fact that, without such techniques, the complexity of the evaluation encourages designers and potential users to make "top-of-the-head" decisions.

The second problem in criteria selection is the lack of a concise statement of bridge system performance requirements. In common with many complex man-machine systems, it does not appear possible to produce a simple measure of system performance. An example of how bridge system functions could be analysed for performance criteria was given by Ramas and Oskaptan in 1973 (ref. 13). Little progress appears to have been made since then in specifying exactly how well some of those functions should be performed. For example, although the accuracy of radio-navigation systems is now being specified (ref. 22), including operational criteria such as the time required to obtain a position fix, the contribution of human error to the accuracy of such systems is much more difficult to specify.

Furthermore, the selection of performance criteria is, in itself, a significant problem. As was emphasised in a paper to the Fifth Ship Control Systems Symposium (ref. 5), it may be important to use measures which indicate the possibility of an error, rather than the error itself. In human engineering terminology this is the distinction between process measures and product measures of performance. The distinction is an important one; for operational personnel the probability of an error is frequently of secondary importance to what actually happened; to behavioral scientists the emphasis is reversed, and this difference in attitude can produce misunderstandings.

CONCLUSION

The foregoing discussion of problems tends to highlight the limitations of the

Design Option Decision Tree technique, rather than the advantages to be derived from its use. Despite the problems outlined above, the analysis has contributed significantly to our understanding, not only of the overall bridge design problem, but also of where our human engineering efforts can be most effectively applied. The technique has been used successfully in three projects, one of them being the redesign of an existing bridge for the Canadian Forces. The analysis has also been used to evaluate proposed bridge designs.

We intend to continue to expand the analysis, to gather more quantitative data, to expand the number of design issues as more operational data are gathered, and to obtain the reaction of system designers and potential operators to the analysis.

We hope that the completed analysis will be used not only to design and evaluate new bridge systems, but also to indicate the areas where future human engineering studies will be most productive.

REFERENCES

(1) W.B. Askren, K.D. Korkan, "Design Option Decision Trees: A Method for Relating Human Resources Data to Design Alternatives", AFHRL-TR-71-52, AD-741 768, Air Force Human Resources Laboratory, Wright-Patterson AFB, Ohio, U.S.A., December 1971.

(2) A.H. Beach, "The Versatile Console System: The Modular Way to a 'Clean' Bridge", Maritime Defence International, Vol. 2, No. 3, March 1977.

(3) D. Beevis, "Polar Icebreaker Bridge Design", DCIEM Report no. 74-R-1069, Toronto, November 1974.

(4) H.I. Chapelle, "The Search for Speed Under Sail, 1700-1855", Bonanza Books, New York.

(5) E.M. Connelly, "Criteria Optimised by Collision Avoidance Strategies", Proceedings, Fifth Ship Control Systems Symposium, Annapolis, Md., U.S.A., October/November 1978.

(6) B. Crabtree, "A Noise Survey of HMCS Iroquois", DCIEM Technical Report 76-X-26, Toronto, July 1975.

(7) J.B. Dahl, G.R. Wilkinson, "The Bridge Area of the Norwegian Coast Guard Ships - A Design History", Symposium on the Design of Ships' Bridges, RINA / NI, London, November 1978.

(8) H. van Donselaar, A. Lazet, H. Schuffel, A. Wepster, "Merchant Vessel Bridge Lay-Out", The Netherlands Institute for Perception, The Netherlands Maritime Institute, Report no. R 144, August 1979.

(9) K.B. de Greene, "Systems Psychology. Ch. 3, Systems Analysis Techniques", McGraw-Hill Book Co., New York, 1970.

(10) J.L. Hanna, A.F.H. Ireland, "Graphic Aids for Console Designs", Information Display, September/October 1969.

(11) B. Ostrofsky, "Design, Planning and Development Methodology", Prentice-Hall Inc., New Jersey, U.S.A., 1977.

(12) G.F. Rabideau, "Field Measurement of Human Performance in Man-Machine Systems", Human Factors, Vol. 6, December 1964, pp. 663-671.

(13) E. Ramas, H. Oskaptan, "Ship Manpower Reduction - Bridge Manning", NATO Defence Research Group Seminar on Man:Machine Relations, Utrecht, The Netherlands, May 1973.

(14) H. Schuffel, A. Lazet, "The Use of Mock-ups and Simulation in Wheelhouse and Bridge Design", Symposium on the Design of Ships' Bridges, RINA/NI, London, November 1978.

(15) H. Schuffel, "Some Effects of Radar and Outside View on Ships' Controllability", in Human Factors in Transport Research. Vol. II, D.J. Osborne, J.A. Lewis, Eds., Academic Press, London, 1980.

(16) A. Shapiro, C. Bates, "A Method for Performing Human Engineering Analysis of Weapon Systems", Wright Air Development Center, Technical Report 59-784, AD 235 920, Wright-Patterson Air Force Base, Ohio, U.S.A., September 1959.

(17) W.T. Singleton, "Ergonomics in Systems Design", Ergonomics, Vol. 10, No. 5, 1967, pp. 541-548.

(18) Cdr. F.S. Underwood, G.D. Buell, "Computer Aided Pilot House Design; A Systems Approach", Proceedings, Fourth Ship Control Systems Symposium, Den Helder, The Netherlands, October 1975.

(19) W.A. Wagenaar, P.J. Paymans, G.M.A. Brummer, W.P. van Wijk, C.C. Glansdorp, "Auxiliary Equipment as a Compensation for the Effect of Course Instability on the Performance of Helmsman", (Comm. 285), Delft, The Netherlands: Netherlands Ship Research Centre, 1972.

(20) "Code Practice for Ships' Bridge Design", Department of Industry, U.K., 1977.

(21) "Human Factors for Designers of Naval Equipment", Medical Research Council, Royal Naval Personnel Research Committee, London, 1970.

(22) "Accuracy Requirements and Harmonisation of Radio Navigation Systems", IMCO, - Note by the Secretariat, Sub-Committee on Safety of Navigation, 24re Session, 3 December 1979.

AN APPROACH TO ANALYSIS OF HUMAN-COMPUTER INTERACTION IN SHIP CONTROL

William B. Rouse
Center for Man-Machine Systems Research
School of Industrial and Systems Engineering
Georgia Institute of Technology
Atlanta, Georgia 30332 U.S.A.

Robert E. Reid
Department of Mechanical and Industrial Engineering
University of Illinois at Urbana-Champaign
Urbana, Illinois 61801 U.S.A.

ABSTRACT

An approach to systematic analysis of human-computer interaction in ship control is proposed. The analytical framework chosen for the problem is that of a multi-processor time-shared computer system where some of the processors are human and other processors are actual computers. Using this framework, task allocation among humans and computers is formulated as an optimization problem where the solution of interest is the assignment of processors to tasks for particular mission phases and situations. The application of the proposed approach to computer aiding, as opposed to automation, is also discussed.

INTRODUCTION

The impact of automation in technical systems has increased substantially in the last decade or so. This has led to a changed role for the human operator who has become a monitor and supervisor of automated systems rather than an in-the-loop controller of manual systems (1,2). A particularly important man-machine systems issue that has arisen because of this trend involves determining how to allocate tasks among humans and increasingly sophisticated computers. This issue is the primary focus of this paper.

While the impact of automation has perhaps been clearest in the aviation industry, the marine industry has been receiving increased attention (3,4). And, as has often been the case within aviation, most of the marine automation efforts appear to have been piecemeal, emphasizing particular control functions and/or hardware possibilities. In contrast to this "bottom-up" approach, what is needed is an overall "top-down" approach for determining the appropriate role for automation. Such an approach will allow one to determine what should be automated rather than what can be automated.

There have been a few attempts to pursue a more top-down view of the problem. Reeves and Spencer (5) discuss approaching automation on various levels ranging from the whole ship down to the individual component. Steinhausen, Orton, and Smalley (6) propose a broad approach to design of man-machine interfaces in the machinery control

domain. Moor and Eberle (7) present a comprehensive and integrated bridge and engine control system.

While all of these efforts are in the right direction, they all suffer from at least one of the following limitations:

1. The total ship for its full range of operations is not considered,

2. Design rather than operation of the ship is emphasized,

3. The solution is presupposed in terms of particular types of hardware.

Nevertheless, the ideas discussed by these authors have contributed to the concepts presented in this paper.

Rouse (8) has proposed a totally top-down systems approach to dealing with the issue of allocating function among humans and computers. The essence of the approach involves structuring the problem in terms of required tasks as a function of mission phase and status, characterizing the performance requirements of each task, and optimizing the allocation of tasks among humans and computers. Rouse illustrated the application of this approach with an example from aviation; in this paper, this approach will be applied to the problem of ship control.

STRUCTURING THE PROBLEM

The overall problem of interest is determination of how the wide variety of tasks encountered in ship control are to be allocated among humans and computers. Solving this problem requires a characterization of the tasks to be performed and quantification of the abilities of humans and computers to perform these tasks. By incorporating this information into an analytical framework, one can rigorously approach the problem of task allocation.

While the literature of man-machine systems and the nature of ship control might lead one to think that linear systems theory is an appropriate candidate for the analytical framework needed, a better choice is that of a multi-processor time-shared computer system. Each of the processors can be either human or computer, with appropriate performance characteristics. From this perspective, the problem can be viewed as involving total automation and the task allocation problem becomes that of deciding which processors should be human and which should be real computers. This type of task allocation problem can be addressed using queueing theory models of computer systems (e.g., Kleinrock (9)).

Thus, restatement of the problem in terms of total automation allows the use of a powerful set of analysis tools. In order to use these queueing theory formulations, the demands on the system and the performance characteristics of each processor must be known. With respect to the types of task required, one need only consider those tasks that could possibly be performed by humans. All other tasks must be automated and therefore, there is no task allocation decision for these tasks.

Task Demands

Rouse (8) has suggested a set of tasks for the flight domain, many of which are applicable in the ship domain. He espouses the following ten tasks:

1. Executing procedures,
2. Scanning,
3. Recognizing,
4. Problem solving,
5. Regulating,
6. Steering,
7. Communicating,
8. Planning,
9. Recording,
10. Maintaining.

This set of tasks was chosen for two reasons. First, each task is fairly high level and thus, at least initially, the fine-grained level of the button pushing and switch flipping can be avoided. Second, there is a reasonably robust set of models of human performance for these tasks, as evidenced by the comprehensive tabulation in Rouse (8) and more thorough treatment in Rouse (10). The use of these models will later be discussed.

Given the above set of tasks to be performed by the multi-processor time-shared computer system, one needs to know the frequency with which these tasks require the system's resources. Rouse (8) has argued that these frequencies vary with task, mission phase, and mission status. For example, in the flight domain an emergency landing places different demands on the system than a normal taxi operation. This aspect of the ship control problem can be represented using the following mission phases for non-military ships (11,12):

1. Predeparture check,
2. Getting underway,
3. Harbor pilotage,
4. River pilotage,
5. Coastal (confined waters) operations,
6. Open seas operations,
7. Coastal operations,
8. River pilotage,
9. Harbor pilotage,
10. Docking or berthing,
11. Cargo unloading/loading.

Mission status can perhaps be defined in a manner similar to the flight domain: normal, abnormal, and emergency.

Considering 10 types of task, 11 mission phases, and 3 levels of mission status, there are 330 combinations of resource demands that can be placed on the multi-processor time-shared computer system. The distribution of interarrival times of each of these types of demand must be estimated. While this might seem to require an enormous investment of effort in data collection, it is quite likely that only the mean interarrival time, perhaps on a ten-point quantized scale, would be necessary for an initial analysis.

Performance Models

Given the above characterization of the time-varying demands placed upon the multi-processor time-shared computer, one must then characterize each processor's ability to perform each task. For the processors that denote actual computers, the performance characteristics can be based on typical engineering models. For the processors that denote humans, models of human performance such as discussed by Rouse (8,10) can be utilized.

The performance predictions required from each type of model include the probability of performing each task within specifications and the distribution of performance times for each task. An alternative to using probability of successful task performance is to use context-specific measures such as rms amplitude, energy consumption, etc.

While predicting performance may seem quite straightforward, it can be rather subtle for the human processors. The most important subtlety is due to the fact that human performance of each of a group of tasks may depend on the particular set of tasks being grouped. For example, having to perform a task involving mental arithmetic while also regulating or steering can lead to degraded performance. On the other hand, some combinations of tasks may complement each other (e.g., simultaneously controlling both lateral and longitudinal velocity of a vehicle). Because of these interaction effects, one has to be careful when predicting human performance in multi-task situations. Rouse (8) considers this issue in more detail.

TASK ALLOCATION

Once one has characterized the task demands and the abilities of humans or computers to satisfy these demands, one would like to determine the allocation of tasks among humans and computers that is optimal with respect to some criterion over a particular time interval of interest. For the control of vehicle systems such as ships, the criterion usually reflects objectives such as maximizing speed of response, minimizing deviations of important variables, maximizing safety, and minimizing time to recover from failure.

The time interval of interest is likely to be the length of a typical mission. Alternatively, the criterion can vary from phase to phase by choosing time intervals equal to phase lengths and optimizing a multi-dimensional criterion. The latter approach may present difficulties in terms of determining the relative values of different phases.

Given a criterion, task allocation can be formulated as an optimization problem where the "return" for allocating a task to a particular processor is the criterion value produced. As noted earlier, the return produced by the human processor may depend on the particular mix of tasks allocated to the human. A constraint on the allocation of tasks to the human is that each human has only 100% of his time to use; in fact, 70% is probably a better number. Thus, crew size versus amount of onboard computer power is an issue that can be addressed with this formulation.

If availability of the human's time is the constraint that dictates the use of computers, then it is likely that non-peak load periods would be such that tasks should be shifted back to the humans from the computers. This workload-sensitive dynamic approach to task allocation has been proposed and evaluated by Chu and Rouse (13).

COMPUTER AIDING

It is quite likely that some tasks can best be performed using some form of human-computer interaction. The formulation espoused in this paper is amenable tc this type of task sharing. This can be accomplished by partitioning tasks into separate functions, each of which can be allocated to human or computer. Thus, it can be seen that the overall approach involves a hierarchical decomposition down to the level necessary to resolve allocation decisions.

Using this task decomposition approach care must be taken to consider interaction effects in the sense that the way in which the computer performs its functions within a task may affect the way in which the human performs his functions. In other words, the effect of a computer aid may be more than just performing a portion of a task; it can affect the strategy chosen and results achieved by the human in his portion of the task. From this perspective, the type of computer aid chosen is likey to affect the type of model of human performance appropriate to the allocation analysis. Or, at least, it may affect the parameters within the general model being used (8).

CONCLUSIONS

The purpose of this paper has been to propose a systematic approach to analysis of human-computer interaction in ship control. In order to encompass the breadth of the problem, an integrated top-down approach was espoused. The essence of the approach is hierarchical decomposition within a framework of a multi-processor, time-shared computer system. The combination of this framework and a variety of models of human performance provide a comprehensive formulation of the problem.

While the methods of analysis proposed in this paper, and elaborated upon elsewhere (8,10), are attractive in that they systematically capture the breadth of the ship control problem, there are considerable difficulties to be overcome before these methods can become standard design tools. The most important of these difficulties are associated with a lack of information in the sense that the product of many past and current research efforts in the ship control domain, in contrast to the flight control area, do not systematically contribute to a unified perspective of the ship control problem. Instead, a more piecemeal approach has been pursued. Hopefully, this paper will contribute to the emergence of a more integrated approach.

REFERENCES

(1) T. B. Sheridan and G. Johannsen, (Eds.), Monitoring Behavior and Supervisory Control, New York: Plenum Press, 1976.

(2) J. Rasmussen and W. B. Rouse, (Eds.), Human Detection and Diagnosis of System Failures, New York: Plenum Press, 1981.

(3) W. J. Blumberg and E. M. Petrisko, "An R & D View of U.S. Navy's Automation Opportunities," Proceedings of the 1981 Joint Automatic Control Conference, Charlottesville, Virginia, June 1981.

(4) V. E. Williams and R. E. Reid, "Experience of the U.S. Maritime Administration in Man-Machine Aspects of Ship Control," Proceedings of the 1981 Joint Automatic Control Conference, Charlottesville, Virginia, June 1981.

(5) P. Reeves and J. B. Spencer, "Ship Automation in the Royal Navy," Proceedings of the Fifth Ship Control Systems Symposium, Annapolis, November 1978.

(6) J.L.P. Steinhausen, J. N. Orton, and J.P.A. Smalley, "A Structured Approach to Man/Machine Interface Design for Command and Control of Ships' Machinery," Proceedings of the Fifth Ship Control Systems Symposium, Annapolis, November 1978.

(7) M. Moor and M. K. Eberle, "New Integrated Bridge and Engine Control System Condition Monitoring and Predictive Maintenance for Slow Running Diesel Engines," Proceedings of the Second International Symposium on Ship Operation Automation, Washington, September 1976.

(8) W. B. Rouse, "Human-Computer Interaction in the Control of Dynamic Systems," Computing Surveys, Vol. 13, No. 1, March 1981, p. 71-99.

(9) L. Kleinrock, Queueing Systems, Vol. II, New York: Wiley, 1976.

(10) W. B. Rouse, Systems Engineering Models of Human-Machine Interaction, New York: North-Holland, 1980.

(11) C. L. Crane, "State of the Art on How to Include Human Control into the Method of Investigation," Proceedings of the Symposium on Aspects of Navigability of Constrained Waterways, Including Harbour Entrances, Delft, April 1978.

(12) K. Kasahara and Y. Nishimura, "Overview of Optimum Navigation Systems," Proceedings of the Symposium on Ship Steering Automatic Control, Genoa, June 1980.

(13) Y. Chu and W. B. Rouse, "Adaptive Allocation of Decision Making Responsibility Between Humans and Computers in Multi-Task Situations," IEEE Transactions on Systems, Man, and Cybernetics, Vol. SMC-9, No. 12, December 1979, p. 769-778.

SIMULATION OF STEAM SHIP PLANTS

by G. Grossmann, W. Milde, H. Xuan
Technical University of Berlin

INTRODUCTION

Ship propulsion systems are getting more complicated continuously and it is rather difficult to reach an optimum setting of the different controllers. To study these problems and to help ship owners in defining the setting of their control systems a simulation program for steam turbine plants was developed at the Technical University Berlin. This program includes a boiler system with natural circulation, a steam turbine coupled to a fixed pitch propeller and the following control systems: turbine load control, boiler pressure control, feedwater supply control and steam temperature control.

The differential equations of the boiler behaviour suggested two changes in the control philosophy. The control of the pressure in the steam drum of the boiler and a load proportional water level should bring a more uniform behaviour of the fuel control valve and the feed water control valve. We are very grateful to Deutsche Shell Tanker AG and Shell International Marine Ltd. that we could test these ideas on TTS "Liotina". These shipboard trials gave us also enough material to evaluate the different time lags of the boiler system.

The now existing simulation program allows the evaluation of conventional steam turbine systems and a prediction of the optimum controller settings. It also allows the development of new control systems using higher controller algorithms for future computer controlled steam systems.

DEVELOPMENT OF THE EQUATIONS FOR THE STEAM SYSTEM

Mathematical boiler model

The boiler is the most complicated part of the whole steam system, so its equations form the greatest part of the simulation program.

Steam drum pressure p_{TR} as function of steam flow $\dot{m}_{DKE}$ and energy input Q_{VD}.

The steam drum pressure p_{TR} and the superheater outlet pressure p_{UE} are connected by the pressure loss Δp_{VUE}

$$p_{TR}(t) = p_{UE}(t) + \Delta p_{VUE}(t) \qquad (1).$$

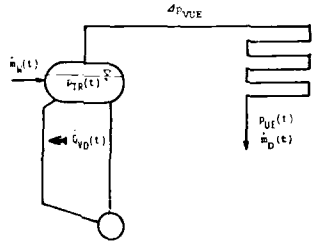

Figure 1. *Boiler - pipes system*

The pressure loss can be described as a function of the losses at design conditions. (Index o)

$$\Delta p_{VUE}(t) = \Delta p_{VUEO} \frac{\dot{m}_D(t)^2}{\dot{m}_{DO}^2} \frac{V_{UE}(t)}{V_{UEO}} \qquad (2)$$

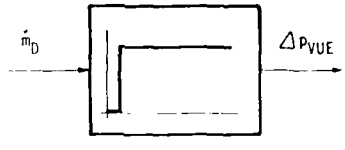

Figure 2. *Block diagram BR1*

As long as the energy input and the energy demand are equal, the pressure level of the system remains constant. When the equilibrium is disturbed by changing the steam demand $\dot{m}_D(t)$ then the pressure loss $\Delta p_{VUE}(t)$ changes and also the steam mass M_{DE} contained within the steam part of the upper boiler drum and the superheater pipes. For a small time step Δt the volume V_{DR} of steam containing part of the drum and the pipes can be considered constant, also the superheater temperature T_{UE}.

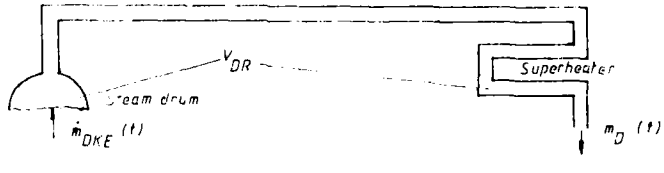

Figure 3. *Steam void V_{DR}*

With $\dot{m}_{DKE}(t)$ as steam output of the boiler and $\dot{m}_D(t)$ as steam demand of the system we get

$$dm_{DR}(t) = (\dot{m}_{DKE}(t) - \dot{m}_D(t))\,dt = \Delta\dot{m}_D\,dt \qquad (3)$$

This change of the steam mass in the pipes effects a change of the specific steam volume v_D and therefore a change of the pressure $p_{UE}(t)$ according to the gas equations.

$$p_{UE}(t) \cdot V_{DR} = m_{DR}(t) \cdot R\,T \qquad (4)$$

$$dp_{UE}(t) = \frac{R\,T}{V_{DR}} \cdot dm_{DR}(t) = \frac{R\,T}{V_{DR}} \Delta\dot{m}_D\,dt \qquad (5)$$

With design conditions there is

$$\frac{R\,T}{V_{DR}} = \frac{p_{UE0}}{m_{DR0}} \qquad (6)$$

$$dp_{UE}(t) = \frac{p_{UE0}}{m_{DR0}} \Delta\dot{m}_D\,dt \qquad (7)$$

$$p_{UE}(t) = p_{UE}(t-\Delta t) + \int dp_{UE}(t) = p_{UE}(t-\Delta t) + \frac{p_{UE0}}{m_{DR0}} \int_{t-\Delta t}^{t} \Delta\dot{m}_D\,dt \qquad (8)$$

$$p_{TR}(t) = p_{UE}(t-\Delta t) + \frac{p_{UE0}}{m_{DR0}} \int_{t-\Delta t}^{t} \Delta\dot{m}_D\,dt + \Delta p_{VUE} \qquad (9)$$

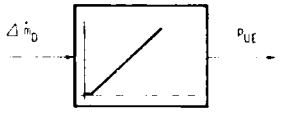

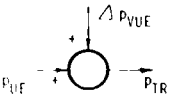

Figure 4. Blockdiagram BR2 *Figure 5. Addition point*

The boiler steam output $\dot{m}_{DKE}(t)$ has two components, one is the evaporation $\dot{m}_{DE}(t)$ from the energy input $\dot{Q}_{VD}$ minus the steam flow $\Delta\dot{m}_{DE}(t)$ needed to bring the feed water from ϑ_{EC} to saturation temperature ϑ_S. The second component is the steam generated by the change of the temperature level of the boiler masses (water m_W, steel m_{St}, brick work m_{MW}) by pressure changes in the steam drum.

Energy balance around the steam drum

$$\dot{m}_{DKE}(t) \cdot h'' = \dot{m}_{DE}(h'' - h') + \dot{m}_{SP} h_{EC} - \dot{Q}_{SV} \qquad (10)$$

$$\dot{m}_{DE}(t) = \frac{\dot{Q}_{KD}(t)}{r} \qquad (11)$$

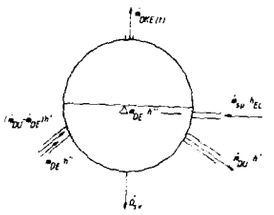

Figure 6. *Energy balance around steamdrum*

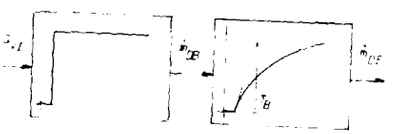

Figure 7. *Blockdiagrams BR 5*

To simplify the equations for the moment the feed water $\dot{m}_{SP}(t)$ is set to be equal to the steam output $\dot{m}_{DKE}(t)$. We then have

$$\Delta \dot{m}_{DE} = \dot{m}_{SP}\frac{h'-h_{EC}}{r} = \dot{m}_{DKE}(t)\frac{h'-h_{EC}}{r} \tag{12}$$

$$\dot{m}_{DKE}(t)h'' = \dot{m}_{DE}(h''-h') - \Delta\dot{m}_{DE}r + \dot{m}_{DKE}h' - \dot{Q}_{SV} \tag{13}$$

$$\dot{m}_{DKE}(t) = \dot{m}_{DE} - \Delta\dot{m}_{DE} - \frac{\dot{Q}_{SV}}{r} \tag{14}$$

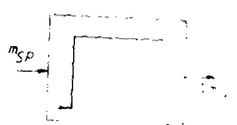

Figure 8. *Blockdiagram* $BR_{E2\,1-4}$

The time constant T_B in BR 5 depends on the steel mass of the evaporator tubes of the boiler.

When the temperature ϑ_S of the boiler changes due to changes of steam pressure p_{TR} in the upper boiler drum, then the energy level of the boiler mass is changed also

$$dQ_{SV} = (m_W c_{pW} + m_{ST} c_{pST} + m_{MW} c_{pMW})\, d\vartheta_S$$

$$= m_W c_{pW} d\vartheta_S \left(1 + \frac{m_{ST}}{m_W}\frac{c_{pST}}{c_{pW}} + \frac{m_{MW}}{m_W}\frac{c_{pMW}}{c_{pW}}\right) \qquad (15)$$

With

$$dh' = c_{pW}\, d\vartheta_S \; ; \quad C = 1 + \frac{m_{ST}}{m_W}\frac{c_{pST}}{c_{pW}} + \frac{m_{MW}}{m_W}\frac{c_{pMW}}{c_{pW}} \; , \quad q = \frac{dh'}{r\, dp_{TR}(t)}$$

equ. (15) becomes

$$dQ_{SV} = m_W \cdot c \cdot q \cdot r \cdot dp_{TR}(t)$$

and the steam m_{SV} released through self evaporation due to pressure changes is

$$m_{SV} = \frac{dQ_{SV}}{r} = m_W \cdot c \cdot q \; dp_{TR}(t) = A \cdot dp_{TR}(t) \qquad (16)$$

The steam flow is governed by equ. (17)

$$T_{SV} \cdot \ddot{m}_{SV} + \dot{m}_{SV} = A \frac{dp_{TR}(t)}{dt} \qquad (17)$$

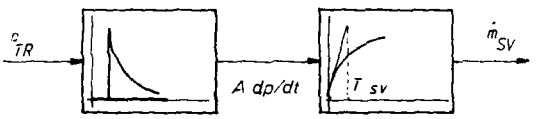

Figure 9. *Blockdiagram BR3*

The boiler output $\dot{m}_{DKE}(t)$ will increase with $\dot{m}_{SV}(t)$ when the steam pressure p_{TR} in the steam drum decreases and vice versa. With a constant drum pressure, $\dot{m}_{SV}(t)$ is zero.

Figure 10 shows the complete block diagram of the pressure system of the boiler incorporating equations (1) to (17).

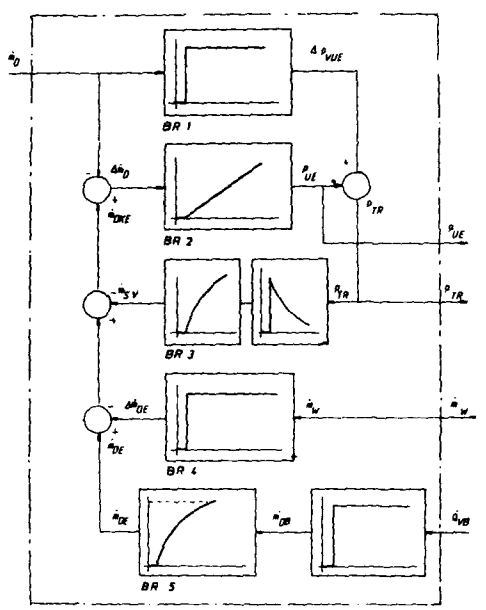

Figure 10. Blockdiagram pressure system

STEAM DRUM WATER LEVEL

Changes in the water level of the steam drum are caused by changes of the water valume V_{WKE} and the steam volume V_{DKE}

$$A_{TR}\frac{dh_{TR}}{dt} = -\frac{dV_{DKE}}{dt} + -\frac{dV_{WKE}}{dt} \qquad (18)$$

$$= v_D\frac{dm_{DKE}}{dt} + m_{DKE}\frac{dv_D}{dt} + v_W\frac{dm_{WKE}}{dt} + m_{WKE}\frac{dv_W}{dt}$$

$$\frac{dV_{WKE}}{dt} = (\dot{m}_{DKE} - \dot{m}_{DS})v_W + m_{WKE}\frac{dv_W}{dt} \qquad (19)$$

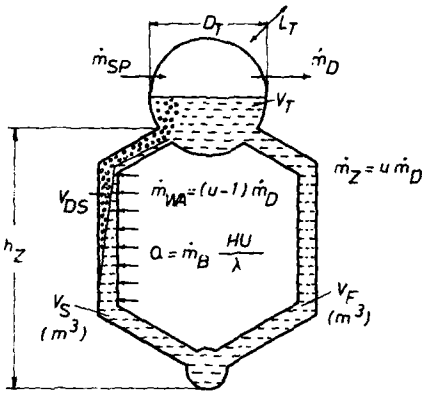

Figure 11. *Circulation*

The greatest influence on the steam volume V_{DKE} is the volume V_D of the steam $\dot{m}_D$ generated by $\dot{Q}_{VD}$. This can be calculated with the following equation

$$V_{DKE} = \dot{m}_{DKE} \frac{V_D}{W_D} (l_S C + l_T) \qquad (20)$$

(l_S = heated length of evaporator tubes, l_T equivalent length of not heated but steam carrying pipes and headers of the boiler.)

$$W_D^2 \cdot W_D = \dot{m}_{DKE} \cdot V_D \frac{\varrho_W - \varrho_D}{\varrho_W} \frac{2gh_Z}{SCI} \frac{l_S C + l_T}{V_S} \qquad (21)$$

h_Z = circulation height, SCI = overall resistance coefficient, reduced to the circulation velocity W_D, V_S = volume of evaporator tubes and steam carrying pipe system.)

$$W_{DW} = W_D - W_W = 0{,}61\left(\frac{A_D}{A_S}\right)^{0{,}2} \sqrt{\frac{\varrho_W - \varrho_D}{\varrho_W}} \qquad (22)$$

(A_D = steam filled area at the upper end of the evaporator tubes A_S = flow area of evaporator tubes, W_D = steam velocity at upper end of evaporator tubes, W_W = water velocity at same place.)

The above equations yield

$$h_{WUL}(t) = \frac{V_{DKE}(t)}{A_{TR}} = \frac{\dot{m}_{DKE}}{A_{TR}} k \qquad \textit{(Block SW1)} \qquad (23)$$

$$h_{WV}(t) = \frac{v_W}{A_{TR}} \int \Delta \dot{m}_{VV}\, dt \qquad \textit{(Block SW3)} \qquad (24)$$

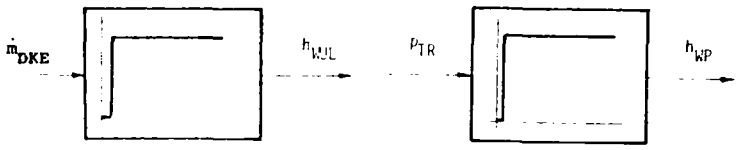

Figure 12. *SW1*

Figure 13. *SW2*

The influence of the boiler pressure on the water volume V_{WKE} of the boiler is covered by

$$dV_{WKE} = m_{WKE} \, dv_W(p) \tag{25}$$

$$h_{WP}(t) = h_{WP2} + \frac{m_{WKE}}{A_{TR}} \int_0^t dv_W(p) \tag{26}$$

$h_{W-1} = 0$ $\qquad$ $h_{WP}(t) = \frac{m_{WKE}}{A_{TR}} v_{W2} \left(\frac{v_W(t)}{v_{W2}} - 1 \right)$ $\qquad$ $v_W(t) = f(p_{TR})$ (Block SW2) $\qquad$ (27)

The complete water level equations is the sum of all the individual components.

$$h_W(t) = h_{WJL}(t) + h_{W-1}(t) + h_{WP}(t) \tag{28}$$

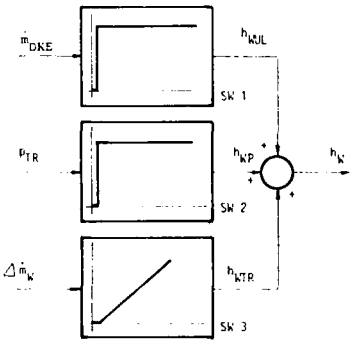

Figure 14. *Blockdiagram of boiler water level*

Superheater temperature system

In the superheater the supplied energy $\dot{Q}_{UE}(t)$ increases the steam temperature ϑ_S to $\vartheta_{NUE}(t)$. Load changes are followed by the superheater temperature $\vartheta_{NUE}(t)$ with a time lag T_Z, as the temperature of steel mass of the superheater tubes has follow the load change too.

$$T_Z \cdot \Delta\dot{\vartheta}_{UE}(t) + \Delta\vartheta_{UE}(t) = \frac{1}{\dot{m}_{DKE}(t)\, c_{pD}} \dot{Q}_{UE}(t) \qquad \text{(Block TE1)} \quad (29)$$

The steam temperature at the superheater outlet is controlled with water of the enthalpy h_{SP}, which is sprayed into the steam.

$$\dot{m}_{DKE}(t)\, c_{pD}\, \vartheta_{NUE} + \dot{m}_{WTE} h_{SP} = (\dot{m}_{DKE} + \dot{m}_{WTE}) c_{pD}\, \vartheta_{UENE} \qquad (30)$$

The amount of spray water $\dot{m}_{WTE}$ is proportional to the deviation of the real steam temperature ϑ_{NUE} from the desired steam temperature ϑ_{UENE}

$$\Delta\vartheta_{UENE} = \vartheta_{NUE}(t) - \vartheta_{UENE} = \frac{\dot{m}_{WTE}(t)}{\dot{m}_{DKE}(t) + \dot{m}_{WTE}(t)} \cdot \frac{\vartheta_{NUE}(t)\, c_{pD} - h_{SP}}{c_{pD}}$$

With consideration of the time delay T_Z this equation becomes

$$\dot{m}_{WTE} \frac{\vartheta_{NUE} c_p - h_{SP}}{\dot{m}_{DKE}(t) + \dot{m}_{WTE} c_{pD}} = T_Z\, \Delta\dot{\vartheta}_{UENE}(t) + \Delta\vartheta_{UENE}(t) \qquad \text{(Block TE2)} \quad (31)$$

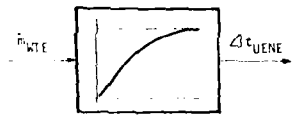

Figure 15. TE2

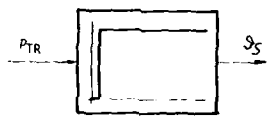

Figure 16. TE3

With the saturation temperature ϑ_S as a function of the boiler pressure p_{TR} the real superheater temperature is

$$\vartheta_{UE}(t) = \vartheta_S + \Delta\vartheta_{UE}(t) - \Delta\vartheta_{UENE}(t)$$

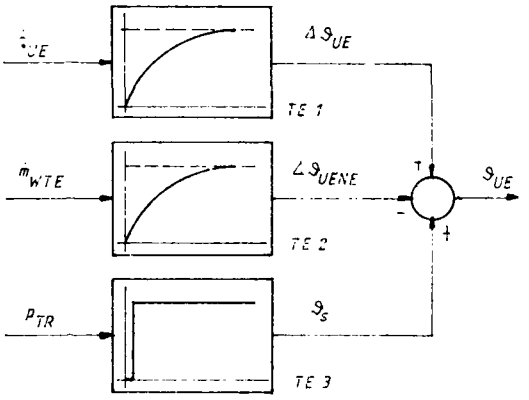

Figure 17. Block diagram of the superheater system.

MATHEMATICAL CONTROLLER MODELS

All controllers are described as normal PID controller

$$y = k_p\left(x_W + \frac{1}{T_N}\int x_W\,dt + T_V\,\dot{x}_W\right) \tag{32}$$

As the simulation usually begins with a state $y_A \neq 0$ at $t=0$ equ. 32 becomes

$$y = y_A + k_p\left(\Delta x_W + \frac{1}{T_N}\int_0^t \Delta x_W\,dt + T_V\,\dot{x}_W\right) \tag{33}$$

Integralpart

$$I = \int \Delta x_W\,dt = \frac{1}{2T_N}\left[\Delta x_W(t) + \Delta x_W(t-\Delta t)\right]\Delta t + \sum_{t=0}^{t-\Delta t}\Delta I \tag{34}$$

Derivativpart

$$D = x \cdot T_V = \frac{\Delta x_W(t) - \Delta x_W(t-\Delta t)}{\Delta t}\,T_V \tag{35}$$

The controller coefficients K_p, T_N and T_V are kept constant during a simulation.

All controller outputs are limited to either $y \geq 0$ and $I \geq 0$ or $y \leq 1$ and $I \leq 1$. If they are connected to a control valve their part of change $\dot{y}$ is also limited.

The water level set point h_{WS} should be adjusted proportional to the boiler load, to keep the boiler water m_{WKE} constant (see chapter 2.1). The best signal for the load proportional component of the water level set point is the velocity of the saturated steam W_{DP} in the main steam pipe.

$$h_{WS} = h_{WSO} + c \cdot W_{DP} \qquad (36)$$

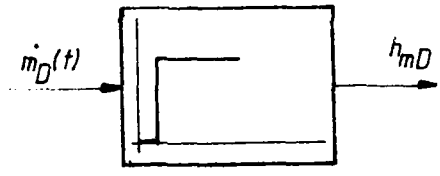

Figure 18. SWE

The feedwatwe controller is a rather simple positioner with the steam flow $\dot{m}_D(t)$ as a proportional part which governs the position of the feed water control valve.

CONTROL SYSTEMS

All control valves are assumed to have a linear characteristic.

For the main turbine all pressures (pressure before turbine or wheel pressure, bled point pressures) are proportional to the steam flow through the turbine.

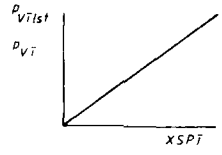

Figure 19.

Fig. 20 shows the complete pressure control cycle. (The air control system is not simulated. The air control has to follow the fuel system with certain restraints, so any improvement of the behaviour of the fuel valve will naturally benefit also the air control system).

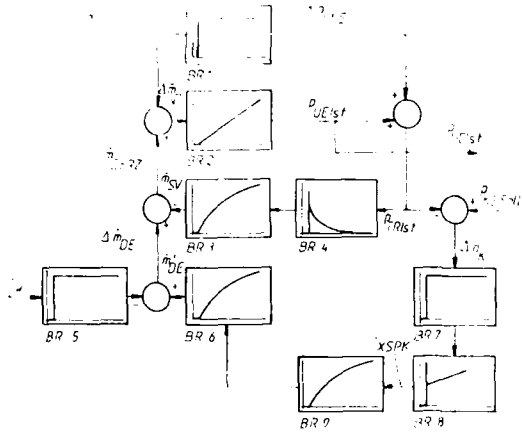

Fig 2(Pressure control cycle

The complete water level control-cycle is shown in figure 2".

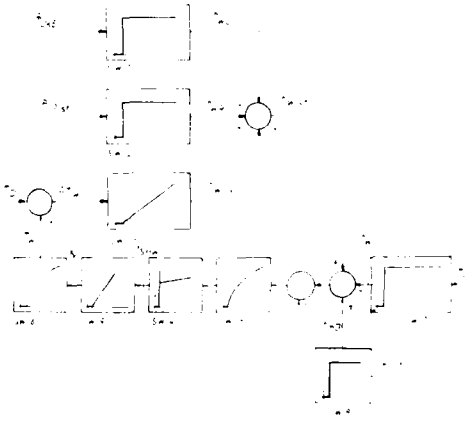

Fig. 2"

E2 1-12

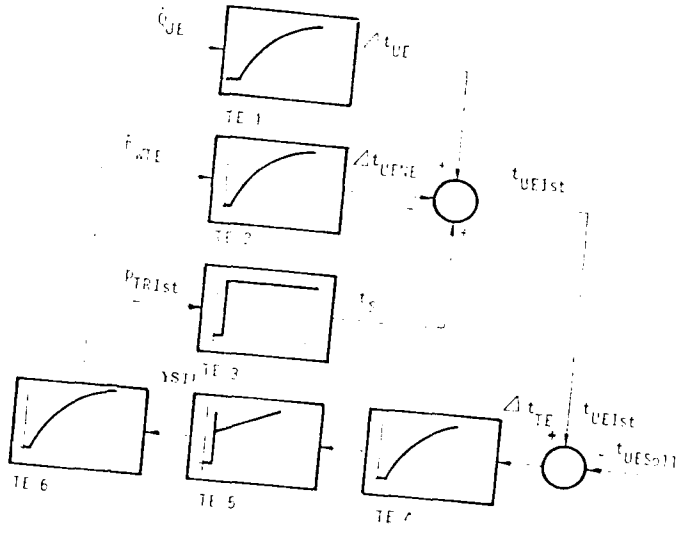

Figure 1-3. Superheater temperature control cycle

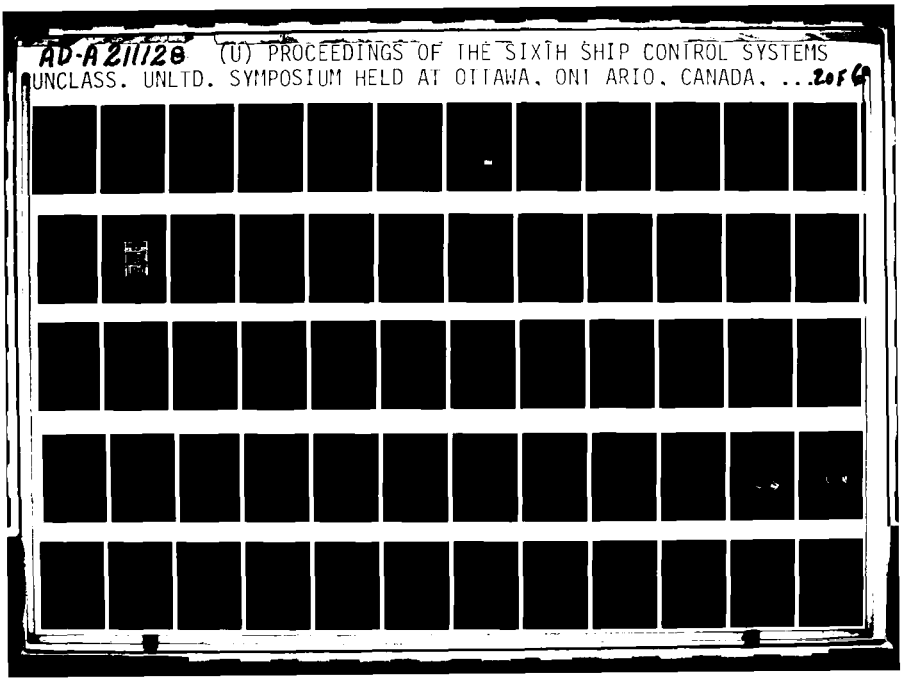

The signal flow diagram of the TTS "Liotina" with two cascaded controllers in the pressure control cycle is shown in Fig. 23.

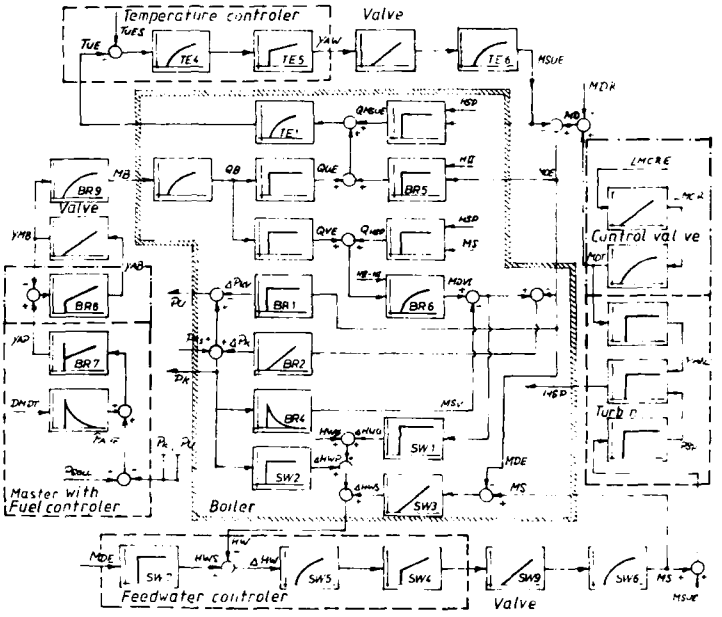

Figure 23. *Block Diagram Steam System TTS "LIOTINA"*

The basis of this system is an economiser heat balance with no high pressure feed water heaters. The energy distribution to the individual heating areas - economiser Q_{EC}; steam generation system Q_{VD}, superheater Q_{UE} - as a function of the boiler load is shown in Fig.24.

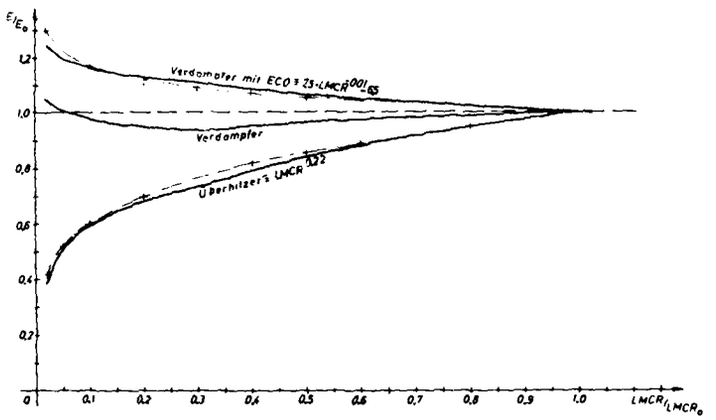

Figure 24. Energy distribution of boiler components

This curves are based on the Foster Wheeler boiler of "L" class ships of Deutsche Shell Tanker AG. Boilers for a high pressure feed water heating will have different energy distribution curves.

The influence of the boiler design is reflected in the cycle constants A, T_{SV} , T_D, which are rather high with this boiler which is of a very heavy design with lots of brickwork. The above constants have to be evaluated from the design drawings of the boiler.

EVALUATION OF THE TIME LAGS AND SIMULATION OF THE "LIOTINA" SYSTEM

In this case the different time lags of the steam system were evaluated from the tests run with the ship's plant. The time constants for the pressure control cycle were found to be as follows.

Time delay for fuel system	T_ϑ	= 1 s
Time lag of heat transfer in furnace	T_D	= 18,5 s
Time delay of self evaporation	T_{SV}	= 4,5 s

Figure 25 shows a comparison of values of the combustion system taken on board and evalues calculated with the computer model.

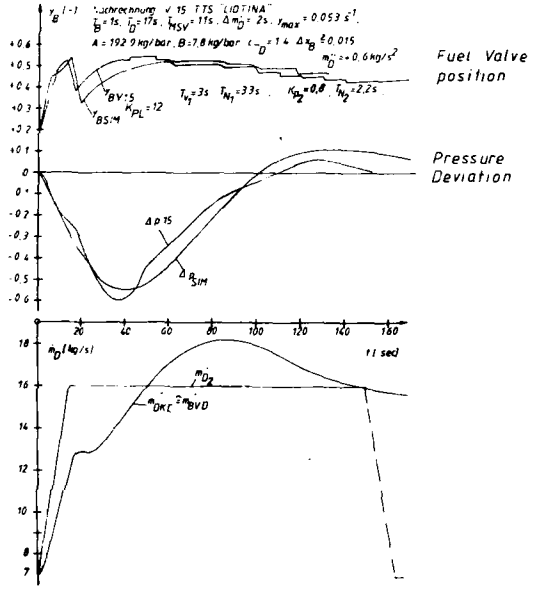

Figure 25. *Comparison Shipboard Test with Simulation*

The calculated values are near enough to the real values - especially the position of the fuel control valve - so that the model fulfils the expectations.

It is very interesting that the steam generation $\dot{m}_{DKE}$ follows the steam demand $\dot{m}_D$ with a delay time constant of T = 14,5 s. The difference between these two values is made up with self evaporation steam $\dot{m}_{SV}$ and with steam from the steam pipes $\dot{m}_{DR}$.

The combustion cycle was disconnected from the rest of the boiler system. This means $\dot{m}_{SP} = \dot{m}_{DKE}$, $\Delta\dot{m}_{DE}$ = const., $\dot{m}_{WTU}$ = const., Q_{VD}/Q_{VDO} = const.

The model is now very simple, it can be programmed for a HP 41 C.

Figure 26 shows this simplified signal flow diagram. With this system the same manœuvre /test 15/ was calculated.

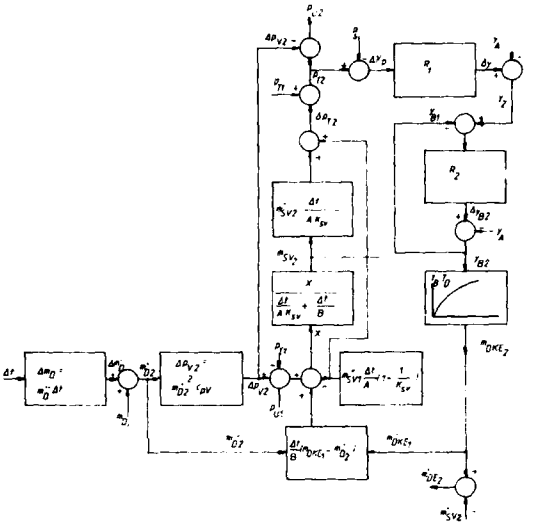

Figure 26. *Boiler pressure cycle*

Figure 27 shows that the deviations from the values calculated with

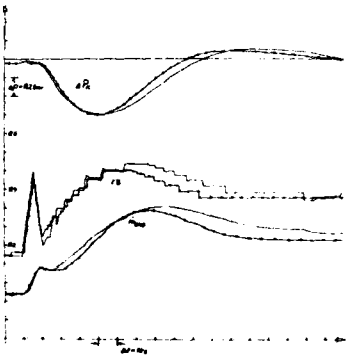

Figure 27. *Comparison*

the complete boiler model are so small, that further development work of t of the fuel control system can be done with the simple system, which is rather fast so that a lot of work can be done in a short time.

One change of the fuel control system is shown in Fig. 28, where the master controller is reduced to just a proportional controller for the pressure deviation. The steam load $\dot{m}_D$ is furnishing the proportional component to the fuel control valve and the derivation part is supplied by the difference of the desired load L_E and the real load L_I.

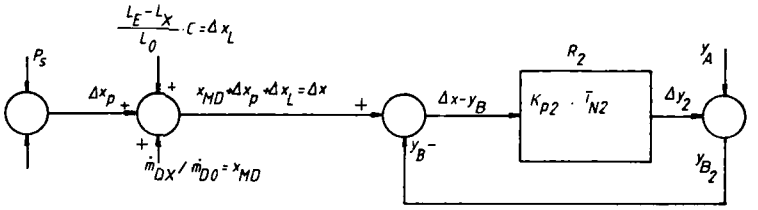

Figure 28.

With the"feed forward" signal the fuel valve moves smoother, the pressure deviations are much smaller and the time lag of the steam generation is nearly compensated. Fig. 29.

Other calculations showed, that the results become better, when the fuel valve moves as fast as possible into a position which is slightly higher than the final position, needed for this load change.

CONCLUSIONS

A computer model of a steam system allows fast evaluations of the optimum controller setting for a given control system. It can be used to developed control systems for different boiler system.

One of the great advantages of such a model is, that parts of it can be incorporated into a micro control computer on bord and that calculated signals, which cannot be measured (for instance the real steam generation $\dot{m}_{DKE}$) can be taken as control signals. This opens many new pathes to improved control systems.

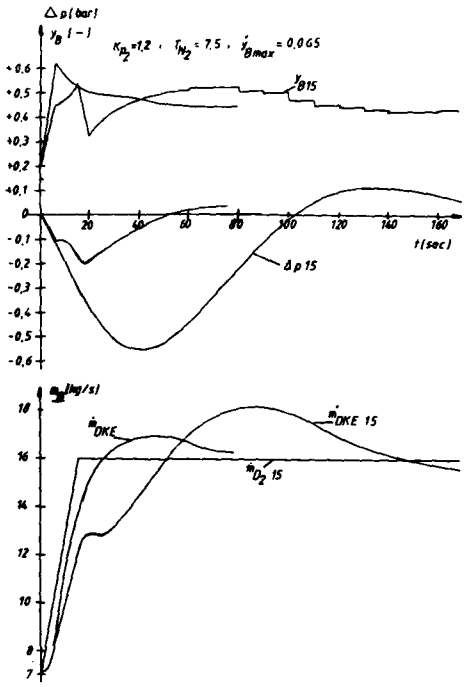

Figure 29. Simplified Boilerpressure-control system

PROPULSION CONTROL FOR HIGH SPECIFIC OUTPUT FOUR STROKE CYCLE DIRECT REVERSIBLE GEARED DIESEL ENGINES IN BULK CARRIERS

By:

R. J. Maddock, Fairbanks Morse Engine Division, Colt Ind.
Bryan Nakagawa, Woodward Governor Co.

ABSTRACT

Modern, medium speed, four stroke cycle, geared marine propulsion engines rely on exhaust gas driven turbo-compressors to achieve their high specific outputs. Use of such engines minimizes engine room space requirement and machinery costs, but requires more precise control than their lower rated ancestors. For the Direct Reversible Engine, the Crash Astern maneuver is the most demanding maneuver the engine will experience.

The exhaust gas driven turbo-compressor contributes little to the engine output at low rotational speeds. It is at such low speeds that direct reversible engines, using friction clutches, must be capable of bringing the propeller shaft speed quickly to synchronism with the running engine.

The microprocessor based Programmable Sequencer provides the flexibility to use techniques otherwise not practical. Closed-loop feedback control of the clutch is used to develop maximum available engine torque and apply it to the propeller shaft without stalling the engine, thereby keeping vessel headreach to a minimum.

Trial data is presented with comment on the problems of translating the planned performance into being, and with discussion of the problems that developed during implementation.

THE DIRECT REVERSING ENGINE

For about the first 40 years of their use as propulsion engines, the direct reversing diesel's natural characteristic of constant torque, instant load response, and short period overload capacity, provided excellent maneuvering power. Even as turbocharging boosted outputs by a third, from about 7.5 bars naturally aspirated, to 12 bars BMEP (Brake Mean Effective Pressure), engines were operated with sufficient excess air to retain the capability of rapidly accepting full load torque throughout their speed range.

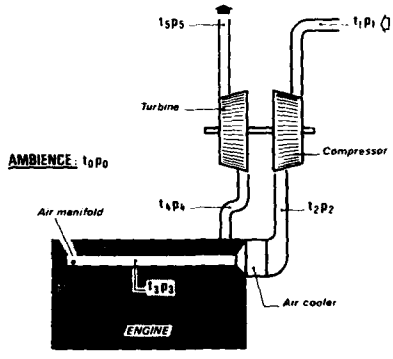

Figure 1. Diesel Engine Turbocharger Gas Flow Schematic

A study of the engine-turbocharger schematic shown in Figure 1 illustrates the gas flow mechanics which impose a systematic increase in engine response time as the boost ratio is increased. The turbine, driven by the hot exhaust gases, drives a compressor which in turn supplies the combustion air. Any load demand, requiring combustion air beyond that available at a given instant, can be satisfied only through a "boot-strap" process of generating more exhaust gas energy to supply more air. At steady-state speed, the engine operates with excess air, making the load increase sequence possible.

As specific power is increased to 15 bars BMEP, with a turbo-charger matched for optimum full power, full torque output is limited to speeds above approximately 2/3 rated RPM. Available torque at 40% speed is limited to about 65% of rated torque. For an engine rated at 19.2 bars, with optimum full power turbo-charger matching, rated torque is available only above about 85% of rated speed, and at 40% speed, torque available shrinks to about one-third of rated. While matching the turbo-charger for less than full RPM will broaden the speed range over which full torque is available, there will be a penalty of lower efficiency and higher peak pressure at full power. Also, within practical limits, little is gained at the lowest speeds. The engines, to which the subject Propulsion Control was fitted, were adjusted to deliver rated torque from 2/3 to full rated speed.

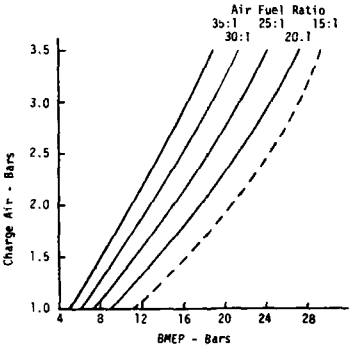

Figure 2. Air Charge Vs. BMEP

Figure 2 shows the BMEP realizable at a given charge air level for various air-fuel ratios. In steady state, an engine will run with an Air/Fuel ratio near 30:1. During a load increase an engine can be temporarily operated with 20:1 ratio. Significantly lower ratios are overfueling, producing black smoke and excessive exhaust gas temperatures. Below a ratio of 16:1, output will decrease. The chart is applicable to normal engine RPM, and does not account for the additional losses that occur at very low speeds. The decreased compression ratio, increased valve overlap and fuel delivery adjustments made for rated speed, full load operation all tend to reduce low speed capability of an engine.

With propeller torque, versus propeller RPM approximating a square law relationship, the torque absorbed (without opposing way on the vessel) at minimum propeller speed is less than 20%. The limitations described are therefore of interest only in engaging the clutch against full opposing vessel way, when backdriving torque from the propeller may reach over 75% of rated engine torque even at zero shaft speed.

Figure 3 shows the probable zones of maximum available low speed torques for a 19.2 and also a 14.8 bar BMEP engine, each superimposed on the third quadrant of a propeller map. The relative loss in capability, on the part of the high BMEP unit is dramatic. The maximum torque zones account for some variation in engine arrangement and adjustment. For a short time interval some undefined additional capacity may be temporarily available, but, there will be a significant delay in engine response to such demand.

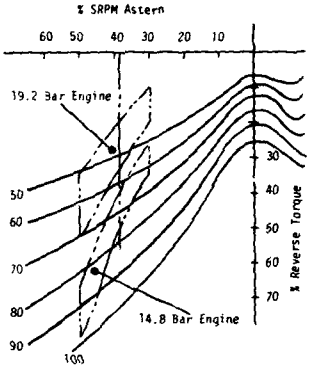

Figure 3. Third Quadrant Propeller Map with Engine Low Speed Available Torque

The propulsion control discussed, is in service on twin screw Integrated Tug-Barge tankers of 45000 dwt tons and 207 meter length overall, powered by two 520 RPM, 9100 BHP engines (19.2 bars BMEP). The ship is equipped with bridge control of the propulsion machinery and also equipped for unattended engine room operation. At 57000 tons displacement, there is a displacement/power ratio of 3.13 tons/BHP. For this class of vessel, if the vessel has attained a full speed steady velocity through the water and then shaft power is quickly reduced to zero, and a shaft brake applied, we find that one full minute after power is removed from the propeller shaft, there will still remain a velocity through the water equal to approximately 85% of the full speed velocity.

Recognizing the foregoing and based on general experience, it was assumed in the initial design stage that satisfactory control characteristics and vessel head reach would be achieved under "crash stop" conditions, if the propeller could be made to turn astern within two to three minutes after the command and movement of the remote control handle. The problem presented by the low torque characteristic at low engine speed of the highly turbo-charged engine and the slow rate of vessel speed decay, was far greater than that previously faced and resolved when 15 bar BMEP engines were used as main propulsion units.

CONTROL DESIGN

Open loop, pre-set engagement rates, of friction clutches do not reliably force the engine to a sustained maximum engine effort in reversing propeller rotation against backdriving torque generated by opposing vessel way. With the engine turning slowly, both it and the conventional mechanical/hydraulic governor respond sluggishly. Friction of the clutch face or drums varies also, and the initial conditions are unpredictable, all dictating a need for conservative load application rates and a limited slip time interval. Therefore the clutch engagement event is the area on which it was decided to focus efforts for improving the relative performance (when maneuvering) of engines having limited low speed lugging capability. The required control functions and devices selected were:

a) An engine fuel control (electronic governor) having precise pre-set speed references, and ability to limit fuel as a function of available combustion air.

b) A clutch with large heat-sink and heat rejection capability.

c) Regulation of clutch slipping torque in accordance with engine speed response.

d) Clutch protection by calculation of the slip work input.

e) Flexible implementation of the Propulsion Control Logic, Control Alarms and Station Transfer.

f) An approximation of vessel speed with a time/power integrator.

The Programmable Sequencer fit the requirements for a primary propulsion control element so well, that only minimal consideration was given to alternative construction. Also, a natural selection was an electronic fuel control having individual plug-in modules for each function.

Having the accurate speed reference setting and fuel rack limit (a), a dynamic clutch control could be programmed in the sequencer to regulate clutch torque for smooth continuous load application to the rack limit, and which would maintain speed control by continued regulation of clutch slipping torque. As the engine is kept operating at the limit of its combustion air supply, it forces a continued increase in this air supply by increased speed of the exhaust driven turbocharger. The larger the heat-sink capacity of the clutch (b), the longer this process could be maintained and in turn increase the torque generated by the engine. The process is terminated either by the propeller being brought to operating speed (and locked-up) or by the work input to the clutch reaching the limit of safe operation. Because there is no preset torque level, the process is self adapting to the engines condition at the moment, and would continue to extract the torque available from a crippled or deteriorated engine, or change in clutch friction coefficient.

The calculation of the heat input due to clutch slip, for each engagement, is also programmed into the sequencer. The set point or work input permitted before aborting the attempted engagement can be modified within limits by the operators. The clutch used has a heat sink capacity of more than 4 BTU's per horsepower rating of the engine. This is about twice the normal capacity for a friction clutch on a 500 RPM engine. It will typically permit slipping to be sustained for about 40 seconds, as compared to 10 to 15 seconds limit in a conventional installation. This is sufficient to reduce ahead way another 10% (of full speed) beyond the coast down curve alone.

SIMULATION MODEL

The block diagram of Figure 4 shows the interrelationships of elements modeled in the computer simulation. The purpose of this simulation study being primarily the validation of the dynamic control algorithms and coefficients, not every element shown in the block diagram needed to be modeled with detailed accuracy. While the governor is accurately modeled, the engine performance is merely a gain and time constant. The ship and propeller do not need detailed

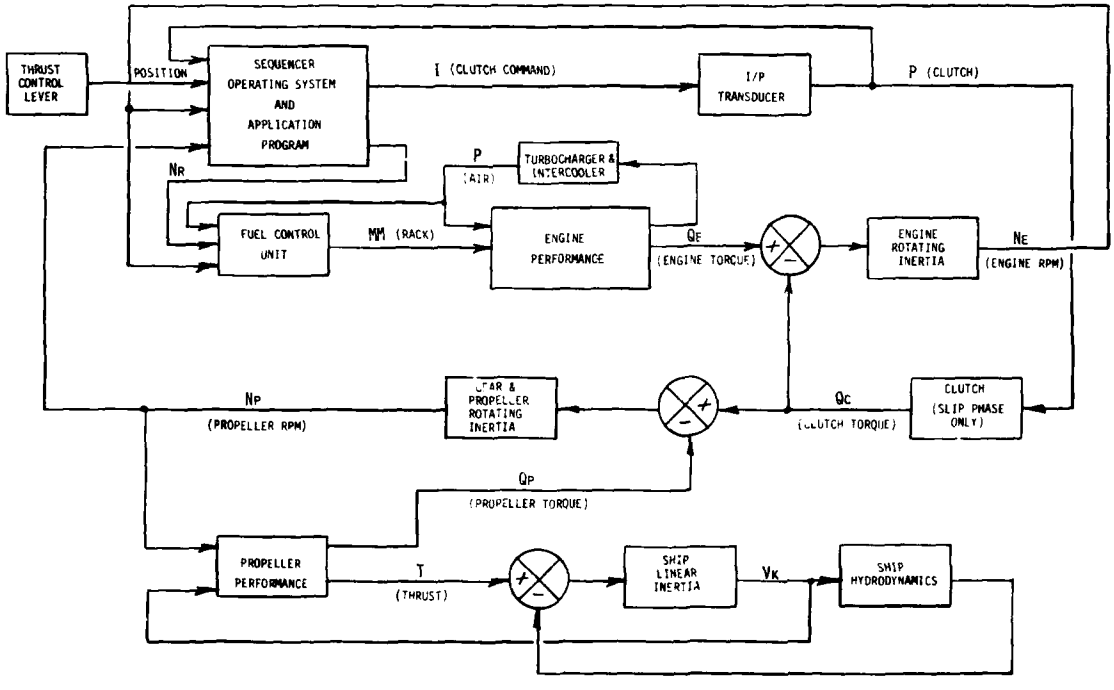

Figure 4. Propulsion Control - Signal Flow

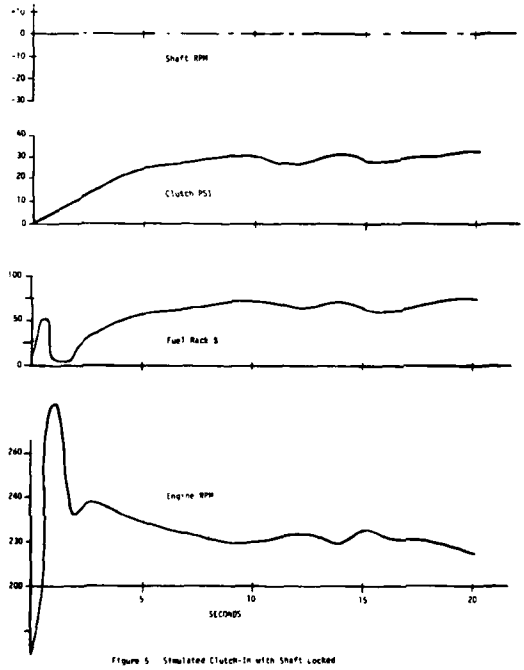

Figure 5 Simulated Clutch-In with Shaft Locked

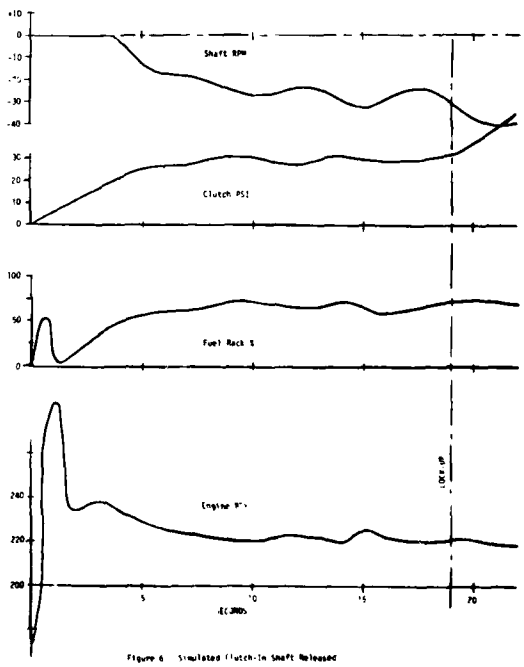

Figure 6 Simulated Clutch-In Shaft Released

modeling; the purpose was not to find the maximum ship's speed that could be used, but rather to extract the optimum effort from the engine without undue hazard to the clutch. The clutch control algorithm is modeled in detail; it is then directly duplicated in the microprocessor including the sampling rate. Only the "Crash Astern" maneuver was studied.

By selection of the speed droop, proportional and velocity error coefficients, and their ratio, both stability and engine loading rate are determined for the period of engine control by torque regulation. Figure 5 shows the calculated engine speed and shaft torque when the propeller shaft was locked. The importance of this exercise is the demonstration that the clutch could be slipped for about 25 seconds even under this most unfavorable velocity difference. Figure 6 shows the result of normal release of the shaft, engine speed and inflation rate are identical to the locked shaft case, up to shaft lock-up, since the loop is controlled from the driving side. The clutch slip work converted to heat is reduced by more than half; the average shaft speed being greater than half the equivalent mean engine RPM.

IMPLEMENTATION

For the twin screw ship application discussed, the propulsion control consisted of:

2	Programmable Sequencers
2	Electronic Fuel Controllers
2	Hydraulic Actuators
2	Combined Control Interface and Local Operating Panels
1	Central Control Panel with Thrust Control Levers
1	Bridge Control Panel with Thrust Control Levers

Figure 7 shows the Fuel Control units and Sequencers.

Fuel Control

The fuel control is primarily analog and accepts input signals of speed, manifold air pressure, and Thrust Control Lever position. A current signal, proportional to the desired fueling level, is output to the hydraulic actuator, to position the fuel rack on the engine. The hydraulic actuator, also contains a complete mechanical ballhead governor for backup, and for use when in the local control mode. The speed setting motor enables an operator to raise or lower the speed from the local control panel located near the engine.

Modular Packaging. The engine speed/fuel control is a modular package housing two functionally independent fuel controls in one chassis; one for each engine. It has been designed to fit in a standard 19 inch rack. Each module performs a single function closely associated with one of the engine parameters for ease of trouble-shooting. Occasionally, a module will have a second function if room can be found for the additional circuitry. Downtime is kept to a minimum by isolating the problem to a module and replacing it. The modules are of the plug-in type and easily replaced. LED indicators located on the front panels of each module aid in monitoring the status of the engine control. For instance, the speed control module pertains primarily to engine speed and the LED's indicate the status of: control, speed pickup failsafe, two speed switches, and an overspeed switch.

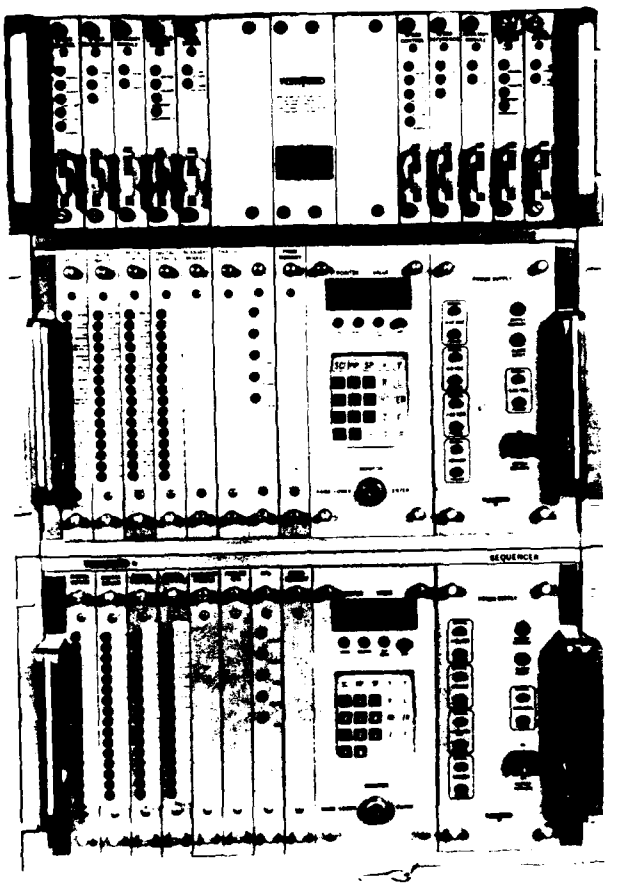

Figure 7: Fuel Control Units (top, Two Controls in One Chassis) and Microprocessor Based Programmable Sequencers

Module Selection. The versatile nature of the hardware enables the selection of the appropriate modules for the functions required. If more inputs and outputs are necessary, the size of the control system can be expanded. A primary reason for selecting this control unit is the Digital Speed Reference module. This module establishes a reference for the Speed Control module via raise, lower, or four other preset selections for a total of six adjustable setpoints. In addition, the reference can move, between set points, at four adjustable rates, including instant. Long term stability is achieved by establishing the speed references in digital circuitry.

To prevent overfueling, with resulting black smoke in the exhaust, a Manifold limiter module is used. This module sets a ceiling on the amount of fuel supplied to the engine as a function of air manifold pressure.

The control dynamics, and stability adjustments, are contained on the Speed Control module. In addition, a 4-20 ma readout, is used to send an accurate analog of engine speed to the sequencer.

The Auxiliary module buffers the speed setting signals from the Thrust Control Levers and compares them to the Digital Speed Reference output. It positions the Digital Speed Reference accordingly to make them match.

The Final Driver module produces the current signal to the actuator. It, also, generates an actuator failsafe if an overcurrent condition is detected.

Programmable Sequencers

At the heart of the system are the sequencers, one for each engine. These are also, modular packages that fit in a standard 19 inch rack. Although, no module has a close association with any of the engine parameters, such as in the engine fuel control, each module still performs a single function. The sequencer is capable of handling 32 digital inputs, 32 digital outputs, 4 analog inputs, and 4 analog outputs.

Most of the modules of the sequencer pertain to digital and analog Input/Output. All I/O, whether digital or analog, is buffered from the external world by special modules that communicate to the CPU (Central Processing Unit) module. The states of the digital inputs and outputs are displayed by LED indicators located on the front panels of their respective modules (see Figure 7).

SOFTWARE

The programming of the sequencers is done in a proprietary language developed especially for programming engine and gas turbine applications. It is capable of manipulating analog and digital I/O, timers, and sequences running concurrently--in addition to the many features of conventional programming languages. The software has been divided into two parts, the operating system and the application program.

Operating System

The operating system is a collection of programs that organize the microprocessor and its peripherals into a sequencer, controller,

and monitor. It serves as an environment in which the application programs run. This allows the application programmer to write programs without knowing the microprocessor and its peripherals in explicit detail.

Concurrency. An operating system feature is concurrency. This enables many sequences to run simultaneously, giving the effect that there is a processor for each sequence. When sequencing or controlling independent equipment this is especially useful.

Timers. A total of 48 precision timers are available. These timers can be used in timing events and flashing lights for annunciation.

Digital and Analog I/O. Discrete inputs and outputs are handled easily in conjunction with the appropriate buffer modules, keeping the Sequencer circuits isolated from external voltages. Analog (4-20 ma) inputs and outputs must, also, be accompanied by their respective buffer modules.

Self Checking Features. The sequencer periodically runs through seven routines to monitor its own health. Whenever a malfunction is detected, it can shut itself down and turn off all the digital outputs. These self checking features include: verifying the internal registers of the microprocessor; verifying the clock and related circuitry; checking the lithium battery, if installed; verifying designated areas of RAM; insuring that no more than 48 sequences are active at once; checking the discrete output modules; and insuring that interrupts are serviced within 15 milliseconds of the request.

Application Program

The application program accomplishes several tasks:

a) All necessary sequencing for starting and stopping the direct reversible engine, which includes checking start permissives.

b) All necessary sequencing for clutch engagement, which includes checking clutch permissives.

c) A proportional-velocity algorithm for clutch engagement.

d) A work computation algorithm for calculating the amount of heat generated by the clutch during the engagement process.

e) A timing integrator algorithm, for predicting the approximate velocity of the ship, used as a clutch permissive for crash asterns.

f) A control transfer sequence for transferring control from the engine room to the bridge and vice versa.

g) A monitor to observe the values of analog inputs and ouputs.

h) An emergency shutdown sequence.

Clutch Control. The dynamic control of clutch pressure during engagement of the pneumatic friction clutch is a primary reason for the design of this system. The control algorithm is implemented in

the application program. During clutch engagement the engine speed is sampled every 85 milliseconds, the speed error and its derivative calculated, and the required corrective action taken thru one of the analog output channels. Since it uses a speed reference lower than that of the fuel control by approximately the speed droop, the achieved result is a smooth increase in engine output power as the speed slows along the droop line.

Thrust Control Lever Monitoring. A sequence monitors the Thrust Control Levers for commands to: Standby Ahead, Clutch in Ahead, Standby Astern, Clutch in Astern, and Stop. As the Control Lever is moved to Standby Ahead, or Standby Astern, it detects the desired direction of rotation, shifts the cams if necessary, and starts the engine in the proper rotation. While in "Clutch in Ahead", or "Clutch in Astern", the Thrust Control Levers produce speed setting signal to the fuel control. Detecting instantaneous changes in the positions of the Thrust Control Levers is a matter of programming.

Setpoint Modification. Setpoints for timers and switchpoints can be modified within a limited range determined by the application program. The Keyboard Monitor module (see Figure 7) allows easy access to the setpoints for viewing, but a key is required for actual modification.

Programmability. The programming capability allowed us to "test and revise" the sequencing and monitoring for improved operation. Once the application program had been established, the RAM (Random Access Memory) module was replaced with a PROM (Programmable Read Only Memory) module which contained the program in permanent form.

Incomplete Sequencing. If for some reason, the start or clutch engage sequences cannot be completed, visual and audio alarms warn the operator. The sequencer will preclude inadvertent continuation of the sequence until the problem has been corrected and the sequence again initiated (reset). To reset the start or clutch engage sequences, overt action is required for obvious safety reasons. The operator must pull the Thrust Control Levers back one level. For instance, a clutch engagement failure would require the Thrust Control Levers to be moved for "Clutch in Ahead" to "Standby Ahead". A start failure would require the Thrust Control Levers to be moved from "Standby Ahead" to "Stop".

INSTALLATION AND TESTING

Three problems became apparent in the installation testing stage.

a) The high flow loss in the pneumatic system, between the electric/pneumatic transducer (I/P) and clutch, resulted in a phase loss that required reducing gain to an unsatisfactory level to stabilize.

b) The slow down, following an engine overspeed transient, on a direct "start and engage clutch" maneuver, as opposed to engagement to a running engine, caused the system to partially fill the clutch then dump completely and re-engage the shaft brake.

c) It was found possible to wipe the throttle directly thru from ahead to astern without triggering the proper shut down - reverse - restart sequence.

The first item resulted from inadequately sized piping in the pneumatic (local) control panel and ship's piping. To a practical extent, the control panel piping was rearranged and enlarged for increased flow, and to locate sensors for more realistic readings during active flow. Although flow head loss was still significant, the changes made resulted in a useable system. Further improvement was made by program changes to place limits on the controlling equation. An upper limit on pressure during slip, minimized the magnitude of flow pressure loss. A minimum clutch pressure limit was established at a level sufficient to avoid violent cycling and brake reengagement, but low enough to present little danger of engine stall. This change, together with a reduction in rate of speed reference change, and the piping modifications, corrected both deficiencies (a) and (b) above. Problem (c) was a program oversight, easily corrected by a program modification made during the initial trials.

SEA TRIAL TESTS

Figure 8 and Figure 9 are records of dynamic variables made on the ships sea trials. In each chart, (a) is the I/P clutch command in millamperes; (b) the actual inflation pressure of the clutch's pneumatic bladder in PSI; (c) the engine rack position in millimeters; (d) the engine RPM; and (e) the shaft RPM.

During clutch slip, the no-load engine speed reference is changed from 170 to 250 RPM (droop would bring full load back to near 200 RPM). This change is made slowly (in contrast to the simulation) as an accommodation to the limited flow of air to the clutch. Had this air flow capacity been greater, the engine loading could have been somewhat faster, reducing unproductive clutch slip at low torque. It is desirable, however, to increase the engine load gradually without wild rack fluctuation; all records show this was done.

Crash Astern

Figure 8 is the record of an aborted crash astern, it illustrates the ability of the dynamic clutch control to regulate engine speed by controlling torque across the clutch. Figure 8(c) shows the rack against a limit from about 18 seconds onward. With the rack blocked the speed governor could no longer regulate, yet, Figure 8(d) shows the speed stable as the result of clutch pressure 8(b) being adjusted for clutch torque exactly equal to the torque generated by the engine. Also note that, although the engine speed remained constant, the shaft speed, Figure 8(e), is very slowly increasing astern, in this instance due primarily to decreasing ship speed. It is probable that another 10 seconds would have brought the propeller speed to synchronism while still remaining well within the clutches heat-sink capacity. The maneuver was the first trial of a new ship, the limit settings were all unnecessarily restrictive, hence, the maneuver was cut off at 30 seconds. Adjustment of the manifold air pressure rack limit to its proper level resulted in a successful shaft reversal.

Figure 9 is the record of a successful "crash stop" from full power at maximum ship's draft. The movement of the Control Lever from Ahead to Astern, removes engine power, applies the shaft brake and declutches the engine from the reduction gear. As the engine approaches a stop, the camshafts are shifted astern, and the engine restarted in astern rotation. The engine remains at idle speed awaiting the astern timing integrator to be cleared (about 140 seconds from original control lever movement for the fully charged case).

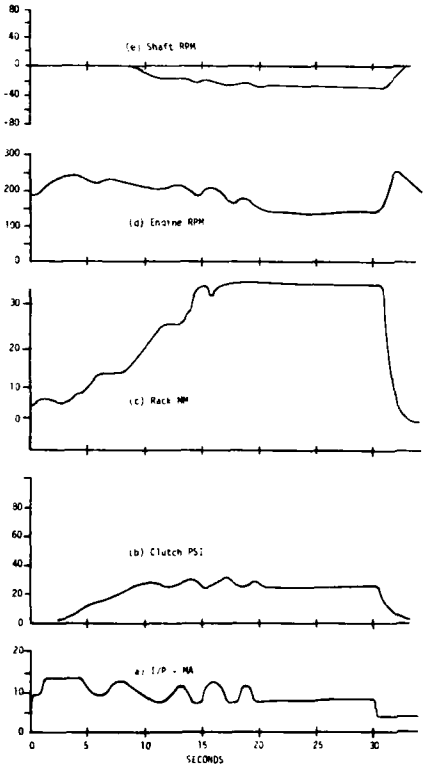

Figure 8. Crash Astern STBD
(Aborted at 30 seconds, Low Rack Limit)

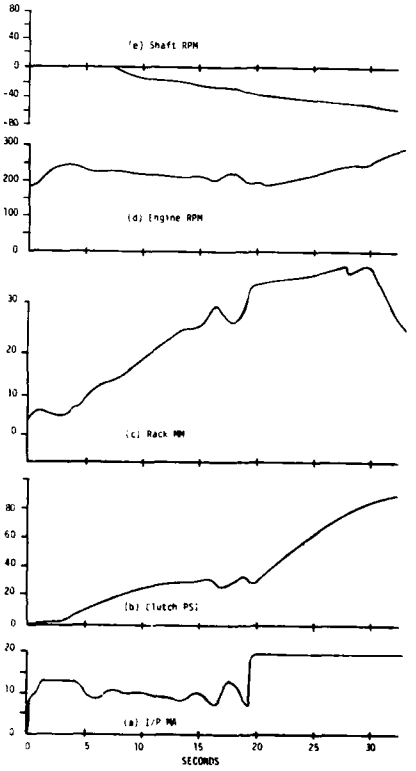

Figure 9. Crash Astern STBD Engine

When this "set point" is reached, clutch engagement starts, corresponding to time zero on Figures 8 and 9. The clutch command current is shown in Figure 9(a) and the resulting clutch air pressure on 9(b). The engine no load speed is changed from 170 to 250 RPM over a 5 second period also beginning at time zero. At this point, the clutch control attempts to regulate engine speed at 200 RPM while the speed control attempts to maintain a higher speed (200 to 250 depending on load). Both Figures 8(d) and 9(d) show the result to be a steady drop in speed between about 240 and 220 RPM as fuel rack (torque) increases, in the time range of 5 to 15 or 20 seconds on the charts. Figure 9(e) is the shaft or propeller speed.

"Raydist" position plots made every few seconds, during several trials similar to that recorded in Figure 9, measured stopping distance, projected along the original heading, and averaged slightly less than 5.5 ship lengths. The time to "Dead In Water", was between 380 and 420 seconds. The actual distance along the ships track is estimated to average 6.5 ship lengths.

While the dynamic clutch control proved capable of accomplishing the crash astern maneuver at slightly higher torque than had been expected, this gain was offset by the back driving propeller torque being higher than expected. The vessels are operating with a control set to attempt a clutch engagement in 140 seconds from command, with the timing integrator fully charged. To fully charge the integrator the vessel must remain at full power for about 20 minutes. For a ship at maximum draft, with a clean hull, the residual vessel speed at 140 seconds from full power is approximately 65 percent. After slipping the clutch for 30 seconds the speed is reduced another 15 to 20% making the clutch lock-up speed 45 to 50% of full vessel speed. While the chart of Fig. 3 shows this to be beyond the engines steady-state torque capacity, they have demonstrated an ability to reliably sustain rotational speed, until the vessel speed is further lowered, and the engine can regain RPM, a matter of only a few more seconds.

EVALUATION

It is probable that the improvement realized in a crash astern maneuver, with the dynamic clutch control as compared to more conventional handling, was on the order of two minutes in time and perhaps 1500 ft. in head reach. The compromise necessary for the restricted flow capacity, of the machinery space interface panel and piping to clutch, generated additional heat in the clutch plates that could have been more productively utilized. This was not an important factor in this instance, the clutch having adequate capacity.

The Programmable Sequencer worked well and its acceptance by operating personnel is not expected to be a problem. The ability to diagnose and correct problems should be improved with respect to a hard wired analog system on PC cards. While operating engineers, perhaps, do not have the understanding or feel of relating functions and control components that they develop with a moving parts pneumatic or relay panel electric control system, it is not felt that this will inhibit servicing. Service of the microprocessor will be by change out of PC cards. Diagnosis will be largely by interpretation of the LED I/O indicators on each card edge.

DYNAMIC PERFORMANCE SIMULATION ANALYSIS IN THE DESIGN OF A MARINE INTEGRATED NAVIGATION SYSTEM

by J.C. McMillan and Dr. D.F. Liang
Electromagnetics Section/Electronics Division
Defence Research Establishment Ottawa
Ottawa, K1A 0Z4

ABSTRACT

This paper presents some of the more significant initial results of recent design and simulation analysis of a Marine Integrated Navigation System. For this phase of the study, the integrated system consisted of a dead reckoning system (Gyrocompass and speed log) and an Omega receiver. Two integration algorithms were designed to combine the data from these instruments using the Kalman filter technique. Extensive simulation results presented consistently indicate the superior performance characteristics of both integration schemes (the 12-state and 16-state filters) over those of a similar system without integration.

1.0 INTRODUCTION

The Canadian Navy is planning to increase its usage of computer assisted command, control and data link communications systems. Increasing emphasis shall be placed on the improvement of navigation accuracy and position reporting efficiency. In addition, in order to successfully carry out joint operations with other ships spread over large areas of the sea, it becomes increasingly essential that each ship be provided with the ability to accurately determine its own position. The availability of powerful digital processors and more accurate sensors makes it possible to satisfy this requirement.

In view of this, a Marine Integrated Navigation System design and development study was undertaken by the Defence Research Establishment Ottawa at the initiation of the Director Marine and Electrical Engineering (DMEE). The aim is to ultimately develop a low-cost marine integrated navigation system, based on modern estimation theory, that will optionally combine diverse and uncorrelated navigation sensor information to provide "optimal" continuous estimates of ship position, speed and various other parameters of interest.

The ultimate marine integrated system may possibly be as depicted in Figure 1, where the navigation systems can be grouped into two general categories: radio navigation systems and dead reckoning systems. The dead reckoning systems are the inertial navigator, underwater log equipment, and gyrocompass. These systems are completely self-contained and provide velocity information which can be integrated to obtain the position information of the ship but they have a tendency to drift, slowly accumulating a large error over the course of a long sea voyage. On the other hand, the radio navigation systems have to rely upon radio signals transmitted from external sources (the beacon or transponder) and they are: Loran, Omega, Decca and Global Positioning System (GPS). These systems can provide direct position information output and the position errors will not grow with the passage of time, because errors are not accumulated through its integration routine.

Because of this complementary nature of the DR and the radio navigation systems, it has been common to manually "reset" the ships DR estimated position to the radio nav. aid position, typically once every few hours. This does not make optimal use of either set of measurements, since at each reset all previous DR and radio nav. aid measurements are essentially forgotten. Moreover, the present-day navigation systems without integration, among other things suffer from the deficiency of incongruity and are burdensome in operation. The success of the navigation operation is highly dependent upon the experience of the operator and the amount of time he can dedicate to this operation.

In order to take advantage of the short-term stability of the DR system and the long term stability of the radio navigation system one can apply the theory of optimal estimation, which can combine the measurements in such a way as to obtain a statistically "optimal" estimate of the ships position and velocity.

The automatic marine integrated system of Figure 1 not only improves operational accuracy, reliability, efficiency and versatility, but also provides performance congruity, CDP information, automatic navigation computation and continuous records of operation. Moreover, it can also provide automatic course alarm and the facility for automatic course correction and fire control integration.

1.1 Scope Of This Presentation

The instruments chosen for simulated integration at this initial phase of the study consist of gyrocompass, speed log and omega receiver. The integrated navigation system data processing algorithm was implemented on a general purpose computer, with "measurement" data numerically simulated, using statistical error models to represent the navigation sensor errors. This allows complete control of the testing conditions and facilitates the rapid and efficient evaluation of the filter performance characteristics for a large number of different test voyages. The alternative would require the costly and time consuming process of collecting vast amounts of real measurement data.

Results of the simulation analysis are of course dependent upon the validity of the models used to simulate the measurement data. Nevertheless the clear success of the initial simulation analysis justifies proceeding to the sea trial validation phase, using real measurements from a ship at sea. Further research is to be conducted to investigate the benefits of incorporating more sensors into this integration scheme, such as DECCA, LORAN-C, GPS etc..

This paper however is devoted to some of the initial results of this development project. In particular this paper examines the improvement in navigation accuracy and robustness that can be achieved by two different sensor integration schemes (a 16-state and a 12-state suboptimal Kalman filter) for a gyrocompass, speed log and omega receiver.

The primary criterion for evaluating these integration algorithm designs will be the absolute and relative accuracy of the position and velocity information obtained, under both normal and unusual error conditions. Another criterion will be the computational processing requirements in terms of execution time and core memory.

2.0 DEAD RECKONING AND OMEGA SIMULATIONS

True Position and Velocity

For the purpose of simulation, "true" velocity ($V_N V_E$) is generated according to

$$V_N = S \cos\theta + V_{NC}$$

$$V_E = S \sin\theta + V_{EC} \qquad (1)$$

where S and θ are the ships water speed and heading, and V_{NC}, V_{EC} are the ocean current components. The ships position (LAT,LONG)is determined by integrating this velocity, or in the discrete case by the update equation

$$\begin{bmatrix} LAT \\ LONG \end{bmatrix}_{t+\Delta t} = \begin{bmatrix} LAT \\ LONG \end{bmatrix}_t + \begin{bmatrix} V_N/R_N \\ V_E/R_E \cos(LAT) \end{bmatrix}_t \Delta t \qquad (2)$$

where R_N and R_E are the radii of curvature of the earth in the north and east direction (functions of position). This representation will be accurate if Δt is sufficiently small.

DR Position and Velocity

Simulation of the DR position estimate is based on these same equations (1) and (2) except that the ocean current is not known and the measured speed and heading are corrupted with drifting errors. Thus the DR position is found by

$$\begin{bmatrix} V_{N1} \\ V_{E1} \end{bmatrix} = \begin{bmatrix} (S + dS) \cos(\theta + d\theta) \\ (s + dS) \sin(\theta + d\theta) \end{bmatrix} \qquad (3)$$

$$\begin{bmatrix} LAT1 \\ LONG1 \end{bmatrix}_{t+\Delta t} = \begin{bmatrix} LAT1 \\ LONG1 \end{bmatrix}_t + \begin{bmatrix} V_{N1}/R_{N1} \\ V_{E1}/R_{E1} \cos(LAT1) \end{bmatrix}_t \Delta t \qquad (4)$$

Comparing equations 1 and 2 to equations 3 and 4, it can be seen that the dominant sources of error in the dead reckoning position and veloctiy estimates are the EM log speed error, the gyrocompass heading error, and the north and east components of the ocean current. Each of these four errors can be modeled by a first order Markov process, so that 4 error states are required to describe the DR error.

Since the ships latitude and longitude are the primary quantities of interest, 2 states are used to represent the error of the DR latitude and longitude. The filter estimates of these two error states can then be used to remove the error from the DR position estimate.

Omega Error Characteristics

Omega is an hyperbolic system that utilizes lines of position based on phase difference measurements from at least three transmitters. It operates in the 10 to 14 KHz band and, since each station has a

range of 13000 Km, only eight stations will be sufficient to provide world-wide coverage.

Changes in the ionospheric propagation characteristics cause anomalous variations in the Omega phase measurements. These errors can be partially compensated for by using skywave correction tables. However, there remain four major components of residual error. The statistical properties of this residual error have been studied in detail by various groups [1],[2] and it is generally agreed that when skywave correction tables have been used, the remaining phase error at the Omega receiver has an autocorrelation function of the form

$$\psi(\tau) = A^2 e^{-\tau/T_1} + B^2 e^{-\tau/T_2} + C^2 e^{-\tau/T_1} \cos(\omega\tau) \qquad (5)$$

where T_1 and T_2 are autocorrelation times, ω is the earth rate $(2\pi/24\ \text{hours})^{-1}$ and A,B and C are constants. This phase error can therefore be adequately described by the sum of three stochastic processes: two first order Markov processes and a periodic process with a period of 24 hours. Since the periodic process is second order, a total of four states are required to properly model each Omega phase error. Determining three different Omega lines of position (LOP) requires reception of Omega signals from 4 distinct stations. Therefore a total of 16 Omega error states are required to represent these Omega errors.

Thus the so called real world model in the simulation program requires a total of 22 error states.

3.0 KALMAN FILTER DESIGNS

The dynamics of the error state vector $\underline{X}$ is mathematically described by the system model

$$\dot{\underline{X}} = \underline{F}(\underline{X}) + \underline{W} \qquad (6)$$

where $\underline{W}$ is a zero-mean Gaussian white noise process. If equation (6) were written out in component form in full detail, it could be seen that the only non-linearity in the system model is due to gyrocompass heading error. Fortunately this error is relatively small, allowing a linear filter to be applied with some success by simply neglecting the heading error.

In fact there are many possible suboptimal filter models that could be derived from simplified world models. The problem is to determine which error states can be ignored to reduce the size of the filter (and hence the computational burden), without significantly degrading the performance. Preliminary results presented here demonstrate that the number of states can be reduced to 16, and even to 12, without significant degradation.

Table 1 lists the error states used for the real world model and for each of the suboptimal filter models. This real world model was used to generate measurement input data to both suboptimal filters for the purpose of performance evaluation and sensitivity analysis.

The general form of a discrete linear Kalman filter is summarized in Table 2 and Figure 2 [4].

DR Errors

Both suboptimal system models neglect the gyrocompass heading error and the speed log error. Partial compensation is achieved by increasing the expected ocean current error to absorb some of this unmodeled velocity error. These DR error states, together with the latitude and longitude errors ($d\lambda$, dL), propagate independently of the Omega errors, according to the linear state equation

$$\frac{d}{dt}\begin{bmatrix} d\lambda \\ dL \\ V_{NC} \\ V_{EC} \end{bmatrix} = \begin{bmatrix} 0 & 0 & 1 & 0 \\ 0 & 0 & 0 & 1 \\ 0 & 0 & -1/T_c & 0 \\ 0 & 0 & 0 & -1/T_c \end{bmatrix} \begin{bmatrix} d\lambda \\ dL \\ V_{NC} \\ V_{EC} \end{bmatrix} + \underline{W} \qquad (7)$$

where Tc is the ocean current correlation time.

Omega Error Model

Since an Omega line of position error is the difference between two independent phase errors, the statistical properties of the LOP error will be basically the same as that of a phase error. By modeling the three LOP errors instead of the four phase errors, the 16-state filter requires only 12 states to represent the Omega errors. The four Omega error states for each LOP error propagate according to

$$\frac{d}{dt}\begin{bmatrix} \text{BIAS} \\ \text{MARKOV} \\ \text{PERIODIC} \\ P_2 \end{bmatrix} = \begin{bmatrix} -1/T_1 & 0 & 0 & 0 \\ 0 & -1/T_2 & 0 & 0 \\ 0 & 0 & 0 & 1 \\ 0 & 0 & -\alpha^2 & -2/T_1 \end{bmatrix} \begin{bmatrix} \text{BIAS} \\ \text{MARKOV} \\ \text{PERIODIC} \\ P_2 \end{bmatrix} + \underline{W} \qquad (8)$$

where the driving noise $\underline{W}$ is the difference between two uncorrelated zero-mean Gaussion white noise processes; one for each Omega signal used to determine the LOP. P_2 is the extra state needed to model the periodic component of the error, T1 and T2 are the Markov process correlation times and α is a constant. Here the strongly correlated Markov process is referred to as a bias to distinguish it from the more weakly correlated one.

Equations (7) and (8) define the continuous state space model for the 16-state filter. The 12-state filter model used the same 4-state DR model but a smaller Omega model. Here phase errors from 4 Omega signals are modelled (rather than from 3 LOPs as in the 16-state filter). Two states are utilized to represent each of these phase errors, for a total of 8 Omega error states. This was accomplished by omitting the periodic states and adjusting the parameters of the weakly correlated Markov processes to maintain the correct mean values and correlation times. The phase error of each Omega signal is therefore modeled by the following two Markov processes

$$\frac{d}{dt}\begin{bmatrix} \text{BIAS} \\ \text{MARKOV} \end{bmatrix} = \begin{bmatrix} -1/T_1 & 0 \\ 0 & -1/T_3 \end{bmatrix} \begin{bmatrix} \text{BIAS} \\ \text{MARKOV} \end{bmatrix} + \underline{W} \qquad (9)$$

where T1 and T3 are the correlation time constants.

Measurements

The measurement model describes the relationship between the inputs to the Kalman filter, $\underline{Z}$, called measurements, and the state vector $\underline{X}$ that is to be determined from these inputs. For linear systems this is generally of the form

$$\underline{Z}(t) = H(t)\underline{X}(t) + \underline{V}(t) \qquad (10)$$

where $\underline{V}$ is the measurement noise and H(t) is the measurement matrix. The same measurement vector was chosen for each of the two filters. It consists of three elements, each of which is the difference between an LOP as measured by the Omega receiver and the corresponding LOP as calculated from the DR position estimate and the known locations of the Omega broadcasting stations. This measurement is related to the 16-state vector according to

$$\begin{bmatrix} Z_1 \\ Z_2 \\ Z_3 \end{bmatrix} = \begin{bmatrix} (\cos\Psi_{i1} - \cos\Psi_{j1}) & (\sin\Psi_{i1} - \sin\Psi_{j1}) & 0\ 0\ 1110\ 0000\ 0000 \\ (\cos\Psi_{i2} - \cos\Psi_{j2} & (\sin\Psi_{i2} - \sin\Psi_{j2}) & 0\ 0\ 0000\ 1110\ 0000 \\ (\cos\Psi_{i3} - \cos\Psi_{j3} & (\sin\Psi_{i3} - \sin\Psi_{j3}) & 0\ 0\ 0000\ 0000\ 1110 \end{bmatrix} \underline{X} + \underline{V} \qquad (11)$$

where the Ψs are the bearings from the ship to the Omega stations, and the LOP used in measurement Zk is defined by the phase difference between the signals from Omega stations ik and jk [3]. The measurement noise $\underline{V}$ is assumed to be zero mean Gaussian white noise with covariance matrix R.

The measurement equation for the 12-state filter is similar to (11) but is more dependent on the choice of Omega stations for the three LOPs. For example if LOPi uses station i and i + 1 then

$$\begin{bmatrix} Z_1 \\ Z_2 \\ Z_3 \end{bmatrix} = \begin{bmatrix} (\cos\Psi_2 - \cos\Psi_1) & (\sin\Psi_2 - \sin\Psi_1) & 0\ 0\ 11\ -1\text{-}1\ 0\ 0\ 0\ 0 \\ (\cos\Psi_3 - \cos\Psi_2) & (\sin\Psi_3 - \sin\Psi_2) & 0\ 0\ 00\ 1\ \ 1\text{-}1\text{-}1\ 0\ 0 \\ (\cos\Psi_4 - \cos\Psi_3) & (\sin\Psi_4 - \sin\Psi_3) & 0\ 0\ 00\ 0\ \ 0\ 1\ 1\text{-}1\text{-}1 \end{bmatrix} \underline{X} + \underline{V} \qquad (12)$$

Discrete Kalman Filter Implementation

Formulating the Kalman filters for implementation on a digital computer requires that the continuous state space models defined by equations (7),(8) and (9) be converted to the equivalent discrete models, of the form

$$\underline{X}(t_k) = \Phi(t_{k-1},t_k)\,\underline{X}(t_{k-1}) + \underline{W}(t_{k-1}) \qquad (13)$$

Here $\Phi(t_{k-1},t_k)$ is the transition matrix, and $\underline{W}$ is a white noise sequence with covariance matrix Q_k. After formulating the discrete equations and developing the necessary software, many computer simulations were run to simulate the true states $\underline{X}$ and measurements $\underline{Z}$. These measurements were then processed by both filters.

The simulated filter estimates $\hat{\underline{X}}$ were compared with the simulated "true" values $\underline{X}$ to determine the absolute accuracy of the two filters. These filter estimates were also compared to the estimates obtained by the conventional method of evaluating DR estimates and correcting with Omega resets at some fixed update interval.

Another criterion for evaluating these filters is the computational burden. The processing time required to implement these filters using the U-D factorization method is roughly proportional to the number of multiplications needed, which according to Bierman [5] varies as

$$n^2-n + (1.5n^2 + 5.5n)m$$

where n is the number of state variables and m is the number of measurements. Thus the 16 state filter should require 1.7 times more processing time than the 12 state filter.

4.0 SIMULATION RESULTS

In the previous section we described two Kalman filters for integrating the DR with the Omega radio navigational aid. Since it is difficult to theoretically compare the performance characteristics of these two filters with those of the same system without integration, it is necessary to conduct extensive numerical simulation and sensitivity analysis to provide meaningful comparisons.

Effects of Filter Update Rate

Table 3 shows the effects of filter update interval on the performance of the 16-state filter, the 12-state filter and the conventional system without integration. The filter update intervals selected are 5 minutes, 30 minutes and 4 hours. For each set of filter update interval, we have simulated two distinct voyages of 28 hours. From Table 3 it is apparent that the RMS radial position errors of both the 16-state and the 12-state filter are significantly smaller for smaller filter update intervals. But the performance accuracy of the conventional reset method does not improve even when the interval between Omega resets is shortened. This is to be expected because the performance accuracy of the reset technique is directly dependent upon the accuracy of the most recent Omega measurement, and not on the frequency of resets. The filters, however, can optimally incorporate all Omega measurement inputs to improve its overall system performance. Since a shorter filter update interval implies the availability of more abundant measurement inputs, this helps the filter to correct its estimates more frequently. Of course, there is a limit to the accuracy achievable by the filters as well, because higher filter updating rates require increased computational burden and also lead to numerical error growth. As seen from Table 3, the filtering update interval of 5 minutes not only provides significant performance improvement over that of the conventional reset techniques but also represents a practical and effective choice of filter update interval, since it does not impose excessive computational burden, nor does it cause noticeable numerical error growth. As a result of this, all subsequent simulation runs were carried out with this 5 minute filter update time interval.

Monte Carlo Simulation

To obtain a meaningful indication of the performance capability of these integration schemes, a large number of 28 hour voyages were simulated. Measurements were generated using the "real world" error model, and processed by both filter algorithms and the conventional reset algorithm. Some of the results are shown in Table 4 which lists the RMS position errors, in meters, for each voyage, and also lists the ratio by which the filter errors are smaller than the reset errors. This table clearly demonstrates the ability of both filters to consistantly produce a significantly more accurate position estimate than the conventional method; even though both filters processed exactly the same measurement inputs used by the conventional reset method. The ratio of the RMS radial position errors show that both filters reduce the position error by a factor of between 2 and 6. The overall improvement ratio for the RMS position error is approximately 4 to 1 for both filters.

Another result that was observed but not listed in this table, is that the position errors of both filters were less than 3 km. at all times during each of these simulation runs, whereas the error using the conventional method was at times greater than 12 km. This indicates that the "worst case" position error can also be effectively reduced by a factor of about 4 by implementing one of these filters.

Table 5 presents the RMS velocity errors of both the filters and the conventional reset technique, for simulated voyages identical to those of Table 4. Here the velocity errors are also consistantly smaller when either of the filters are used instead of the conventional reset method. However the range of improvement ratio for both filters is between 1.3 and 1.6, which is considerably smaller than the improvement achieved for position errors. This agrees well with theoretical expectation since Omega measurements only provide additional position information and therefore the synergistic integration of the DR and Omega can improve the accuracy of the position to a much greater extent than the velocity.

To further illustrate and compare the performance behaviour of the two filters with that of the conventional reset technique, typical simulation results are presented in Figure 3, where the radial position errors for one particular voyage are plotted. Statistically more reliable indication of the expected filter performance is obtained from the 12-voyage RMS averages, which are presented in Figure 4. From these it is obvious that the position error for the DR is the most severe and tends to grow with the passing of time; accumulating a position error of 15 km. for a journey of 28 hours. The position error for the conventional reset technique also has the same tendency to drift in the time interval between resets. When the reset is performed, the position error is corrected down to the 3-km. accuracy level of the Omega measurement. On the other hand, both filters consistently display stable error behaviour. Their position errors are bounded to about 1 km. and they do not display any time-dependent error growth characteristics after the first few hours of operation.

From Figure 4 it can also be observed that there is no significant difference between the performance of the 16-state and the 12-state filters. This is rather significant, since the 12-state filter is computationally 1.7 times more efficient than the

16-state filter, yet it can perform almost as well as the 16-state filter.

Sensitivity Analysis

In the previous subsection, all performance results presented were based upon numerical simulations that assumed perfect *a priori* knowledge of subsystem error characteristics and its operational environment. However, considering the variety of operational environments the naval vessels will encounter, it is impossible to use one error model representation to characterize all the true operational system error behaviour. Therefore it is important to systemtically examine the performance of these two filters under abnormal conditions, when there are serious discrepancies between the prior statistics assumed by the filters and the error characteristics of the true operational environment. For this, extensive sensitivity analysis was conducted to evaluate the performance of the conventional reset technique and both of the filters under abnormal conditions. Conditions used were such that each significant error source statistic was either increased or decreased by a factor of three, while all other error statistics remained unchanged at their normal values.

The results of this study are presented in Table 6, where for brevity each position error represents the RMS over two simulated runs. It is apparent that both filters respond in a very similar manner to each of the abnormal conditions. The improvement ratio of the filter position errors over those of the conventional reset method is within the range of 3.1 to 6.3 under all of these conditions. It should be noted that the absolute error of the filter position estimates was most seriously degraded when the Omega phase error was three times larger than the assumed nominal value. Here the RMS position errors of the filters and the conventional reset are 2,930. meters for the 16-state filter, 3,289. meters for the 12-state filter and 10,428. meters for reset.

For this worst case under abnormal conditions, the simulation results in terms of position errors versus time are illustrated in Figure 5. Here it should be kept in mind that not only does this represent the use of Omega measurements three times less accurate than normal, but also that the filters were designed using nominal error parameters. Furthermore, even though there is such a discrepancy between the error models used to generate the abnormal measurements and the nominal error model used to design the filters, both filters remained amazingly stable and are consistently superior to the conventional reset method over a very broad range of possible operational error conditions.

5.0 CONCLUSIONS

In this initial design and simulation study, we have briefly discussed the advantages of synergistic integration of various navigation sensors. In particular, two integration schemes based on modern estimation techniques were designed to integrate a dead reckoning system and an Omega receiver. Extensive numerical simulation and sensitivity analysis work was conducted to compare the performance of these two filters against that of the dead reckoning and the conventional reset approaches.

Using the conventional method of periodically reseting the DR position estimate to the Omega position, the RMS position error was found to be 4,488 meters, under normal conditions. With 5 minute filter update intervals, the implementation of 16 and 12-state filters are shown to be capable of reducing this RMS position error to 1,181 meters and 1,213 meters respectively, which is a very significant improvement. Relative improvement ratios of these filter position accuracies are therefore 3.8 and 3.7 respectively.

Both filters also improve the velocity accuracy, reducing the RMS velocity error from .6m/sec. to .4m/sec. under normal conditions. Furthermore the improvement in position accuracy was seen to persist under all conditions tested, even when the modelling mismatch was rather serious. The robustness and stability of both filters are some of the essential characteristics that can help to ensure the success of naval operations in a great variety of operational environments.

The extensive simulation results also indicate that a computationally more efficient 12-state filter performs virtually as well as the larger 16-state filter. The implementation of this 12-state filter, at a 5 minute filter update rate, can easily be carried out in a medium-speed microprocessor. The real-time implementation of this integration scheme and its sea-trial validation is part of the follow-up activities of this project.

ACKNOWLEDGEMENTS

The authors wish to thank DMEE-7 and DMRS-4 for their support and encouragement in this development project. Thanks are also due to Professor W.S. Widnall of M.I.T., U.S.A. for his valuable suggestions.

REFERENCES

(1) The Analytic Sciences Corporation, "Models For Aided Inertial Navigation System Sensor Errors", TASC Report No. 312-3, 1975.

(2) Duckenfield, M.J., Marsh, J. and Milbourn, A.J.,"Studies in Integrated Navigation Systems", Brunel University, Uxbridge, Middlesex, 1979.

(3) McMillan, J.C., "A Kalman Filter for Marine Navigation", M. Phil. thesis, U. of Waterloo, Waterloo, Ontario, 1980.

(4) Gelb, A., Applied Optimal Estimation, "The M.I.T. Press, Cambridge, Massachusetts, 1974

(5) Bierman, G.J., Factorization Methods for Discrete Sequential Estimation, Academic Press, New York, 1977

Figure 1. Marine Integrated Navigation System

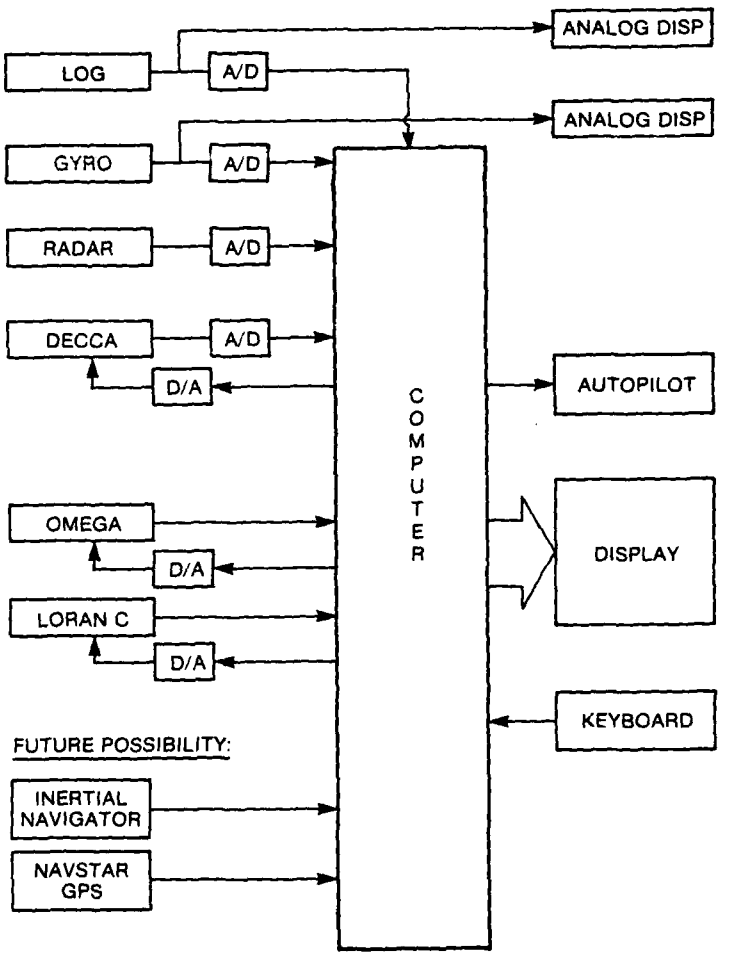

TABLE 1: SYSTEM ERROR STATES

ERROR SOURCE	ERROR STATES		
	REAL WORLD	16-STATE FILTER	12-STATE FILTER
GYROCOMPASS	1	2	2
EM LOG	1		
OCEAN CURRENT	2		
DR POSITION	2	2	2
OMEGA PHASE PROPAGATION			
BIAS	4	3	4
MARKOV	4	3	4
PERIODIC	8	6	
TOTAL NO. OF STATES	22	16	12

Table 2. Discrete Kalman Filter Equations

Assumptions

System Model	$x_k = \phi_{k-1}x_{k-1} + w_{k-1}$ $\quad w_k \sim N(0,Q_k)$
Measurement Model	$z_k = H_k x_k + v_k$ $\quad v_k \sim N(0,R_k)$
Initial Conditions	$\hat{x}_o = E\{x_o\}$ $\quad P_o = E\{(\hat{x}_o - x_o)(\hat{x}_o - x_o)^T\}$
White Noise	$E\{v_j v_k^T\} = 0$ $\quad E\{w_j w_k^T\} = 0$ for all $j \neq k$
Independence	$E\{w_j v_k^T\} = E\{x_o v_k^T\}$ $\quad E\{\hat{x}_o v_k^T\} = 0$ for all j,k
	P_k is positive definite for all k

Recursion Formulae

Propagation	$\hat{x}_k(-) \quad \phi_{k-1}\hat{x}_{k-1}$
	$P_k(-) = \phi_{k-1}P_{k-1}\phi_{k-1}^T + Q_{k-1}$
Filtering	$\hat{x}_k = \hat{x}_k(-) + K_k[z_k - H_k\hat{x}_k(-)]$
Error Covariance	$P_k = [I - K_k H_k]P_k(-)[I-K_k H_k]^T + K_k R K_k^T$
Kalman Gain	$K_k = P_k(-)\, H_k^T\, [H_k P_k(-)\, H_k^T + R_k]^{-1}$

Figure 2. Block Diagram for Kalman Filter Integrating Dead-Reckoning System and Omega Receiver

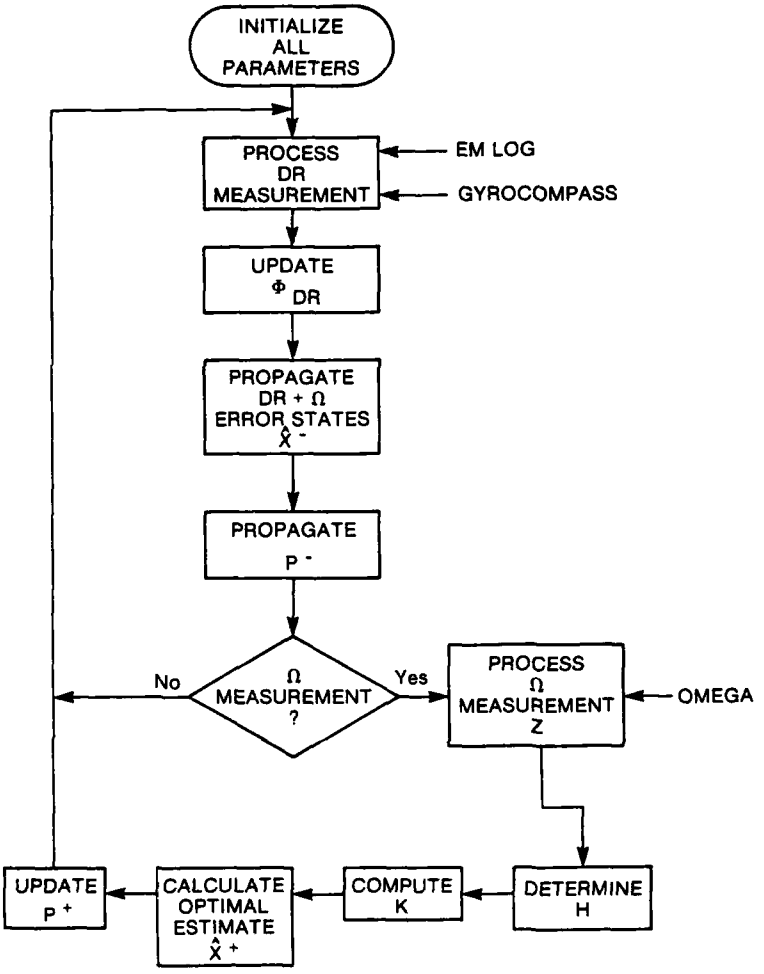

Table 3. Effect of Filter Updating Rate On Position Error.

FILTER UPDATE INTERVAL	VOYAGE NUMBER	RMS POSITION ERROR (METERS)				
		RESET	16-STATE FILTER		12-STATE FILTER	
		RMS ERROR	RMS ERROR	IMPRV'T RATIO	RMS ERROR	IMPRV'T RATIO
5 MIN.	3	5,018.	1,148.		1,106	
	4	2,295.	1,041.		1,180	
	RMS	3,902.	1,096.	3.6	1,144	3.4
30 MIN.	3	4,834.	1,485.		1,247.	
	4	2,372.	1,484.		1,370.	
	RMS	3,807.	1,485.	2.6	1,310.	2.9
4 HRS.	3	4,356.	4,472.		4,227.	
	4	3,842.	3,115.		2,965.	
	RMS	4,107.	3,854.	1.1	3,651.	1.1

Table 4. RMS Radial Position Errors (METERS)

VOYAGE NUMBER	RESET	16-STATE FILTER		12-STATE FILTER	
	RMS ERROR	RMS ERROR	IMPROVEMENT RATIO	RMS ERROR	IMPROVEMENT RATIO
1	3,996	1,107	3.9	985	4.1
2	5,083	1,020	5.0	1,235	4.1
3	4,356	1,148	3.8	1,106	3.9
4	3,842	1,041	3.7	1,180	3.3
5	3,627	1,438	2.5	1,205	3.0
6	4,030	1,307	3.1	1,375	2.9
7	2,841	1,359	2.1	1,290	2.2
8	3,645	1,303	2.8	1,253	2.9
9	5,093	1,404	3.6	1,556	3.3
10	7,152	1,206	5.9	1,342	5.3
11	5,029	860	5.9	1,031	4.9
12	3,607	883	4.1	822	4.4
WORST CASE	7,152	1,438		1,556	
TOTAL	4,488	1,181	3.8	1,213	3.7

Table 5. RMS Velocity Errors (Meters/Second)

VOYAGE NUMBER	RESET	16-STATE FILTER		12-STATE FILTER	
	RMS ERROR	RMS ERROR	IMPROVEMENT RATIO	RMS ERROR	IMPROVEMENT RATIO
1	.6507	.4018	1.62	.3984	1.63
2	.6033	.4062	1.49	.4072	1.48
3	.6077	.4012	1.51	.4021	1.51
4	.5817	.3977	1.46	.3940	1.48
5	.5965	.3912	1.52	.3989	1.50
6	.5631	.4250	1.32	.4166	1.35
7	.5000	.3980	1.26	.3901	1.28
8	.6023	.4237	1.42	.4209	1.43
9	.5332	.3943	1.35	.3921	1.36
10	.5298	.3972	1.33	.3908	1.36
11	.5725	.3989	1.44	.3909	1.46
12	.6102	.4179	1.46	.4160	1.47
WORST CASE	.6507	.4250		.4209	
TOTAL RMS	.5806	.4046	1.43	.4016	1.45

Figure 3. TYPICAL RADIAL ERRORS UNDER NORMAL CONDITIONS

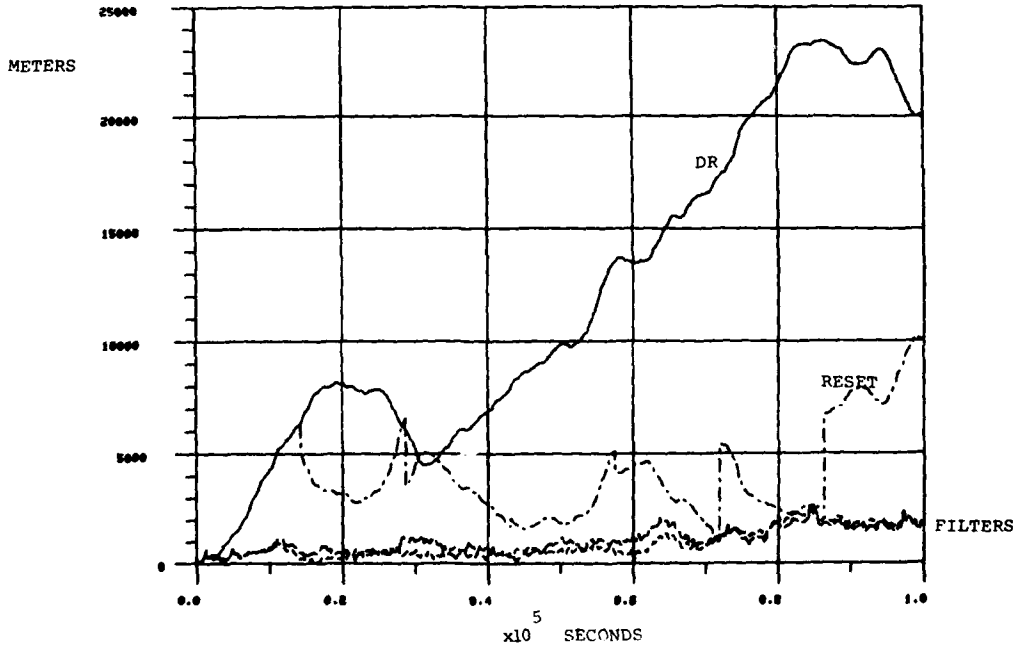

Figure 4. RMS RADIAL ERRORS UNDER NORMAL CONDITIONS

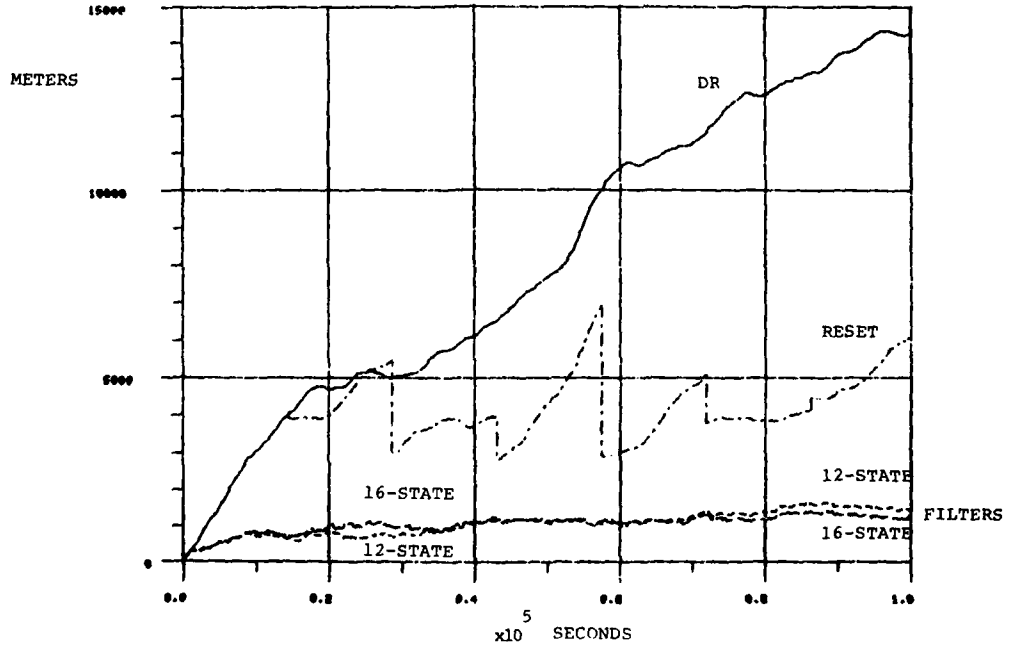

Table 6. Abnormal Conditions, RMS Position Errors

ERROR CONDITION	RESET	16-STATE FILTER		12-STATE FILTER	
	RMS ERROR	RMS ERROR	IMPROVE. RATIO	RMS ERROR	IMPROVE. RATIO
NORMAL CONDITION	4,107	1,096	3.7	1,144	3.6
DR VELOCITY ERROR					
LARGE*	8,309	1,670	5.0	1,319	6.3
SMALL+	3,470	1,016	3.4	1,102	3.1
MEASUREMENT NOISE					
LARGE*	4,037	1,253	3.2	1,213	3.3
SMALL+	4,103	1,063	3.9	1,133	3.6
OMEGA PHASE ERROR					
LARGE*	10,428	2,930	3.6	3,289	3.2
SMALL+	2,762	590	4.7	463	6.0
DR CORR. TIME					
LARGE*	4,206	1,224	3.4	1,187	3.5
SMALL+	3,845	1,037	3.7	1,122	3.4

* 3 TIMES NORMAL

+ 1/3 TIMES NORMAL

Figure 5. RADIAL ERRORS UNDER WORST ABNORMAL CONDITIONS

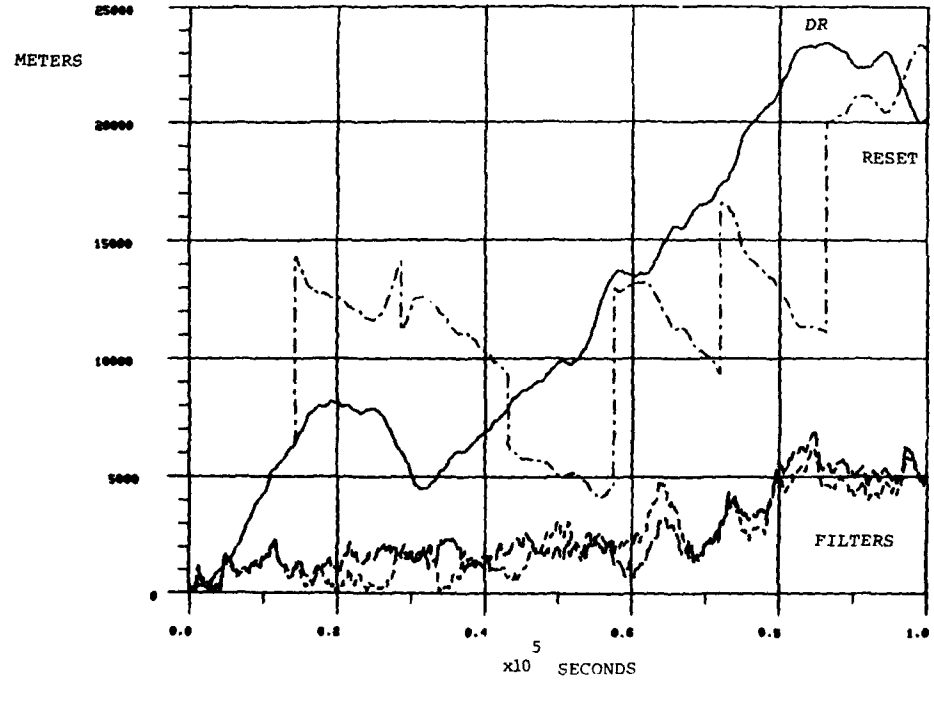

LOW VISIBILITY APPROACHES TO AN OFFSHORE DEEPWATER PORT: A SIMULATOR STUDY OF BEHAVIORAL FACTORS IN SHIP CONTROL

John S. Gardenier, D.B.A., U.S. Coast Guard*
Roger C. Cook, Ship Analytics, Inc.
Richard B. Cooper, Ship Analytics, Inc.

ABSTRACT

This paper reports specific results of a study of approaches to the Louisiana Offshore Oil Port (LOOP). More generally, it adds to the evidence that ship simulator behavioral studies are a valuable addition to other evaluative techniques in ship control systems engineering.

Congress specifically directed research into a broad range of issues regarding offshore port operations relating to the Deepwater Port Act of 1974. Some of those studies involved ship navigation and control. The study reported here was a simulator experiment in which twelve master-mate teams faced various port approach problems with different on-ship and off-ship navigation aids. Four of the twelve had received "team training" or "bridge management training;" eight had not. All teams were current VLCC personnel, many with experience in the Gulf of Mexico.

Three types of output were generated. Track plots of all runs can be interpreted directly to reveal differences in strategy and overall success or failure. In addition, where sufficient consistent data were obtained, statistical results are available regarding rudder and engine orders, fix frequencies, track deviations, and closest points of approach (CPAs) to obstacles or other vessels. Finally, subjective opinions were expressed by the mariners both on a debriefing form and by spontaneous comments.

The "bottom line" result for the problem directly at hand was that all teams solved all approach problems successfully, in that no collisions, rammings or groundings occurred. Still, near misses and some apparent temporary disorientation show room for improvement. Minor changes to the navigational approach system were recommended for consideration. A very interesting finding, but one which limited our ability to analyze all factors statistically, was a distinct variability of strategies in solving each problem. Two scenarios revealed a dominant strategy selected by the majority of crews, with the minority (one quarter to one third) splitting into equal subgroups which took distinctly different strategies from the majority and from each other.

The value of on-ship and off-ship aids varies, as would be expected, with the scenario, the approach strategy selected, and the training of the team. The behavioral effects of control aids,

*Facts and opinions stated in this paper are the sole responsibility of the authors; this paper does not represent official positions or policies of the U.S. Coast Guard.

therefore, are too variable and complex to evaluate in a practical sense. It is apparent that any evaluation which addresses only the mathematical and engineering aspects of equipment, displays, or controllers will fall short of predicting real safety value.

INTRODUCTION

On April 25, 1981, Captain Berna brought the loaded 274,347 ton tanker, TEXACO CARIBBEAN, into the Louisiana Offshore Oil Port (LOOP) from Ras Tanura, Saudi Arabia. He became the first very large crude carrier (VLCC) master to bring a revenue vessel into a United States off-shore deepwater port. Captain Berna may have rehearsed the approach in his mind many times, and although constrained by a variety of parameters, he was the master of his ship with relatively free choice of his actions. The approach was not unusually difficult or eventful and yet it was the first; soon to be followed by hundreds of others, none which will be identical to Captain Berna's and many which will be very difficult. A recent innovative application of simulator research by the United States Coast Guard, previewed Captain Berna's and other approaches. Most will be predictably conventional and safe. The research method employed for this prediction, however, also indicated that within the lifetime of the port there would be many different strategies used by VLCC masters. Many of the approaches would not be so conventional and some would not be so safe. The simulation further indicated why the different approaches will occur and what, if necessary, can be done to prevent them.

This use of simulation techniques not only provided design criteria for offshore and near-shore deepwater ports, but demonstrated the ability of simulators to predict and evaluate human behavior over a broad spectrum of ship control tasks. The same research technique can define (1) how various mariners will react to given circumstances, (2) what ship control behavior will represent the norm and what will be exceptions, (3) what factors influence ship control behavior, and (4) how those factors can be changed to produce a more desirable behavior. The experiment described herein provides evidence that behavioral studies are beneficial for ship control and port systems engineering, and that the most cost-effective tool for these studies is the dynamic ship simulator.

BACKGROUND

As early as 1974, in response to proposals for the contruction of two off-shore oil terminals off the coast of the United States, Congress enacted legislation directing and funding research relevant to the danger and pollution hazards of a deepwater port (DWP). Apart from investigations conducted by the applicants, the United States Coast Guard also undertook to conduct its own research. Two studies were initiated specifically to address the operational hazards of navigation (Gardenier, 1981). The first study systematically analyzed hazards and risks associated with navigating VLCC's in the vicinity of a deepwater port, and the oil unloading operation itself.

The hazard and risk analysis indicated that aside from potential problems at the port, the human factor posed serious uncertainties during approaches to the port (Faragher et al; 1979). Problems of rig density, low visibility and small craft

operations were found to warrant further investigation. To this were hypothesized the effects of different navigation equipment, bridge personnel training or organization, and the type of approach. To investigate these man-in-the-loop parameters the use of a dynamic ship's simulator was essential.

In the 1970's the technology of marine simulators improved rapidly, until today training and research on simulators has become commonplace, both in the United States and abroad (CAORF, 1981). Further, the requirements for dynamic ship simulators appear to be ever increasing (Gardenier 1979). They have been used to investigate port design, the effectiveness of bridge equipment, shipboard and waterborn aids to navigation, and personnel capabilities; to name but a few, (CAORF, 1977 -1980). Using simulators, research can be conducted in the classical scientific design or as loosly controlled experiments using simplified yet relevant measures (Keith et al, 1977). Simulator research is, therefore adaptable to the study of both man and his environment. Simulators always simplify the real world, but sound research starts from simulations verified as adequately realistic by highly experienced mariners. Quantitative and statistical analyses are employed when appropriate and accompany sophisticated measures of both ship and personnel performance.

Two major benefits, then, evolve from simulator research. First, the simulators themselves provide an automatic record for direct reconstruction and analysis of each voyage. Secondly, effective design of the simulation cues mariners to address and consider aspects of a voyage which could not otherwise be revealed. The mariners themselves can be used both to evaluate the simulation and make suggestions concerning the research problem.

Real-time simulation was selected as most appropriate for investigating potential human factors problems in approaches to deepwater ports. Scandinavian investigators, Istance and Ivergard, have reported (1976) that errors are committed by highly skilled personnel; individuals experienced, sober and well regarded by their peers and managers. Such problems the authors contend, should be termed "competent", rather than "incompetent", errors. A Shell study (Butt, 1978) also confirmed this thinking in independent research. Studies by the Coast Guard (Paramore et al; 1977 a, b) revealed relatively few cases of grossly negligent or incompetent licensed mariner behavior in marine accident records. Further, catastrophic failures of ship control systems are rare (Gardenier, 1976). Yet accidents have occurred and could be expected to reoccur which would involve the most competent seamen. Are there elements in port design which could contribute to "competent" error? If "competent" errors occur can the port design be made sufficiently "foregiving" to prevent an ecological disaster? These two questions were foremost during the development of the simulation.

Under ordinary conditions, the approach of VLCCs to deepwater ports should be safe, routine and relatively easily executed. The designation of two-mile safely fairways and provisions for a vessel traffic service will enhance safety during approaches and departures. Unfortunately, the safety fairways do not always provide the shortest route to the port, and their use is not

mandatory. While the safety fairways are areas in which no oil drilling or production operations can be conducted, there may also be adequate water depth and clearance from obstacles outside the fairway. As such, there is no compelling reason of law, regulation, or prudent seamanship to require the master to stay in the fairway. While many mariners prefer to stay in the fairways because of the predictability of traffic and assurance of no obstructions, there will inevitabely be occasions for all masters in which their adherence to the safety fairway would take them so far out of the way that the added distance would offset the fairway advantages.

Within the geographic area of the deepwater ports, low visibility and unusual current conditions are not uncommon. While the arrival of VLCCs will be coordinated to assure the availability of a mooring master, occasionally unexpected delays in the mooring master's arrival can be anticipated. Both the moorings and the anchorage are beyond the mooring master pick-up point. There is no guidance to the master suggesting what to do in the event of the mooring master's delay. Questions arose over the ability of masters to maintain their position and orientation in the fairway under such conditions. There might also be problems of disorientation during landfall due to the rig-cluttered radar screen and increased traffic. If such problems did exist, they might best be solved by electronic aids or the introduction of procedural measures aboard the tankers or during communications between the tankers and the deepwater ports.

In developing the simulation, the objective was to determine which combinations of hazards, if any, present serious precision navigational problems to VLCC masters in the vicinity of deepwater ports. Secondly project personnel were asked to ascertain what mechanisms might be helpful for alleviating the potential problems.

THE SIMULATION

Licensed masters, some with experience operating in the Gulf of Mexico and all with VLCC experience were consulted prior to the design of the simulation scenarios. Based upon the objectives of the research and what the masters said they would expect, and probably do, four unique scenarios for approach to a deepwater port were constructed. The Louisiana Offshore Oil Port (LOOP) was selected as the gaming area primarily because of the availability of charts and operational data. It was intended, however, that the research apply to all off-shore and near-shore deepwater ports; so unique characteristics of LOOP such as vessel communications were not simulated. It was also decided that the simulation should portray "worst case" visibility conditions requiring primary reliance on the radar and electronic navigation systems. A two-knot northeast current, severe but not uncommon in this area, was also introduced. Various navigational displays were evaluated: radar with the existing aids for LOOP, radar with beacons (RACONS) installed on selected existing rigs south of LOOP, an automated radar plotting aid (ARPA) to augment radar, and the addition of an artificial navigation display of the fairway and port superimposed on the ARPA display. This latter feature is characteristic of the "navigation option" found on many commercially available ARPA systems. Finally, the bridge team management concept was used as a procedural variable.

A high fidelity simulation of shiphandling characteristics was assured by using a recently validated VLCC motion model. This model included low speed hydrodynamic coefficients suited to the final approach to the mooring master pickup point. Traffic ships were introduced to perturb the initial course of ownship and require the master to establish "his own" course for the port. Slow speed fishing vessels and off-shore workboats were included to produce a radar observer workload characteristic of the area. These radar returns had to be properly interpreted to distinguish them from buoys or oil rigs. One scenario provided the greatest opportunity for disorientation, were it to occur in this research. On the final run, after achieving maximum credibility between the subject and experimenter, the mariners were given an inaccurate position estimate (they were told it was an estimated position based on a ten hour old fix), failed electronic navigation equipment, and an actual location where the radar picture supported the false position. Even in this case, all elements were potentially realistic. Clues and instrument capability were available to permit a solution. At the end of the run, masters agreed that such an event is not unrealistic.

PERFORMANCE MEASURES

The development of performance measures was based on a fundamental difference between this experiment and previous ship control simulations. In simulation research, subjects are traditionally provided with a goal which they are to attempt to achieve. One example is to stay on the centerline of the channel; another might be to achieve a 2.0 mile closest point of approach. Such goals were not provided to the subjects in the deepwater port experiment, since the simulation was specifically intended to see how, if left to his own discretion, each master would make the approach. In order to conduct an objective evaluation of the overall safety and effectiveness of all approaches, a method of grouping and comparing all runs of simular "strategy" was adopted. This meant that all masters had to declare their strategy prior to each approach. If they deviated from their original strategy the resulting data was included in the next most similar one. Some strategies were modified during the approach leading to a further establishment of "substrategies." Performance measures within each strategy were compared statistically and graphically. These performance measures included, (1) a description of the mean track, (2) the crosstrack variability of runs, (3) mean speed and and propeller speed in revolutions per minute (RPM), (4) mean frequency of engine, rudder and course orders, (5) mean frequency of radar, loran, radio direction finder (RDF), depthfinder and deduced reckoning (DR) fixes (6) mean closest point of approach (CPA) to each traffic ship and rig, (7) lowest CPA to each traffic ship and rig, (8) maneuver decision and ability to perform the maneuver following the mooring master's delayed arrival, and finally (9) for the disorientation scenario, the amount of time required until the master first doubted his original position, confirmed his enrroneous position and set a new course for the port.

Statistical applications included a two-way analysis of variance to test main effects of the navigation displays and bridge organization variables. Results were indicated as "significant" if there was only a ten percent or lower chance of

those results being due to random variation. The final analysis combined these results with behaviors observed during the simulation and masters' verbal comments to provide a logical "chain of evidence" from which all conclusions of the research could be derived.

SOME CONCLUSIONS

The simulations were run with 12 master-mate teams, each making approaches to the port from four different directions. Figure 1 shows the tracks of all ships in an approach from the east. The deepwater port complex and mooring master pickup point are located in the upper left corner of the figure. Adherence to the fairways would impose a distinct time and fuel cost penalty. About two-thirds of the crews came south of all rigs, sailed west to intersect the north-south approach fairway, and then turned north to make their final approach up the fairway. One-sixth ignored the fairways altogether and sailed a clear path through the rigs directly toward the port entrance. In analyzing approaches from this direction, one dominant and two secondary strategies emerged (see Figure 2). Results of this analysis suggests that these three strategies are characteristic of the type which can be expected in deepwater port operations (i.e., the non-adherence to safety fairways when they are "out-of-the-way").

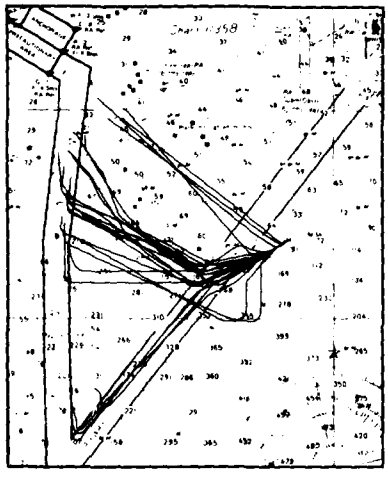

Figure 1. Tracks of Ships Which Approached from the East

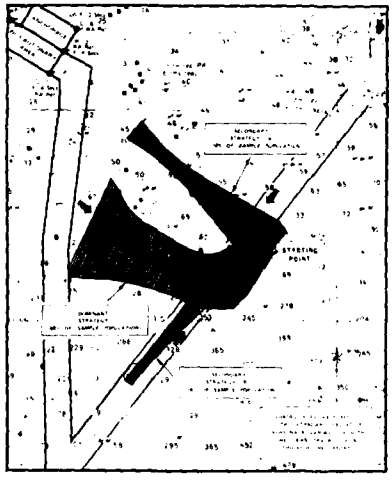

Figure 2. Strategies Approaching from the East

Another scenario, Figure 3, was characteristic of a typical approach from the south. Here the port complex is off the figure directly to the north. Although originally on a course for the fairway intersection, a stand-on ship crossing ahead was introduced to modify this original decision. As shown in Figure 4, seventy-six percent of the subjects made a sharp turn to the fairway entrance as soon as they were safely past the traffic close aboard. Twelve percent made a gentler turn, crossing ahead of the second ship, but entered the fairway north of the intersection. The remaining twelve percent stayed well astern of both traffic ships and then proceeded directly to the port outside the fairway. The resultant lowest CPA to the second traffic ship for the strategy turning directly toward the intersection was more than 1.5 nautical miles with a mean of more than 2.5 nautical miles. Secondary strategy "A" and "B" experienced 1.8 and 2.3 nautical mile mean CPAs respectively, with comparably smaller lowest CPAs. The finding suggests that adherence to the safety fairway will be independent of traffic near the fairway entrance.

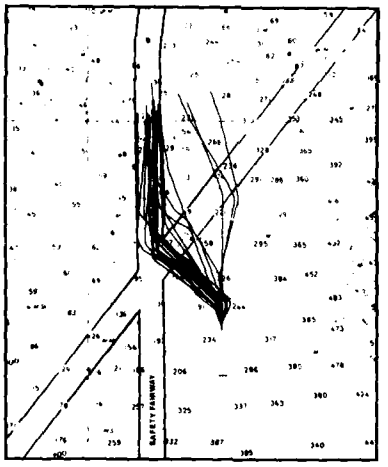

Figure 3. Tracks of Ships Which Maneuvered for Traffic

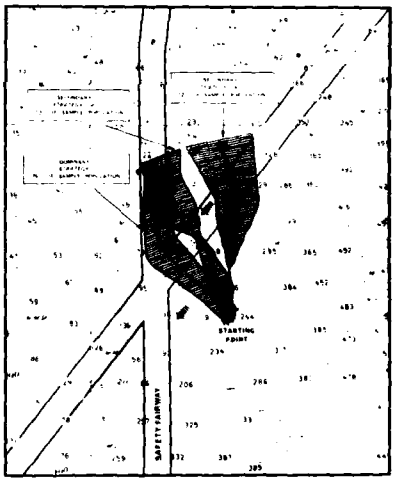

Figure 4. Strategies of the Maneuver and Approach

Figure 5 shows the variety of tracks and station-keeping techniques employed in the final approach to the mooring master pick-up point. In this scenario, the arrival of the mooring master was "delayed." With the good radar returns from the port entrance buoys, all masters maintained full control of their ships. As is seen, however, they elected different techniques for slowing the vessel while maintaining a posture from which an

indefinite delay of the mooring master could be endured. No master became disoriented; no tanker was endangered. One problem is that the mooring master must be on board for a tanker to proceed to the LOOP anchorage. Several masters, however, suggested designating an alternative acceptable anchorage in the immediate port vicinity for cases where the delay entering the port is substantial. Another suggestion was to move the pick-up point further south to avoid the need for making the dogleg turn at dead slow speed, when maneuvering is difficult. Assuming that adherence to the safety fairways would be desireable for port operations, the relocation of this pick-up point further south should discourage approaches from the east through the rig fields.

Individual ship tracks from the final scenario are shown in Figure 6. Of primary interest was the possibility of a master being off position but improperly reassured by the similarity of rig returns on his radar to these associated with the correct approach path. The scenario was designed to introduce ownship within radar range of rigs at a location other than that indicated by the information available. The LORAN was made "inoperative" and ownship was situated on the same radio bearing as the erroneous position estimate. Water depths were somewhat comparable. The ship tracks of Figure 6 indicate that there were a wide variety of techniques employed for determining ownship's actual position as well as masters' responses once their position was determined.

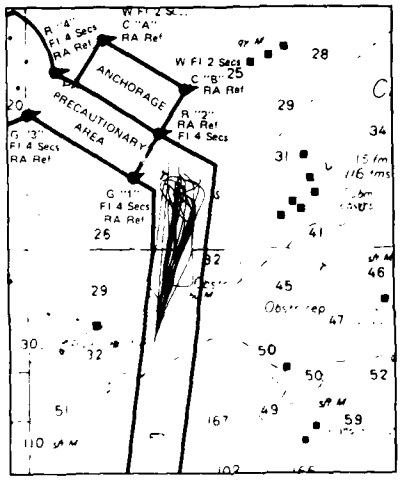

Figure 5. Tracks of Ships Maneuvering to Pickup the Mooring Master

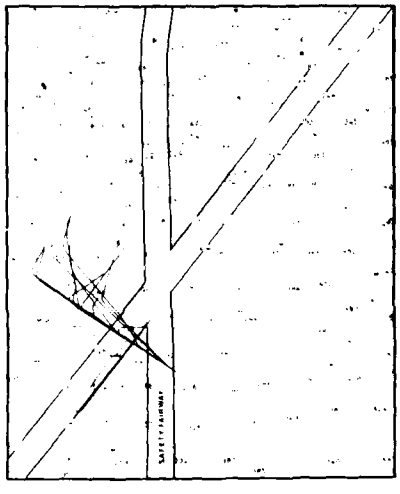

Figure 6. Tracks of Ships on an Erroneous DR

Results indicate that at no time did functional disorientation (loss of reasoning and logical process) or extreme anxiety occur for any subject. Further, although many subjects acknowledged that they were temporarily, in their own words, "lost" none considered their situation dangerous or irretrievable. All set about methodically to determine their actual position while maintaining a safe and judicious operational posture.

SUMMARY OF FINDINGS

Among the findings of this experiment which primarily pertained to VLCC operations in and around a deepwater port, there was also a demonstration of the effectiveness of simulators for examining the human interaction in port systems. By presenting all requirements of the task to be performed (i.e., approach to a deepwater port and pickup of the mooring master) and providing suitable simulation of information and ship response, it was possible to observe and measure adequacy of the port approach design before it actually became operational. Such an endeavor shows promise not only for the evaluation of other ports; but for the development of port regulations, port communications, training or organizational requirements, and the use of navigation and ship control systems.

The project final report (Cook et al, 1980) provides many more details than can be summarized here. Aside from those already discussed, the study showed that when racons are provided, masters use them as a single point range or for radar parallel indexing. The result is a focusing of tracks toward the racon. Use of ARPA with a navigation option display produced varied effects. The clear delineation of fairway boundaries and implied high precision of the system enabled masters to choose alternative tracks either in the center or along the right edge of the fairway. While both of these behaviors were shown to result in safe operation during the simulation, this study alone could not determine which of the behaviors is more desirable in terms of deepwater port safety and operating effectiveness.

The study also found that traffic encounters as they were simulated presented no undue hazard or difficulty during the port approach. There were indications based upon demonstrated navigation capability and achieved CPAs that if additional fairway traffic had been present it would have been handled safely. Traffic separation schemes and a traffic advisory service for deepwater ports were not examined in this project. Decisions on these topics should be derived from a more explicit and comprehensive study of the traffic situation.

Comparisons in navigation and shiphandling performance between traditionally organized bridge personnel and team organized crews showed no difference with respect to achieved safety or overall operational effectiveness in this experiment. Nonetheless, there were a number of techniques employed by the team organization which improved the approaches and demonstrated an increased capability to deal with contingencies. These techniques include preplanning the approach, delegation of duties, review of contingency actions, cross-checking procedures and assuring effective communications.

References

(1) Butt, J. A. 1978. "Recent Developments in Navigation Training." In Proceedings of the Safe Navigation Symposium, Oil Companies International Marine Forum, New York, NY

(2) CAORF (Computer-Aided Operations Research Facility). 1977-1980. Proceedings of the Annual CAORF Symposium. National Maritime Research Center, Kings Point, NY

(3) CAORF, 1981. Proceedings of MARSIM '81: The Second International Conference on Marine Simulation.

(4) Cook, R., K. Marino, and R. Cooper. 1981. A Simulator Study of Deepwater Port Approach Shiphandling and Navigation Problems in Poor Visibility. National Technical Information Service, Springfield.

(5) Faragher, W. E., J. T. Pizzo, L. R. Reinburg, et al. 1979. Deepwater Port Approach/Exit Hazard and Risk Analysis. National Technical Information Service, AD A074529, Springfield, VA

(6) Gardenier, J. S. 1976. "Toward a Science of Merchant Marine Safety," Marine Traffic Systems, Netherlands Maritime Institute, Rotterdam. (Major extract reprinted in Schiff and Hafen, 1976, 7, pp. 613-616).

(7) Gardenier, J. S. 1979. "Where Are We Headed With Vessel Bridge Simulators?" In Proceedings of the Third CAORF Symposium, National Maritime Research Center, Kings Point, NY, pp -1 to 8-11.

(8) Gardenier, J. S. 1981. "Navigational Safety Approaching Off-Shore Deepwater Ports," 1981 Oil Spill Conference (Prevention, Behavior, Control, Cleanup), Atlanta, Georgia, pp 609-616.

(9) Istance, H., and T. Ivegard. 1975. Ergonomics and Reliability in Shiphandling Systems-Theories, Models, and Methods, "In Porceedings of the Fourth Ship Control Systems Symposium, Den Helder, Netherlands.

(10) Keith, V. F., J. D. Porricelli, J. P. Hooft, et al., 1977. "Real-Time Simulation of Tanker Operations for the Trans-Alaska Pipeline System," In 1977 Transactions of the Society of Naval Architects and Marine Engineers, New York, NY, pp 419-458.

(11) Paramore, B., R. B. Dayton, J. D. Porricelli, and R. M. Willis. 1979a. Human and Physical Factors Affecting Collisions, Rammings, and Groundings on Western Rivers and Guld Intercoastal Waterways. National Technical Information Service, AD A074290, Springfield, VA

(12) Paramore, B., V. Keith, P. King, J. Porricelli, and R. Willis. 1979b. Study of Task Performance Problems in Reports of Collisions, Rammings, and Groundings in Harbors and Entrances. National Technical Information Service, AD A071058, Springfield, VA

AUTOMATIC CONTROL FOR COURSE AND STATION KEEPING

by M. Policarpo, Portugese Navy
A. Gerba, and G. J. Thaler
U.S. Naval Postgraduate School

ABSTRACT

Course and Station keeping are achieved by generating course commands and station error and using these signals to control the ship. The command and error signal are generated by using a preprogrammed trajectory and Telstar measurements of position.

INTRODUCTION

Manual steering of ships consists of maintaining ship's heading, the desired heading being reset at intervals. The usual ship's autopilot merely replaces the helmsman. The intent of this paper is to start with the familiar autopilot and interface it to a navigation computer which uses Telstar (or perhaps Loran III). The combination then provides options of course keeping with automatic reset of the heading command, or station keeping which adds a position error into the loop and forces the ship to follow a desired trajectory. The basic philosophy is shown in the block diagram of Fig. 1.

DEFINITIONS

To provide quantitative data for simulation studies we chose to apply the ideas of Fig. 1 to a 200,000 DWT supertanker of the following characteristics:

Length 310 meters
Breadth 47.16 meters
Draft 18.90 meters

Steering quality indices:

T_1 = -269.3 seconds
T_2 = 9.3 seconds
T_3 = 20.0 seconds
K = -0.0434 rad/sec
Maximum rudder deflection = 30°
Maximum rudder rate = 2.32 degrees/second

The transfer function from rudder angle to yaw rate is

$$\frac{\dot{\theta}(s)}{\delta(s)} = \frac{K(sT_3 + 1)}{(sT_1 + 1)(sT_2 + 1)}$$

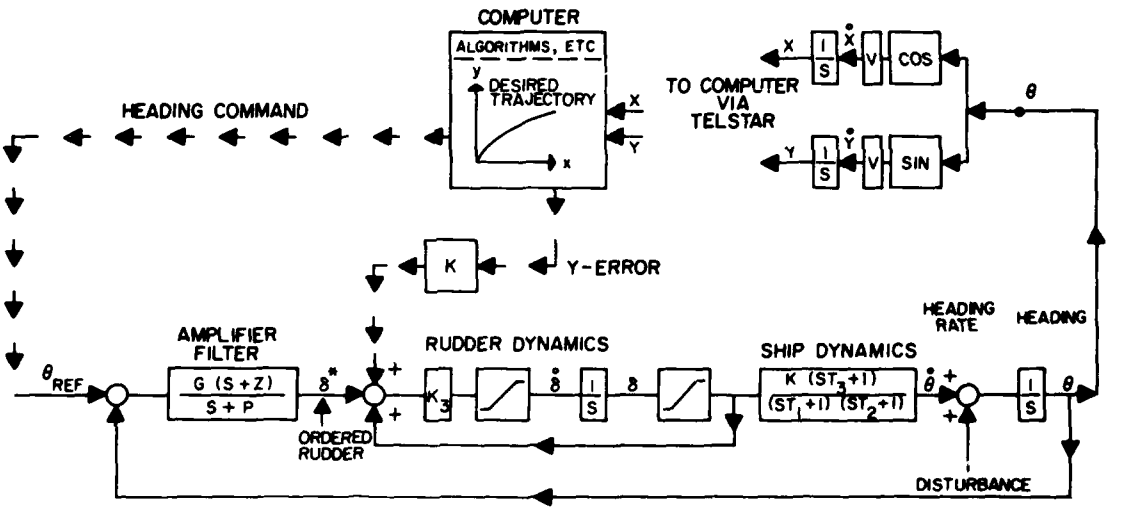

Figure 1. Block Diagram of the Course and Station Keeping Controller.

Since T_1 is negative the hull is directionally unstable and the autopilot loop must be stabilized. Alternatives are yaw rate feedback using a rate gyro or a cascaded lead (high pass) filter. Both were studied but only the latter is used here (see Fig. 1).

FILTER PARAMETERS

It was decided to use a single section of filter (one zero, one pole) with a separation of one decade. Root locus analysis aided by simulation studies (rudder servo nonlinearities included) led to the choice

$$\text{FILTER} = 4.6\left(\frac{2.5s + 1}{25s + 1}\right)$$

Fig. 2 shows the rudder response and heading response of the autopilot controlled ship for a 10° step change in heading command. Note that the rudder reaches its 30° limit for a short time on its initial excursion, thus sudden large changes in heading are to be avoided if possible. Note also that the response is slightly oscillatory. These results are due, in part, to the abitrary decision to use only one section of filter with zero-pole separation set at one decade. The result given here is near optimum under these constraints, but a design using more zeros and poles without separation constraints can produce responses that might be considered preferable. Such variations were not explored. The given filter and resulting autopilot are used in the rest of this study.

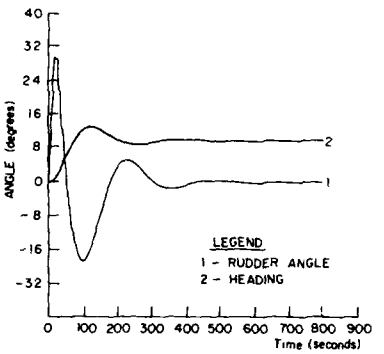

Figure 2 Rudder Angle and Heading Response to a 10 Degree Step Change in Heading Command

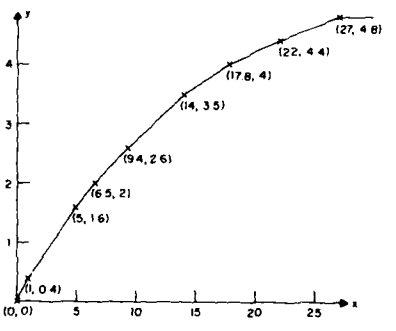

Figure 3 Definition of Trajectory Used

THE DESIRED TRAJECTORY

The desired trajectory is a specific track which the ship is to follow from port of origin to destination. It would be defined by the navigator in advance by selecting coordinate points on his charts. This could be done by drawing a desired track on the chart and reading coordinates from it. The coordinates are then stored in computer memory and an algorithm used which may

(a) Interpolate linearly between points,

(b) Interpolate nonlinearly using a suitable function,

(c) Obtain a least squares fit through the points.

For use in simulation tests we used the trajectory defined by the solid line in Fig. 3. We have used x-y coordinates; latitude and longitude would be more natural for course control. In this study the curve is always entered with a value of x, and interpolation was linear. Note that one could just as easily enter the curve with a value of y. The only change required is the renaming of variables in the algorithm.

COURSE CONTROL

The automatic course control system is shown on Fig. 1 if we eliminate the y-error signal from the computer. Operation is as follows:

1. Enter trajectory with value of x, read y_1.
2. Enter trajectory with $x + \Delta x$ (here $\Delta x = .125$ miles), read y_2.
3. Calculate $\Delta y = y_2 - y_1$.
4. Desired heading = $\tan^{-1} \Delta y/\Delta x$.

Since Telstar provides essentially continuous measure of positions, the above calculations can provide nearly continuous variation in the desired heading. Since this procedure does not consider the position (off-track) error, we would expect the ship to follow the trajectory reasonably well in calm water (no ocean currents), but with a slowly accumulating position error. This is shown by Figs. 4a,b,c,d. On Fig. 4a the commanded heading is given by the straight line segments. The line segments are straight because we used linear interpolation, the discontinuities are due to the step changes in slope at the coordinate points on Fig. 3.

STATION KEEPING

In order to follow the track more accurately we must measure the position error and try to force it to zero. The computer calculates this error easily by

$$y_{ERROR} = y_1 - y_{TELSTAR}$$

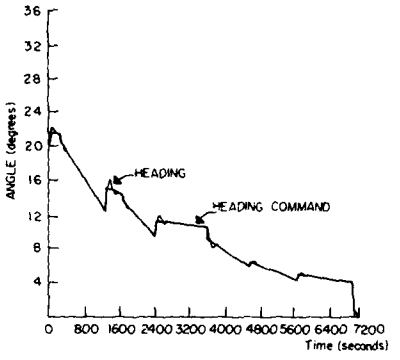

Figure 4a Heading and Heading Command Versus Time

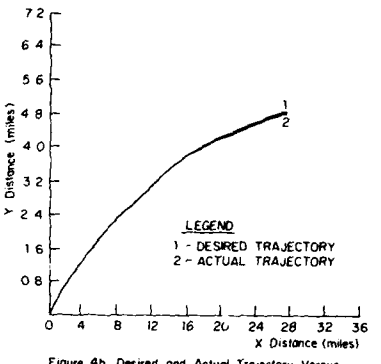

Figure 4b Desired and Actual Trajectory Versus Time

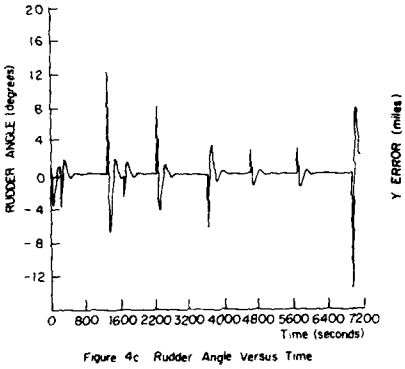

Figure 4c Rudder Angle Versus Time

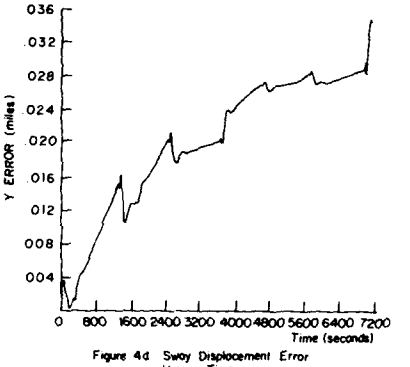

Figure 4d Sway Displacement Error Versus Time

If we amplify this error and use it to add a correction to the ordered rudder we obtain a station keeping system which tries to follow the track closely even in ocean currents and/or in sea-state. This station keeping loop is obtained on Fig. 1 by activating the y-ERROR path. Figs. 5a,b,c,d show that the error remains small in calm water.

Simulation of a sea-state in the usual context was not considered since we are interested only in the ability of the controller to keep the ship on track. It is known that one effect of waves is to cause a turning (yawing) rate, which can reach magnitudes of 0.2 degrees per second. As a simple test of the controller's ability to follow track in sea-state, we added to the simulation (see

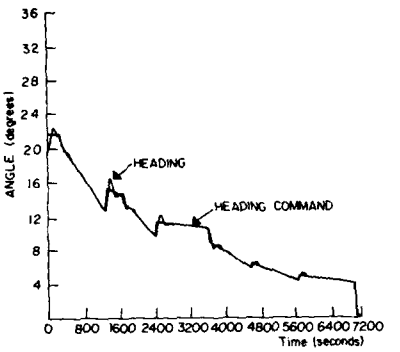

Figure 5a Heading and Heading Command Versus Time

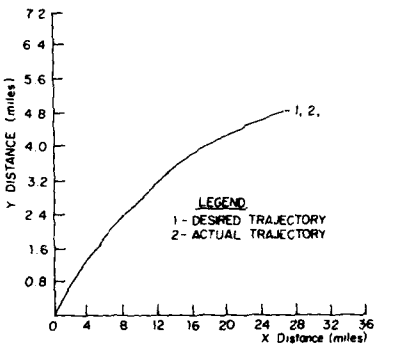

Figure 5b Desired and Actual Trajectory Versus Time

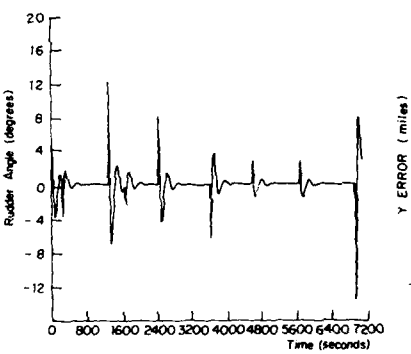

Figure 5c Rudder Angle Versus Time

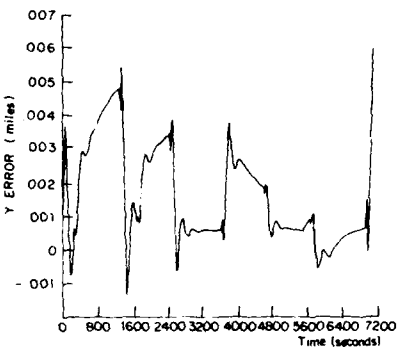

Figure 5d Sway Displacement Error Versus Time

Fig. 1) a constant heading rate disturbance of 0.2 degrees/second. The results are shown on Fig. 6 . Note that the controller develops a steady rudder offset of about 4.5 degrees, and the trajectory is followed quite closely with a small steady state position error of 0.027 miles (50 meters) which is approximately the breadth of the ship (47.16 meters).

DISCUSSION AND CONCLUSIONS

From the results obtained we may conclude that automatic guidance of a ship along a prescribed trajectory may be obtained by combining navigation information from Telstar with a relatively simple autopilot design. The autopilot designed in this paper

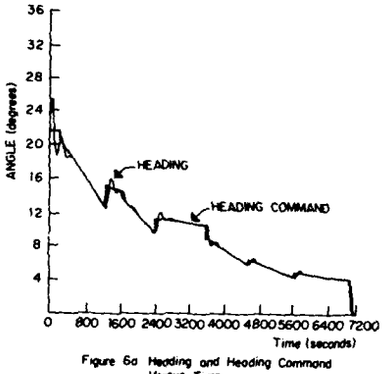

Figure 6a Heading and Heading Command Versus Time

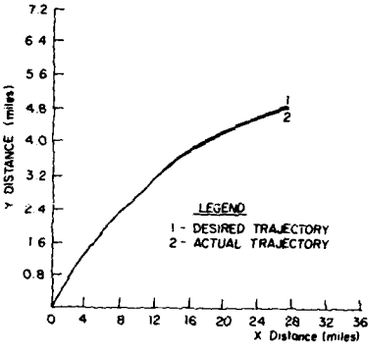

Figure 6b Desired and Actual Trajectory Versus Time.

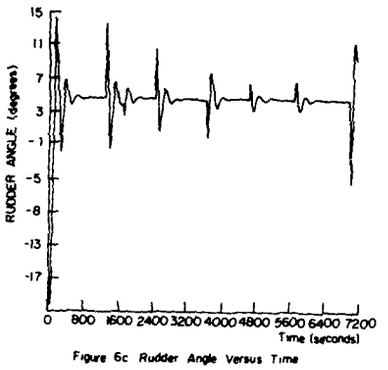

Figure 6c Rudder Angle Versus Time

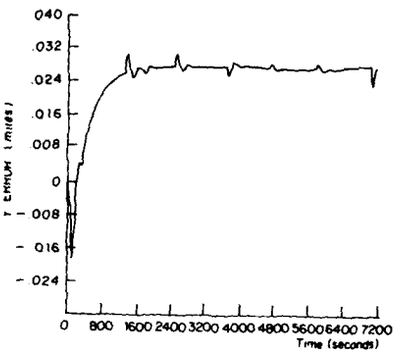

Figure 6d Sway Displacement Error Versus Time

requires no new control components or techniques, it simply resets the desired heading continuously and adds a correction to the rudder command both based on comparison of Telstar data with the prescribed trajectory.

Additional control features not studied here, such as speed control, minimization of fuel and/or transit time in sea-state, etc., should be obtainable using the basic concepts of this course and station keeping design. In order to study additional control features a more detailed model of this ship is needed, including the dynamics of the propulsion system, drag characteristics, etc. We hope to continue our studies in this direction.

REFERENCES

1. Davidson, Kenneth S.M., and Schiff, Leonard J., "Turning and course keeping qualities of ships," Transactions SNAME, Vol. 54, 1946.

2. Davidson, K.S.M., "On the turning and steering of ships," Transactions SNAME, Vol. 52, 1944.

3. Nomoto, K., Taguchi, T., Honda, K., and Hirano, S., "On the steering qualities of ships," International Shipbuilding Progress, Vol. 4, No. 35, 1957.

4. Schiff, L., and Gimprich, M., "Automatic steering of ships by proportional control," Transactions SNAME, Vol. 57, 1949.

5. Koyama, T., "Improvement of course stability by the subsidiary automatic control," International Shipbuilding Progress, Vol. 19, No. 212, 1972.

6. Minorsky, N., "Directional stability of automatically steered bodies," Journal ASNE, 1922.

7. Millikem, R.J., and Zoller, C.J., "Principle of operation of NAVSTAR and system characteristics," Navigation, Journal of the Institute of Navigation, Vol. 25, No. 2, 1978.

8. Henderson, D.W., and Strada, J.A., "NAVSTAR field test results," Navigation, Journal of the Institute of Navigation, Vol. 26, No. 1, 1979.

9. Van Amerongen, J. and Van Nauta Lemke, H.R., "Optimum steering of ships with an adaptive autopilot," Proc. 5th Ship Control Systems Symposium, Annapolis, Maryland, U.S.A., 1978.

10. Brink, A.W., Baas, G.E., Tiano, A., and Volta, E., "Adaptive automatic course-keeping control of a supertanker and a containership--a simulation study," Proc. 5th Ship Control Systems Symposium, Annapolis, Maryland, U.S.A., 1978.

11. Koyama, T., "On the optimum automatic steering system of ships at sea." J. Soc. Nav. Archit. Japan, 122. 142, 1967.

12. Ware, J.R., Fields, A.S., and Bozzi, P.J., "Design procedures for a surface ship steering control system," Proc. 5th Ship Control Systems Symposium, Annapolis, Maryland, U.S.A., 1978.

13. Källström, C.G., Aström, K.J., Thorell, N.E., Eriksson, J.E., and Stem, L., "Adaptive autopilots for tankers, Automatica, Vol. 15, pp. 241-254.

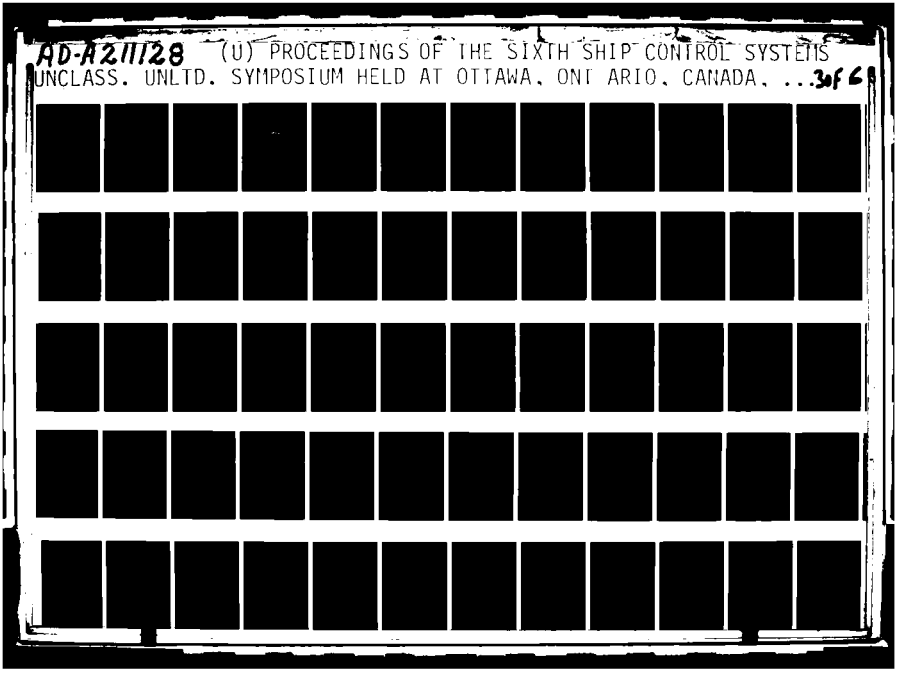
AD-A211128 (U) PROCEEDINGS OF THE SIXTH SHIP CONTROL SYSTEMS
UNCLASS. UNLTD. SYMPOSIUM HELD AT OTTAWA, ONTARIO, CANADA, ...3 of 6

OPTIMAL CONTROL OF SHIP-TUG OPERATIONS IN RESTRICTED WATERWAYS

by William McIlroy, Ph. D.
Head of Research, CAORF, Grumman Data Systems
and Gilbert Carpenter, Ph. D.
Research Scientist, Grumman Aerospace Corporation

ABSTRACT

This paper describes how off-line mathematical models can complement the real time simulation experiments performed at CAORF (Computer Aided Operations Research Facility), Kings Point, N.Y. The Optimal Ship Maneuvering Program was developed as an off-line model to evaluate piloted ship performance during harbor entrance and transit maneuvers and to evaluate ship-tug control policies during docking maneuvers. The program employs essentially the same ship dynamic model and waterway description as used by the CAORF Simulator.

When navigating through a restricted waterway the master or pilot is required to perform several efficient course changes coupled with periods where he must exhibit a high proficiency in course-keeping ability. In addition, he will have to be able to perform safe evasive maneuvers when either obstructions or other ships present a collision situation. With the introduction of new and larger ship designs and the addition of uncertainties in local wind and currents the pilot will not be able to rely solely on his years of experience for making control decisions. His knowledge of the ship's maneuvering capability and handling characteristics can be limited and therefore his decisions need to be augmented by an onboard computer to advise him of the optimal maneuver to perform.

These considerations resulted in the development of a maneuvering program to generate optimal ship trajectories through sinuous restricted waterways, with many turns and under varying wind and current conditions. The program generates optimal time histories for both the rudder and propeller revolutions which minimize the ship's deviation from a prescribed track while either maintaining constant speed during the transit, following a specified speed envelope or varying speed optimally to reach a specified terminal speed condition. This off-line simulation program is an invaluable means of predicting the required maneuvering capabilities or limitations of a ship transiting a given waterway or a proposed port or harbor design. For man-in-the-loop simulator studies such as CAORF's pilot controllability experiments, the program provides a datum or optimal reference trajectory for comparison with the individual subject's performance. Thus it provides an absolute rather than just a relative figure of merit for pilot evaluation.

Some applications of the optimal control program will be described: for example, (1) anticipation distance as a function of initial range from turn point, (2) optimal rudder history as a function of path curvature in channel transfer, (3) effect of wind speed and direction.

Ship/Tug navigation through a restricted waterway and tug rescue of disabled ships are some of the additional problems which are being studied as the program is developed further. In the navigation problem the optimal tug control is derived so that the ship transits a channel complex with a minimum cross track deviation. For the rescue problem which is often caused by the failure of a ship's steering and/or propulsion system the tug control policy is to either return the ship to its original track or, alternatively, abort the mission while avoiding groundings and rammings due to the presence of obstacles and other ship traffic. Optimized policies determine a cost effective means for conducting docking and rescue with limited tug resources.

INTRODUCTION

When navigating through a restricted waterway the master or pilot is required to perform several efficient course changes coupled with periods where he must exhibit a high proficiency in course-keeping ability. In addition, he must be able to perform safe evasive maneuvers when either obstructions or other ships present a collision situation. With the introduction of new and larger ship designs and the addition of uncertainties in local wind and currents the pilot will not be able to rely solely on his years of experience for making control decisions. His knowledge of the ship's maneuvering capability and handling characteristics can be limited and therefore his decisions need to be augmented by an on-board computer to advise him of the optimal maneuver to perform.

These considerations resulted in the development initially of a computer code called the Optimal Ship Maneuvering Program which generates optimal ship trajectories through restricted waterways. The program determines the rudder control as a continuous function of time so as to maneuver the ship along established channel centerlines or assigned tracks with minimum cross track deviation. In addition the program can handle the situation encountered by the helmsman when he must contend with unknown forces due to wind and water currents.

This Optimal Ship Maneuvering Program was recently extended by enhancing its capabilities to evaluate piloted ship performance during harbor entrance and transit maneuvers and to evaluate ship-tug control policies during docking maneuvers. The extended program generates optimal time histories for both the rudder and propeller revolutions which minimize the ship's deviation from a prescribed track while either maintaining the ship's speed or following a prescribed speed variation through the transit or attaining an assigned terminal speed. This off-line simulation program is an invaluable means of predicting the required maneuvering capabilities or limitations of a ship transiting a given waterway in the presence of cross currents and winds. For man-in-the-loop simulator studies such as CAORF's piloted controllability experiments, the program provides a datum or optimal reference trajectory for comparison with the individual subject's performance. Thus it provides an absolute rather than just a relative figure of merit for pilot evaluation.

Ship-tug navigation through restricted waterways, docking and tug rescue of disabled ships are high priority items in the CAORF on-line research program. These simulator experiments will be supported with off-line studies using the Optimal Ship-Tug Maneuvering Program presently under development. This off-line program offers a technique whereby a datum or optimal strategy can be evolved against which individual pilot performance on CAORF can be compared.

For the ship/tug navigation problem the optimal tug control (tug pull force and angle) is derived using the criterion that the ship should transit a channel complex with minimum cross track deviation while maintaining a prescribed speed variation. In addition, the tugs are required to bring the ship to rest in an area designated as the turning basin and orient the ship with a prescribed heading. For docking operations the program generates optimal control policies that take the ship from the turning basin to a docking position at the berth with a null speed at termination so as to guarantee minimum damage to the ship and dock facilities. For the rescue problem, which is often caused by failure of the ship's steering system or its engines, the tug control policy is to return the ship to its original track or to a track 180^{o} to its original track while avoiding groundings and rammings due to the presence of obstacles or other ship traffic. These optimized policies can lead to cost effective strategies for conducting docking and rescue missions with limited tug resources.

The mathematical modeling of the coupled ship-tug dynamic system can be extremely complex depending on the number of tugs, their type, and their individual placement. In addition, under certain operating conditions for a ship and a tending tug, the tug can cause interference effects which influence the ship's hydrodynamic coefficients. Since this interaction phenomenon is poorly understood, the basic ship's hydrodynamic coefficients for shallow water have not been altered in this study.

The tugs considered initially are highly maneuverable tugs having a 360^{o} rotatable Kort nozzle design. Recent tests using a tug of this type ("Tina," 1000 HP) indicated that this class of tug could provide essentially a constant bollard pull in all relative ship-tug directions for ship speeds up to six knots (1). In order to reduce some of the tug burden in the longitudinal direction an option for either preselecting or optimizing an rpm sequence for the ship's engine has been provided.

Whenever the maneuvering program has to optimize the control of more than two tugs, serious computational difficulties arise due to the number of control variables and their counteracting effects, which can cause instabilities in the numerical algorithm. Consequently, several options for consolidating the operation of several tugs were investigated. One of the first methods was to consider the resultant forces and moment acting on the ship's center of gravity due to the contribution of each tug as illustrated in Figure 1.

The advantage of this method is that the maneuvering program has to optimize only the resultant tug forces F_X, F_Y and the resultant moment M_T. Unfortunately synthesizing individual bow and stern tug orders from this form of a control structure can be extremely ambiguous without an additional set of auxiliary equations of constraint.

To simplify the tug control synthesis a second method was considered whereby the tugs are consolidated with respect to their bow or stern placement as shown in Figure 2.

In this configuration the maneuvering program has to optimize the four controls: the resultant bow tug force and pull angle and the resultant stern tug force and angle. The advantage here is that bow and stern tug operations can be synthesized independently but at the expense of having to optimize one additional control parameter.

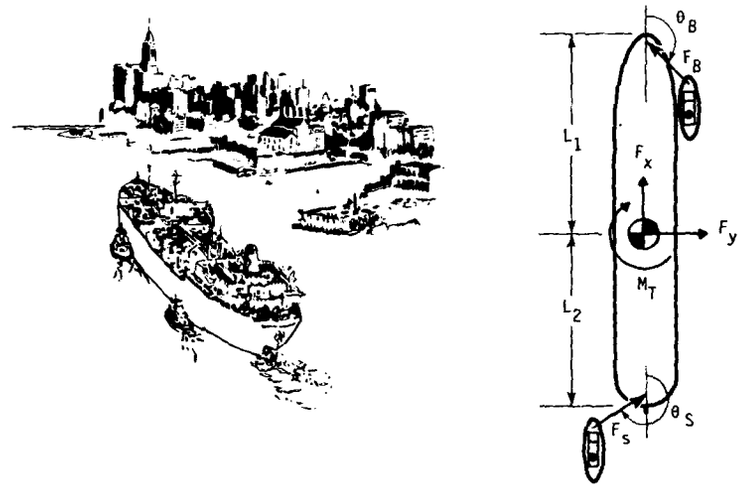

Figure 1. Tug Placement

SHIP-TUG DYNAMIC MODEL

The ship coordinate nomenclature and dynamic model used in the Optimal Ship-Tug Maneuvering Program are summarized in this section. Figure 3 shows the coordinate system used to define ship motions in calm water and indicates the positive direction of all quantities. The force and moment equations are written with respect to the ship's body axes (x, y) which are oriented along the longitudinal and transverse axes of the ship, with the origin fixed at the ship's center of gravity. The equations describing the motion of the ship in the horizontal plane for yaw, sway, and surge are given by:

$$
\begin{aligned}
I_z \dot{r} &= N = N_{hydro} + N_{rudder} + N_{prop} + N_{wind} + N_{tug} \\
m\,(\dot{v} + ur) &= Y = Y_{hydro} + Y_{rudder} + Y_{prop} + Y_{wind} + Y_{tug} \\
m\,(\dot{u} - vr) &= X = X_{hydro} + X_{rudder} + X_{prop} + X_{wind} + X_{tug}
\end{aligned}
\qquad (1)
$$

where N, Y, X represent the total moment and forces acting on the ship due to the hull and rudder hydrodynamics, propulsion, winds, and external effects due to banks, passing ships, tugs, etc.

The terms u and v are fore/aft and athwartship velocities respectively, along and normal to the ship's centerline. In addition, r is the rotational rate of the ship, m the mass in slugs, and I_z the moment of inertia about a vertical axis through the center-of-gravity.

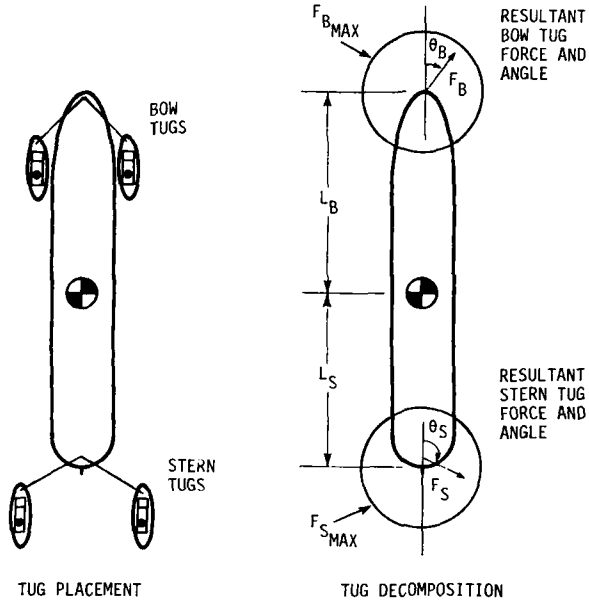

Figure 2. Consolidated Tug Placement

The hydrodynamic and rudder forces and moments appearing on the righthand side of these equations are functions of the ship's speed relative to the water. These can be expressed in terms of u, v, r, and δ and their derivatives, and are expanded in a Taylor series about the instantaneous state of motion (2, 3). The ship speed components relative to the ground are $u_g = u + u_c$ and $v_g = v + v_c$ where u_c, v_c are current velocity vectors along and perpendicular to the ship's centerline. The resultant ship speed through the water is $U = (u^2 + v^2)^{\frac{1}{2}}$.

The adopted format is to expand the hydrodynamic terms in a polynomial series formed from the products of dimensionless coefficients N', Y', X' and dimensional quantities such as ρ (water density), U (resultant ship velocity relative to the water), L (ship length), and A (reference area, $A = L^2$) where

$$N = \tfrac{1}{2} \rho U^2 AL N'$$

$$Y = \tfrac{1}{2} \rho U^2 A Y' \qquad (2)$$

$$X = \tfrac{1}{2} \rho U^2 A X'$$

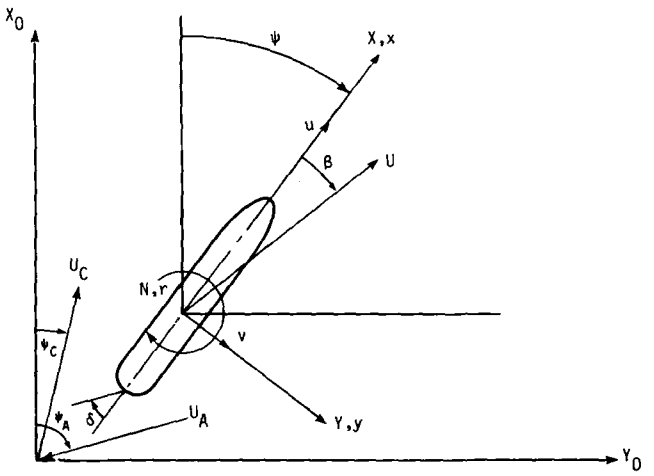

Figure 3. Ship Coordinate Nomenclature

The equations of motion for the degree of expansion included in this study with the effects of ship propulsion, tug, and aerodynamic forces are summarized as follows:

$$\dot{r} = \left[\frac{1}{L^2(I'_z - a_{11})}\right]\left[a_0U^2 + a_1 Uv + a_2L\, Ur + a_3U^2\delta + a_5\frac{Lv^2r}{U} + a_6\frac{L^2vr^2}{U} + a_7\frac{v^3}{U} + a_8\frac{L^3r^3}{U} + a_9U^2\delta^3 + \frac{2}{\rho L^3}(N_{PROP} + N_{WIND} + N_{TUG})\right] \quad (3)$$

$$\dot{v} = \left[\frac{1}{L(m' - b_{12})}\right]\left[b_0U^2 + b_1 Uv + b_2L\, Ur + b_3U^2\delta + b_5\frac{Lv^2r}{U} + b_6\frac{L^2vr^2}{U} + b_7\frac{v^3}{U} + b_8\frac{L^3r^3}{U} + b_9U^2\delta^3 - Lm'ur + \frac{2}{\rho L^3}(Y_{PROP} + Y_{WIND} + Y_{TUG})\right]$$

$$\dot{u} = \left[\frac{1}{L(m' - C_4)}\right]\left[C_0U^2 + (C_1 + m')\, Lvr - C_2v^2 + C_3U^2\delta^2 + \frac{2}{\rho L^2}(X_{PROP} + X_{WIND} + X_{TUG})\right]$$

while the inertial position and heading of the ship are given by:

$$\begin{aligned} \dot{x}_o &= u\cos\psi - v\sin\psi + U_c\cos\psi_c \\ \dot{y}_o &= u\sin\psi + v\cos\psi + U_c\sin\psi_c \\ \dot{\psi} &= r \end{aligned} \tag{4}$$

The ship's propulsion system is expressed in terms of the longitudinal velocity, u, and the propeller revolutions, n, according to:

$$\begin{aligned} X_{PROP} &= c_{p1}u^2 + c_{p2}un + c_{p3}n^2 \\ Y_{PROP} &= b_{p1}u^2 + b_{p2}un + b_{p3}n^2 \\ N_{PROP} &= a_{p1}u^2 + a_{p2}un + a_{p3}n^2 \end{aligned} \tag{5}$$

In forward motion and with clockwise rotation of the propeller ($u > o$, $n > o$) Y_{PROP} and N_{PROP} are set equal to zero.

The aerodynamic forces and moments acting on the ship due to the wind (U_{AR} magnitude, ψ_{AR} direction relative to the ship) are expressed as Fourier series expansions. Assuming that the absolute wind magnitude U_A and direction ψ_A are specified as referenced in Figure 3 and the ship's speed and direction are known, the relative wind can be determined from the following relations. Note that the convention used to indicate the direction of the absolute wind refers to *the angle from which the wind is blowing.*

The direction of the absolute wind, as measured from the ship with a heading of ψ as shown in Figure 4, is given by

$$\psi' = \psi_A - \psi$$

The absolute wind vector $\underline{U}_A$ can be expressed as components in the ship body axis system (x, y).

$$\begin{aligned} U_{AX} &= -U_A\cos\psi' \\ U_{AY} &= -U_A\sin\psi' \end{aligned} \tag{7}$$

Note that the negative signs in the above expressions are due to the convention of specifying ψ_A as "where the wind is blowing from." The relative wind components are simply given by:

$$\begin{aligned} U_{ARX} &= U_{AX} - U_X = -U_A\cos\psi' - u \\ U_{ARY} &= U_{AY} - U_Y = -U_A\sin\psi' - v \end{aligned} \tag{8}$$

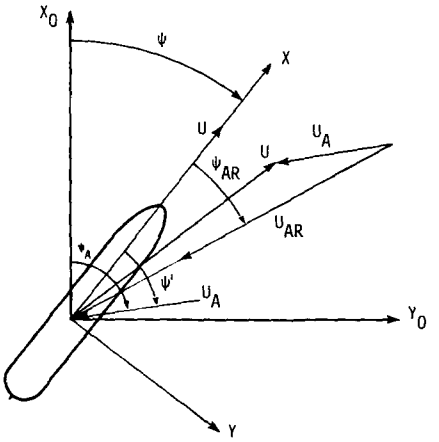

Figure 4. Geometrical Relationsnip Between Absolute and Relative Wind

and from which the relative wind magnitude U_{AR} and direction c_{AR} can be determined according to

$$U_{AR} = (U_{ARX}^2 + U_{ARY}^2)^{1/2}$$
$$\cos \psi_{AR} = - U_{ARX}/U_{AR} \qquad (9)$$
$$\sin \psi_{AR} = - U_{ARY}/U_{AR}$$

The aerodynamic forces and moments are modelled by the following Fourier series:

$$X_{wind} = \frac{1}{2} \rho_A L^2 U_{AR}^2 \sum_{i=1}^{5} C_{x_i} \cos (i\psi_{AR})$$
$$Y_{wind} = \frac{1}{2} \rho_A L^2 U_{AR}^2 \sum_{i=1}^{5} C_{y_i} \sin (i\psi_{AR}) \qquad (10)$$
$$N_{wind} = \frac{1}{2} \rho_A L^3 U_{AR}^2 \sum_{i=1}^{5} C_{N_i} \sin (i\psi_{AR})$$

where ρ_A is the air density.

The hydrodynamic coefficients are, in general, functions of position, attitude, rudder angle, propeller slip, ship velocity, etc. With

appropriate changes in these coefficients the above model is capable of representing a ship operating in open deep waters, shallow water, canals, or dredged channels. For each of these operating conditions the coefficients are essentially constant except that in all cases the rudder coefficients are affected by the propeller slip.

The rudder effectiveness depends upon the resultant speed of water flowing over the rudder which is due to the ship's forward motion augmented by the propeller wash over the rudder. It is related to the propeller slip, based on an empirical formulation derived from the literature (4). Specifically the rudder coefficient a_3 (and similarly a_9, b_3, b_9, and c_3) is changed from its equilibrium value by the relation

$$a_3 = \frac{(1 + KS^{3/2})}{(1 + KS_e^{3/2})} \; a_{3e}, \text{ etc.} \tag{11}$$

where a_{3_e} = equilibrium value of rudder coefficient

$S = 1 - u/pn$ = propeller slip

$S_e = 1 - u_e/pn$ = equilibrium slip

p = propeller pitch

n = propeller revolutions per second

K = empirical constant

Thus, this relationship models the effect of the rudder being "less effective" in situations of increased propeller slip such as during hard maneuvering.

This model was used extensively in developing the library of CAORF ship models. Unfortunately the validity of the model for many operating conditions has been questioned, especially in the low speed regime. When the propeller revolutions (n) approach zero the definition of slip is ill-defined both theoretically and numerically and results in poor estimates of rudder effectiveness. Consequently, an improved rudder model based on a quadratic function of surge velocity and propeller speed to approximate the rudder effectiveness coefficients was developed. For the improved model the coefficients a_3, a_9, b_3, b_9, and c_3 take on the form

$$\begin{aligned}
a_3 &= \frac{2}{\rho U^2 AL} (a_{R1} u^2 + a_{R2} un + a_{R3} n^2) \\
a_9 &= \frac{2}{\rho U^2 AL} (a_{R4} u^2 + a_{R5} un + a_{R6} n^2) \\
b_3 &= \frac{2}{\rho U^2 A} (b_{R1} u^2 + b_{R2} un + b_{R3} n^2) \\
b_9 &= \frac{2}{\rho U^2 A} (b_{R4} u^2 + b_{R5} un + b_{R6} n^2) \\
c_3 &= \frac{2}{\rho U^2 A} (c_{R1} u^2 + c_{R2} un + c_{R3} n^2)
\end{aligned} \tag{12}$$

It is clear that the above relations are free from singularities as either u or n approaches zero.

The resultant tug forces and moment acting on the ship's center of gravity for the tug configuration shown in Figure 2 are summarized as:

$$\begin{aligned} X_{TUG} &= F_B \cos\theta_B + F_S \cos\theta_S \\ Y_{TUG} &= F_B \sin\theta_B + F_S \sin\theta_S \\ N_{TUG} &= L_B F_B \sin\theta_B - L_S F_S \sin\theta_S \end{aligned} \tag{13}$$

The ships considered in this study are the 165,000 DWT and the 80,000 DWT tankers taken from the library of ships available on the CAORF Simulator. The physical properties, hydrodynamic, propulsion, and aerodynamic coefficients for these ships are summarized in Tables 1 through 4 (see Appendix).

A trajectory describing the state of the ship (x_O, y_O, ψ, r, v, u) as a function of time is generated by integrating Eqs. (3) and (4) forward from an initial condition using a rudder command $\delta_C(t)$ and an engine or propeller speed command $n_C(t)$. The responses of the rudder and propeller to the commanded values are modeled based on first-order linear systems; that is,

$$\begin{aligned} \dot{\delta}(t) &= \frac{1}{\tau_R}(\delta_C - \delta) \\ \dot{n}(t) &= \frac{1}{\tau_n}(n_C - n) \end{aligned} \tag{14}$$

δ, n - actual rudder angle and propeller speed

τ_R, τ_n - time constants associated with changes in rudder angle and propeller speed

In addition, the command values must not violate rate and limitation constraints, i.e.,

$$\begin{aligned} |\delta| &\le \delta_{lim} & |\dot{\delta}| &\le \dot{\delta}_{lim} \\ |n| &\le n_{lim} & |\dot{n}| &\le \dot{n}_{lim} \end{aligned} \tag{15}$$

SHIP-TUG TRAJECTORY SIMULATION

An inherent feature of the maneuvering program is the capability of simulating ship-tug trajectories for arbitrary control inputs and immediately viewing the results on an interactive graphics terminal. The ship-tug trajectories are generated in a fraction of real time with the ability to plot, in addition to the trajectory, the time histories for yaw, yaw rate, sway, surge, rudder, propeller rpm and tug controls for immediate evaluation. After the simulation program has been given the initialization parameters the interactive graphics allows the user to enter tug commands at selected time intervals. Interactively, he can view the resulting ship motions and assess the next tug command. If

the user wishes to compare his tug command skill with the optimal tug command for the same scenario, he can, while still in the interactive mode, generate the optimal maneuvering solution. The optimization program begins with the last trajectory generated by the user and iteratively calculates the optimal tug control. The resulting optimal ship trajectory, the time history of the optimal bow and stern tug commands or any of the other ship parameters can be plotted for the user to analyze.

The capabilities of the Maneuvering Program were extended to not only minimize the ship's cross track deviation but to minimize changes in the ship's speed through the channel transfer. Consequently, appropriate changes were made to the performance index to represent these optimization goals.

The performance index was originally selected as an integral square error criterion, a commonly accepted criterion used in optimal tracking studies. The index was augmented with a term representing the error or deviation in ship speed along with an appropriate weighting coefficient to provide the proper scaling between the two criteria, i.e.,

$$PI = \int_{t_o}^{t_f} (\Delta^2 + k\nu^2)dt \tag{16}$$

Δ = cross-track deviation

$\nu = U - U_o$, speed deviation

k = weighting constant

The cross track deviation is defined as the perpendicular distance to the channel centerline from the c.g. of the ship as illustrated in Figure 5. In order to smooth the transition between the two channel centerlines a blending arc can be specified of arbitrary radius in the region designated. This feature of the program eliminates the fictitious error peak which occurs when the ship passes the point of channel centerline intersection (way-point) and allows for a more realistic specification of the desired path.

OPTIMAL CONTROL ALGORITHM

Among the many numerical methods available for control optimization, the conjugate gradient method was selected because prior experience has proved it to be efficient in treating problems comparable in scope and mathematical complexity to the channel transfer problem. Experience has shown that the method converges more rapidly than the method of steepest descent and exhibits greater stability than the second-variational and Newton methods.

The conjugate gradient method developed for control problems in function space by Lasdon, et al. (5) is an extension of the Davidon-Fletcher-Power methods in the field of finite dimensional optimization (6). The iterative procedure which is designed to solve only the unconstrained optimal control problem requires storage of the ship trajectory, gradient trajectory, computation of the norm of the gradient, and storage of the actual direction of search. For the case where terminal conditions and inequality constraints are present, penalty

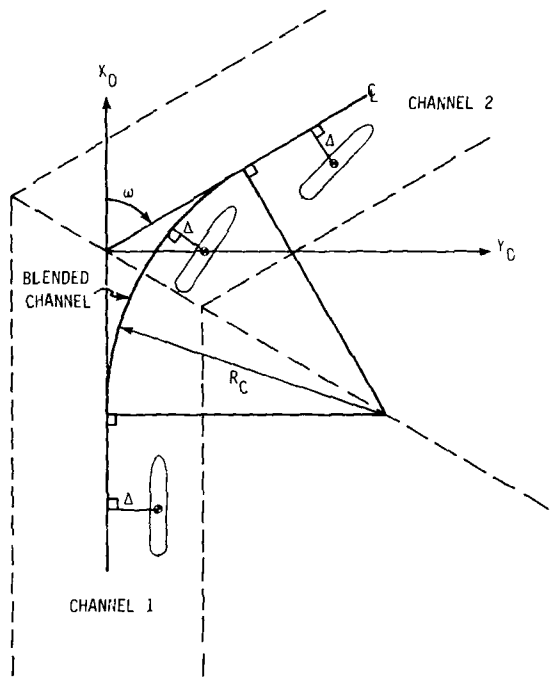

Figure 5. Channel Transfer Geometry

functions can be introduced to convert the problem to solving a sequence of unconstrained problems.

Using the notation of Lasdon the problem can be stated as:

minimize $J = \emptyset\ (x(t_f))$

subject to the constraints on the state vector, $\underline{x}$

given by $\dot{\underline{x}} = \underline{f}\ (\underline{x}, \underline{u}, t)$

with the initial conditions

$$\underline{x}\ (t_o) = \underline{c}$$

where t_o and t_f are fixed. In general, the state vector $\underline{x}$ is an n vector, while the control $\underline{u}$ is an m vector. For the ship channel transfer problem the state vector is composed of $\underline{x}^T = (x_o, y_o, \psi, r, u, v, E)$ determined by system state equations and is controlled by $\underline{u}^T = (\delta, n, F_B, \theta_B, F_S, \theta_S)$ composed of the rudder deflection, propeller speed and the bow and stern tug forces and pull angles.

This program can be a valuable asset in a wide spectrum of applications including extensive parametric studies to assess the sensitivity of optimal channel transfers to changes in ship design parameters, physical characteristics of the channel, and to changes in the strength and direction of local winds and tides. Oftentimes ships are controlled by a sequence of discrete rudder commands rather than in the continuous manner assumed in this study. The optimization program is being extended to include this type of restricted control format. The program would generate the optimal set of discrete rudder deflections to be used for a set of prespecified time intervals. An evaluation of the use of this type of suboptimal control will be based on the degree of degradation in the performance index.

OPTIMAL TRANSFERS USING RUDDER COMMANDS

Effect of Range from Way-Point

The maneuver begins with the ship, a 165,000 DWT CAORF tanker, at a range of 3000 ft. from the channel entrance and moving in a trimmed equilibrium condition along the x_o axis at a speed of 25 ft/sec (approximately 15 knots). The maneuver is completed within a 5 minute period and occurs at a time when the channel is assumed to be at slack tide with zero wind.

The optimal solution is shown as the solid trajectory line in Figure 6(a) with the ship location and relative attitudes given at several times along the trajectory. Note that the optimal rudder solution initially commands a slight heading change to port and then proceeds with the expected hard over turn to starboard. The rudder remains against the starboard stop (-35^o) for 60 seconds and just before the ship reaches the way-point (112 sec) a rudder reversal begins with the rudder held against the port stop for 18 seconds. The optimal solution then slowly returns the rudder to the trimmed condition.

Since the optimal rudder control here commands hard over deflections, a further study was carried out to determine whether a greater initial range would improve the channel transfer and reduce the use of maximum rudder deflections. The range was therefore increased to 6000 feet, thus doubling the maneuvering time to the way-point to 4 minutes. With this additional maneuvering time, the use of maximum starboard rudder is slightly reduced and the need for maximum port rudder is eliminated as seen in Figure 6(a). In both results the beginning of the hard-over starboard command occurs at a range of 2400 feet from the way-point. This is equivalent to approximately 2.5 shiplengths and a time of 96 seconds from the way-point in anticipating the 45^o change in course.

Effect of Path Curvature

Circular arcs were drawn connecting the entrance and exiting legs of the channel, with radii of 2000 ft., 5000 ft., and 10,000 ft. respectively, to represent the designated tracks, as illustrated in

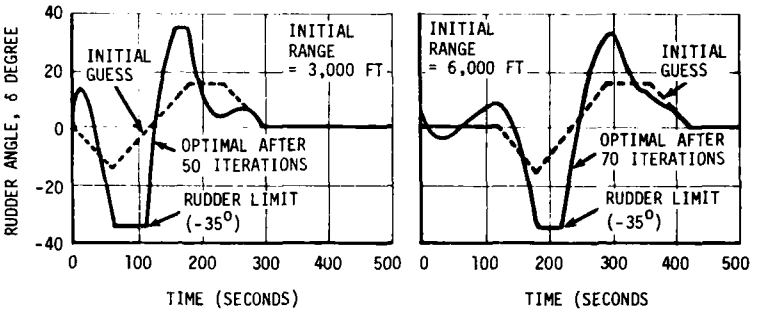

(a) OPTIMAL RUDDER COMMAND

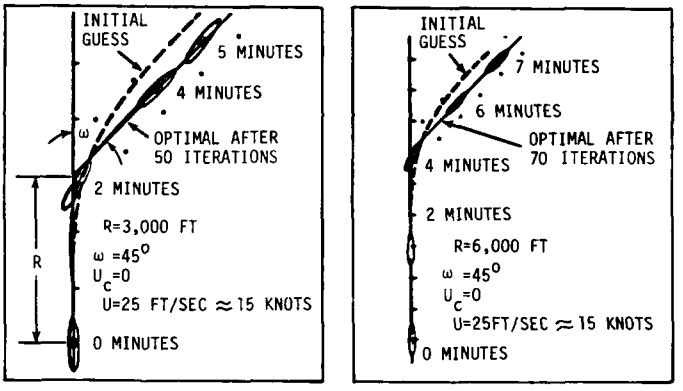

(b) OPTIMAL CHANNEL TRAJECTORY

Figure 6. Optimal Channel Transfer for 165,000 DWT Tanker; Channel Centerline is Designated Track , Initial Range 3000 and 6000 Feet

Figure 7. The optimal rudder angles to achieve minimum deviation off these assigned tracks were calculated and are shown in Figure 8 for the 165,000 DWT tanker initially moving at 15 knots and starting at a point 3000 feet from the way-point with zero wind and zero current.

The maximum deviations off track with these rudder histories were ± 20 feet, + 10 feet, +6 feet and -10 feet respectively. It should be noted that large rudder angles are required in the tighter turn. Also, before the main rudder command is given to initiate the turn, the rudder is moved slightly back and forth to prepare for the turn.

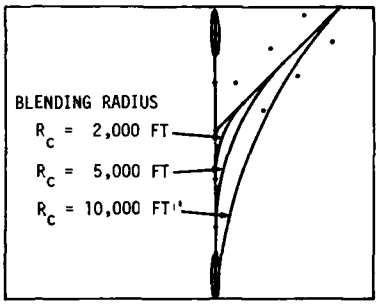

Figure 7. Transitional Arcs for 45° Turn

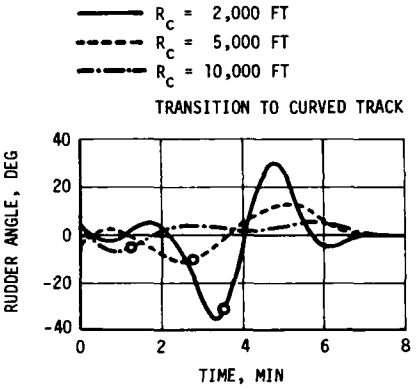

Figure 8. Optimal Rudder Angle for Various Radius Turns; 165,000 DWT Tanker, 15-Knot Ship Speed, No Current, No Wind, 6000 Foot Initial Range

At the point where the right rudder is applied to initiate the turn, the ship has developed in all cases a small counterclockwise turn rate. The right rudder is increased until the ship reaches the transition point, and thereafter the rudder is moved steadily over to the left during the turn. At the transition point, although the ship is

perfectly on track, it has developed a substantial turn rate and lateral velocity before beginning the turn. The same behavior is indicated for each turn curvature. For the 2000 ft. radius turn, the right rudder is applied 1.10 minutes (1673 feet or 1.76 ship lengths) before reaching the transition point. The yaw rate developed at the beginning of the arc is 0.6°/second and the lateral velocity 1.76 knots. For the 5000 ft. curvature bend, right rudder is applied about 1.37 minutes from the transition point (approximately 2080 feet or 2.19 ship lengths). The corresponding yaw rates and lateral velocity are 0.2°/second and 0.5 knots.

Figure 9 shows the ship trajectory when a step input of 35° right rudder is applied to the 165,000 DWT tanker. Superimposed is an arc with a 2000 ft. radius of curvature, which very closely fits the trajectory over a considerable portion of the initial turn. From this it appears that a 2000 ft. radius turn is about the minimum that can be attained by the ship with a minimum deviation off track. Tighter turns result in larger deviations and overshoots.

Figure 10 shows the transitional arcs that were established as desired tracks in three areas of New York Harbor for which optimal studies were performed. The radii of these arcs are 6500 ft., 3500 ft. and 11,000 ft., respectively, which approximately cover the range of values that were compared above.

OPTIMAL TRANSFERS USING RUDDER AND PROPELLER COMMANDS

The purpose of this study is to illustrate the capabilities of the optimization program to minimize the average cross-track deviation while maintaining the ship's initial speed. The steering task is to navigate through a channel transfer characterized by a 45 degree change in heading with a 5,000 ft. blending arc as depicted in Figure 7. The maneuver begins with the 80K DWT CAORF Tanker at an initial range of 5,000 ft. from the channel entrance and moving in a trimmed equilibrium

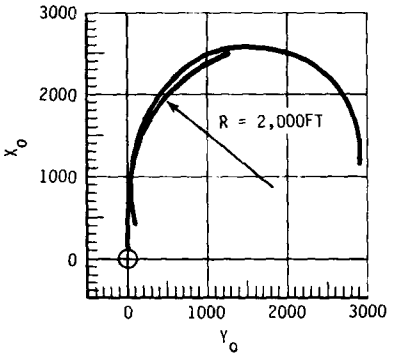

Figure 9. Turn Trajectory for Step Input δ = -35; 165,000 DWT Tanker, 15-Knot Ship Speed, No Wind, No Current

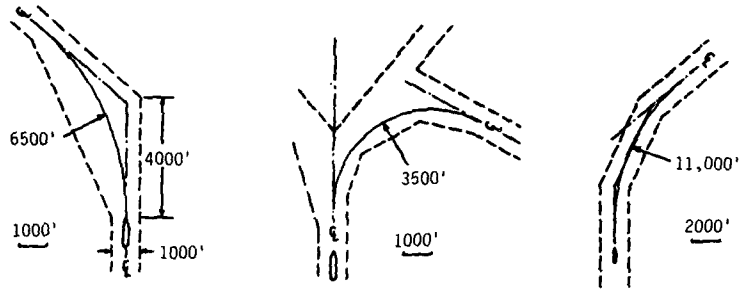

Figure 10. Transitional Arcs for Three Areas in New York Harbor

condition along the X_o axis at a speed of 10 knots. The maneuver is completed within a 10 minute period and occurs at a time when the channel is assumed to be at slack tide with no wind.

The optimal solution is difficult to distinguish from the desired path in Figure 7 since the maximum cross track deviation is only $\pm$10 ft. while the maximum deviation in ship speed is less than 0.1 knots throughout the transfer. The optimal rudder solution given in Figure 11 initiates a starboard rudder command 1.0 minutes into the trajectory indicating that the anticipation range to the transition point is approximately 2,000 ft. or 2 ship lengths. Note that the 5,000 ft. blending arc only requires a maximum rudder deflection of 5 degrees to minimize cross track deviation. The starboard rudder input lasts for a period of 4.5 minutes followed by a rudder reversal to port to align the ship with the second channel centerline. The optimal propeller rpm solution which maintains the speed is summarized in Figure 11. It is evident from the optimal propeller command that as the ship traverses the region of the blending arc additional power is required to offset the increased drag induced in the turn. A maximum increase of only 10% in propeller rpm is required to maintain the ship's speed to within 0.1 knots of its initial speed.

This study was repeated for the same channel transfer conditions with the addition of a 50 knot wind blowing from the SW (225°). The wind is crossing the port beam during the first leg and becomes a following wind as the ship completes the turn.

For the transfer with wind the maximum cross track error is less than $\pm$12 feet while the maximum speed error is once again held to $\pm$ 0.1 knots. The corresponding optimal controls for the rudder and propeller rpm are shown in Figure 12. At the initialization of the trajectory with the wind blowing at 50 knots from 225° the equilibrium values for the rudder and propeller rpm are -4.5° and 57.1 rpm respectively. The optimal rudder command initiates the starboard turning maneuver essentially at the same point (1 minute) as in the case of no wind. A maximum starboard rudder of -10.5 deg. is reached at 2.5 minutes into the

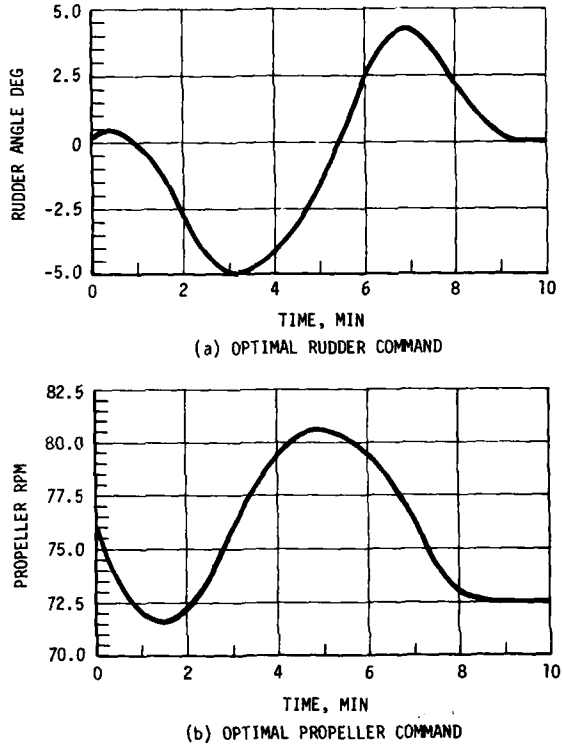

Figure 11. Optimal Rudder and Propeller Commands; 80,000 DWT Tanker, 10-Knot Initial Speed, No Current, No Wind, 5000 Foot Initial Range

trajectory but this represents only a 5 degree variation from the equilibrium value (-4.5 deg), the same as developed in the study without wind.

OPTIMAL TRANSFERS USING TUG CONTROL

The purpose of this study is to illustrate the capabilities of the ship-tug maneuvering program to navigate the 80K CAORF Tanker with the aid of only bow and stern tugs through a channel transfer characterized by a 45 degree turn and smoothed with a 4000 ft. blending arc as depicted in Figure 13. Once again the objective is to minimize the average cross-track deviation from the prescribed path while maintaining the ship's initial speed of 4 knots. The maneuver begins with the

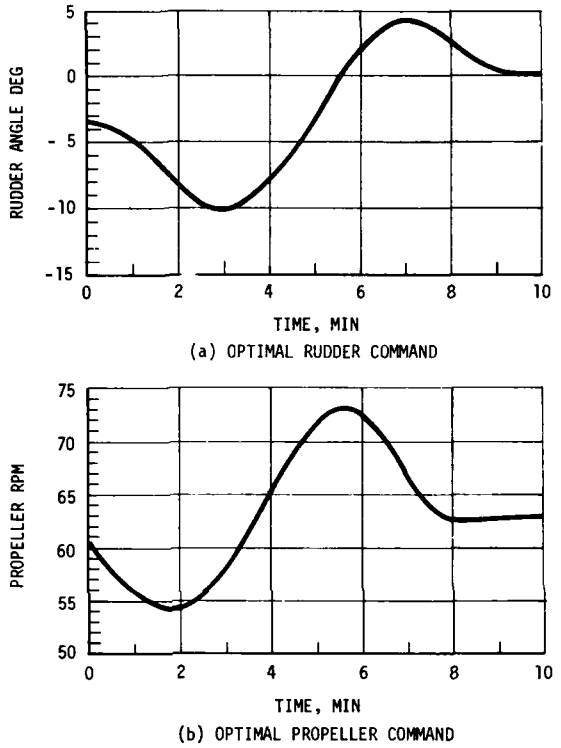

Figure 12. Optimal Rudder and Propeller Commands; 80,000 DWT Tanker, 10-Knot Initial Speed, No Current, 50-Knot Wind S.W., 5000 Foot Initial Range

tanker at an initial range of 3000 ft. from the channel entrance and with its propeller turning at only 0.1 rpm. This propeller speed is maintained with the rudder held amidships throughout the transfer. For the duration of the maneuver only a single bow and stern tug are in attendance and are ordered to use 15,000 lbs of bollard pull, approximately one half of their maximum capability. Therefore with the tanker's engine shut down and with its rudder held fixed, the task of maneuvering the tanker is solely dependent on the two tugs.

The Ship-Tug Maneuvering Program generated the optimal pull angle time histories for the bow and stern tugs which result in minimizing the performance criterion. It is difficult to distinguish the optimal ship trajectory from the desired path in Figure 13 since the maximum

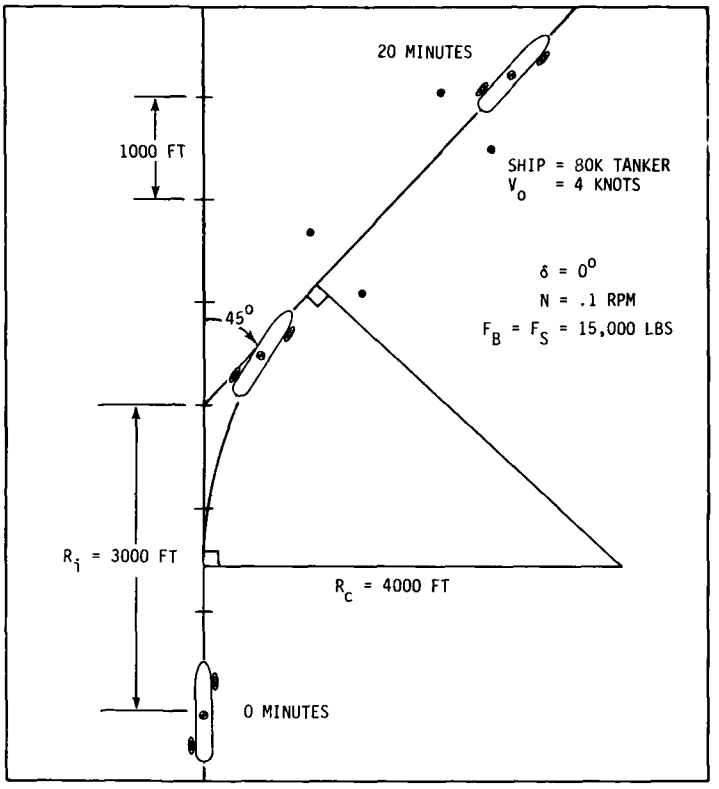

Figure 13. Optimal Channel Transfer with Tugs

cross-track deviation is only ±25 ft. The cross-track deviation and the deviation in ship speed are more clearly shown as time histories in Figure 14. The extent of the errors in path and speed deviation are indicative of the rather limited tug resources used in this example; that is, with the tugs restricted to only half power the average path error is 13 ft. while the average speed variation is 0.3 knots. It is expected that as the allowable tug forces are increased to their maximum values or as additional tugs are used there should result a corresponding reduction in path and speed deviations.

The optimal time histories for the tug pull angles are summarized in Figure 15. Note that the pull angle for the bow tug has a much larger angular excursion than that of the stern tug. The bow tug begins with a pull angle of 230^o, retarding forward motion and initially

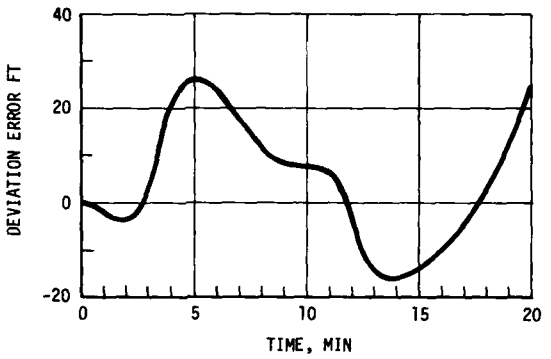

(a) CROSS-TRACK DEVIATION ERROR

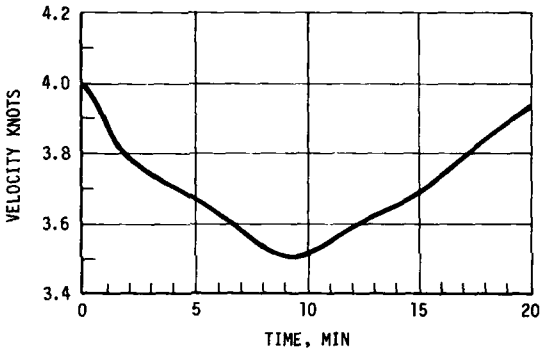

(b) SHIP SPEED

Figure 14. Optimal Channel Transfer with Tugs, Cross-Track Deviation and Ship Speed

turning the ship to port. This is quickly modulated within the next 2-3 minutes so that the bow tug pulls at 90° to initiate the starboard turn. The 90° pull direction is maintained for more than 7 minutes and as the ship reaches the channel intersection the bow tug starts to reverse its direction of pull to the port side (at 13 minutes the tug is pulling at -45° in the port direction). At the completion of the transfer the ship's yaw rate has been nulled and the bow tug is pulling at 0°.

In contrast to the 230° change in pull angle required for the bow tug, the stern tug varies its angle by only ±18°. During the period when the bow tug maintains a starboard pull direction the stern tug varies its pull (push) direction to port with a sinusoidal variation up to a maximum of only -18°. The optimal solution appears to assign the

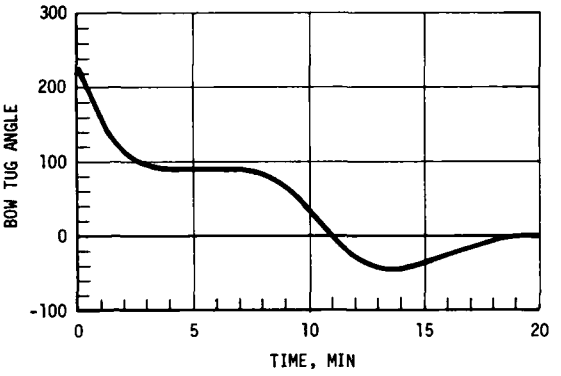

(a) BOW TUG PULL ANGLE

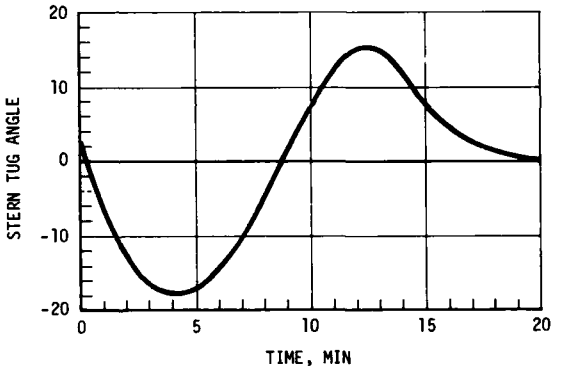

(b) STERN TUG PULL ANGLE

Figure 15. Optimal Tug Pull Angle Commands

task of turning to the bow tug while relying on the stern tug to maintain speed through the channel transfer.

CONCLUSION

The Optimal Ship Maneuvering Program and its extension to ship-tug operations have provided a valuable insight into the capabilities and limitations of ships with and without tug support in performing safe maneuvers in restricted waterways. These studies support on-line experiments on the CAORF simulator, which permits the evaluation of man-ship performance in "real time." Some of the most recent experiments at CAORF have emphasized ship-tug operations involving tug control in maneuvering and under conditions of impaired maneuverability.

The optimal programs described previously provide a basis for comparing the observed pilot strategies and ultimate performance with a theoretical optimal. The present programs are based on continuous controls, but are being extended to consider discrete control, which will be more appropriate in describing real-life operations.

Ultimately, these programs could lead to the development of shipboard equipment to assist the mariner in decision making, etc., and used in training programs to demonstrate strategies for ship and tug maneuvering.

REFERENCES

(1) Kelley, J. R. and Drazin, D. H., "Tanker Berthing Evaluation," Full Scale Trail Results Employing the MSC Tanker Yukon and a Rotatable, Right-Angle Drive Tugboat Tina, David Taylor Naval Ship Research and Development Center Report, DTNSRDC - 79/066, July 1979.

(2) Eda, H., "Low Speed Controllability of Ships in Wind," Journal of Ship Research, Vol. 12, No. 3, pp 181-200, September 1968.

(3) McIlroy, W. and Carpenter, G., "Technical Aspects of Fast-Time Simulation at CAORF," Proceedings of the Third CAORF Symposium," Oct. 1979, USMMA, Kings Point, NY.

(4) Fujii, H. and Tsuda, T., "Experimental Researches on Rudder Performance, (2) and (3)," Journal Society Naval Architects, Japan, Vol. 110, Dec. 1961; Vol. 111, June 1962.

(5) Lasdon, L., Mitter, S., and Waren, A., "The Conjugate Gradient Method for Optimal Control Problems," IEEE Transactions on Automatic Control, Vol. 12, No. 2, April 1967.

(6) Fletcher, R. and Powell, M., "A Rapidly Convergent Descent Method for Minimization," British Computer Journal, pp. 163-168, June 1963.

Dr. McIlroy is a member of Grumman Data Systems Corporation and Head of Research at CAORF, Kings Point, New York, USA. Dr. Carpenter is a Research Scientist with Grumman Aerospace Corporation, Bethpage, New York, USA.

This work was performed under contract with the U.S. Maritime Administration in support of the CAORF (Computer Aided Operations Research Facility) operation at Kings Point, N.Y. We wish to acknowledge the enthusiastic support given to this project by J. J. Puglisi, CAORF Managing Director, and J. J. Johnsen, CAORF Operations Manager.

APPENDIX

SHIP CHARACTERISTICS AND MODELLING COEFFICIENTS

Table 1. Hydrodynamic Coefficients for the 80K DWT Tanker

Draft = 40 ft.	$A = L^2$	
$m' = 1.380$ E-2	Water Depth = 48 ft.	
$I_z' = 8.045$ E-4	Length, L = 763 ft.	
	Beam B = 125 ft.	
Length-beam ratio	L/B	6.10
Beam-draft ratio	B/H	3.13
Block coefficient	C_B	0.80
Trim	TRIM	EVEN
Draft/water depth	H/DW	0.83
Beam/water width	B/W	--

Hydrodynamic Moment Coefficients	a_0	0	0.0
	a_1	V	-8.285 E-3
	a_2	R	-3.094 E-3
	a_3	D	0.0
	a_4	Y	0.0
	a_5	V2R	-6.450 E-2
	a_6	VR2	2.520 E-2
	a_7	V3	5.622 E-4
	a_8	R3	-4.400 E-4
	a_9	D3	0.0
	a_{10}	Y3	0.0
$I_z' - a_{11}$		RDOT	1.743 E-3
	a_{12}	VDOT	0.0

Table 1. Hydrodynamic Coefficients for the 80K DWT Tanker (Cont)

Hydrodynamic Force Coefficients	b_0	0	0.0
	b_1	V	-2.888 E-2
	b_2	R	3.023 E-3
	b_3	D	0.0
	b_4	Y	0.0
	b_5	V2R	1.096 E-1
	b_6	VR2	-8.028 E-2
	b_7	V3	-1.582 E-1
	b_8	R3	1.810 E-3
	b_9	D3	0.0
	b_{10}	Y3	0.0
	b_{11}	RDOT	0.0
	$m' - b_{12}$	VDOT	3.090 E-2
	c_0		-7.246 E-4
	$m' + c_1$		3.090 E-2
	c_2		-6.509 E-3
	c_3		0.0
	$m' - c_4$		1.440 E-2

Table 2. Propulsive, Aerodynamic, Rudder Coefficients for the 80K DWT Tanker

Propulsive Coefficients ($u > o$, $n > o$) u = ft/sec n = rps	C_{P_1}	-5.090 E+1
	C_{P_2}	-4.452 E+3
	C_{P_3}	1.560 E+5
Aerodynamic Coefficients	C_{X_1}	-1.985 E-2
	C_{X_2}	9.644 E-4
	C_{X_3}	5.939 E-3
	C_{X_4}	-7.369 E-4
	C_{X_5}	1.017 E-3
	C_{Y_1}	-3.108 E-2
	C_{Y_2}	7.963 E-4
	C_{Y_3}	5.145 E-3
	C_{Y_4}	3.094 E-4
	C_{Y_5}	5.513 E-5
	C_{N_1}	2.141 E-3
	C_{N_2}	-2.014 E-3
	C_{N_3}	2.161 E-4
	C_{N_4}	2.632 E-5
	C_{N_5}	-2.264 E-4

Table 2. Propulsive, Aerodynamic, Rudder Coefficients for the 80K DWT Tanker (Cont)

Rudder Coefficients	a_{R_1}	-8.350 E+5
	a_{R_2}	7.038 E+6
	a_{R_3}	-1.369 E+8
	a_{R_4}	6.104 E+5
	a_{R_5}	-5.143 E+6
	a_{R_6}	9.998 E+7
	b_{R_1}	2.329 E+3
	b_{R_2}	-1.963 E+4
	b_{R_3}	3.816 E+5
	b_{R_4}	-1.443 E+3
	b_{R_5}	1.216 E+4
	b_{R_6}	-2.365 E+5
	c_{R_1}	-3.120 E+2
	c_{R_2}	2.630 E+3
	c_{R_3}	-5.111 E+4

Table 3. Hydrodynamic Coefficients for the 165K DWT Tanker

Draft = 52.2 ft.		$A = L^2$	
m' = 1.46 E-2		Water Depth = 56 ft.	
I_z' = 9.13 E-4		Length, L = 951 ft.	
		Beam B = 155 ft.	
Length beam ratio	L/B	6.12	
Beam draft ratio	B/H	3.00	
Block coefficient	C_B	0.81	
Trim	TRIM	EVEN	
Draft/water depth	H/DW	0.93	
Beam/water width	B/W	--	
Hydrodynamic Moment Coefficients	a_0	0	0.0
	a_1	V	-8.500 E-3
	a_2	R	-3.300 E-3
	a_3	D	-1.450 E-3
	a_4	Y	0.0
	a_5	V2R	-2.500 E-2
	a_6	VR2	1.400 E-2
	a_7	V3	3.300 E-3
	a_8	R3	0.0
	a_9	D3	-2.000 E-3
	a_{10}	Y3	0.0
$I_z' - a_{11}$		RDOT	1.800 E-3
	a_{12}	VDOT	0.0

Table 3. Hydrodynamic Coefficients for the 165K DWT Tanker (Cont)

Hydrodynamic Force Coefficients	b_0	0	0.0
	b_1	V	-1.750 E-2
	b_2	R	4.300 E-3
	b_3	D	3.300 E-3
	b_4	Y	0.0
	b_5	V2R	2.000 E-2
	b_6	VR2	-2.000 E-2
	b_7	V3	-4.200 E-2
	b_8	R3	0.0
	b_9	D3	-1.000 E-3
	b_{10}	Y3	0.0
	b_{11}	RDOT	0.0
	$m' - b_{12}$	VDOT	2.640 E-2
	c_0		-5.200 E-4
	$m' + c_1$		2.640 E-2
	c_2		-2.000 E-3
	c_3		-1.000 E-3
	$m' - c_4$		1.540 E-2

Table 4. Propulsive and Aerodynamic Coefficients for the 165 DWT Tanker

Propulsive Coefficients ($u > o$, $n > o$) u = ft/sec n = rps	C_{P_1}	-7.380 E+1
	C_{P_2}	-4.168 E+3
	C_{P_3}	2.085 E+5
Aerodynamic Coefficients	C_{x_1}	-1.140 E-2
	C_{x_2}	0.0
	C_{x_3}	0.0
	C_{x_4}	0.0
	C_{x_5}	0.0
	C_{y_1}	-2.880 E-2
	C_{y_2}	0.0
	C_{y_3}	0.0
	C_{y_4}	0.0
	C_{y_5}	0.0
	C_{N_1}	4.400 E-3
	C_{N_2}	-1.700 E-3
	C_{N_3}	0.0
	C_{N_4}	0.0
	C_{N_5}	0.0

VESSEL AND MARINE TRAFFIC BEHAVIOUR ANALYSIS IN CONSTRAINT WATERS

by dr. J.P. Hooft*
and ir. C.C. Glansdorp**

1. Introduction

This paper discusses the analysis of the navigability of a fairway.
The navigability of a fairway is determined by the behaviour of the ships sailing in this fairway and by the behaviour of the traffic flow resulting from the manoeuvres of the ships as they influence each other.
When information on the behaviour of the ships and the resulting traffic flow is available a judgement can be given about the navigability of the fairway from a nautical point of view. This judgement will be subjective when the predicted navigability is compared to the traffic behaviour known from existing situations. However a more objective judgement can be made when use can be made of criteria which have been developed from the analysis of navigability under a variety of conditions.
The criteria on which the navigability will be judged should be independent of the situations to be considered.

The behaviour of one ship is described by a set of actions and resulting phenomena which will be observed during the passage through of the fairway such as for example:

- the trajectories of the ship and the space needed by the ship
- the physical efforts (use of rudder and main engine, tug assistance, etc) to perform the intended manoeuvres.
- the efforts of the control systems (including human actions) to realize the intended manoeuvres.

The combination of actions of the controlled vessel is a result of the behaviour of each of the elements in which the controlled ship can be assumed to consist of, such as:

1. the manoeuvrability of the vessel which is determined by the vessel's reactions to control devices and/or the environmental disturbances.
2. the characteristics of the control system (behaviour of pilot or navigator and helmsman or the automatic pilot)
3. the characteristics of the navigation aids.

The part of the ship's manoeuvrability that is determined by the relation between the control action (rudder angle) and ship's manoeuvre is called the attainability of the steered ship. Sailing in the fairway considered, one describes the attainability of the ship by the collection of all manoeuvres generated by any kind of rudder order that can be realised. It should be noted that the attainability will depend on environmental conditions such as wind and current.

Aside of the attainability one also may be interested in other aspects of the ship's manoeuvrability such as the dynamic stability or the sensitivity. In this aspect the sensitivity is related to changes in the manoevrability due to changes in, for example the following conditions: a break down of the main power, a change in waterdepth etc.

From the above considerations it will be seen that for the prediction of the behaviour of vessels and of the resulting traffic in the fairway a proper description is needed of all factors that effect the sailing conditions; this will be discussed in section 2.

* Head Ship-Handling Research, MARIN
** Head of the Navigation and Ship-Handling Department, MARIN

In section 3 a discussion will be given with regard to the methods at which the navigability of a fairway can be analyzed. In the following sections some elucidation will be given of the possible results that can be acquired when performing such analysis.

2. Factors influencing the ship's behaviour

In this section a brief discussion will be given about the factors that have to be considered when analysing the navigability of a fairway.

Ships: For most fairways the navigability largely depends on the behaviour of a reference ship. Such a ship on which the dimensions of a fairway is based can either be the largest vessel that is to be expected to use the fairway, a special type of ship with unconventional manoeuvring properties or a vessel loaded with hazardous or noxious cargoes.

The manoeuvrability of ships can often be analysed by means of static considerations about the disturbing forces (wind and current) that have to be counteracted by the steering forces (rudders, lateral thrusters, tugboats or by means of simplified dynamic descriptions (K and T values of Nomoto [1]). These considerations are especially valuable when comparable information is available from full scale observations.
However when detailed information is required about the manoeuvrability of special type of ships the complete mathematical model and the relevant coefficients of this model should be determined by means of an elaborate program which provides all manoeuvring characteristics of the ship. A simulation using this mathematical model can be used to derive these manoeuvring characteristics assuming artificial control functions.

Ship's control: When during normal operations all the hardware is functioning correctly then the most important part of the control is the human behaviour (pilot, navigator, helmsman etc). Though human behaviour is predictable to a certain extent it has not been possible to describe the human behaviour properly by means of mathematical formulae for all possible conditions.
Those predictions of human behaviour which are available are related to known situations in which observations have been made of special groups of people under specified conditions. For this reason often use is made of the results of simulator tests.
Special attention in the analysis of vessels control should be devoted to the characteristics of the navigational aids and traffic management on the ship and on shore such as leading lights, Decca system, shore based traffic guidance etc.

Environmental conditions: For the analysis of the navigability of a fairway all details with regard to the environmental conditions such as changes of the bottom profile, the currents, the allowable speeds (e.g. due to bank erosion), the availability of tugs etc. should be properly included.

An operational analysis of the fairway may require some additional information about the hydraulic characteristics. These can be obtained by physical model-testing in addition to full scale observations.

3. Considerations concerning navigability

Each system will be acceptable when the pre-set aims of the system will be reached by means of "acceptable" efforts. Mostly the definition of these aims are clear: the shipping will not exceed the pre-set boundaries of the fairway. However the criteria at which these aims are reached are mostly lacking. These criteria are especially important when the aims are not reached so that the

(visual-, wind- and current) conditions have to be established under which the aims can still be reached.

To be more specific the analysis of the navigability refers to such items as:
a. the trajectories of the ship: often some rules of thumb are used in which the channel width (or width of lane) is presented as a number of ship's breadths. In such considerations one assumes some additional distance beteen the channel banks and the sailing lane of the vessel though in practice vessels often sail close along the banks without problems.
b. the efforts at which the ships are navigated through the fairway: in this aspect one often considers the amount of changes of the rudder angle, propellor r.p.m., the use of tug assistance etc. The efforts undertaken by the human operators are also considered sometimes though measurements of these efforts (e.g. expressed by the heart beat) are seldomly performed.

Generally the navigability of a fairway is defined by "the ease at which the ship can be manoeuvred through the fairway". This does not mean that the fairway is well navigable when the ships can pass through it smoothly with little effort, but also that a change of conditions in the fairway will not affect the ship's behaviour very much. This consideration leads to the conclusion that the fairway is well navigable when:
a. the ship's can be manoeuvred well in the fairway and,
b. the behaviour of the controlled ship will not alter much at changing conditions of the fairway.

4. Methods of analysis

In this section a discussion will be given in relation to the methods in which the navigability of a fairway can be analysed. It is assumed that when adopting these methods all relevant information about the characteristics of the fairway is available in addition to the information of the characteristics of the ships, of the manoeuvres to be executed and of the environmental conditions.
The several options of analysis may be discussed in such a hierarchical order that each following method will be more specific and detailed when the previous method has not lead to a reasonable conclusion.
In the remainder of this paragraph the two extreme methods will be discussed: a feasibility study on the one hand and a complete simulator study on the other. They are called method A and method B respectively.

Method A: This method is based on finding the answer of the following query: When the manoeuvrability of the reference vessel van be sketchily described, is it possible that this vessel can be navigated through the fairway under the condition that adequate steering power remains available? For this kind of analysis the vessel's controllability must be roughly estimated. Especially some information with respect to the manoeuvres which are induced by the rudder angle should be known to determine the attainability of the ship in the fairway concerned. Generally this information is available from current literature. Hydrographic details and information with regard to the tidal regime are also necessary to this analysis. This method may be defined: a feasbility study.

After having evaluated the navigability of the fairway in this way it may happen that one can not reach a decision. This might be the case when too little information is available or when the traffic situation of the fairway is so complicated that a more detailed analysis is required. One then applies method B.

Method B: In order to evaluate the controllability of a reference vessel or the navigability of the fairway and to locate possible bottlenecks one generates a complete simulation of the anticipated real life situation with the aim of a manoeuvring simulator.
Comments with respect to method B are: When there is no possibility for simulation to estimate the controllability of a given ship, then the practical consequence will be to perform the first passage of the reference vessel in the fairway concerned with great care. During such a trial special attention is given to the other ships; more pilots are on the bridge; more tugboats are available etc. Based on this experience acquired during one or more of such trials, conclusions may be drawn about the acceptability of the ship to navigate this fairway or with regard to additional precautions to be taken.

It will be obvious that in method B for analyzing the navigability of a fairway full credit can be given to the specific skill of the mariners. In this way insight will be gained with respect to the question: "How will the passage through the fairway be realized?" This information is of importance for establishing the changes in exceeding limits within which the manoeuvres of the ship should remain. Such limits refer to the location of the ship, but also to the use of the control devices and of the (mental) load of the mariners.
This method will be referred to as the simulator method.

5. Feasibility study of the navigability of a fairway
A feasibility study of the navigability of a fairway may be based upon the relations between various parameters such as[2]:
- dynamic sailing characteristics of a vessel
- configuration of the fairway
- external effects like the tidal regime, wind and waves
- characteristics of the aids to navigation

An illustration of such a study may be given by the following steps:
- Calculation of required under keel clearance
- Calculation of minimum required path-width, ignoring effects of wind and tidal stream
- Calculation of available depths below chart datum and of required depths and the specification of locations where available depths are smaller than the required depths.
- Calculation of time intervals when the required depth is less than the available depth without taking into account meteorological effects (sea state zero, no wind).
- Calculation of these time intervals but now taking into account the meteorological effects like wind and sea state provided the equilibrium rudder angle to compensate for wind effects does not exceed a given preset value.

The under keel clearance consists of a number of factors which may be regarded as stochastic variables which are normally distributed. To all contributing factors an average value and a standard deviation should be assigned.

Main factors in the determination of the under keel clearance are: squat and draught increase due to motions of the vessel in a certain sea state.

The draught and depth accuracy do not contribute significantly to the average values but the accuracy of the hydrographic survey is reflected in the standard deviation of the depth. The vessel's loading condition sometimes causes a hog or a sag thus the nominal draughts do not apply and have to be corrected, even though the reading of draughts and the calculation of the corrected draughts due to fuel consumption are accurate to a certain extent.

When using "visual navigation" it is impossible to determine a vessel's position in a fairway exactly so a certain width should be provided to compensate for this inaccuracy. It is obvious that in case of visual navigation the configuration of leading lines and buoy-gates is important together with the characteristics of the unaided eye of the navigator in charge.

Another factor contributing to the required path-width in ideal circumstances is the way a vessel behaves when one is trying to maintain a course whether by the helmsman or by autopilot. The path width as a result of course keeping ability is sometimes called manoeuvring lane. One will often resort to the results of measurements in real life when making an estimate of the width of this lane.

The use of visual aids to navigation alone implies the need for specification of visibility limits below which the use of the leading lines and buoy-gates is not possible.

The minimum value of the required path-width under ideal circumstances alone is not sufficient to determine the extreme limit of navigability of the fairway. Since this value of the required path-width is known for various locations (although variable due to variations in accuracy of the visual aids to navigation) the available depth should be greater than the required depth. When Fair Sheets are available the determination of available depths is more precise then when using the normal charts for this purpose. As usual, these depths are given below chart datum and hence the vertical tidal motion is not taken into account in this step. When the fairway is divided into a number of locations (these locations have to be carefully selected) all the depths across the fairway at a given location and within the required path-width are carefully scrutinised to find the maximum depth.

This scrutiny should be extended to all locations of the fairway when the depths required for the vessel based on the Under Keel Clearance are smaller than the available depths the fairway is said to be navigable in a vertical sense. When the depths required for the vessel are greater than the available depths we must pay attention to the tidal regime.
Therefore knowledge of this regime is necessary.

Generally the mean extremes in the tidal regimes are considered: neap and spring tide. Often use is made of a socalled mean tide but the definitions of this tide vary. It should be remembered however that even neap and spring tide values vary with time since they represent an average condition. The calculation starts with the selection of a tidal range. It is necessary to calculate the tidal height at all locations of the fairway as a function of time. This is generally not an easy task to perform, since tedious calculations are involved. Co-Tidal charts may be used to good purpose in this connection. When vertical tidal motions are used, naturally also the horizontal tidal motions have to be used. The strength and direction of the tidal stream should be known at all locations of the fairway for all relevant times. In fact the draught of the reference vessel will govern which rate of the tidal streams to use when it turns out that these rates vary with depth.

When it is assumed that a vessel will sail parallel to the axis of the fairway the tidal stream vector should be decomposed into components along the fairway axis and at a right angle to it.
The along axis components will affect the vessel's groundspeed and consequently the times of passage for all locations can be calculated as a function of time relative to some arbitrary zero. This zero is usually chosen at the time of HW or LW of a primary or secondary port in the vicinity of the fairway.

Cross channel components of the tidal stream are normally compensated for by changing the heading of the vessel to ensure that its track coincides with the fairway axis or is parallel to it.
This difference between heading and track contributes to the vessel's path-width. Now the minimum required path-widths for all locations and at all times relative to "zero time" can be calculated when the effects of the tidal regime are taken into account.

The available depths at the time of passage within this newly calculated required path-width are now determined. The depths below chart datum and the calculated tidal heights at the passage times are added to obtain the available depths. It is now possible to construct a time window with the constraint that the required depths are smaller than the available depths. This time window specifies an interval within which departure times from the entrance of the fairway must fall for the speed selected. It is also possible that no transit is possible for the selected reference vessel. Sometimes an increase in speed (when possible) is necessary to open the time window, but no spectacular results should be expected. The results so far have shown the possibilities of transit for the reference vessel through the fairway in almost ideal conditions.

It should be pointed out that the results only apply to the selected tidal range. So at least the extremes -neap and spring tide- should be taken to arrive at definite conclusions as regards transit limitations for the vessel considered.

A calculation of the equilibrium rudder - and driftangle when the vessel is subjected to an arbitrarily chosen windload is necessary to counter the effects of wind. For this calculation we require the hydrodynamic damping derivatives as a function of the depth/draught ratio, the rudder-area and the wind-area to obtain values for the required rudder angle and drift angle which will maintain an equilibrium condition.

It may be argued that when this required rudder angle exceeds a certain value the room to manoeuvre the vessel is restricted when traffic conditions require the use of rudder. An attempt to fix a value for this preset rudder angle implies a consideration of the rudder angle in use when negotiating bends in the fairway. Sometimes 15 degrees rudder angle are used as the preset value, so that 20 degrees are left for negotiating bends and to manoeuvre the vessel when the traffic condition requires such.

Now we have the possibility that wind conditions should be restricted in order to maintain the required rudder angle at the preset value. The wind forces are only slightly affected by the ship's speed through the water and are largely dependent on the windspeed.
The compensating hydrodynamic forces vary with the square of the vessel's speed through the water. Hence the vessel's speed is an important factor. The lower the vessel's speed the lower the resulting windspeed which induces the maximum permissable rudder angle. The vessel's damping derivatives are very sensitive to under keel clearance and this means that a number of calculations should be performed with varying depth/ draught ratios. The driftangle contributes to the path-width which should be calculated. There is no need, however, to extend these lane-width calculations to windspeeds and -directions which are not allowed for the vessel concerned.
The required path-width in ideal conditions is known and the lane width contribution due to wind is now added to it to establish required path- widths at all possible times of passage for each location taking into account the limitations in wind conditions. It may be anticipated that the newly calculated required path-width is larger than the one calculated for the ideal condition. Now the smallest depth below chart datum should be found within this path-width.

When the minimum depth below chart datum has been found at all locations within this required path-width the actual depths at all times of passage may be calculated by adding the tidal height to the depths found. Since we know the required depths at various states of the sea, again time intervals may be constructed provided the available depth at each location is larger than the required depth in a given sea state.

When it turns out that no time intervals can be constructed no transit is possible under the assumed conditions. Note that it has been assumed that windloads do not change materially the vessel's speed through the water, so that a new calculation of times of passage of any location has been omitted.

The specification of the time intervals, which is done by stating a range of departure times from the starting point of the fairway, should indicate as well the reference vessel, the tidal range, the average assumed speed through the water of the vessel and the restrictions in wind conditions and sea states that are applicable to those intervals. An example of a time interval is given in Fig. 1. This Figure is borrowed from a study on the navigability of VLCC's in the Southern part of the North Sea [3].

It is most convenient to list the locations which govern the time interval as well. It is obvious that these locations of constraint in the fairway should draw the attention of the analyst when remedial measures are proposed and eventually taken.
So far one vessel in a fairway has been considered. But this is highly hypothetical and real life often demands the incorporation of some aspects of traffic in the analysis. The aspects considered here are: overtaking and passing. Now the required path widths of both vessels are needed and the possible times of passing a given location in the fairway.
By comparing the vessel draughts one vessel can be designated as the largest vessel. This designation is important at a later time to select the appropriate distance between the fairway boundary and fairway axis.

The analysis now proceeds with the determination of the "shore-side" boundary of the required path width of the largest vessel. This required path-width is considered to be a measure of the lateral dimension of a "ship-domain". This domain is defined as the area of water around the ship which the navigator wants to keep free of any obstruction while the ship is underway.

The "shore-side" boundary may be determined by the location of depth -including the tidal height- which equals the required depth for the largest vessel concerned.

This location should be within the fairway boundary. It is now possible to determine the location of the vessel's centre of gravity by assuming that this centre is located at half the distance of the required path-width for this vessel measured from the location of the "shore-side" boundary.

The location of the vessel's extremity (not necessarily the stem or the stern) which is towards the passing vessel may be calculated taking into account the driftangles due to wind and tidal stream at the time of passing the given location.

Figure 1:
Length of period, inside which the time of departure from the MPC-Buoy must fall, as a function of the ship's draught and using the basic under keel clearance of 5.2 m.

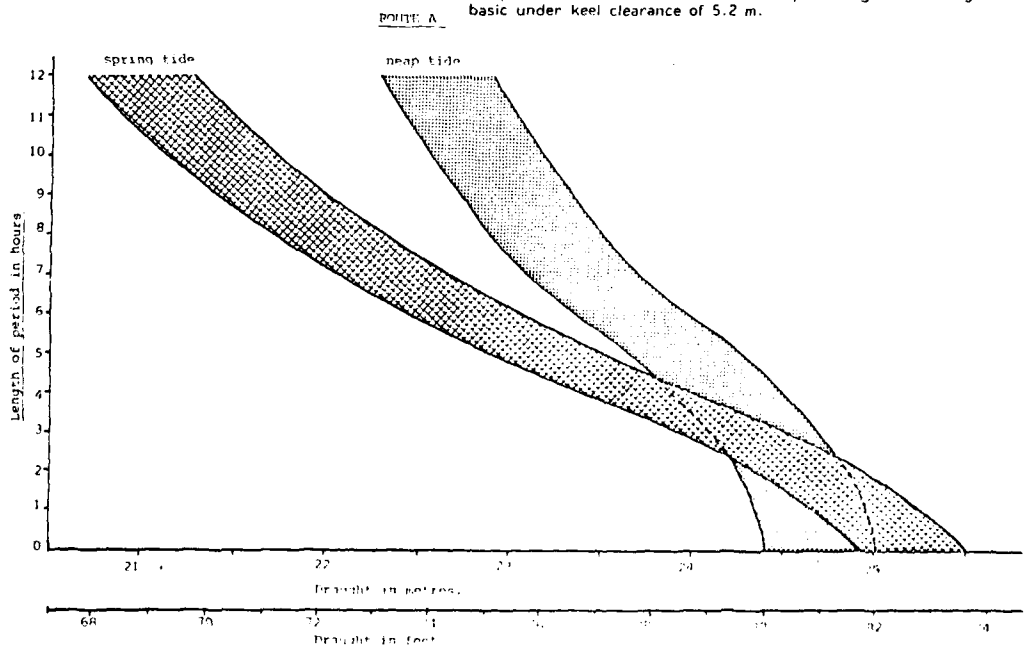

FI 5-8

In order to find the position of the other vessel one should determine a safe passing distance. The factors which may affect the choice of a safe passing distance may be summarized as follows:

- nature of cargo of each vessel
- speed of each vessel
- total time required for the passing manoeuvre
- hydrodynamic suction or repulsion during the passing manoeuvre.
- navigator's ability to deal with the hydrodynamic phenomena.

When the nature of cargo is such that the cargo comprises no pollutants or explosives the governing factor for the passing distance is often the hydrodynamic suction and repulsion between the two vessels and the ability of the navigators to deal with these phenomena.
However since a human being is in charge of navigation incidents cannot entirely be prevented.

When a safe passing distance is determined, the location of the other vessel may be computed as well as the "shore-side" boundary of this vessel in relation to the fairway axis.
When this "shore-side" boundary is nearer to the fairway axis than the real shore-side, passing of the two vessels may be possible provided that the smaller vessel has a sufficient Under Keel Clearance.

The calculation may be repeated for other possible times of passage. For various sea states it will now be possible to construct a time window or time interval inside which the two vessels are permitted to pass each other at the given location. This procedure may be repeated for a variety of ships of different sizes which will enable one to find limiting dimensions for ships passing the reference vessel at the given location. The calculation as set out here may be repeated for all locations of the fairway. This will result in a list showing the locations where it is possible for the reference vessel to pass any other vessel together with the applicable time windows.

In order to calculate the required path-width for the overtaking manoeuvre the overtaken ship is always the vessel which is positioned first in the calculation. The question as to the safe overtaking distance is even harder to answer than the question in the aforegoing step in relation to the safe passing distance.

The speed difference of both vessels involved in an overtaking manoeuvre determines the duration of the manoeuvre. Analyses of accidents involving overtaking have shown that various distances between the vessels exist which cause the same type of accidents. A clear answer on the required passing distance may not be expected from hydrodynamics alone.

The policy maker may be reluctant to increase the passing distance beyond practical limits since the implication might be for example that no downstream traffic is allowed during an upstream voyage of a gascarrier, which may be undesirable for economic reasons. The policy maker will not be very reluctant, however, to increase the overtaking distance, because it is obviously a more dangerous manoeuvre than the passing manoeuvre and the effects of such an increase upon shipping in general are small, since in river traffic the speeds do not vary much and lie in fact within a relatively narrow band.

It is clear that often no overtaking manoeuvres involving gastankers and oiltankers are permitted.

Again a specification of overtaking-time windows for all locations can be made at various sea states. The list provides an indication of the bottlenecks and suggested possible solutions to remove them.

6. Elucidation by means of a case study for the simulator method

In this section a discussion will be given with regard to an evaluation of the dimensions of the entrance of a port of which no similar situation exists. By means of simulation of the manoeuvrability into this port, decisions will be taken regarding the navigability for a reference vessel.

The harbour to be designed for the docking of only LNG carriers of 125,000 m^3 or smaller is located along a coast. The port is designed for the arrival of 136 ships per year over a period of 20 years which leads to about 5500 passages in the harbour. In the approach channel the ships sail through current and waves while the channel depth is designed for a keel clearance of 15% of the ship's draft.

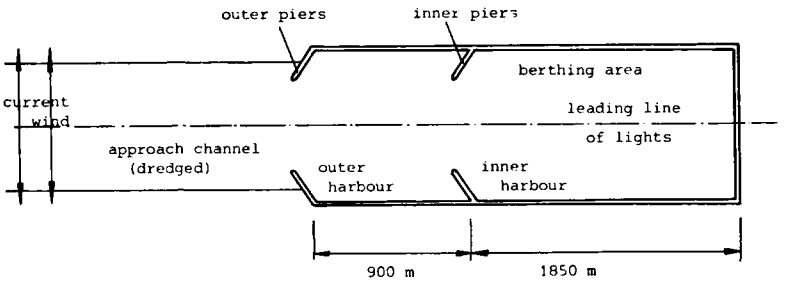

Figure 2. Schematic plan of the design.

The maximum current amounts to 3 kn. while the ships sail in prevailing winds of either 5 Bft or 8 Bft.

The first decision to be made refers to the approach speed of the vessel. With respect to the first conception of a 2750 m length of inner and outer harbour -based on experience from earlier studies- it is stipulated that the ships will pass the outer piers at a speed of approximately 5 kn. with a maximum variation of 1 kn. while 2½ miles in front of the outer piers their velocity still is 8 kn.

The port design will also be based on the fact that the tugs will fasten inside the outer harbour region.

The next requirement in relation to the design refers to the stipulation that only one ship at a time will approach and dock in the harbour. At this stage of the design the question arises what the dimensions of the approach channel (to be dredged) and the distance between the piers should be. When "design charts" about the width of shipping lanes would have been available, a compromise could be attained to an optimum harbour. This compromise would lie between as wide a harbour mouth as possible for the navigation and as small a harbour mouth as possible from a hydraulic point of view leading to minimum wave penetration in the harbour.

In order to explore the waterway dimensions required to facilitate the vessel to enter the harbour it is seen that the inherent controllability will lead to a width of the approach channel dependent on the ship's drift angle against current and wind while the dimensions of the harbour mouth and the area thereafter will depend on the current shear in front of the outer piers.

A further exploration will show that the initial controllability of the ship (navigated ship) will lead to the following factors:

When approaching in a 500 m wide channel under the condition of no current while wind disturbances can not be neglected during normal operations one finds the following dimensions:

a. Available width of outer harbour mouth 500 m:
the required width of lane in the approach channel appr. 290 m
the required width of lane between the outer piers appr. 240 m
the required width of lane in the outer harbour appr. 230 m

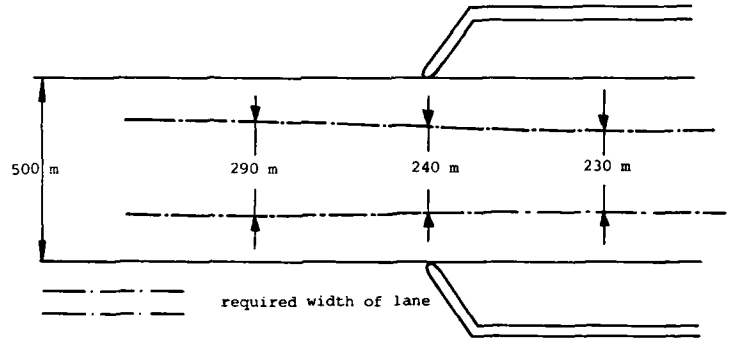

Figure 3: Initial controllability of ship in design alternative a.

b. Available width of outer harbour mouth 300 m:
the required width of lane in the approach channel appr. 600 m
the required width of lane between the outer piers appr. 220 m
the required width of lane in the outer harbour appr. 245 m

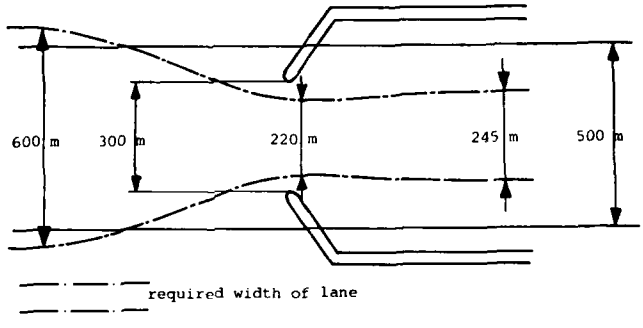

Figure 4: Initial controllability of ship in design alternative b.

Note: The results presented in Figures 3 and 4 have been deduced from the average value and standard deviation of many manoeuvres of ships entering the harbour under the conditions specified.
For the winds blowing from starboard side, half of the required width of lane is determined by the average and the standard deviation presented in Figure 5.

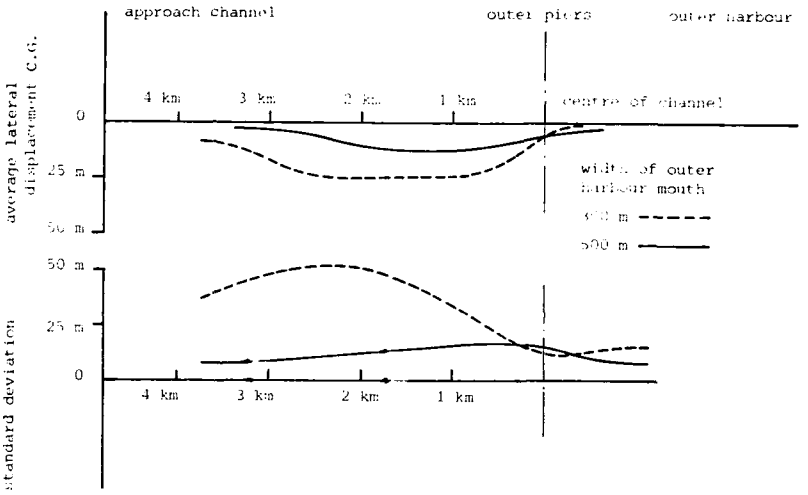

Figure 5: Description of the ship's tracks in design alternative a or b.

From the aforegoing it is seen that in the option of a 300 m wide outer entrance the ship's controllability is such that at least a 600 m wide approach channel is required. The channel width has to be 600 m "at least" because the initial controllability is considered to provide the minimum deviation between actual and intended manoeuvre. During normal operations the ship's controllability in practice will be less (leading to larger channel widths) than the initial controllability, as will be shown later on.

The navigability of the waterway can only be improved when the starting points of the waterway design are changed or when one refers to another ship system (manoeuvring characteristics of the ship in combination of control method). The controllability of the ship can be improved for instance by special training of the pilots or navigators, by providing other aids to navigation to the pilots or by increasing the water depth by which the turning ability of the ship increases.

In order to proceed the design of the harbour some decisions have to made from a practical point of view. One assumed the following decisions:

1. At this stage it is not recommended to change the starting points of the design in order to improve the initial controllability of the ship.

2. It is assumed that a harbour entrance of 500 m is acceptable from a point of view of wave penetration in the berthing area.
3. Widening of the approach channel from a point of view of initial controllability of the ship has to be rejected.

Based on these arguments the development of the harbour design now continues with alternative A presented in Figure 3.

It is decided that the waiting time of the ships to enter the port at an appropriate current velocity has to be minimal.
When the vessels have to enter the port at any moment of the tide then the following values are found:

required width of lane in the approach channel	appr. 620 m
required width of lane in the outer entrance	appr. 410 m
required width of lane in the outer harbour	appr. 525 m
required width of lane in the inner entrance	appr. 385 m

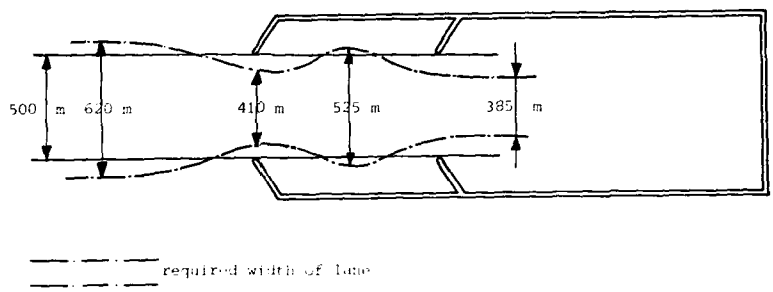

Figure 6: Required width of lane of the ship in the first draft design.

With respect to the values indicated in Figure 6 the following comments should be made:
1. The widths of lanes determined are prelimanary values which only hold for the initial design stage in which the starting points of the design have not yet been evaluated from an economic, hydraulic etc. point of view.
2. The widths of lanes have been determined in a more or less ideal environment in which for instance the visibility was good and the information of the current speeds was known to the pilots. When the hydrographical information to the pilots is not accurate then the waterway has to be much wider allowing the pilot to experience the environmental conditions in which he is sailing.
3. The widths of lanes have been determined using the average track and standard deviation of many manoeuvres.

The values shown in Figure 6 are a consequence of the high level of safety used in the calculations presented above.
However, in the initial stage of design the harbour dimensions seem acceptable relative to the controllability of the ship considered when one neglects these required widths of lane while instead the chances of exceedance of the given waterway dimensions are reviewed. One then obtains the following picture:

chance of exceedance of an extreme in the 500 m approach channel 1.5%
change of exceedance of an extreme between the 500 m outer pier 0.1%
change of exceedance of an extreme in the 500 m outer harbour 0.4%

From the preliminary values in Figure 6 determined by the ship's controllability it can be decided that a first draft design of the harbour can be:
-width of channel 500 m
-width of outer entrance 500 m
-width of inner entrance 500 m

This draft should be further evaluated from a point of view of hydraulic and economical aspects. It is advised that a detailed draft developed in that way will be tested afterwards on its navigational merits. In such a final nautical studay a search can be made to the optimization of the navigability by improving the ship's controllability by a variety of measures specific to the harbour.

In such a detailed nautical study also due attention should be devoted to real life disturbances which influence the ship's controllability adversely. Such disturbances can be a breakdown of machinery on board the ship, failures in connecting tug boats, hindrance of unforeseen obstacles (maintenance dredger) etc.

The values presented in this paper have been deduced from experiments performed at the MARIN Wageningen, Ship manoeuvring simulator [4]. These Figures only hold for the conditions of this specific harbour design and can not be copied for any other situation as long as no correlation is available with a range of experiences acquired under other conditions. The above Figures have only been used in this paper to demonstrate the recommended line of thinking of assessing the ship's controllability in the design of ports and harbour entrances.

7. Epilogue

Two extreme cases of studies of the navigability of fairways, and port entrances are presented. The first one treats a feasibility desk study which often can be used to assess the navigability in the preliminary stages. The latter one refers to use of a shiphandling simulator as a tool for the final lay-out of a fairway. Although economic and hydraulic aspects play sometimes a dominant role it is believed that both types of study are the core of a succesful lay-out design of a fairway or a basin in the prelimenary and final phases of the design process. Furthermore both types can aid to predict restricting conditions for vessel operation with regard to wind and visbility, as is succesfully demonstrated by several MARIN-studies.

8. References

[1] Nomoto, K.
"Analysis of the Standard Manoeuvre Test of Kempf and Proposed Steering Quality Indices"
Symposium on Ship Manoeuvrability
Washington, 1960

[2] Glansdorp, C.C. and Goldsteen, G.H.
"Hydronautical Bottleneck Analysis in Relation to Risk Analysis"
4th International Symposium on Vessel Traffic Services
Bremen, 1981

[3] Glansdorp, C.C., Goldsteen, G.H., Wepster, A., Donselaar, H. van, Keuning, J.J. de, Melissen, P.
"From Greenwich Buoy to Euro Channel"
Report no. R-213, August 1981
Netherlands Maritime Institute

[4] Hooft, J.P and Paymans, P.J.
"Four Years Operation Experience with the Ship Control Simulator"
STAR-Symposium, 1975

BIOGRAPHY

Cornelis C. Glansdorp

Born in 1941, Cornelis C. Glansdorp finished his M Sc. Naval Architecture at Delft University in 1966.
Early in 1967 he joined the Royal Netherlands Navy to perform full scale manoeuvring tests with frigates as an Royal Netherlands Reserve Navy Officer. In 1968 he joined the Shipbuilding Laboratory of the department of Naval Architecture Delft of the University of Technology, specialising in manoeuvring of surface vessels. Subjects which were covered: PMM-test, simulator tests, calculation of linear manoeuvring derivatives.
In 1974 he joined the chair of navigation of same department. In 1976 he became a part-time consultant of the Navigation Research Centre of the Netherlands Maritime Institute, which was founded in late 1973.

In 1978 he was appointed as a fellow of the Royal Institute of Navigation.

At May 1st, 1981 he succeeded captain Wepster as head of the Navigation Research Centre of NMI, which was renamed after the merger with N.S.M.B (Jan 1st, 1981) to Navigation and Shiphandling Department of the Maritime Research Institute Netherlands (MARIN).

MATHEMATICAL MODELLING FOR RUDDER ROLL STABILIZATION

by J. van Amerongen
and J.C. van Cappelle

Control Laboratory
Electrical Engineering Dept.
Delft University of Technology
Postbox 5031, 2600 GA Delft,
The Netherlands

ABSTRACT

Modern passenger ships as well as naval ships are equipped with roll stabilization systems in order to improve the passenger's comfort or to keep the ship fully operational in bad weather conditions. Fins and tanks are most commonly used but both have disadvantages. Tanks require a lot of space, fins introduce a considerable drag and are expensive. Besides, fin motions disturb the heading control system, while rudder motions not only effect a ship's heading but influence the rolling motions as well. In present systems this interaction is generally disregarded. However, by explicitly modelling the interaction it can purposefully be used by applying the rudder for roll stabilization as well. This paper describes a simple mathematical model for the transfer between the rudder angle and the two outputs: rate of turn and roll angle. The parameters of this model can be estimated from full-scale trials such as zig-zag manoeuvres. Examples are given of the parameter estimation of two different ships, a pilot vessel and a naval ship.

INTRODUCTION

Since a long time ago automatic control systems have been applied to controlling the motions of a ship. In most cases an autopilot for controlling the heading has replaced the helmsman, although manual steering remains possible. To reduce the rolling motions, tanks and fins have been applied which always work fully automatically. Until recently the controller structure of these systems was simple. But the availability of small and inexpensive digital computer systems offers a possibility to apply more advanced control algorithms into a wide range of practical systems. This has already led to a series of new autopilot designs, which all claim more accurate and more economical control of a ship's heading, by introducing adaptive properties into the controller (see for instance Van Amerongen and Van Nauta Lemke, 1978; Van Amerongen , 1981).

Although an autopilot which generates only smooth rudder motions implicitly causes less roll, this is seldom explicitly used as a design criterion. On the other hand, the coupling between the stabilizer fins and yawing are disregarded in the design as well. To get an optimal performance of both systems the ship should be considered as one multi-variable system with two inputs: rudder angle and fin angle, and two outputs: heading and roll angle; one integrated controller should be designed for both actuators.

Another possibility with promising properties is to use the rudder no control of the heading but for roll stabilization as well (Carley, 1975; Lambert, 1972, 1975; Lloyd, 1975, Baitis, 1980). Although this will req powerful steering machine the savings realized by not installing stabi are apparent. Also with respect to fuel economy a rudder roll stabiliza system may be advantageous. This aspect is of growing importance. Fo ships the total operational cost is already for more than sixty percent by the fuel cost. (See figure 1 , according to Milch, 1980.)

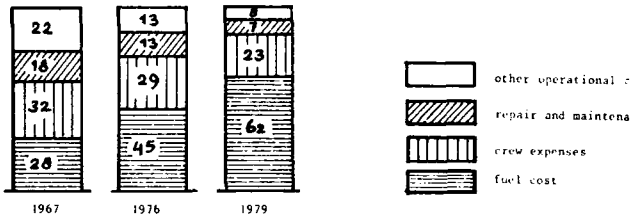

Figure 1 Increasing importance of fuel cost

Rough estimates indicate that the loss of speed due to the drag of the fins is approximately ten percent. Recently several papers have di perfomance criterion for a course autopilot (Koyama, 1967; Norrbin, Amerongen and Van Nauta Lemke, 1980). It can be shown that the loss of minimized by minimizing the rate of turn of a ship, for instance by appl small and smooth rudder motions. However, the rudder itself caus neglectable small drag. From the data provided by Norrbin, 1972 it foll for a cargo liner with 33000 tons displacement and a length of 200 meters of speed due to steering is described by (Van Amerongen and Van Nauta Lem :

$$\frac{0.0076}{T}\int_0^T \left(\varepsilon^2 + 1600\dot{\psi}^2 + 6\delta^2 \right) dt \quad [\%] \qquad (1)$$

The loss of speed caused by the rudder only is thus:

$$\frac{0.0076}{T}\int_0^T \left(6\delta^2 \right) dt \quad [\%] \qquad (2)$$

A rudder angle of, for instance, 10 degrees gives a loss of speed of ne percent, supposed that the ship does not start turning.

It can be shown that for control of the heading high-frequency rudder mot no positive effect on the course-keeping accuracy (Van Amerongen and Lemke, 1980): course control only necessitates low-frequency rudder moti respect to the frequencies of these motions the rolling motion is high Quick rudder motions, to suppress the rolling motion, with a mean value c

the course controller, will therefore hardly influence the ship's heading. Because of eqn.'s (1) and (2) the loss of speed caused by these quick rudder motions can be kept on a reasonable value as long as turning is prevented.

MATHEMATICAL MODELLING

The basic equations which describe the motions of a ship, important with respect to steering and roll stabilization are:

$$Y = m (\dot{v} - ur) \tag{3}$$

$$K = I_x \ddot{\varphi} \tag{4}$$

$$N = I_z \dot{r} \tag{5}$$

where m is the ship's mass, included the added mass of the water.

Ix and Iz are the moments of inertia about the x-axis and z-axis.

Y is the hydrodynamic force in the y-direction.

K and N are hydrodynamic moments.

The other variables have been defined in figure 2a and 2b.

The eqn.'s (3) - (5) can be expanded into a Taylor series. See for instance Eda, 1978. Disregarding all higher order terms and introducing the fin angle α yields the following simplified equations:

$$Y = Y_v v + Y_r r + Y_\varphi \varphi + Y_\delta \delta + Y_\alpha \alpha \tag{6}$$

$$K = K_v v + K_r r + K_\varphi \varphi + K_{\dot{\varphi}} \dot{\varphi} + K_\delta \delta + K_\alpha \alpha \tag{7}$$

$$N = N_v v + N_r r + N_\varphi \varphi + N_\delta \delta + N_\alpha \alpha \tag{8}$$

Substitution of eqn.'s (3) and (6) into (7) and (8), and substitution of eqn. (4) into (7) and eqn (5) into (8) yields, after Laplace transformation:

$$\varphi = \omega_n^2 \frac{K_\delta \delta + K_\alpha \alpha - K_r r}{s^2 + 2z\omega_n s + \omega_n^2} \tag{9}$$

$$r = \dot{\psi} = \frac{n_\delta \delta + n_\alpha \alpha - n_\varphi \varphi}{T_r s + 1} \tag{10}$$

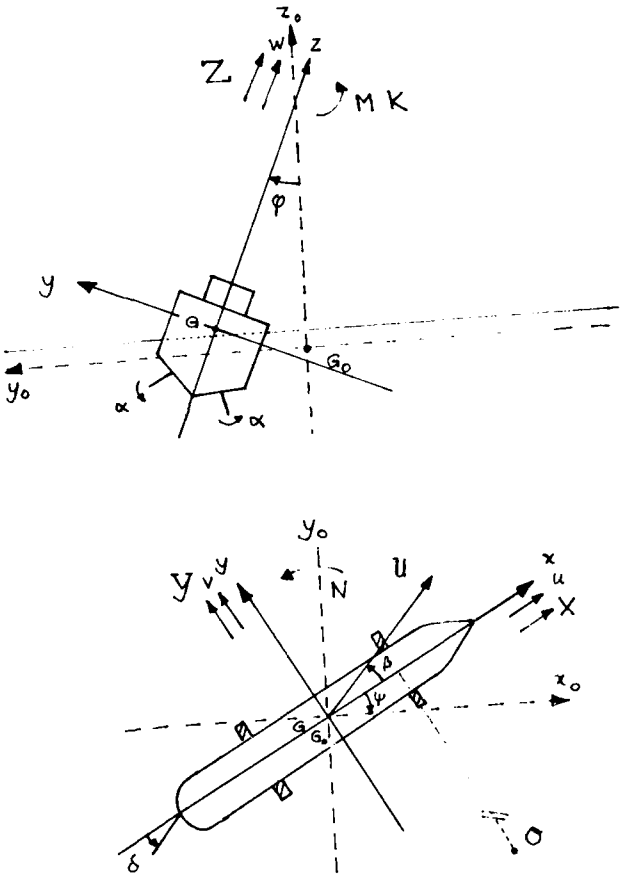

Figure 2 Definition of variables

Disregarding the influence of the fins and the roll angle on the rate of turn, eqn. (10) transforms into the well known Nomoto model. Equations (9) and (10) can be combined into one block diagram as shown in figure 3.

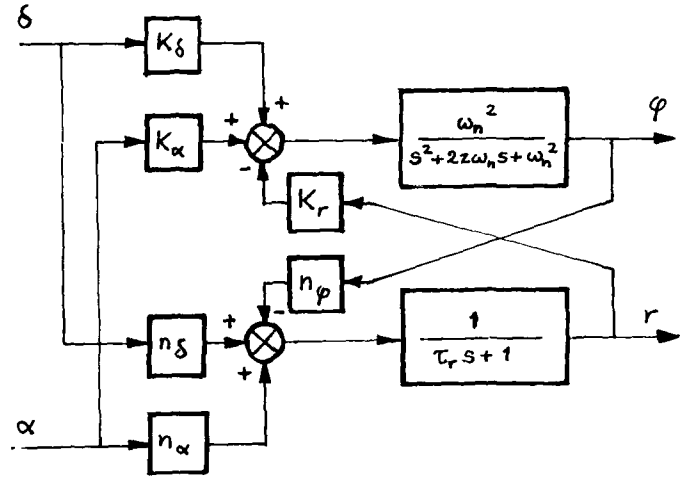

Figure 3 Blockdiagram of the dynamics between rudder and roll

When the ship has no stabilizing fins and the coupling of φ and r is disregarded, this blockdiagram simplifies into the system of figure 4. In figure 4 the parameters K_N and τ_N have replaced n_δ and τ_r. This model will be useful for investigation of rudder roll stabilization systems.

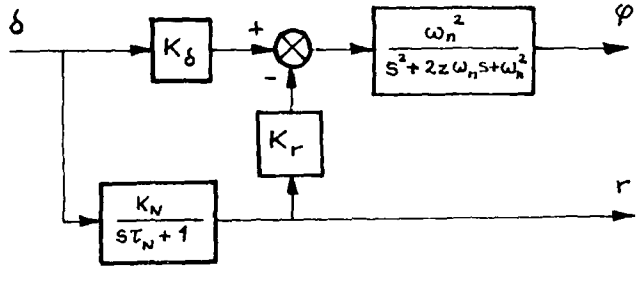

Figure 4 Simplified blockdiagram

PARAMETER ESTIMATION FROM FULL-SCALE TRIALS

The simplicity of the model of figure 4 enables to estimate its parameters from full-scale trials. Zig-zag manoeuvres are well suited as test signals. During the trials the rudder angle, the rate of turn and the roll angle should be recorded. This enables a two-stage identification procedure:

1. Determine the parameters K and T from the rate of turn and rudder signals. $_N$ $_N$

2. Use the rate of turn signal computed by the now identified Nomoto model, together with the rudder and roll angle signals to estimate K_δ, K_r, z and ω_n.

For both stages hiliclimbing with the aid of a digital computer works well. In case that the circumstances are not ideal, for instance when there is wind, it is necessary to estimate two additional constants r_0 and φ_0, which must be subtracted from the measured r and φ signals. For obtaining accurate results the constants r_0 and φ_0 should be small.

The parameter-estimation procedure was tested on data which were available from earlier measurements with a pilot ship. It appeared that for this ship the second order part of the transfer function could be well approximated by one single pole. This yields the block diagram of figure 5.

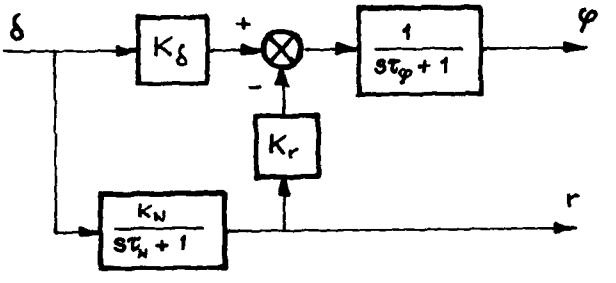

Figure 5 First order rol dynamics

For this pilot ship,with a lentgh of 60 meters and sailing with a speed of 12 knots the parameters are given in table 1.

The same procedure was used to estimate the parameters of a naval ship, about twice as long and sailing with a speed of 21 knots. For this ship the parameters of the model of figure 5 have also been determined, but the responses clearly indicated the need of using the second-order roll dynamics of the model of figure 4. Parameters of both models are given in table 2.

In figures 6 and 7 the measured responses and model responses are given for the pilot ship, (first-order roll dynamics) and for the naval ship (second-order roll dynamics).

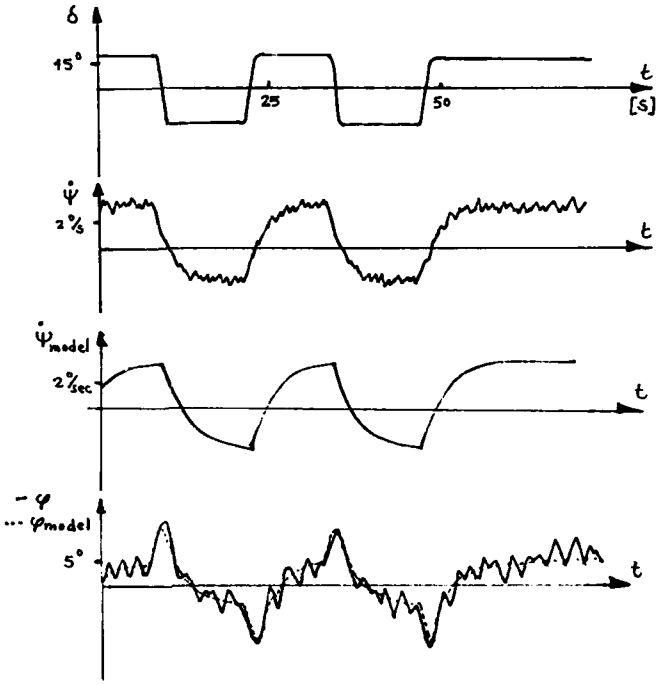

Figure 6 Results of identification of a pilot vessel

Table 1 parameters of a pilot vessel

yaw dynamics	roll dynamics
$K_N = 0.125$	$K_\delta = 0.4$
$\tau_N = 10$	$K_r = 6$
	$\tau_\varphi = 1.9$

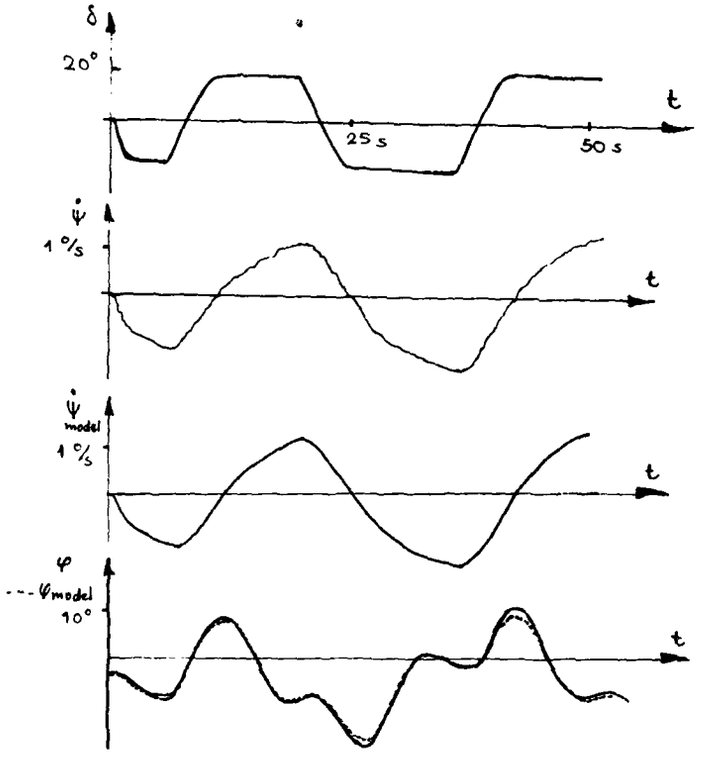

Figure 7 Results of identification of a naval ship

Table 2 parameters of a naval ship

yaw dynamics	first-order roll dynamics	second-order roll dynamics
$K_N = 0.06$	$K_\delta = 0.22$	$K_\delta = 0.25$
$\tau_N = 6$	$K_r = 5.2$	$K_r = 5.4$
	$\tau_\varphi = 1.9$	$\zeta = 0.23$
		$\omega_n = 0.55$

CONCLUSIONS

It has been shown that relatively simple models can be derived to describe the transfer between rudder and roll. The parameters of these models can be estimated from full-scale zig-zag manoeuvres. For some ships a model with first-order roll dynamics appears to give a reasonably good description.

The models also give some insight into the ability of the rudder to stabilizing a ship's roll. Due to the non-minimum phase character of the responses the rudder will never be able to compensate a stationary roll angle, what fins are able to do. Only in the high frequency range the rudder has the desired effect. For low frequencies the roll in opposite direction, caused by the rate of turn will be dominant. However, as the course control system requires the rate of turn to be kept small.

Figure 8 shows bode diagrams for the transfers between rudder and heading and between rudder and roll, calculated with the second-order roll parameters of table 2. The low-frequency character of the rudder-heading transfer function and the more high-frequency character of the rudder-roll transfer function can clearly be seen.

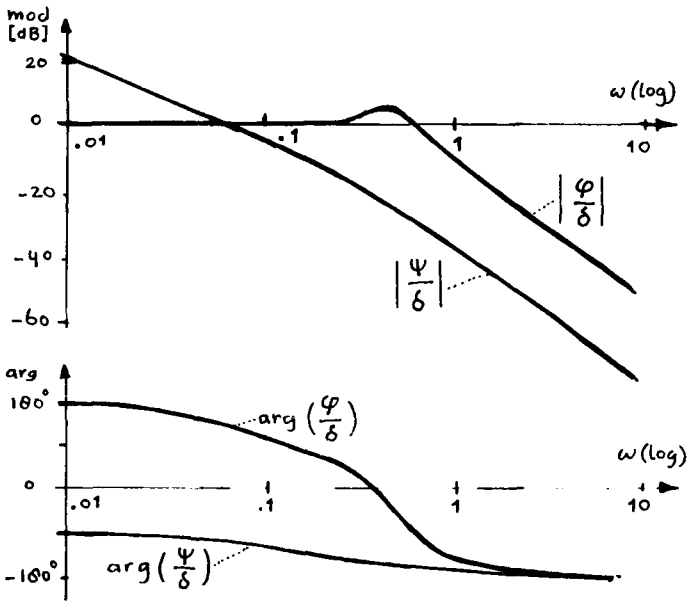

Figure 8 Bode diagrams for the rudder-heading and the rudder-roll transfer functions.

REFERENCES

J. van Amerongen and H.R. van Nauta Lemke, "Optimum steering of ships with an adaptive autopilot", Proceedings 5th Ship Control Systems Symposium, Annapolis Md., USA, 1978

J. van Amerongen and H.R. van Nauta Lemke, "Criteria for optimum steering of ships", Proceedings Symposium on Ship Steering Automatic Control, Genoa, Italy, 1980

J. van Amerongen, "A model reference adaptive autopilot for ships - Practical results", Proceedings 8th IFAC World Congress, Kyoto, Japan, 1981

A.E. Baitis, "The development and evaluation of a rudder roll stabilization system for the WPEC Hamilton Class", DTNSRDC Report, Bethesda, Md., USA, 1980

J.B. Carley, "Feasibility study of steering and stabilizing by rudder", Proceedings 4th Ship Control Systems Symposium, The Hague, The Netherlands, 1975

W.E. Cowley and T.H. Lambert, "Sea trials on a roll stabiliser using the ship's rudder", Proceedings 4th Ship Control Systems Symposium, The Hague, The Netherlands, 1975

W.E. Cowley and T.H. Lambert, "The use of the rudder as a roll stabilizer, Proceedings 3rd Ship Control Systems Symposium, Bath, UK, 1972

H. Eda, "A digital simulation study of steering control with effects on roll motions", Proceedings 5th Ship Control Systems Symposium, Annapolis Md., USA, 1978

T. Koyama, "On the Optimum Automatic Steering System of Ships at Sea", J.S.N.A. Japan, Vol. 122, 1967

A.R.J.M. Lloyd, "Roll stabilization by rudder", Proceedings 4th Ship Control Systems Symposium, The Hague, The Netherlands, 1975

S. Milch, "Hull forms and propulsion plants in the 1980's - Improved fuel economy", Schip en Werf, Vol 47 (26), pp. 443 - 447, 1980

N.H. Norrbin, "On the added resistance due to steering on a straight course", 13th ITTC, Berlin, Hamburg, W. Germany, 1972

AUTO STEERING AND STABILISER TRIALS IN HM SHIPS

By W B Marshfield
AMTE(H)

ABSTRACT

Auto steering and stabiliser trials in four ships of the Royal Navy are described.

The main objective of the auto steering trials was to measure the open loop rudder demand to yaw response of the ships at several forward speeds. The autopilot time constants were then adjusted to give an acceptable course keeping and course changing performance. PRBS or BLN signals were used in addition to sinusoidal signals to obtain the frequency responses.

On two of the ships stabiliser tuning trials were also carried out using similar techniques, and in both of these ships autopilot and stabiliser effective trials have been attempted.

A secondary objective of the trials was to obtain information to identify multivariable models of ship yaw and roll dynamics, and while this analysis has not yet been undertaken some indications as to the quality of the results is given.

Also given is some measured information on roll damping and the speed loss due to fin activity.

INTRODUCTION

Objectives

The paper was written to describe autopilot tuning trials on four Royal Naval ships. It gives the techniques used, presents the criteria adopted in tuning the autopilots and gives examples from the trial results. Autopilot effectiveness trials were also undertaken and these are briefly described.

On two of the ships roll stabiliser tuning trials were also carried out and these are described in similar terms.

In addition to the primary rudder angle to yaw and fin angle to roll responses other parameters were measured and some examples from these results are given.

Background Information

Previous to 1978 autopilot trials had been the responsibility of the Admiralty Engineering Laboratory (AEL), now part of the National Gas Turbine Establishment (NGTE) and responsibility for stabiliser trials was shared between AEL and the former Admiralty Experiment Works, now part of the Admiralty Marine Technology Establishment (AMTE),

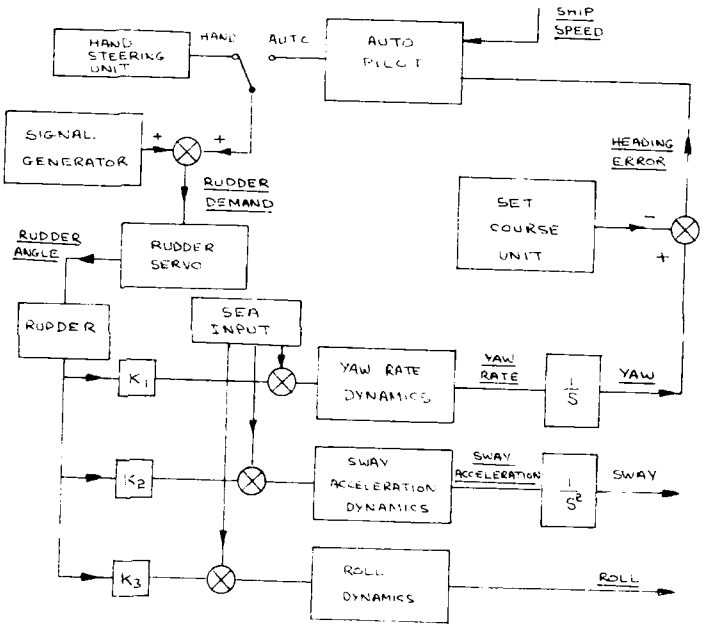
HAND STEERING UNIT
HAND
AUTO
AUTO PILOT
SHIP SPEED
SIGNAL GENERATOR
+
+
HEADING ERROR
RUDDER DEMAND
SET COURSE UNIT
−
+
RUDDER ANGLE
RUDDER SERVO
RUDDER
SEA INPUT
K_1
YAW RATE DYNAMICS
YAW RATE
$\frac{1}{S}$
YAW
K_2
SWAY ACCELERATION DYNAMICS
SWAY ACCELERATION
$\frac{1}{S^2}$
SWAY
K_3
ROLL DYNAMICS
ROLL

AD-A211128 (U) PROCEEDINGS OF THE SIXTH SHIP CONTROL SYSTEMS
UNCLASS. UNLTD. SYMPOSIUM HELD AT OTTAWA, ONTARIO, CANADA, ... 4 of 6

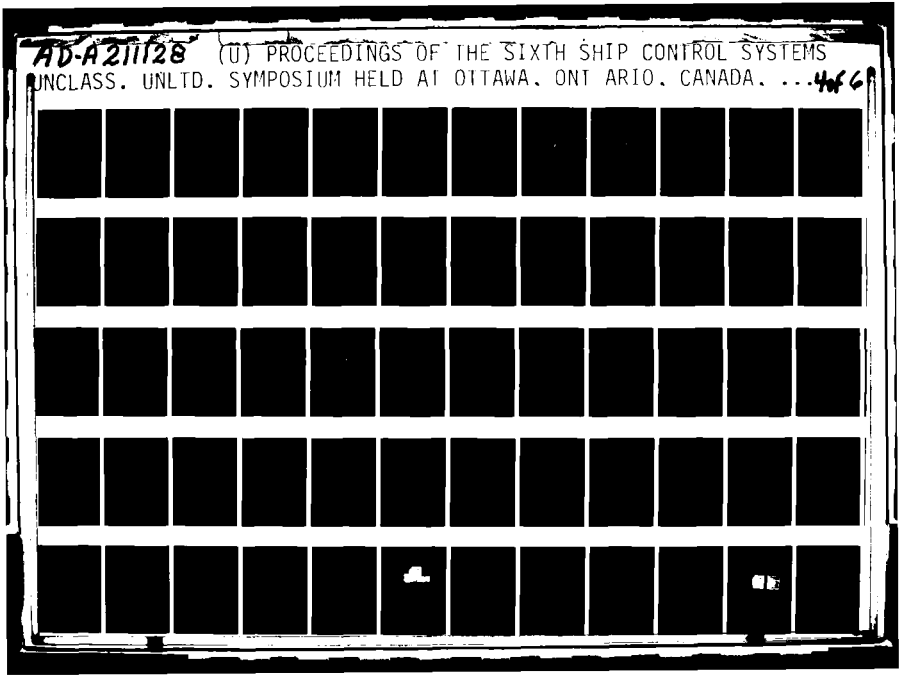

to give the best compromise between course keeping and course changing performance. The course changing performance of the chosen autopilot was then checked by conducting further trials, with step changes in course demand of 5, 30 and 50 degrees with the ship in autopilot control.

In the case of the MCMV and the Frigate, the autopilots had previously been set using data obtained from model experiments, and in the event no changes were made for the subsequent course change manoeuvres. For the Frigate and Aircraft Carrier, trials were later carried out to check the course keeping performance of the autopilots in rough weather. For the MCMV the only trial attempted so far was abandoned when a sea state 8 to 9 left no one with an inclination for conducting autopilot trials.

Roll Stabiliser Trials

These were carried out on the Frigate and Carrier, both ships being fitted with two pairs of trapezoidal fins.

The techniques used were similar to those used in the autopilot trials, with the signal generator in this case providing fin demand signals as shown in Figure 2.

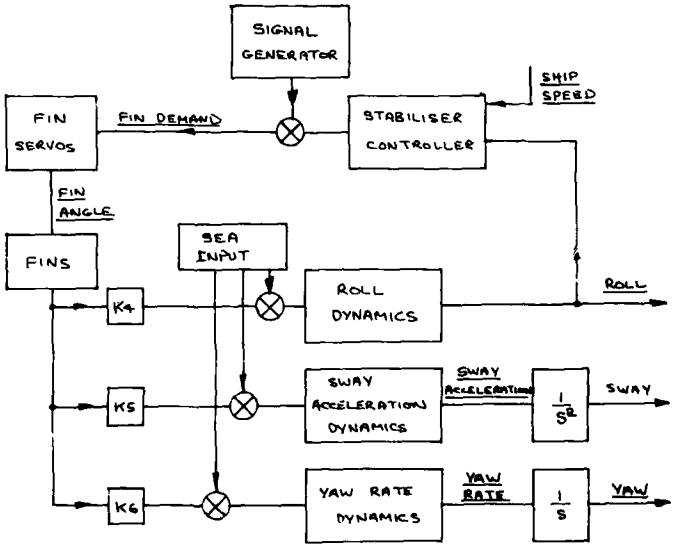

Figure 2. Block Diagram for Stabiliser Trials

Again the recorded quantities are shown underlined.

The principal objective of the trials was to measure the fin demand to roll angle frequency response of the ships at a number of forward speeds. The cruising speed response was then used to tune the stabiliser controller. Subsequently performance trials were carried out on both ships, although in both cases the seas encountered were not very severe.

QUALITY OF RESULTS

Measurement of Yaw

The yaw rate signal was generally used for the determination of the rudder demand to yaw response in preference to the yaw or heading error signals as these tended to saturation. It was sometimes difficult to prevent large variations from the base course, especially during low frequency measurement or towards the end of a PRBS serial especially when wind/sea disturbances were present. The weather helm control on the hand steering unit was used to try and correct excessive departures from the base course - but this was not always successful. During one PRBS run on the Destroyer the ship turned through 360 degrees!

To obtain the yaw response, at a particular frequency ω, the yaw rate response is divided by $j\omega$ ($j = \sqrt{-1}$). This facility is automatically available on the DSA. Where it was possible to use the yaw signal direct this corresponded well (as expected) with the yaw response obtained from the yaw rate signal.

When considering the yaw response of a ship for autopilot tuning it is necessary to consider frequencies down to 1 mHz. In one instance one cycle at 1 mHz was measured on the Aircraft Carrier but 3 mHz was the lowest frequency used where repeats were carried out. Where responses down to 1 mHz are shown these are the results of extrapolation.

Sinusoidal Responses

In both autopilot and stabiliser trials the results were averaged over 10 cycles for frequencies above 10 mHz. For measurements between 3 and 10 mHz three to 8 cycles were individually measured and averaged. Repeatability was good in most cases.

It took 2½ to 3 hours to carry out one complete frequency response.

PRBS and BLN Measurements

As stated these were analysed using a Hewlett Packard 5420A DSA, some details of which are given in Appendix B. The record lengths taken were usually between 25 and 30 minutes, although in a few cases the runs were truncated to about 15 minutes. If the sea was calm then the results corresponded well in amplitude and phase with the sinusoidal measurements and the measured coherence values were near unity. Figure 3 shows a result obtained on the Destroyer where the coherence is between 0.9 and 1.0 over most of the measurement range. The gain and phase here correspond very well to the sinusoidal response values. Figure 4 shows a less acceptable result from the MCMV with poor coherence over most of the range. The gain response

looks deceptively [illegible] at low frequencies because the values at 4, 6 and 1[illegible] mHz lie on a straight line; [illegible] are in fact too high.

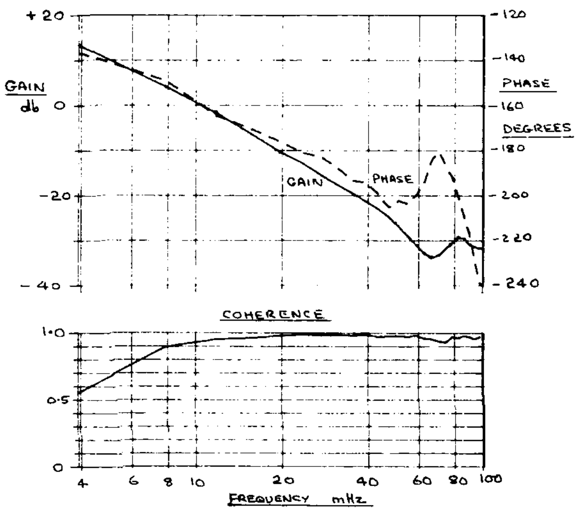

Figure 3. Destroyer 24 Knots Rudder Demand to Yaw

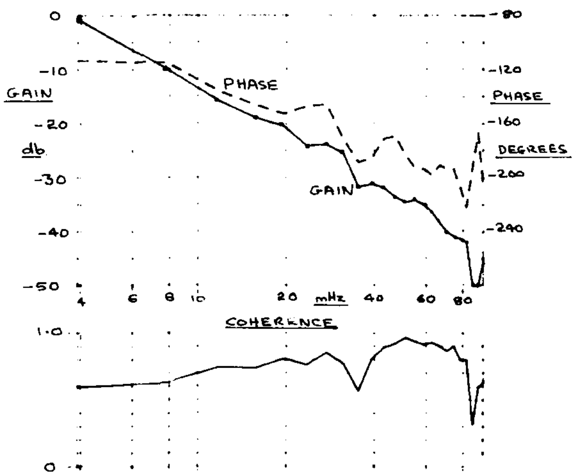

Figure 4. [illegible] 3 Knots Rudder Demand to Yaw

Figures 4 and 5 show results where narrow band interference produced unacceptable results over part of the measurement range. The important peak of the roll response is preserved in Figure 4 but has been rendered useless in Figure 5.

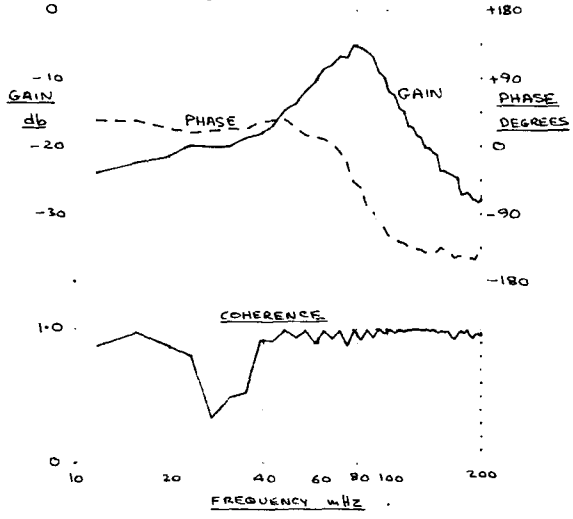

Figure 5. Frigate 13 Knots Fin Demand to Roll

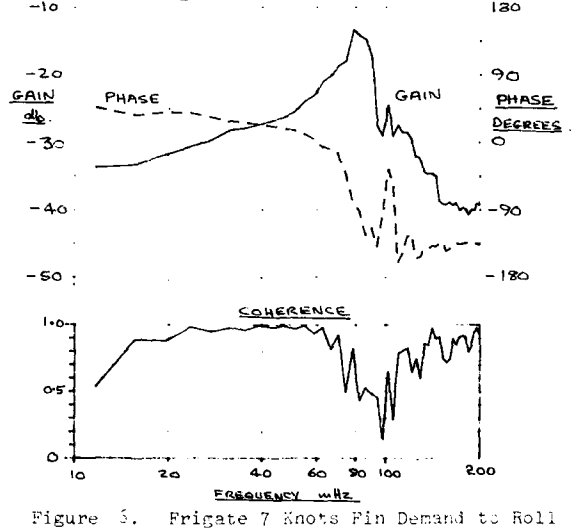

Figure 6. Frigate 7 Knots Fin Demand to Roll

It is concluded that while PRBS responses are easily and quickly obtained, it is desirable to reinforce the collected data at critical points using sinusoidal measurements. Adopting this principle during subsequent forced rolling trials it was possible to obtain a useful frequency response measurement in about one hour of trials time.

YAW RESPONSE AND AUTOPILOT TUNING

Details of Autopilot

Figure 7 shows a block diagram of an autopilot system.

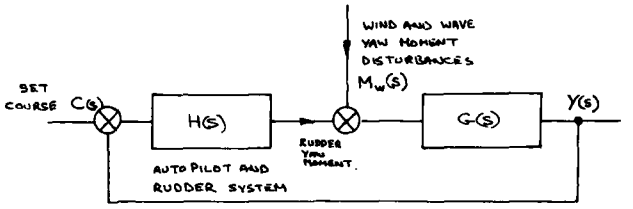

Figure 7. Autopilot System

The transfer function of the system is given by:

$$Y(s) = M_w(s) \frac{G(s)}{1 + GH(s)} + C(s) \frac{GH(s)}{1 + GH(s)} \qquad (1)$$

G(s) gives the ship yaw response to a yaw moment (note GH(s) should more strictly be written G(s).H(s)). s is the Laplace operator.

In a calm sea Y(s) = C(s) for a constant set course. In a seaway if $M_w(s)$ is not zero mean then the mean course is not equal to C(s) unless H(s) contains an integrator - usually termed the weatherhelm integrator.

The autopilot used by the Royal Navy are designed by S G Brown Limited and consist essentially of a phase advance circuit, to which can be added a weatherhelm integrator. Its transfer function is therefore of the form

$$\frac{\text{Rudder Demand}}{\text{Heading Error}} = R_1 R \left[\frac{(1 + T_1 L s)}{(1 + T_1 s)} + \frac{1}{T_2 s} \right]$$

L (lift) and R_1 (Rudder quantity) are switch selectable with T_1 and T_2 determined by either component selection, or as in the latest design, by pin board selection. Having selected T_1 and T_2 for a particular ship speed these values are changed, for other speeds, in discrete steps by a signal from the ship's log according to an inverse speed law, as shown in Figure 8. The other autopilot controls are:-

(1) Rudder Limit Switch, which allows the selection of a maximum rudder angle between 2½ and 30 degrees.

(2) The Yaw Switch, with settings from 0 to 5 degrees in 1 degree steps.

With the yaw switch to 1 degree for example, the heading error must exceed ± 1 degree before corrective action is taken. The error is then reduced to zero before the yaw dead band is reset to ± 1 degree.

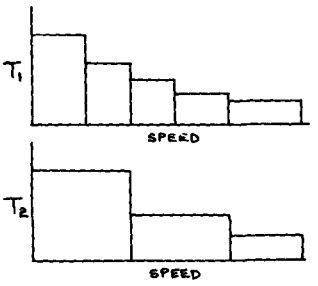

Figure 8. Autopilot Speed Compensation

Tuning of Autopilots

I am indebted to John Warren of S G Brown Limited for demonstrating the use of Nichols Charts when tuning autopilots. We should therefore consider the frequency domain version of equation (1). Thus

$$Y(j\omega) = M_w(j\omega)\,\frac{G(j\omega)}{1 + GH(j\omega)} + C(j\omega)\,\frac{GH(j\omega)}{1 + GH(j\omega)} \qquad (2)$$

The open loop frequency response of the system is $GH(j\omega)$ which is made up of the measured rudder demand to yaw response and the heading error to rudder demand response of the autopilot.

Figure 9 shows on a Nichols chart the response of an 'ideal' autopilot. This is perhaps arguable, but the response has been arrived at as follows.

For $|GH(j\omega)| = |1 + GH(j\omega)|$ then the response must follow the 0 db (closed loop) contour; which it does above the 0 db (open loop) line. Below this if $|(1 + GH\ j\omega)| \geq 1$ then the yaw motions due to waves will not be enhanced by the presence of the autopilot system. The frequency at which the response crosses the 0 db line we will call the transition frequency ω_T. In practice it is sufficient that ω_T occurs at a frequency where the rudder demand to yaw response is around - 20 db.

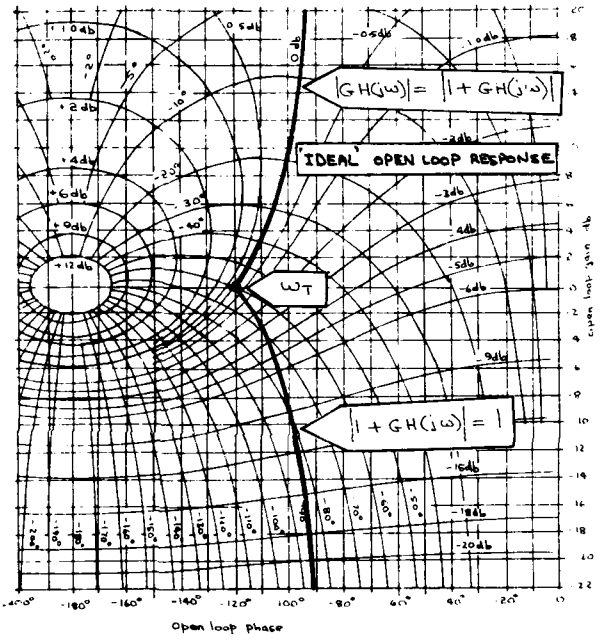

Figure 9. 'IDEAL' Autopilot Response

Figure 10 shows the tuning results for the aircraft carrier. Curve A is the measured yaw response at 18 knots, to which has been added the autopilot response without the weatherhelm integrator (curve B) and the autopilot with weatherhelm integrator, curve C. ω_T is about 0.14 rad/sec (23 mHz).

Curve B follows the 0 db closed loop contour very well, and this was supported by the step response to a heading demand which had zero overshoot. Including the weatherhelm integrator introduced about a 1 degree overshoot in the step response.

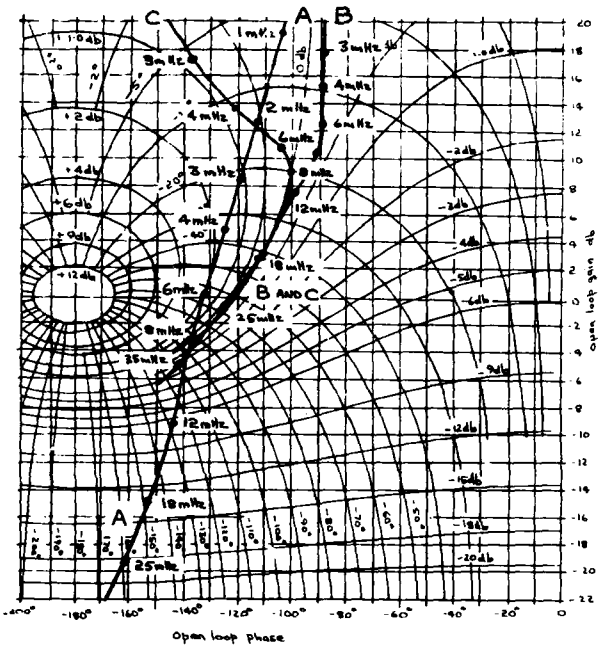

Figure 10. Carrier 18 Knots Response

The matching of the autopilot to speeds above 18 knots was good but at lower speeds the compensation was not so well maintained. See Figure 11.

In fact no step responses were carried out at 12 knots, but experience at other times where step responses were carried out did indicate that these were a fairly sensitive test of autopilot tuning.

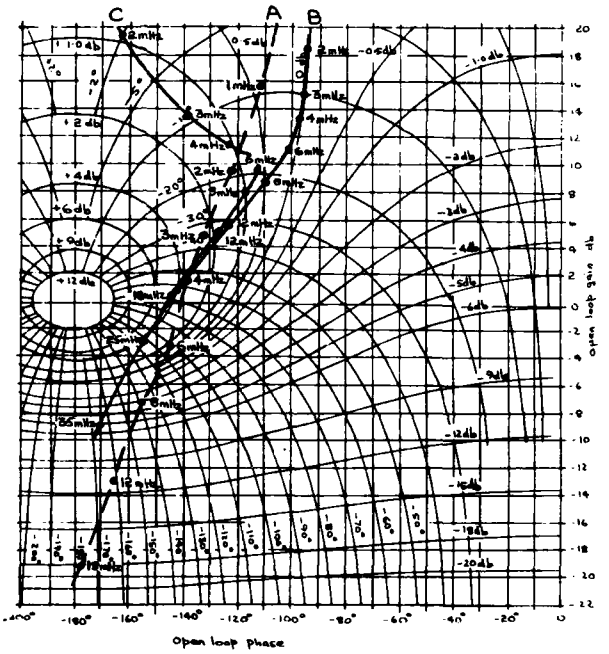

Figure 11. Carrier 12 Knots Response

Autopilot Effectiveness Trials

Having tuned the autopilots attempts were made to measure their performance in a seaway.

The trial objectives were to measure the yaw disturbance of the ship at three separate headings to the prevailing sea, ie bow, beam and quartering seas with

(1) The ship unsteered.

(2) In Auto.

(3) In Auto, with weatherhelm integrator.

This procedure was usually carried out at two forward speeds, 30 minutes recordings were taken for each steering mode.

So far these trials have been carried out on the frigate and the aircraft carrier. As they were carried out on passage it was not possible to deploy a wave buoy and only visual estimates of the sea state were possible.

For the unsteered runs a manual weatherhelm was initially set to maintain as near a straight course as possible. Small adjustments were allowed if the course deviated by more than 20 degrees from the desired directions. In general the ships maintained course well under these conditions, although at 12 knots in quartering seas the aircraft carrier could not maintain a course unsteered.

The power spectral densities and rms values of yaw and rudder angle (where applicable) were determined using the DSA and compared for each speed and heading. From these it would appear that trials of this sort are not suitable for distinguishing between the finer points of autopilot tuning. The general conclusions are predictable ie, an unsteered ship, while it might follow a reasonably straight course is unlikely to achieve precisely the desired course. With no weather helm integrator the autopilot course steered is within a degree or so of the desired course. With the weatherhelm integrator the required course is well maintained.

Figure 12 shows some results from the Aircraft Carrier in quartering seas in sea state 5. The autopilot yaw band was set to zero. The steering of the ship actually takes place in the 0 to 6 mHz frequency band, and by 25 mHz the rudder demand to yaw response is around - 20 db. It is therefore interesting to note that small yaw disturbances still occur at frequencies around 50 mHz (20 seconds period) and it is these that caused the major rudder activity.

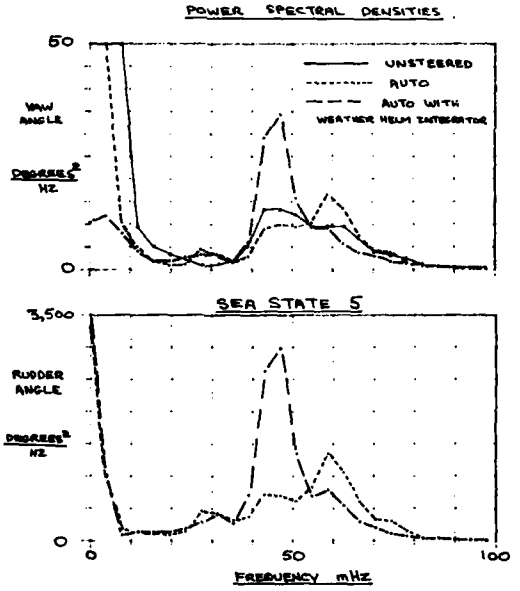

Figure 12. Carrier 18 Knots Quartering Seas

The rms measurements taken from Figure 12 were as follows.

	Degrees rms	(10-100 mHz Band)
	Yaw	Rudder
Unsteered	0.61	-
Auto	0.70	6.6 degrees
Auto with WH	0.60	5.5 degrees

Figure 13 shows some results for the Frigate in bow seas in a similar sea state. Here the actual motions are much less, but there is a small peak at about 100 mHz that does cause perceptible rudder motions.

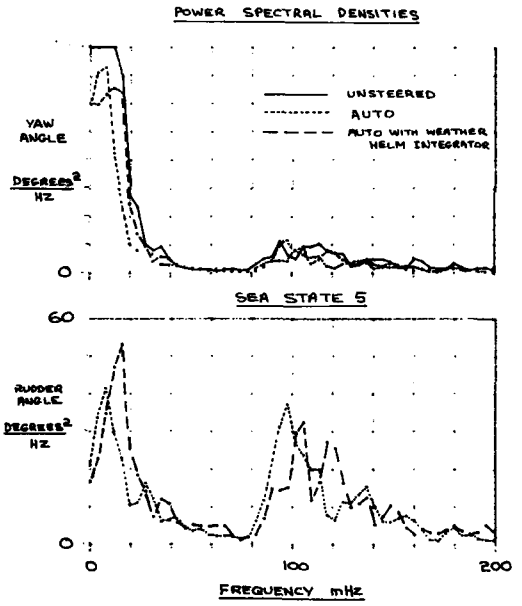

Figure 13. Frigate 11 Knots Bow Seas

Quantities measured from the data are:-

Condition	Mean Heading Error	Degrees rms		Measurement Band
		Yaw	Rudder Angle	
Unsteered	-	0.43	-	20-200 mHz
Auto	0.6 degrees starboard	0.53	1.46	4-200 mHz
Auto with WHI	0.2 degrees port	0.58	1.54	4-200 mHz

In both ships the yaw dead band of the autopilot was set to zero so that the rudder responded to all heading error signals. It was not possible to investigate the effects of yaw band changes during the planned serials but some measurement were later carried out on the carrier.

Figure 14 shows a result obtained in beam seas at 20 knots in sea state 5. The quantities measured from the data are:-

Yaw Band	Degrees rms		Measurement Band
	Heading Error	Rudder Angle	
Min	0.84	6.54	3-120 mHz
± 1 degree	1.47	5.51	3-120 mHz

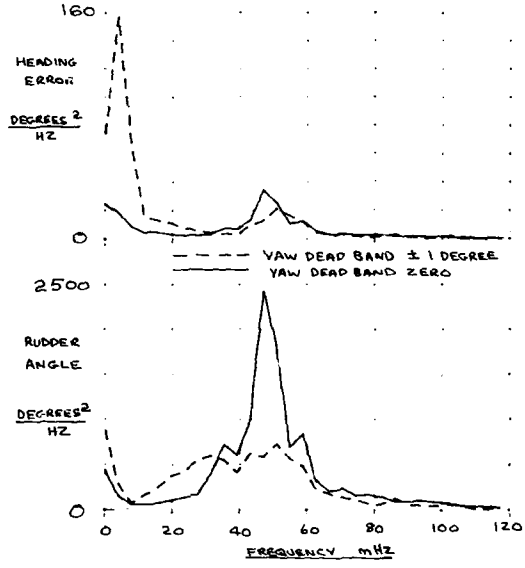

Figure 14. Carrier 20 Knots Beam Seas

It seems that, here at least, the rudder angle has been decreased by the yaw dead band but at the expense of a larger heading error.

MCMV Yaw Response

The MCMV is designed to tow mine sweeping equipment which essentially consists of drag loads towed with steel cables of considerable length, some of which are fitted with diverters to spread the sweeps. The original autopilot trials were carried out before the sweep gear had been embarked. Some five months later it was possible to repeat two of the yaw responses with the sweeps deployed. Figure 15 shows the sinusoid test results at 10 knots.

Clearly the increased flow over the rudders for the same speed and the presence of sweeps attached at the stern have a marked effect on the high frequency response of the system.

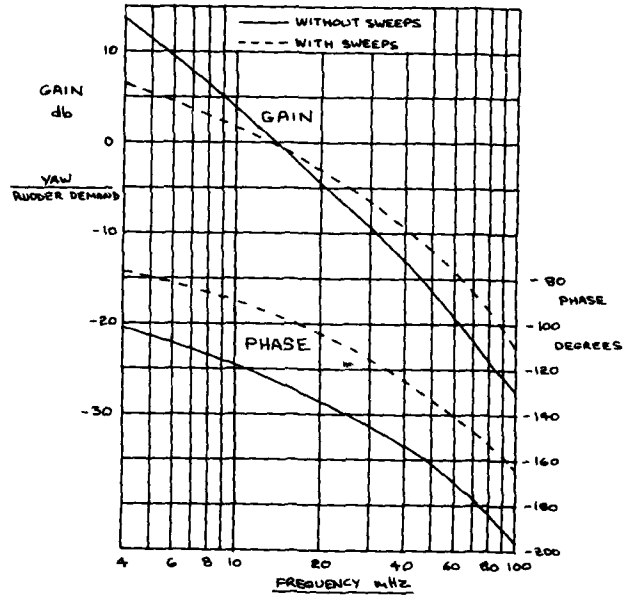

Figure 15. MCMV 10 Knots With and Without Sweeps

ROLL RESPONSES AND STABILISER TUNING

Tuning Controllers

The stabiliser controller principally used by the Royal Navy on newly constructed ships is one designed at the Admiralty Engineering Laboratory and manufactured by Muirhead-Vatric Limited. It accepts a roll angle signal from the ship's gyro and uses analogue computer

techniques to develop a transfer function of the form:

$$\frac{\text{Fin Demand Angle}}{\text{Roll Angle}} = 0.24\ \frac{K4.K5(K1 + 6.06\ K2s + K3s^2)}{(s^2 + 10s + 100)(s + 3)}$$

for the "stabilise to vertical" mode of operation.

There is a "stabilise to list" mode, where a zero is introduced at the origin (s = 0) but this does not affect the frequency response of the controller in its working range.

The controller gains are:

K1	Roll angle	range 0 to 10 in integer steps
K2	Roll velocity	range 0 to 10 in integer steps
K3	Roll acceleration	range 0 to 10 in integer steps
K4	Gain	range 0 to 10 in integer steps
K5	Speed dependent gain	3 settings: (1) High speed = 0.15; (2) Low speed = 0.3; (3) Auto: = 0 V<6, = 1 6<V<12, = $\frac{144}{V^2}$ 12<V

where V is ship speed in knots.

The fin demand to roll angle response of the ship forms the major part of the open loop response of the stabiliser system, which is completed by the frequency response of the controller. A typical roll response was shown in Figure 5.

The phase advance at low frequencies is quite usual for ships where the fins are not horizontal.

If the K1, K2, and K3 gains are chosen to provide a phase advance, at the ship roll natural frequency, equal to the phase lag between roll and fin demand at that frequency, then optimum stabilisation is achieved. The settings of K1, K2 and K3 to achieve this are not unique but it is advisable to ensure that K3 is not zero - which produces too much phase advance at low frequencies, or too large which means that high frequency (around 1 Hz) gain of the controller is too large.

The auto setting of K5 is normally used so that it remains to fix the value of K4. The method used at AMTE is described in Reference 2. Basically it consists of using a roll prediction computer program (Reference 3) which uses the Conolly roll prediction method (Reference 4) to calculate the rms roll motion at worst heading in a particular sea state for various values of K4. K4 is then selected so that the rms roll angle does not exceed a given level on the worst heading in a particular sea state at a specified speed. The degree of stabilisation required is not large and it is usual to have an open loop gain at the roll natural frequency of between 1 and 3.

Roll Response

Figure 16 shows the complete open loop response of the frigate in polar form, which illustrates the salient points of stabiliser tuning. Figure 17 gives the same information for the carrier.

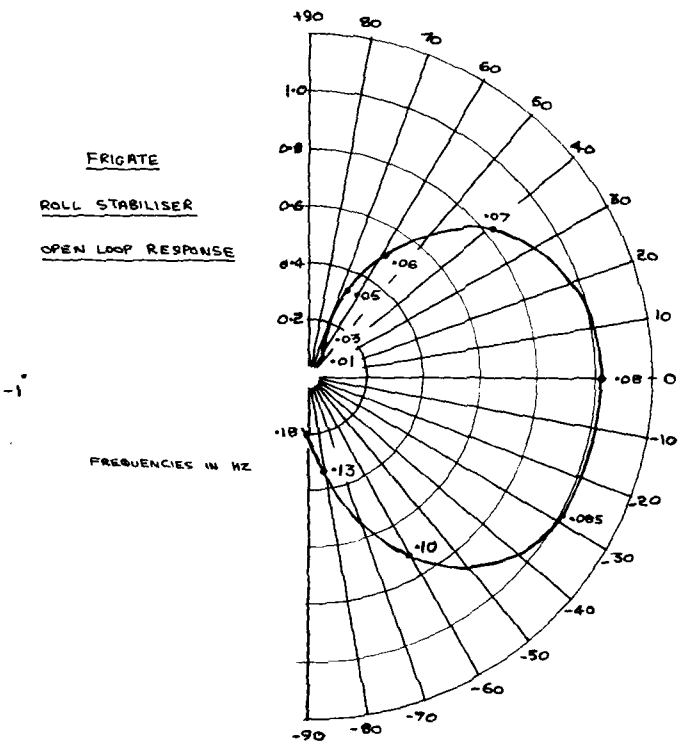

Figure 16. Frigate Stabiliser Open Loop Response

The forced rolling trials were carried out at a number of forward speeds for both ships and since the roll natural frequency remained sensibly constant with speed and the measured phase lag at the roll natural frequency did not alter by more than ± 15 degrees then a single set of settings suffices for all speeds.

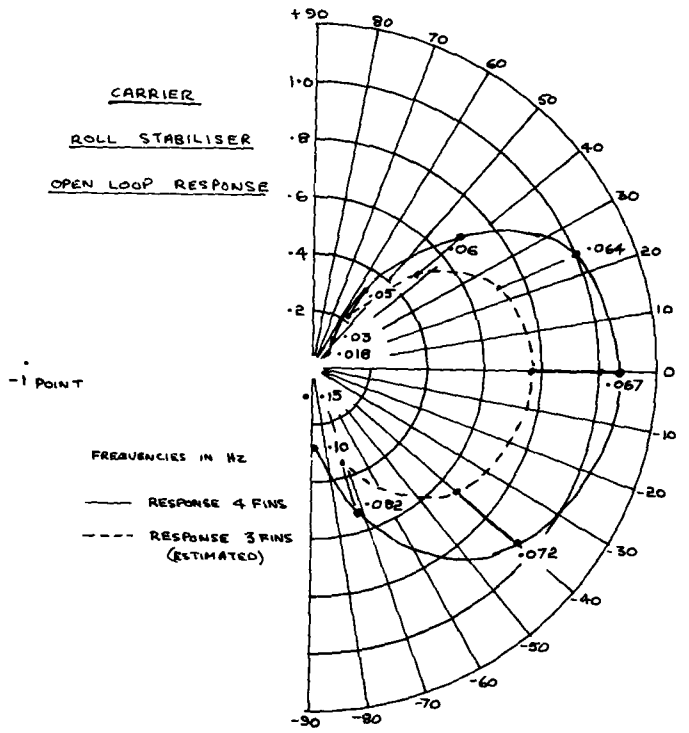

Figure 17. Carrier Stabiliser Open Loop Response

Roll Stabiliser Effectiveness Trials

These have been attempted in both ships, with only partial success. The trials objectives were to measure the stabilised and unstabilised roll motions at two speeds with three headings to the prevailing seas, ie bow, beam and quartering seas. As with the auto-pilot trials they were carried out on passage and only visual estimates of the sea state could be obtained.

The frigate trials were disappointing because the sea state was too low to provide a rigorous test of the system. Figure 18 shows some typical results in quartering seas with the controller used to calculate Figure 16. An unstabilised roll of 1.2 degrees rms is reduced to 0.74 degrees rms for an rms fin motion of 1.0 degrees.

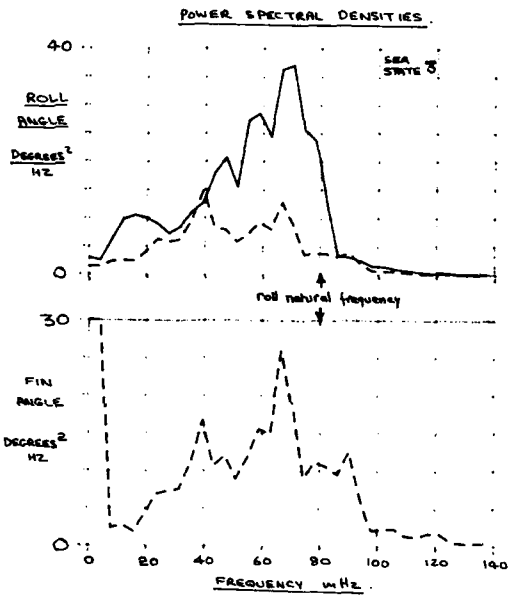

Figure 18. Frigate 18 Knots Quartering Seas

For the trials in the Carrier only three stabilisers were working as one of the fin servos became unserviceable just after the trials began. Figure 19 shows a result for beam seas. (Figure 17 gives the estimated open loop response with three fins working.)

Although the sea state is 5 the unstabilised roll is only 1.9 degrees rms. The stabiliser reduces this to 1.6 degrees with a fin angle of 5.6 degrees rms.

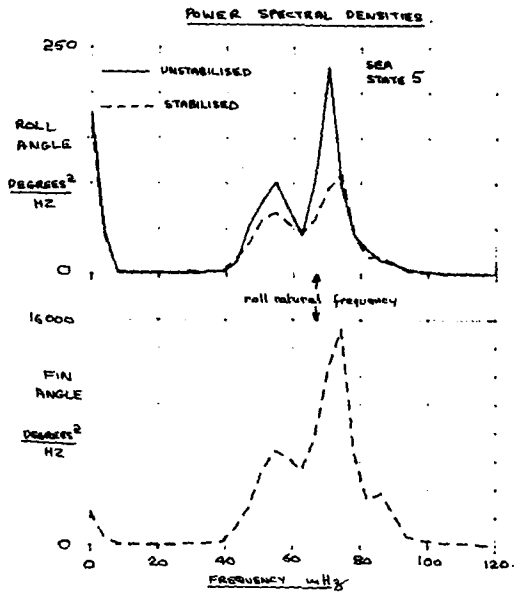

Figure 19. Carrier 18 Knots Quartering Seas

ANALYSIS OF SECONDARY DATA

So far only a limited analysis of the secondary data has been undertaken - this being mainly on the frigate results.

Autopilot Trials

Figure 20 shows an analysis of the rudder angle to roll response of the frigate at 16 knots. Figure 21 shows the results for rudder angle (degrees) to sway accelerations (metres per sec^2) from the same serial. Both sets of data were obtained using the DSA to analyse recordings taken during a sinusoidal response.

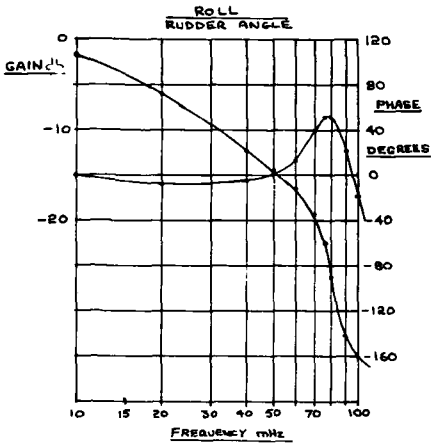

Figure 20. Frigate 16 Knots Rudder Angle to Roll

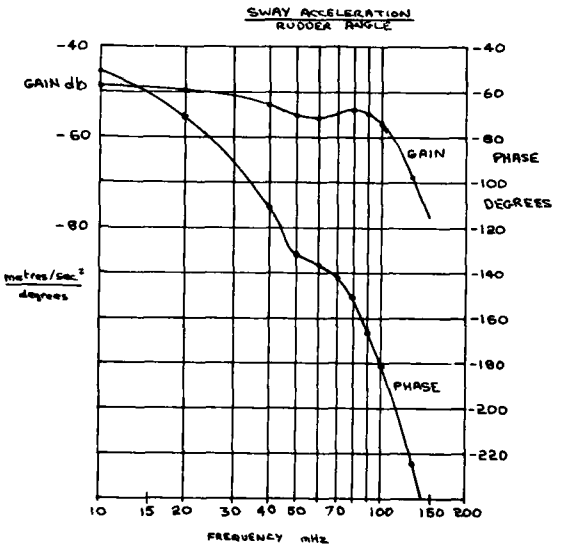

Figure 21. Frigate 16 Knots Rudder Angle to Sway Acceleration

Stabiliser Trials

The roll response of a ship to a roll moment M(t) is usually represented by a simple second order system with an equation of the form:-

$$I\ddot{\phi}(t) + B\dot{\phi}(t) + \Delta g\overline{GM}\,\phi(t) + M(t) = 0.$$

(I is the roll moment of inertia, B the damping force per unit velocity Δ the ship mass, g the acceleration due to gravity and $\overline{GM}$ the metacentric height.)

Dividing through by I and converting to the usual nomenclature we get

$$\ddot{\phi}(t) + 2\zeta\omega_o\dot{\phi}(t) + \omega_o^2\phi(t) + \frac{M(t)}{I} = 0$$

where ζ is the roll damping coefficient and ω_o is the roll natural frequency.

The fin to roll response of a ship is obviously more complicated than a simple 2nd order system but the peak is dominated by the pair of complex poles represented in the simple roll equation. The roll damping coefficient can therefore be estimated by the formulae

$$\zeta = \frac{\text{Bandwidth}}{2\omega_o}$$

where the bandwidth in question is the - 3 db bandwidth around the peak of the forced roll response.

The results of this simple analysis of the frigate and carrier roll responses are given in Figure 22.

Also shown on the Frigate results are the analysis of some of the roll decays recorded at the end of some of the sinusoidal runs after the excitation was switched off. This time domain analysis agrees reasonably well with the frequency domain results.

Figures 23 and 24 show some further analysis of PRBS serials. Figure 23 gives the fin angle to sway acceleration with all fins working. The ship speed was 12 knots. The coherence is extremely good for this serial but at other speeds the results were more scattered. The sway acceleration due to fins measured on the carrier was so small that it was lost in noise and in no cases were analysable data obtained from the PRBS results.

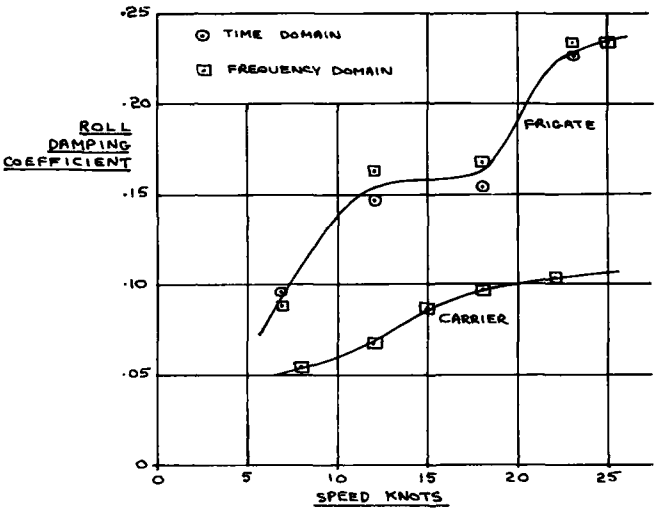

Figure 22. Roll Damping Coefficients

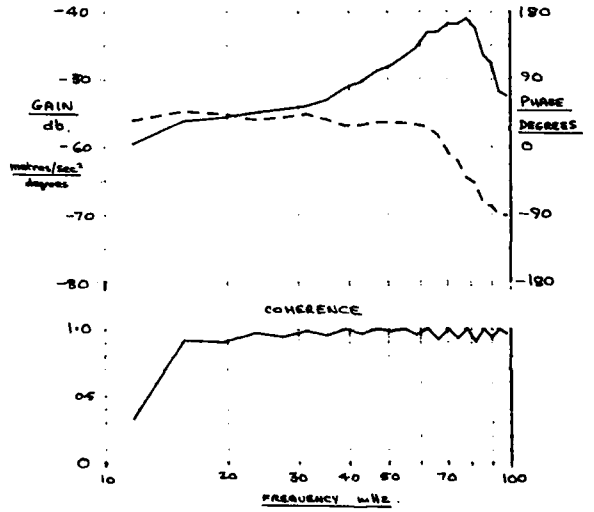

Figure 23. Frigate 12 Knots Fin Angle to Sway Acceleration

Figure 24 is the only result obtained for yaw velocity due to fin angle where the coherence is at all reasonable over part of the frequency range. The rapdily and continuously changing phase characteristic is typical of a time delay, and it may be that the yaw measured was due to wash from the stabiliser fins interacting with the rudders.

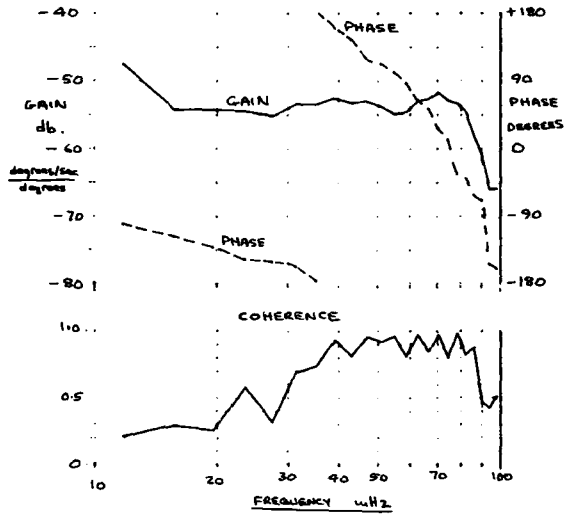

Figure 24. Frigate 12 Knots Fin Angle to Yaw Velocity

On the Frigate it was possible to get some idea of the speed losses due to fin action as the speed recordings from the log signal showed recognisable speed reductions in response to a step input to the fins. The speed loss, with both sets of fins, was quantified as being:-

$$\text{Speed Loss (Knots)} \approx -\frac{0.09\ |\beta|}{(1 + 28s)} \quad \text{where } \beta = \text{fin angle.}$$

This was reasonably constant over a speed range of 12 to 26 knots. This means that an rms fin angle of 5 degrees is likely to cause a speed loss of about 0.45 knots.

Similar analysis was not possible for the carrier as flow from the fins increased the noise levels on the log signal to such a degree that any small change in speed went undetected.

DISCUSSION AND CONCLUSIONS

1. The trials show that in a calm sea situation PRBS signals can provide frequency domain information of equal quality to those derived using sinusoidal signals. However if sea disturbances occur then it is seen that sinusoidal responses with their higher signal to noise ratio provide more reliable data. The combination of the two techniques in these trials have ensured that valuable trials time was not wasted.

2. An efficient trials procedure for tuning autopilots has emerged from these trials. The frequency domain measurements, plotted on a Nichols chart, provided the necessary information of the required phase and gain from the autopilot in an easily digested form.

3. The autopilot effectiveness trials were shown not to be a sensitive test of autopilot tuning. This was possibly due to the changing input from the sea during the trials. Nugatory rudder action was shown to occur but it is not clear how this can be avoided as such measures as reducing the rudder bandwidth or filtering the heading error signal are likely to introduce unacceptable phase lags into the open loop response.

4. The stabiliser trials showed that the forced rolling characteristics of a ship, with regard to natural frequency and the phase lag at the natural frequency are relatively insensitive to speed. This means that one set of controller gains is capable of providing good stabilisation over the entire speed range.

Changes in natural frequency due to changes in $\overline{GM}$ were not investigated during the trials and it seems unlikely that this can be achieved in practice. Fortunately during normal operations in a warship changes in condition are kept to a minimum. At worst, typical information suggests that a reduction in natural frequency of 30 per cent is possible in going from the deep to the light condition. While ideally such a change should be compensated for, in actual fact the reduction in efficiency would be small.

5. Roll damping coefficients have been determined from the frequency response data, and these agree reasonably well with values obtained from time domain roll decay information.

6. While the present autopilots have proved satisfactory and reliable in service the technology used is now somewhat dated. There is also some evidence that the speed scaling could be improved. These autopilot trials have provided a full set of data on the rudder angle to yaw response of a wide range of RN ships. This should be of considerable help in the design of future autopilot systems.

7. The analysis of the secondary data (such as rudder induced sway, etc) has been included to show the quality of the data collected. It shows that some of the PRBS records can provide sufficient data for the identification of multivariable mathematical models of ship steering and roll dynamics. This analysis may bring the dream of a combined steering and roll control of a ship nearer reality.

ACKNOWLEDGEMENTS

While this work was carried out for the Ministry of Defence (Procurement Executive) the responsibility for statements of fact or opinion rests with the author.

The author would like to acknowledge the influence of Dr J B Carley and Mr C Bruce, formerly of AEL, and Mr J Warren of S G Brown who have informed his thinking on autopilots and stabiliser systems. Also the assistance and co-operation given by his colleagues in AMTE(H) and at Ship Department Bath is acknowledged. Finally he would like to acknowledge the kindness and co-operation received from the Captains and crews of the ships which took part in these trials.

Also the coolness they have exhibited while their ships have been driven, out of control on erratic courses, often at night; and the patience they have shown during the hours of roll motion in calm seas.

REFERENCES

(1) C. H. Bruce, J. B. Carley, "HMS SHEFFIELD - Identification of Roll Dynamics," AEL Report No 447, August 1977.

(2) G. P. Windett, J. O. Flower, "Measurement of Ship Roll Dynamics by Pseudo-random Binary Sequence Techniques," Trans 4th Ship Control Systems Symposium, 1975.

(3) W. B. Marshfield, "The Selection of Roll Stabiliser Controller Coefficients," AMTE(H) R80006, 1980.

(4) A.R.J.M.Lloyd, "AMTE(H) Computer Program LM175."

(5) J. E. Conolly, "Rolling and its Stabilisation by Active Fins," Trans RINA Vol 11, 1969.

Appendix A

THE PSEUDO RANDOM BINARY SEQUENCE

The PRBS used in the trials were generated by a Solartron Type JM 1861 PRBS generator.

A normal PRBS is one in which there are only two possible signal levels which can change only at regularly spaced event points. It is generated using a shift register with the outputs of two of its stages connected to an exclusive OR gate the output of which controls the state of the first stage of the shift register. For a shift register N stages long it requires $2^N - 1$ clock pulses before the sequence repeats itself.

Multi-level sequences can be generated by summing the outputs of a number of shift register stages. During the trials 3 level sequences were used; and these are generated using the outputs from two stages. Figure A1 illustrates 2 and 3 level sequences of amplitude A volts.

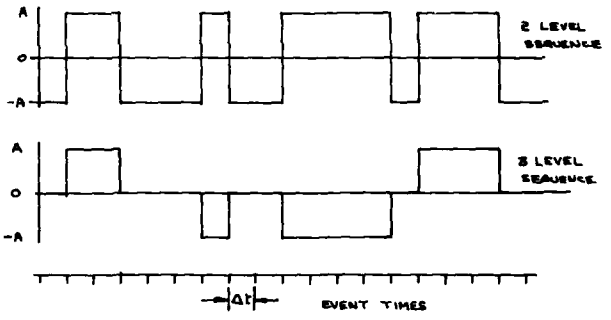

Figure A1

If the event time is Δt and the clock frequency $fc = \frac{1}{\Delta t}$ then the period repeats is $\Delta t.p$ where $p = 2^N - 1$.

The power spectral density of the sequence is a series of discrete lines occurring at intervals of $\frac{fc}{p}$.

Details of the sequences used on the trials are shown in the following table.

Ship	Type of Trial	fc Hz	N	Sequence Length Seconds	Number of Levels
MCMV	AP	0.3	7	423.3	2
Frigate	AP STAB	1.0 1.0	7 7	127 127	2 2
Destroyer	AP	0.3	7	423.3	3
Carrier	AP STAB	BLN* 0.3	- 7	- 423.3	- 3

* BLN (Band Limited Noise) see Appendix B.

Figure A2 shows the power spectral densities of the sequences used, the amplitude A being 5 volts. Note that 100 mHz is about the maximum useful frequency for the 3 level sequence with fc = 0.3 Hz. Unfortunately the signal generator used produces only a limited range of clock frequencies with no alternative values between 0.3 and 1 Hz.

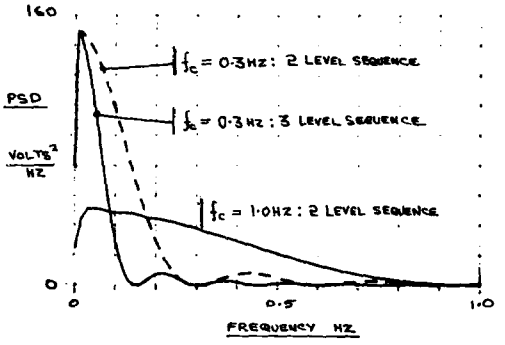

Figure A2. PSD of Trial Sequences

Appendix B

DIGITAL SIGNAL ANALYSER

The Hewlett Packard 5420A Digital Signal Analyser is a two input device. It digitises the signals connected to the inputs and operates on that data according to a pre-programmed set-up state specified by the user.

The two modes of analysis used in the trials were auto power spectrum (power spectral density) and transfer function.

Using the HP nomenclature consider:

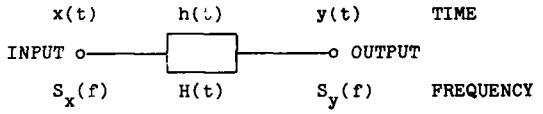

where

$x(t)$ = time domain input

$y(t)$ = time domain output

$S_x(f)$ = linear Fourier spectrum of $x(t)$

$S_y(f)$ = Linear Fourier spectrum of $y(t)$

$H(t)$ = System impulse response

$H(f)$ = System transfer functions (frequency response)

For the auto power spectrum the DSA calculates, for example,

$$\overline{G_{xx}(f)} = \overline{S(f).\ S^*(f)}$$

Where * denotes the conjugate of the function and —— averaging. The DSH averages the results from over lapping samples from the data, the number of samples being set by the operator.

For the transfer functions measurement we have

$$H(f) = \frac{\overline{G_{yx}(f)}}{\overline{G_{xx}(f)}} = \frac{\overline{S_y(f).\ S_x^*(f)}}{\overline{S_x(f).\ S_x^*(f)}}$$

where $G_{yx}(f)$ is the cross power spectrum of $y(t)$ and $x(t)$.

Incidentally when calculating $H(f)$ all the ingredients of the coherence function are generated, so that this can also be displayed by the DSA, thus

$$\gamma^2(f) = \frac{\overline{|G_{yx}(f)|^2}}{\overline{G_{xx}(f).\ G_{yy}(f)}}$$

Where $\gamma^2(f)$ is the coherence function, whose value lies between 0 and 1.

The coherence function gives the signal to noise ratio (S/N) of the measurement, ie

$$\frac{S(f)}{N(f)} = \frac{\gamma^2(f)}{1 - \gamma^2(f)}$$

In practice is seems that the measurements become unreliable when $\gamma^2(f)$ falls below about 0.85.

Band Width of Measurement

The measurement bandwidth of the DSA can be adjusted to suit the particular signals being analysed. All the DSA analysis given in this report was carried out over a frequency range of 0 to 1 Hz, which gave a sampling interval of 0.25 sec. For most of the illustrations reproduced here only a small portion of this bandwidth is reproduced.

The values of the ordinates in the PSD measurement are calculated as follows:-

$$PSD = \frac{(K\ V_{rms})}{\Delta f.\ L_s}$$

where

K is the calibration factor

L_s = 1.5 (to correct for the use of the Hanning Window)

$\Delta f = \frac{\text{Measurement Bandwidth}}{256}$ = 3.90625 mHz (for 1 Hz BW)

V_{rms} is the voltage at the frequency ordinate in question.

Note also that all the DSA data presented here is in discrete frequency form with a frequency spacing of Δf.

The other consequence of the selected bandwidth is that the bandwidth of the noise source is also adjusted.

When the Carrier autopilot trials were carried out the DSA noise source was used instead of the PRBS signals, and in order to limit the violence of the rudder movements to acceptable limits the measurement bandwidth was reduced to 0.25 Hz. The PSD of the noise source in this condition is shown in Figure B1.

Note that Figure B1 is obtained from a recording and the measurement bandwidth is again 1 Hz.

The consequence of using the 0.25 Hz bandwidth during the autopilot trials is that the time taken to obtain the first complete sample of data is increased 4 fold over the 1 Hz bandwidth. This limited the number of averages obtained during a ½ hour recording period to about 30 as compared with 120 when a 1 Hz bandwidth was used.

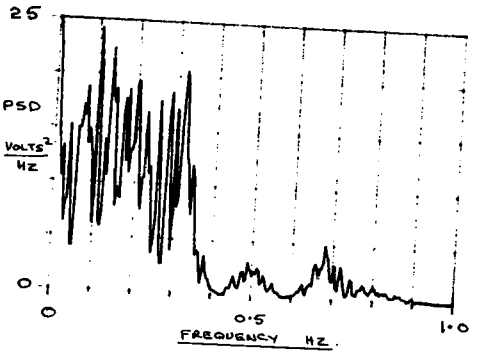

Figure B1. PSD of BLN

CONTROL OF YAW AND ROLL BY A RUDDER/FIN-STABILIZATION SYSTEM

by Claes G. Källström
Swedish Maritime Research Centre, SSPA

ABSTRACT

Different discrete time regulators for control of a ship's yaw and roll motions are designed using linear quadratic control theory. A simulation study to investigate the performances of the different regulators is presented. A ro-ro ship equipped with two active stabilizing fins sailing in irregular beam seas is used as test ship in the simulation study.

1. INTRODUCTION

Traditionally course-keeping and roll stabilization of ships are treated as two separate control problems. Since both yaw and roll motions are induced by deflections of rudder as well as stabilizing fins, it is, however, important to consider the interactions when designing the regulators. This can be done in different ways. Regulators based on de-coupling of the yaw-roll motions were discussed in references (1) and (2). Linear quadratic control theory was employed in (3) to design continuous time regulators.

Efforts to design regulators for reducing the roll by the rudder only have also been made. See references (4), (5), (6), (7) and (8). The key problem using this approach is, of course, that two outputs, yaw and roll, have to be controlled by one input. An autopilot for course-keeping, where not only the yaw motion was considered but also the roll motion, was discussed in (9).

In this paper different discrete time regulators for a ro-ro ship are designed based on linear quadratic control theory. This theory is described in several text books, for example reference (10). A loss function approximately describing the rate of fuel consumption is used as a criterion for the design of an ordinary course-keeping autopilot. This loss function is based on a linear combination of squared heading and rudder angles. The autopilot is then modified by using a criterion, where not only heading and rudder angles are penalized but also roll motions. A regulator for reduction of roll by an active fin-stabilization system is also designed without considering the yaw-roll interactions. Finally, an optimal multivariable controller for a rudder/fin-stabilization system is described, where fuel consumption as well as roll motions are minimized. The performances of the different regulators are compared in a simulation study. A relatively complex non-linear mathematical model of a ro-ro ship sailing in irregular beam seas is used in the simulations.

The paper is organized as follows. The test ship is described in Section 2 and the mathematical simulation model is summarized in Section 3. The performance criteria and the design of the different regulators are discussed Section 4. The simulation results are given in

Section 5 and the major conclusions to be drawn can be found in Section 6. An appendix with the detailed simulation model is also given.

2. TEST SHIP

A single screw/single rudder ro-ro ship was selected for the simulation study. The bow and stern draught is 11.0 m and the displacement is 52 010 m^3. The metacentric height $\overline{GM}$ is 0.45 m. The ship particulars are summarized in Table 1.

Table 1. Particulars of Test Ship

HULL DATA	
Length between perpendiculars (L)	173.2 m
Beam	32.3 m
Draught, bow	11.0 m
Draught, stern	11.0 m
Displacement (∇)	52 010 m^3
Metacentric height ($\overline{GM}$)	0.45 m
PROPELLER DATA	
Propeller diameter (D)	6.3 m
Pitch ratio (P/D)	0.715
Number of blades	4
RUDDER DATA	
Total rudder area	35.8 m^2
Aspect ratio	1.4

Propulsion and Rudder

A diesel engine of 13 000 HP delivers the propulsion power. The ship is fitted with a four-blade propeller with a diameter of 6.3 m. The rudder is of "Mariner" type with a total area of 35.8 m^2. The propeller and rudder data are given in Table 1.

Active Fins

The test ship has no roll stabilization system. However, in the simulation model the ship is fitted with two active fins. See Fig. 1. Each fin has an area of 25.0 m^2 and the aspect ratio is 1.0. The active fins are placed 50 m aft of L/2.

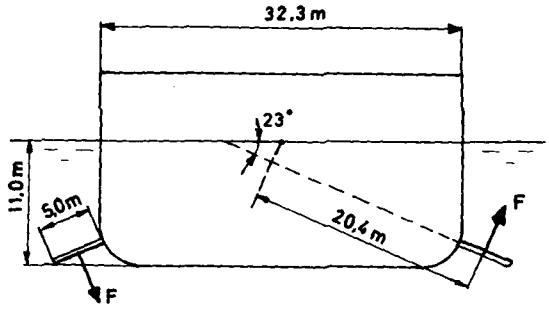

Figure 1. Active Fins Designed for the Test Ship.

3. MATHEMATICAL MODEL

The simulation model, which describes the surge, sway, yaw and roll motions of a ship sailing in waves, is briefly outlined in this Section. The complete simulation model is given in the appendix, where parameter values for the test ship are also summarized. The numerical values have been obtained from captive scale model tests and theoretical estimations. Another alternative of determining the parameters for a specific ship is the application of system identification to full-scale experiments or free-sailing scale model tests. See references (11), (12), (13), (14) and (15).

The structure of the basic mathematical model was given by Norrbin (16) and further developed by Norrbin (17). The mathematical model, excluding the roll equation, has been used in many simulation studies, for example in (14) and (18).

Equations of Motion

The equations of motion are conveniently expressed using a coordinate system fixed to the ship. The origin is placed in the free water surface plane half-way between the perpendiculars and in the centre-line of the ship.

The variables used to describe the surge, sway, yaw and roll motions are explained in Fig. 2. The projections of the total ship speed V on the x- and y-axes are the surge velocity u and the sway

velocity v. The yaw rate is denoted r and the heading and rudder angles are denoted ψ and δ. The roll motion is characterized by the roll angle ϕ and the roll rate p. The angle α of the active fins is defined positive when a negative roll moment is induced.

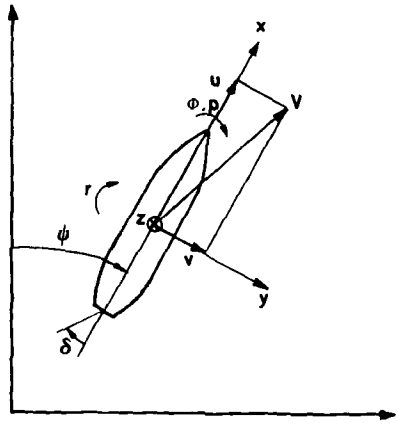

Figure 2. Variables Used to Describe the Surge, Sway, Yaw and Roll Motions of a Ship.

The equations of motion are obtained from Newton's laws expressing conservation of linear and angular momentum:

$$
\begin{aligned}
m(\dot{u} - vr - x_G r^2 + z_G rp) &= X + T(1-t_p) + X_R + X_F + X_w \\
m(\dot{v} + ur + x_G \dot{r} - z_G \dot{p}) &= Y + Y_R + Y_F + Y_w \\
I_{zz}\dot{r} - I_{zx}\dot{p} + mx_G(\dot{v} + ur) &= N + N_R + N_R + N_w \\
I_{xx}\dot{p} - I_{zx}\dot{r} - mz_G(\dot{v} + ur) + mg\cdot\overline{GM}\cdot\sin\phi &= K + K_R + K_F + K_w
\end{aligned}
\qquad (3.1)
$$

where X and Y are the components of the hydrodynamic forces on the x-axis and y-axis, N and K are the z-component and x-component of the hydrodynamic moments, m is the mass of the ship, I_{zz} and I_{xx} are moments of inertia, I_{zx} is a product of inertia, and x_G and z_G are x and z co-ordinates of the centre of gravity. Note that the y co-ordinate of the centre of gravity is equal to zero, because the co-

ordinate origin has been set in the centre-line of the ship. The propeller thrust is denoted T and the thrust deduction factor t_D. X_R, X_F and X_W are forces in the x-direction from rudder, active fins and waves, respectively. The added forces and moments of the other equations of (3.1) are defined analogously.

Propeller Thrust

The propeller thrust is computed as

$$T = K_T \cdot \rho D^4 n^2 \tag{3.2}$$

where ρ is the water density, D is the propeller diameter and n is the propeller rate of revolution. The propeller is characterized by a polynomial expression for K_T, which is given in the appendix. A constant propeller rate of revolution n equal to 1.93 1/s (116 rpm) is assumed in the simulations. This propeller rate corresponds to a nominal ship speed of 7.7 m/s (15 knots).

Rudder and Active Fin Forces

The lift forces from the rudder and one of the active fins are obtained as:

$$\begin{aligned} Y_R &= (k_1 u^2 + k_2 T)(1 + s_1 \delta^2)\delta \\ F &= k_3 u^2 (1 + s_2 \alpha^2)\alpha \end{aligned} \tag{3.3}$$

Note that $Y_F = 2 \cdot \sin\gamma \cdot F$, where γ is the angle between the fin axis and the free water surface plane (cf. Fig. 1). The details of (3.3) and the other forces and moments from rudder and active fins are given in the appendix.

First-order models describing the rudder and active fin dynamics are included in the simulation model:

$$\begin{aligned} \dot{\delta} &= (-\delta + \delta_c)/T_R \\ \dot{\alpha} &= (-\alpha + \alpha_c)/T_F \end{aligned} \tag{3.4}$$

where δ_c and α_c are the commanded angles and T_R and T_F are the time constants. Both rudder and fin rates of (3.4) are limited as well as the maximum rudder and fin angles.

Wave Forces

The forces and moments from beam seas acting on the ship are approximated by:

$$X_W = 0$$

$$Y_w = m \cdot \bar{a}_1 \cdot S(t)$$

$$N_w = mL \cdot \bar{a}_2 \cdot \xi(t) \qquad (3.5)$$

$$K_w = mL \cdot \bar{a}_3 \cdot S(t)$$

where $\xi(t)$ is the z co-ordinate of the sea level at origin and $S(t)$ is the wave slope.

A Pierson-Moskowitz wave spectrum given by (see ref. (19))

$$\Phi_{\xi\xi}(\omega) = \frac{A}{\omega^5} e^{-B/\omega^4} \qquad (3.6)$$

is simulated by feeding a white noise signal into a filter. A significant wave height of 7 m and a mean wave period of 9.4 s are chosen in the simulations. This corresponds to A = 0.78 and B = 0.063 in (3.6). A rational spectrum

$$\tilde{\Phi}_{\xi\xi}(\omega) = \frac{b_2^2\omega^2}{\omega^6 + (a_1^2-2a_2)\omega^4 + (a_2^2-2a_1a_3)\omega^2 + a_3^2} \qquad (3.7)$$

with $a_1 = 0.5$, $a_2 = 0.33$, $a_3 = 0.07$ and $b_2 = 0.415$ is used as an approximation of (3.6) for the chosen sea state. The spectra (3.6) and (3.7) are illustrated in Fig. 3.

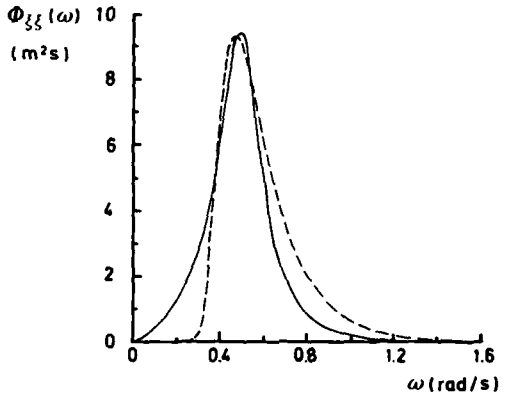

Figure 3. The Rational Spectrum (3.7) (continuous line) and the Pierson-Moskowitz Spectrum (3.6) (dashed line) for a Significant Wave Height of 7 m and a Mean Wave Period of 9.4 s.

A stochastic process with spectral density (3.7) is obtained as output from the filter

$$G_\xi(s) = \frac{b_2 s}{s^3 + a_1 s^2 + a_2 s + a_3} \tag{3.8}$$

when the input is white noise (see ref. (20)). An approximation of the wave slope spectrum

$$\Phi_{SS}(\omega) = \frac{\omega^4}{g^2} \Phi_{\xi\xi}(\omega)$$

is given analogously by

$$G_S(s) = \frac{c\, b_2 s^2}{s^3 + a_1 s^2 + a_2 s + a_3} \tag{3.9}$$

where $c = -0.065$ for the chosen sea state.

The two filters (3.8) and (3.9) are represented in the simulations by the differential equation system:

$$\begin{bmatrix} \dot{x}_1 \\ \dot{x}_2 \\ \dot{x}_3 \end{bmatrix} = \begin{bmatrix} -a_1 & 1 & 0 \\ -a_2 & 0 & 1 \\ -a_3 & 0 & 0 \end{bmatrix} \begin{bmatrix} x_1 \\ x_2 \\ x_3 \end{bmatrix} + \begin{bmatrix} 0 \\ b_2 \\ 0 \end{bmatrix} e$$

$$\begin{bmatrix} \xi \\ S \end{bmatrix} = \begin{bmatrix} 1 & 0 & 0 \\ -a_1 c & c & 0 \end{bmatrix} \begin{bmatrix} x_1 \\ x_2 \\ x_3 \end{bmatrix} \tag{3.10}$$

where e is a discrete time white noise signal with zero mean and standard deviation 2.22. A time step of 0.5 s was used. Realizations of the wave level ξ and the wave slope S are shown in Fig. 4. These realizations are used in all the simulations.

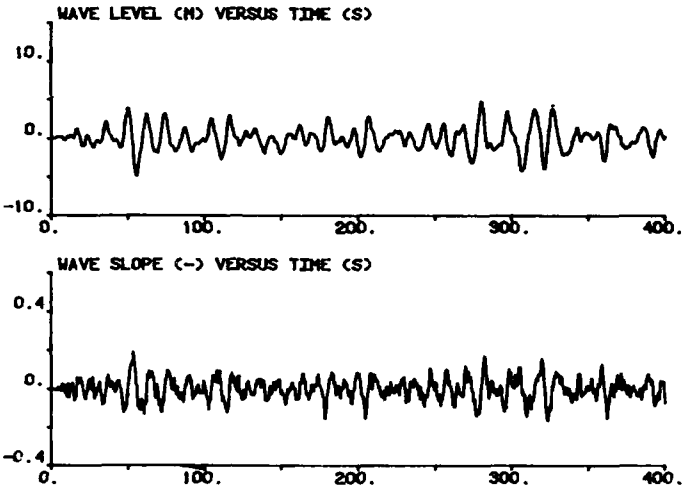

Figure 4. Realizations of wave level ξ and wave slope S.

4. DESIGN OF REGULATORS

The regulator design is based on linear quadratic control theory (see ref. (10)). The design is carried out efficiently by use of the interactive computer program SYNPAC, ref. (21).

A preliminary investigation showed that a sampling interval of 1-5 s was appropriate. It was decided to use the interval 2 s in all the simulations.

Linearized Models

The following linearized state space model is the basis for the design:

$$\begin{bmatrix} \dot{v} \\ \dot{r} \\ \dot{p} \\ \dot{\psi} \\ \dot{\phi} \end{bmatrix} = \begin{bmatrix} -0.019 & -3.1 & 0.069 & 0 & 0.031 \\ -0.0012 & -0.087 & 0.00055 & 0 & -0.000031 \\ 0.00066 & -0.14 & -0.018 & 0 & -0.022 \\ 0 & 1 & 0 & 0 & 0 \\ 0 & 0 & 1 & 0 & 0 \end{bmatrix} \begin{bmatrix} v \\ r \\ p \\ \psi \\ \phi \end{bmatrix} + \begin{bmatrix} 0.044 & 0.015 \\ -0.0018 & -0.00026 \\ -0.0017 & -0.0040 \\ 0 & 0 \\ 0 & 0 \end{bmatrix} \begin{bmatrix} \delta_c \\ \alpha_c \end{bmatrix} \tag{4.1}$$

where the equations of surge, rudder and fin motions have been excluded and the linearization is performed around $u = 7.7$ m/s, $v = r = p = \psi = \phi = \delta = \alpha = 0$.

If the roll motion is neglected in equation (4.1), an analysis shows that the time constants of the v and r equations are $T_1 = 8$ s, $T_2 = -50$ s and $T_3 = 22$ s. Thus, the steering equations have a very unstable mode. Nomoto's steering model:

$$\begin{bmatrix} \dot{r} \\ \dot{\psi} \end{bmatrix} = \begin{bmatrix} -\frac{1}{T} & 0 \\ 1 & 0 \end{bmatrix} \begin{bmatrix} r \\ \psi \end{bmatrix} + \begin{bmatrix} K/T \\ 0 \end{bmatrix} \delta_c \tag{4.2}$$

where $T = T_1 + T_2 - T_3 = -64$ s and $K = 0.040$ 1/s, is used for the design of a simple yaw regulator.

If the couplings of v and r into the roll equations of (4.1) are neglected, the ship's natural period of roll is then calculated to 42 s and the damping coefficient ξ to 0.061. The design of a simple roll controller is based on the model:

$$\begin{bmatrix} \dot{p} \\ \dot{\phi} \end{bmatrix} = \begin{bmatrix} -0.018 & -0.022 \\ 1 & 0 \end{bmatrix} \begin{bmatrix} p \\ \phi \end{bmatrix} + \begin{bmatrix} -0.0040 \\ 0 \end{bmatrix} \alpha_c \tag{4.3}$$

Performance Criteria

A simple criterion for steady state course-keeping has been proposed by Koyama (22) and Norrbin (23):

$$J^* = \int_0^\infty (\psi^2 + \lambda_\delta \delta_c^2)\, dt \tag{4.4}$$

It was verified in reference (24) by full-scale experiments that the criterion (4.4) with an appropriate value of λ_δ gave a good description of the rate of fuel consumption in weather conditions varying between light and fresh breeze. In hard weather the criterion (4.4) has not been verified. Based on formulas in reference (23) the value of λ_δ was calculated to 0.17 for the test ship. A corresponding value for the active fin deflections was also calculated: $\lambda_\alpha = 0.24$.

A suitable criterion for the design of roll regulators is:

$$J = \int_0^\infty (\lambda_p p^2 + \lambda_\phi \phi^2 + \varepsilon_\alpha \alpha_c^2)\, dt \qquad (4.5)$$

where λ_p and λ_ϕ should be chosen in such a way that a good roll reduction is obtained. A few preliminary simulations resulted in the following values: $\lambda_p = 55\ s^2$ and $\lambda_\phi = 0.5$. The values can probably be improved by a more comprehensive simulation study.

Regulator 1

A simple yaw controller is designed based on Nomoto's model (4.2) and the criterion (4.4):

$$\delta_c = -112 \cdot r - 2.3 \cdot \psi \qquad (4.6)$$

Regulator 2

A yaw and roll controller, where the rudder only is used, is designed based on the criterion:

$$J = \int_0^\infty (\lambda_p p^2 + \psi^2 + \lambda_\phi \phi^2 + \lambda_\delta \delta_c^2)\, dt \qquad (4.7)$$

and a combination of the models (4.1) and (4.2):

$$\delta_c = -27 \cdot r - 5.0 \cdot p - 2.3 \cdot \psi - 1.4 \cdot \phi \qquad (4.8)$$

Regulator 3

This regulator consists of one rudder/heading loop and one fin/roll loop. The yaw-roll interactions are not considered. The yaw controller is the same as (4.6) and the roll controller is designed using the model (4.3) and the criterion (4.5):

$$\alpha_c = -13 \cdot p + 0.10 \cdot \phi \qquad (4.9)$$

Note that the roll rate gain is the important factor and that the roll gain is almost negligible.

Regulator 4

A true multivariable controller is designed based on a combination of the models (4.1) and (4.2), and the criterion:

$$J = \int_0^\infty (\lambda_p p^2 + \psi^2 + \lambda_\phi \phi^2 + \lambda_\delta \delta_c^2 + \lambda_\alpha \alpha_c^2)\, dt \qquad (4.10)$$

The following controller was obtained:

$$\begin{aligned} \delta_c &= -26 \cdot r - 2.8 \cdot p - 2.4 \cdot \psi - 0.87 \cdot \phi \\ \alpha_c &= 5.0 \cdot r - 13 \cdot p + 0.020 \cdot \psi - 0.21 \cdot \phi \end{aligned} \qquad (4.11)$$

The reason for excluding the sway velocity v is simply that it is usually difficult to obtain reliable measurements of v.

5. RESULTS OF SIMULATIONS

The simulations were carried out efficiently by use of the interactive simulation program SIMNON, reference (25). The results of the simulations are shown in Figs. 5-8. A summary of root-mean-square (rms) values and maximum values are given in Table 2, where the steering loss function J^* (eqn. (4.4)) is also tabulated. Note that the maximum rudder and fin angles were limited to 20° in all the simulations.

Table 2. Simulation Results

Regulator	rms (δ) deg	rms (α) deg	rms (ψ) deg	max $\lvert\psi\rvert$ deg	rms (ϕ) deg	max $\lvert\phi\rvert$ deg	J^* $(\text{deg})^2$
1	8.84	-	0.50	1.29	5.32	16.38	13.53
2	7.87	-	1.14	2.71	4.86	14.93	11.81
3	8.78	12.12	0.48	1.32	4.86	14.58	13.34
4	4.22	12.28	0.87	1.93	4.70	13.37	3.79

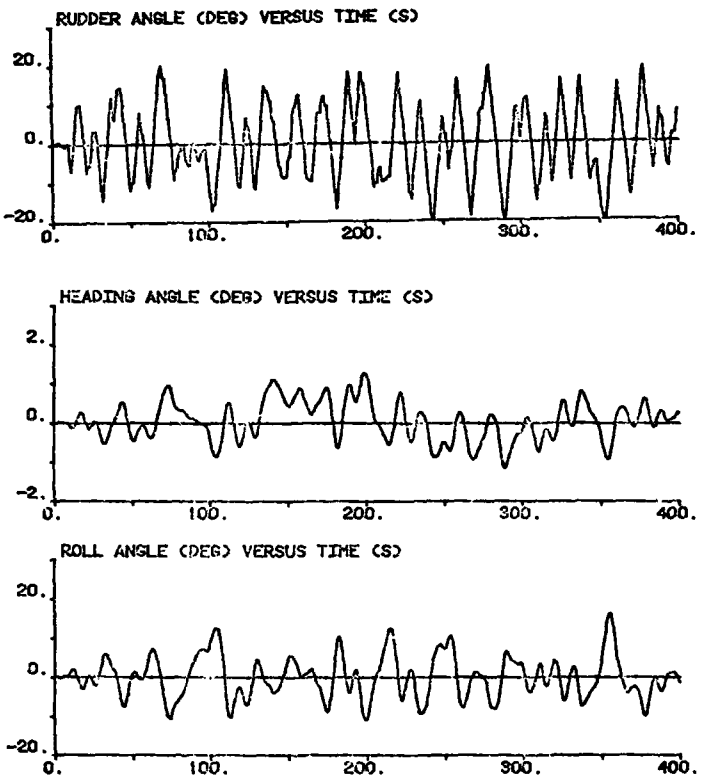

Figure 5. Regulator 1 - Simulation Results.

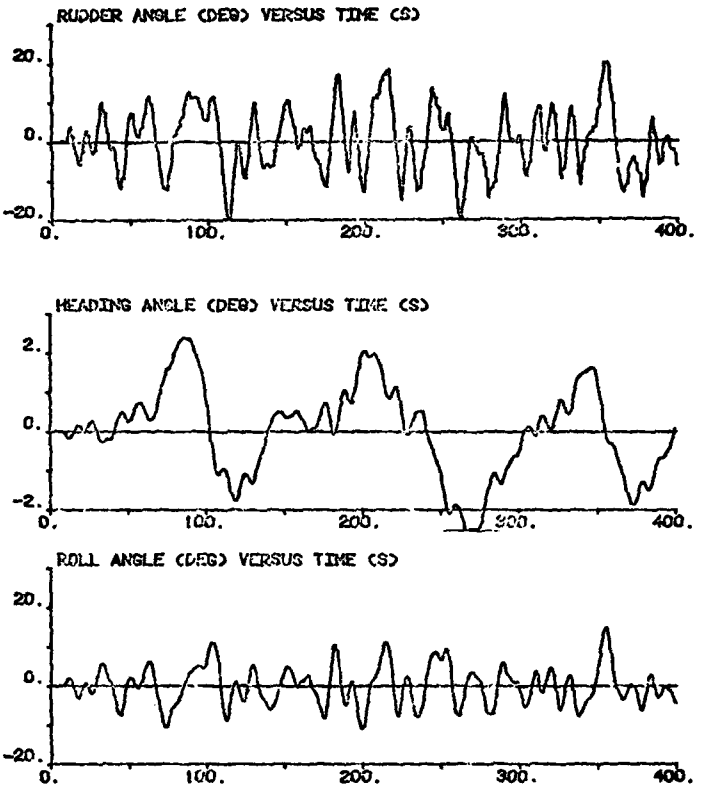

Figure 6. Regulator 2 - Simulation Results.

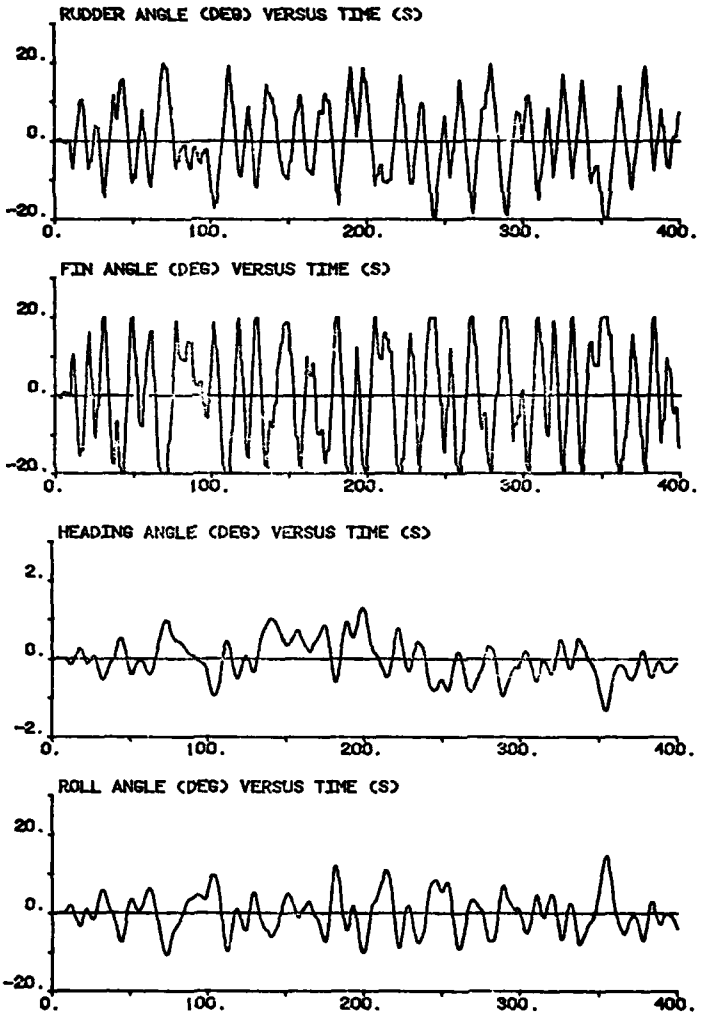

Figure 7. Regulator 3 - Simulation Results.

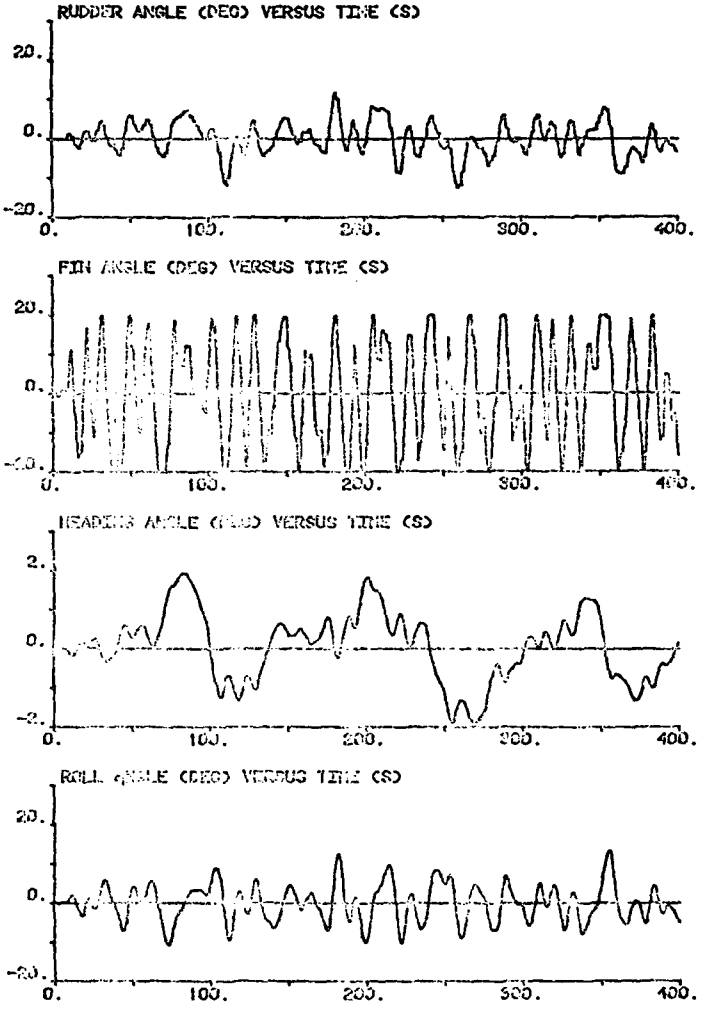

Figure 8. Regulator 4 - Simulation Results.

By comparing the simple course-keeping regulator 1 with regulator 2 (yaw/roll-control by rudder), it is concluded that the rms of roll is reduced by 8.6 % and the maximum roll angle by 8.9 %. Thus, roll stabilization by rudder is a reasonable concept for the test ship. Also note that the J^* is decreased for regulator 2. This result indicates that the roll motion should be considered in all autopilot designs for ships (cf. ref. (9)).

Traditional yaw/roll-control by rudder/fins (regulator 3), without considering the yaw/roll-interactions, improved the roll performance approximately as much as regulator 2 did. However, it should be noted that the value of J^* is larger for regulator 3 than for regulator 2 because of the induced resistance of the active fins.

Regulator 4, the true multivariable controller, reduced the rms of roll by 11.7 % and the maximum roll by 18.4 % compared to regulator 1. The improvements compared to regulator 3 were 3.3 % and 8.3 %, respectively. Note the extremely low value of J^* obtained for regulator 4.

6. CONCLUSIONS

A relatively complex non-linear mathematical model for a ship moving in irregular seas has been presented. An approach to simulate continuous wave spectra by feeding white noise into a filter was given.

Different discrete time yaw/roll-regulators were designed using linear quadratic control theory. These were investigated by simulations, where a ro-ro ship was sailing in irregular beam seas of a significant wave height of 7 m. It was concluded:

- o A true multivariable rudder/fin-controller improved both roll and steering performances significantly.
- o Some, not insignificant, improvements of both roll and steering behaviour were obtained with a system for yaw/roll-control by the rudder.

However, not many simulations of this type have been carried out up to now, so the simulation results must be considered as preliminary.

Future work should include a feasibility study of applying advanced filtering techniques, for example Kalman filtering, and adaptive control techniques for the combined yaw/roll-control problem. Adaptive autopilots for yaw-control only and Kalman filters were designed in references (14) and (26). Kalman and adaptive filters have also been designed for wave filtering in connection with dynamic positioning systems (references (27) and (28)).

7. REFERENCES

(1) J. B. Carley, A. Duberley, "Design considerations for optimum ship motion control", 3rd Ship Control Systems Symposium, Bath, England, 1972, Proceedings Vol. 2, Paper No VI C-1, 19 p.

(2) R. A. Savill, M. G. Waugh, and I. N. Britten, "Micro-computer implementation of a de-coupling pre-compensator for ship steering-stabilization interaction", Symposium on Ship Steering Automatic Control, Genova, Italy 1980, Proceedings, pp. 377-382.

(3) P. H. Whyte, "A note on the application of modern control theory to ship roll stabilization", 18th General Meeting of the American Towing Tank Conference, Annapolis, Md, Proceedings, Vol. 2, pp. 517-532.

(4) W. E. Cowley, T. H. Lambert, "The use of the rudder as a roll stabiliser", 3rd Ship Control Systems Symposium, Bath, England, 1972, Proceedings Vol. 2, Paper No VII C-1, 25 p.

(5) F. F. van Gunsteren, "Analysis of roll stabilizer performance", International Shipbuilding Progress 21(1974):237, May, pp. 125-246.

(6) W. E. Cowley, T. H. Lambert, "Sea trials on a roll stabiliser using the ship's rudder", 4th Ship Control Systems Symposium, the Hague, the Netherlands 1975, Proceedings Vol. 2, pp. 195-213.

(7) J. B. Carley, "Feasibility study of steering and stabilising by rudder", 4th Ship Control Systems Symposium, the Hague, the Netherlands 1975, Proceedings Vol. 2, pp. 172-194.

(8) A. R. J. M. Lloyd, "Roll stabilisation by rudder", 4th Ship Control Systems Symposium, the Hague, the Netherlands 1975, Proceedings Vol. 2, pp. 214-242.

(9) K. Ohtsu, M. Horigome, and G. Kitagawa, "A new ship's auto pilot design through a stochastic model", Automatica 15(1979), pp. 255-268.

(10) B. D. O. Anderson, J. B. Moore, "Linear Optimal Control", Prentice-Hall, Englewood Cliffs, New Jersey, USA 1971, 399 p.

(11) K. J. Åström, C. G. Källström, "Identification of ship steering dynamics", Automatica 12(1976), pp. 9-22.

(12) K. J. Åström, C. G. Källström, N. H. Norrbin, and L. Byström, "The identification of linear ship steering dynamics using maximum likelihood parameter estimation", SSPA, Göteborg, Sweden, Publication No 75, 1975, 105 p.

(13) L. Byström, C. G. Källström, "System identification of linear and non-linear ship steering dynamics", 5th Ship Control Systems Symposium, Annapolis, Maryland, USA 1978, Proceedings Vol. 3, 21 p.

(14) C. G. Källström, "Identification and adaptive control applied to ship steering", Department of Automatic Control, Lund Institute of Technology, Lund, Sweden, CODEN: LUTFD2/(TFRT-1018)/1-192/(1979).

(15) C. G. Källström, K. J. Åström, "Experiences of system identification applied to ship steering", Automatica 17(1981):1, p. 187-198.

(16) N. H. Norrbin, "Theory and observations on the use of a mathematical model for ship manoeuvring in deep and confined waters", SSPA, Göteborg, Sweden, Publication No 68, 1971, 117 p.

(17) N. H. Norrbin, "A method for the prediction of the manoeuvring lane of a ship in a channel of varying width", Symposium on Aspects of Navigability of Constraint Waterways, Including Harbour Entrances, Delft, the Netherlands 1978, Proceedings Vol. 3, Paper 22, 16 p.

(18) N. H. Norrbin, S. Göransson, R. J. Risberg, and D. H. George, "A study of the safety of two-way traffic in a Panama canal bend", 5th Ship Control Systems Symposium, Annapolis, Maryland, USA 1978, Vol. 3, 34 p.

(19) W. G. Price, R. E. D. Bishop, "Probabilistic Theory of Ship Dynamics", Chapman and Hall, London 1974, 318 p.

(20) K. J. Åström, "Introduction to Stochastic Control Theory", Academic Press, New York and London, 1970, 299 p.

(21) J. Wieslander, "Synpac commands - User's guide", Department of Automatic Control, Lund Institute of Technology, Lund, Sweden, CODEN: LUTFD2/(TFRT-3159)/1-130/(1980).

(22) T. Koyama, "On the optimum automatic steering system of ships at sea", Selected Papers from Journ. Society of Naval Arch. of Japan, Vol. 4(1970), pp. 142-156.

(23) N. H. Norrbin, "On the added resistance due to steering on a straight course", 13th Int. Towing Tank Conference Berlin/Hamburg 1972, Vol. 1, pp. 382-408.

(24) C. G. Källström, N. H. Norrbin, "Performance criteria for ship autopilots", Symposium on Ship Steering Automatic Control, Genova, Italy 1980, Proceedings, pp. 23-40.

(25) H. Elmqvist, "SIMNON - An interactive simulation program for nonlinear systems - User's manual", Department of Automatic Control, Lund Institute of Technology, Lund, Sweden 1975, Report 7502.

(26) C. G. Källström, K. J. Åström, N. E. Thorell, J. Eriksson, and L. Sten, "Adaptive autopilots for tankers", Automatica 15(1979):3, pp. 241-254.

(27) J. G. Balchen, N. A. Jenssen, and S. Sælid, "Dynamic positioning using Kalman filtering and optimal control theory", Symposium on Automation in Offshore Oil Field Operation, Bergen, Norway 1976, Proceedings, pp. 183-188.

(28) N. A. Jenssen, "Estimation and control in dynamic positioning of vessels", The Norwegian Institute of Technology, Division of Engineering Cybernetics, Trondheim, Norway 1980, Report 80-90-W, 174 p.

APPENDIX - SIMULATION MODEL

The simulations are based on the following mathematical model describing the surge, sway, yaw and roll motions of a ship moving in waves:

$$(1-X''_{\dot{u}})\dot{u} = \frac{1}{L}\frac{1}{2}X''_{uu}u^2 + \frac{1}{L\sqrt{gL}}\frac{1}{2}X''_{uvv}uv^2 + L(x''_G+X''_{rr})r^2 + (1+X''_{vr})vr -$$

$$- Lz''_G pr + (T/m)(1-t_p) + X''_{YR\delta}(Y_R/m)\delta + X''_{F\alpha}\cdot 2\cdot(F/m)\alpha + X_w/m$$

$$\begin{bmatrix} 1-Y''_{\dot{v}} & L(x''_G-Y''_{\dot{r}}) & -L(z''_G+Y''_{\dot{p}}) \\ x''_G-N''_{\dot{v}} & L((k''_{zz})^2-N''_{\dot{r}}) & -L(I''_{zx}+N''_{\dot{p}}) \\ -(z''_G+K''_{\dot{v}}) & -L(I''_{zx}+K''_{\dot{r}}) & L((k''_{xx})^2-K''_{\dot{p}}) \end{bmatrix} \begin{bmatrix} \dot{v} \\ \dot{r} \\ \dot{p} \end{bmatrix} =$$

$$\begin{bmatrix} \frac{1}{L}Y''_{uv} & Y''_{ur}-1 & Y''_{up} \\ \frac{1}{L}N''_{uv} & N''_{ur}-x''_G & N''_{up} \\ \frac{1}{L}K''_{uv} & K''_{ur}+z''_G & K''_{up} \end{bmatrix} \begin{bmatrix} uv \\ ur \\ up \end{bmatrix} +$$

$$\begin{bmatrix} C\frac{L^3}{2\nabla}f_Y(v,r) \\ C\frac{L^3}{2\nabla}f_N(v,r) \\ L\frac{1}{2}K''_{p|p|}p|p| - g\frac{\overline{GM}}{L}\sin\phi \end{bmatrix} + \begin{bmatrix} 1 & \lambda_{12} \\ \lambda_{21} & \lambda_{22} \\ \lambda_{31} & \lambda_{32} \end{bmatrix} \begin{bmatrix} Y_R/m \\ 2\cdot F/m \end{bmatrix} +$$

$$\begin{bmatrix} Y_w/m \\ N_w/(mL) \\ K_w/(mL) \end{bmatrix}$$

The model is normalized using the 'bis' system (Norrbin (16)).

The propeller thrust is computed as:

$$T/m = K_T D^4 n^2/\nabla$$

where

$$K_T = c_1 + c_2 J + c_3(P/D) + c_4 J^2 + c_5(P/D)^6$$

and the propeller advance coefficient

$$J = \frac{u(1-w)}{nD}$$

The nonlinear functions $f_Y(v,r)$ and $f_N(v,r)$ have been derived by Norrbin (17). They are reprinted in Källström (14).

The lift forces from the rudder and one of the stabilizing fins are computed as:

$$Y_R/m = [\frac{1}{L}\frac{1}{2} Y''_{uu\delta} u^2 + Y''_{T\delta}(T/m)](1+s_1\delta^2)\delta$$

$$F/m = [\frac{1}{L}\frac{1}{2} F''_{uu\alpha} u^2](1+s_2\alpha^2)\alpha$$

The rudder and fin angles are governed by first order differential equations:

$$\dot{\delta} = (-\delta+\delta_c)/T_R \quad , \quad |\dot{\delta}| < \dot{\delta}_{lim} \quad , \quad |\delta| < \delta_{lim}$$

$$\dot{\alpha} = (-\alpha+\alpha_c)/T_F \quad , \quad |\dot{\alpha}| < \dot{\alpha}_{lim} \quad , \quad |\alpha| < \alpha_{lim}$$

where δ_c and α_c are the commanded angles.

The heading angle ψ and roll angle ϕ are obtained as:

$$\dot{\psi} = r$$

$$\dot{\phi} = p$$

In beam seas the wave forces can be approximated by:

$$X_w/m = 0$$

$$Y_w/m = \bar{a}_1 \cdot S(t)$$

$$N_w/(mL) = \bar{a}_2 \cdot \xi(t)$$

$$K_w/(mL) = \bar{a}_3 \cdot S(t)$$

where $\xi(t)$ is the z co-ordinate of the sea level at origin and $S(t)$ is the wave slope.

The following parameter values for the test ship are used in the simulation study:

L = length between perpendiculars = 173.2 m

∇ = displacement = 52 010 m^3

m = mass = $53.3 \cdot 10^6$ kg

g = acceleration of gravity = 9.81 m/s^2

x''_G = normalized x co-ordinate of centre of gravity = 0.018

z''_G = normalized z co-ordinate of centre of gravity = -0.015

k''_{xx} = normalized radius of gyration around x-axis = 0.074

k''_{zz} = normalized radius of gyration around z-axis = 0.25

I''_{zx} = normalized product of inertia = 0

$\overline{GM}$ = metacentric height = 0.45 m

D = propeller diameter = 6.3 m

P/D = propeller pitch ratio = 0.715

n = propeller rate = 1.93 1/s

$X''_{\dot{u}}$ = -0.060

$\frac{1}{2} X''_{uu}$ = -0.032

$\frac{1}{2} X''_{uvv}$ = 0.00040

X''_{rr} = 0

X''_{vr} = 0.15

t_p = thrust deduction factor = 0.19

$X''_{YR\delta}$ = -0.40

$X''_{F\alpha}$ = -0.67

$Y''_{\dot{v}}$ = -0.73

$Y''_{\dot{r}}$ = 0

$Y''_{\dot{p}}$ = 0.0011

Y''_{uv} = -0.78

Y''_{ur} = 0.22

Y''_{up} = 0.010

$N''_{\dot{v}}$ = 0

$N''_{\dot{r}}$ = -0.040

$N''_{\dot{p}}$ = 0

N''_{uv} = -0.50

N''_{ur} = -0.19

N''_{up} = 0.0014

$K''_{\dot{v}}$ = 0.017

$K''_{\dot{r}}$ = 0

$K''_{\dot{p}}$ = -0.0012

K''_{uv} = 0.018

K''_{ur} = -0.0051

K''_{up} = -0.0027

C = 0.75

$\frac{1}{2} K''_{p|p|}$ = -0.0040

λ_{12} = 0.39

λ_{21} = -0.48

λ_{22} = -0.11

λ_{31} = -0.031

λ_{32} = -0.12

c_1 = -0.020

c_2 = -0.37

c_3 = 0.52

c_4 = -0.063

c_5 = -0.0016

w = wake fraction = 0.27

$\frac{1}{2} Y''_{uu\delta}$ = 0.14

$Y''_{T\delta}$ = 0.95

s_1 = -0.45

$\frac{1}{2} F''_{uu\alpha}$ = 0.057

s_2 = 1.6

T_R = time constant of rudder = 0.5 s

$\dot{\delta}_{lim}$ = rudder rate limit = 0.077 rad/s (= 4.4 deg/s)

δ_{lim} = rudder angle limit = 0.35 rad (= 20 deg)

T_F = time constant of fin = 0.4 s

$\dot{\alpha}_{lim}$ = fin rate limit = 0.14 rad/s (= 8.0 deg/s)

α_{lim} = fin angle limit = 0.35 rad (= 20 deg)

$\bar{a}_1$ = 27 m/s^2

$\bar{a}_2$ = -0.017 1/s^2

$\bar{a}_3$ = 0.23 m/s^2

} Assumptions: u ≈ 7.7 m/s (15 knots), beam sea on port side

DESIGNING A MICROPROCESSOR BASED FIN STABILISER CONTROL SYSTEM

By Michael Clarke B.Sc.
Muirhead Vactric Components Ltd

ABSTRACT

This paper will outline the various stages in the design and development of a low cost microprocessor based fin stabiliser control system (FSCS) suitable for a wide range of surface ships. There are several critical areas such as cost, performance, reliability, maintainability and safety which must be realised in any new design before the equipment becomes acceptable to the user. The paper explains how these have been met to provide a cost-effective roll stabiliser without the frills or gimmicks that have become commonplace in many modern microprocessor based systems.

INTRODUCTION

Muirhead have been in the ship stabiliser field since 1946 and have, to date, supplied more than half the stabilised ships in the world including naval vessels with control systems. The current range of stabiliser control systems in production number three, and are all analogue in principle. The low cost K-426 system introduced in 1970 utilises an in-built velocity gyroscope as the ship's motion sensor and was designed for smaller vessels where the degree of sophisticated control is not always necessary. For larger vessels, the K-373 system again uses an in-built velocity gyroscope but computes roll angle, roll velocity and roll acceleration signals from the gyroscope and combines these to produce the stabilised signal. For naval applications, the AEL system designed by the Royal Navy Admiralty Engineering Laboratory and manufactured by Muirhead is used, although many navies, including the Royal Navy, also use the K-373. All three systems provide automatic fin angle reduction with ships speed by utilising an output from the ship's log.

In March 1978 Muirhead were awarded a design subcontract to produce a prototype microprocessor FSCS for the U.S. Navy's FFG 7 class ships, which was duly completed by the end of 1979.

The Royal Navy and other customers in the U.K. and abroad requested design studies into systems using modern technology and therefore, Muirhead decided to update its current range. The result of this work is the new FSCS shown in Fig.1

DESIGN AIMS

From market research and customer liaisons, a draft specification was compiled detailing all the parameters and design aims for the new control system. It was Muirhead's intention that the new equipment should, in the first place, extend our current range and then eventually replace or supersede the AEL and K-373 systems. Therefore, the equipment would need to meet both military and commercial specifications.

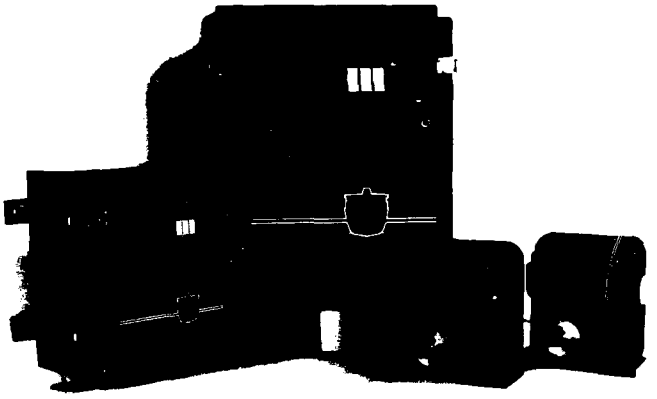

Fig.1 Microprocessor FSCS for a Two-Fin Installation

The new control system would be microprocessor based as it had been demonstrated in various studies that this offered many advantages over conventional analogue controllers. This would be more adaptable to future requirements so long as the overall cost was kept to within that of our existing equipment. These advantages can be defined as follows:-

a) All signal filtering would be software based thereby allowing more complex functions to be implemented.

b) All time-dependent elements used in the control algorithm etc. would be software based thus allowing ramping techniques to be used, thereby enabling the system to come on-line faster.

c) Drift problems would be eliminated.

d) Characteristics or the principle of the control algorithm can be changed easily during the design life of the equipment.

e) Self-adaptive control can be implemented.

f) Extensive self-test facilities can be in-built to give warning of system failure or impending failure.

g) Automatic fault diagnostics for the majority of fault conditions.

h) Predefined test waveform generation during installation and maintenance for ease of calibration and checkout.

The need to meet both military and commercial applications with one equipment design can prove detrimental to the commercial equipment in terms of cost. However, military FSCS are not deemed critical

equipment and therefore the reduced shock requirement can be met easily without incurring a cost penalty. Also, most electronic components nowadays are manufactured to both military and commercial specifications, and in the design phase, this was kept very much in mind so that for the military equipment, all the components could be purchased to an acceptable Quality Assurance screened level.

Briefly, the functional requirements for the FSCS can be listed as follows:-

a) The equipment life expectancy shall be 10 years, minimum.

b) The equipment shall function continuously during sea-going periods of a ship for up to 30 days at a time.

c) The equipment shall incorporate performance monitoring and test facilities to enable rapid diagnosis to be made of faults down to printed wiring board or replaceable subassembly level. The Mean Time To Repair for the system shall not exceed 1/2 hour for all repair actions intended to be performed by the ship's crew underway, and not more than 3 hours maximum for any single repair action.

d) The equipment shall be repaired onboard ship by the replacement of complete printed wiring boards or equivalent subassemblies. The printed wiring boards and other replaceable subassemblies shall be suitable for repair ashore by skilled staff employing normal electronic workshop techniques.

e) The Mean Time Between Failure for the FSCS equipment shall not be less than 2000 hours.

f) The equipment shall be suitable for controlling ships with a roll period between 7 to 25 seconds.

MICROPROCESSOR

Today there is a vast bewildering range of microprocessors available to the design engineer and too often the wrong choice is made right at the start of the project. By the time some of the flaws become apparent, it is too late to change to a more suitable device.

The choice of microprocessor for this application, the 16 bit Texas 9900, was based on previous experience with the device and a similar application. The important aspects that the microprocessor must fulfill can be summarised as follows:-

a) A 16 bit data word length compatable with I/O and system resolution, thereby reducing access and computation time.
In parts of the control algorithm double length arithmetic (32 bits) is required to maintain sufficient accuracy etc. and therefore a 16 bit microprocessor is obviously preferred.

b) Comprehensive instruction set with fast multiply and divide facility.

c) Fast instruction cycle time.

d) Comprehensive software development system with in-circuit emulation

capability.

e) Available in both military and commercial versions.

f) Preferably at least dual sourced.

g) Iteration time of less than 100 m.Sec. for the complete task.

Some explanation should be given to the statement in Section g) above.

Since the FSCS is digital in nature, it has a finite resolution and therefore the information given to the fin/hydraulic system is, in effect, a series of steps whose magnitude is directly proportional to the iteration time of the Central Processor Unit. This would place undue strain on the fin/hydraulic system if the iteration time was not sufficiently short, i.e. ideally less than 100 m.Secs.

Other techniques used in an effort to overcome the problem where the iteration time causes concern, such as averaging the step and outputing at a faster rate, or analogue filtering at the fin/hydraulic system, only exacerbate the problem by introducing appreciable phase delays which, in turn, affect stabilisation performance. Thus, whether the iteration time required is achievable, depends upon factors mentioned in previous Sections a), b) & c) and the complexity of the control algorithm principle. Muirhead's policy has been to adopt a proven control algorithm with a microprocessor that has spare computation facilities, so that with future development of the FSCS, more complex algorithms can be implemented if the demand exists.

ROLL MOTION SENSING

As with the choice of microprocessor, care must be exercised with the selection of the sensor. The following text examines the requirements for a suitable ship motion transducer.

There are many choices of transducer that can be used which measure roll angle, or roll velocity, or roll acceleration. Gyroscopes have been used successfully for many years in this type of application, either by fitting an acceleration or velocity gyroscope in the equipment, or by taking information from the ship's stabilised gyro-compass. The main problems with these types of transducers have been size, weight, sensitivity and reliability. To increase the sensitivity of these basically mechanical devices, normally involves a cost and/or reliability penalty.

A very early conception (around 1950) of the purpose and possible performance of stabilisation control, was that it was assumed that the residual motion of the vessel when stabilised, would be sinusoidal in character. Experience has shown however, that this assumption is not true; it implies that roll damping alone is being achieved. The present conception is that ship stabilisation should result in holding the vessel substantially vertical on the sea and that whatever motion remains will be an aperiodical motion with no recognisable character.

In an ideal theory, acceleration control alone is needed since the first result of a wave motion on the ship is an acceleration in the direction of the roll. If this were measured instantaneously, and the fin angle correction applied in the opposite sense, stabilisation

will be achieved. In practice, a certain amount of ship motion is a prerequisite to sensing the acceleration, and to ensure that this motion is of small amplitude, a high sensitivity accelerometer is needed. Therefore, in this design a sensitive angular accelerometer was chosen to give optimum stabilisation performance. By using an angular device, 'heave' and 'sway' elements of the ship are eliminated from the output information that would be present if a linear device were used. From the acceleration information, velocity and angle can be computed for the control algorithm by using standard integration techniques. If, however, a transducer is used that gives velocity or roll information, computation of the other two terms required can introduce appreciable problems of digital noise, when differentiation is used on information which has a limited and finite resolution. This can be overcome by additional filtering within the control algorithm and therefore does not preclude other types of transducers that measure roll angle or velocity from being used with this FSCS.

SYSTEM CONFIGURATION

The FSCS has been configured around three units - a) the Central Processor Unit (CPU); b) the Angle Transmitter Unit (ATU) and c) the Acceleration Sensor Unit (ASU) which connect together as shown in Fig.2

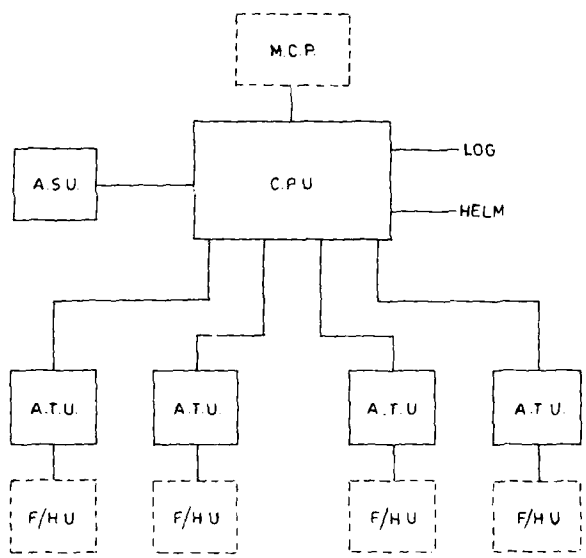

Fig.2 System Configuration for FSCS

In Fig.2 the units shown dotted are other parts of the installation to which the FSCS interconnect, and the diagram is not meant to represent or show a complete Fin Stabiliser System.

In an effort to minimise cost as far as possible, the number of units that comprise a FSCS was evaluated in depth and has resulted in the configuration shown. This could have been reduced still further by the inclusion of the Angular Accelerometer and the electronics from the ATU into the CPU, but the configuration chosen freed the equipment from several important constraints:-

a) The need for the CPU to be mounted on an aft or forward bulkhead and near to the ship's roll centre.

b) The CPU size and weight could be reduced.

c) Other types of ship motion sensor could be accommodated if required.

d) The Fin/Hydraulic system needs to be complete in its entirety for maintenance, installation, checkout and fault diagnostic purposes.

Electrical noise or EMI has for many years caused problems to all types of equipment fitted to ships. Muirhead's FSCS have not suffered this sort of problem in the past due mainly to the fact that 3-wire synchro type signals have been used within and between units for the transference of information. However, with the new design, this is no longer so, hence the problem of EMI has been investigated thoroughly. From this work, the following has been found.

Careful design is needed with respect to

a) how the equipment grounds and zero volts are connected together along with the ship's supply ground.

b) the choice of logic level voltage between units (in this case,24V) so that sufficient magnitude is provided to ensure an adequate noise margin.

c) all signals between units should be transmitted and received differentially along two separate lines. One line for the signal and one line for the return.

Using these techniques, with overall screened twisted pair cabling between units, it has been demonstrated that the equipment will survive the most hostile EMI environment found, even aboard naval vessels.

It can be seen from Fig.2 that the FSCS was designed to control up to a maximum of 4 fins, utilising one ATU per fin. Each ATU has a mechanical coupling (to measure fin angle) and an electrical connection (error signal to drive hydraulics) to its respective Fin/Hydraulic Unit (F/H.U.).

The CPU requires the following inputs, the log and helm signals, and control signals, Power On, Normal/Quiet mode, True Vert/Natural List mode, Forced Roll and Fin Angle Zero (one for each fin) which are all normally taken from the machinery control panel (MCP) which commands the complete stabiliser operation.

Lastly, the configuration depicted in Fig.2 was deemed to provide the greatest flexibility and simplicity such that the FSCS could be tailored to meet the range of different installations required by today's vessels.

CENTRAL PROCESSOR UNIT (CPU)

The majority of this paper is concerned with the design and operation of the CPU and thus the other two units will only be dealt with briefly in later sections.

The CPU exterior and interior view with the outer door open are shown in Fig.3.

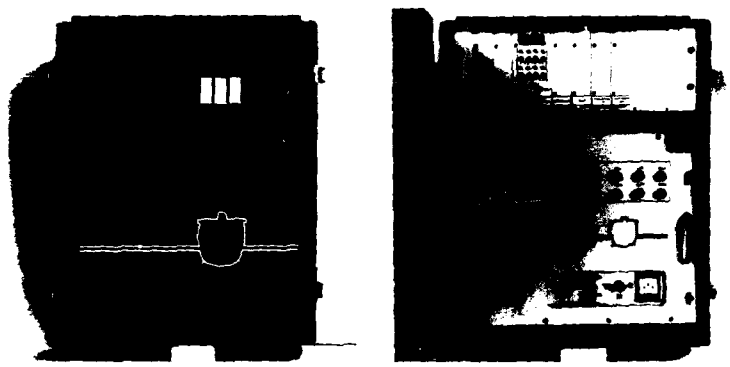

Fig.3 Exterior and Interior Views of the C.P U.

The purpose of the CPU is to compute stabilising or fin angle demand signals, in accordance with the control algorithm from information supplied by the ASU. However, the function and parameters of the control algorithm are controllable by the MCP and the Configuration and Test Module housed within the CPU. (see Fig.3, interior view).

It has already been stated that the control algorithm is a three term controller comprising roll angle, velocity and acceleration. The angular accelerometer signal, by the time it reaches the CPU, has already undergone some simple filtering to remove the relatively high frequency content due to ship vibrations. It is again further filtered by software before being integrated twice to obtain roll velocity and angle. Each term, i.e. angle, velocity and acceleration, is adjustable to one of sixteen attenuated levels, set by switches within the Configuration and Test Module. These switches are used to input the parameters deduceable from the natural frequency and damping ratio of the ship. It had been the intention to have three switches calibrated in natural frequency, damping ratio and gain, but this presupposed the best mix of the three terms in the algorithm thereby not allowing enough flexibility. The arrangement chosen might make the setting up more complicated during installation and sea trials, but once set, it is not the intention that they should be changed or be operator adjustable during the normal operational life of the ship.

The signals from the helm transducer and the list transducer are summed together with the selected attenuated roll angle, velocity and acceleration signals to form the fin angle demand signal. The helm signal is used to anticipate the roll induced by sudden large changes in helm angle and is adjustable by switches on the Configuration and Test Module to one of several curves that best fits the ship. The list transducer is fitted within the CPU to correct for the list of ship if the True Vertical Mode command is in operation from the MCP.

The log signal is used to limit the maximum fin angle demand signal obtainable to the curve shown in Fig.4

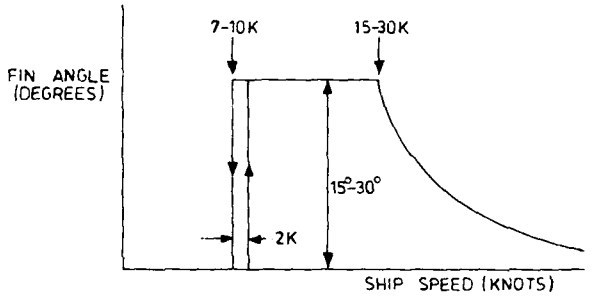

Fig.4 Fin Angle v Ship Speed Curve

Again, the variable parameters of the curve are set by switches within the Configuration and Test Module. It should be explained that these switches are only accessible after the module has been removed from the equipment and are not the switches shown mounted on the front panel. The point where, with decreasing ship speed, the fin angle goes from maximum to zero, can be set in one knot steps from seven to ten knots. Maximum fin angle demand can be set in one degree steps from fifteen to thirty degrees and the point where the inverse square law part of the curve starts to operate can be set in one knot steps from fifteen to thirty knots. At the start, there is a built-in two knot hysteresis to stop the system oscillating between zero and maximum fin angle demand. A switch mounted on the front panel of the Configuration and Test Module can be used in the event of log failure to manually select a ship speed of 14 or 40 knots.

The curve shown in Fig.4 is further modified by the Normal/Quiet Mode signal from the MCP. In the Normal Mode the curve remains unchanged, but along the vertical axis it is reduced by 50% when the Quiet Mode is in operation. This is a useful feature for naval vessels when it is necessary to reduce the accoustic noise of the ship passing through the sea.

The fin angle demand signal is individually sent to each ATU depending upon its respective Fin Zero signal from the MCP. This signal is independently acted upon by both software and hardware from safety

AD-A211128 (U) PROCEEDINGS OF THE SIXTH SHIP CONTROL SYSTEMS
UNCLASS. UNLTD. SYMPOSIUM HELD AT OTTAWA, ONTARIO, CANADA, ...5 OF 6

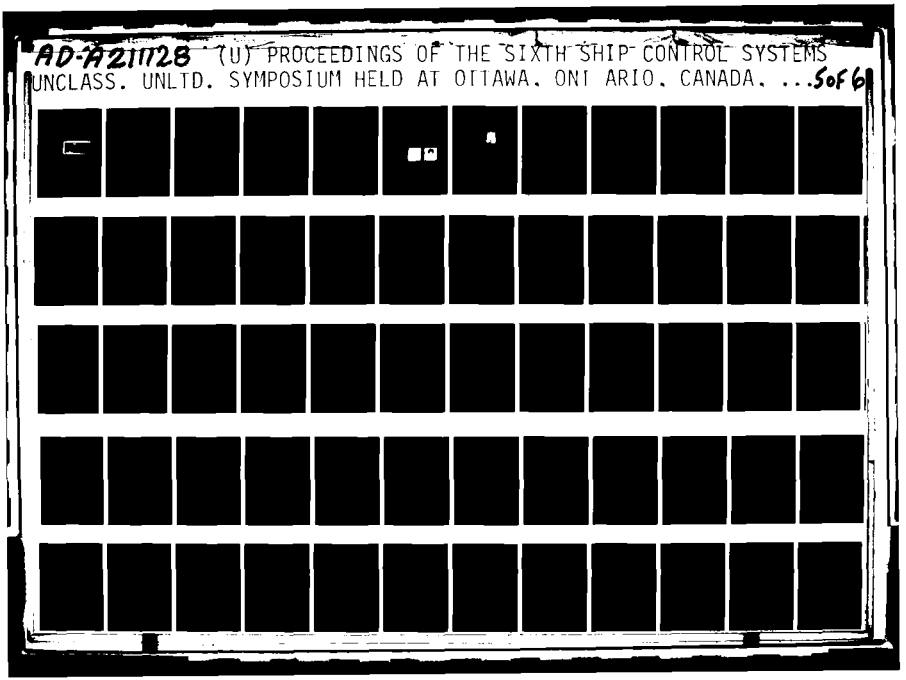

considerations to hold the fin angle demand signal to zero if commanded by the MCP.

The Forced Roll signal, either to Port or Starboard, from the MCP overrides the control algorithm and sets the fin angle demand signal to maximum (dependent upon the curve in Fig.4, the ship's speed and the Normal/Quiet Mode signal).

The above text has briefly described the function of the CPU when in the stabilising mode. The operating mode is selected by the eight switches on the front panel of the Configuration and Test Module (see Fig.5 for a close-up view of the CPU modules).

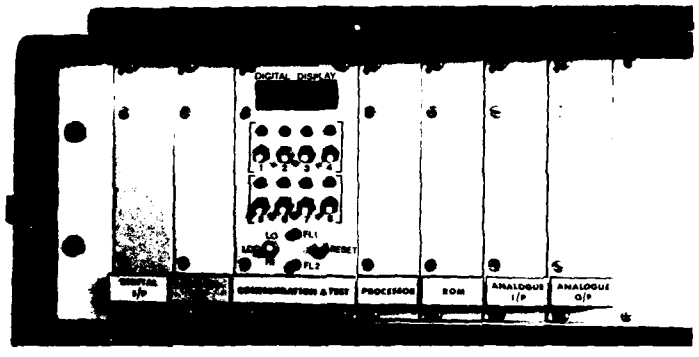

Fig.5 C.P.U. Electronic Modules

There are four operating modes; Stabilisation, Fin Test, Maintenance and Fault Diagnostics. Switches numbered 1 and 2 select the mode and those numbered 3 to 8 are used to select functions for the processor to perform during that mode of operation.

In the stabilisation mode, setting switches numbered 3 to 8 accesses information within the CPU for presentation on the digital display. This covers such things as individual fin angles, power supply voltages, last angle, roll angle, helm angle, ship's speed etc. Again, while in the maintenance mode, similar information is supplied but the fin angle demand signals are held at zero.

In the fin test mode, various waveforms selected both in frequency and shape are generated as fin angle demand signals for the purpose of exercising the fins. All the fins would move in the same direction thereby not inducing any rolling action on the ship if it were in motion. The fin angle demand signals would still be influenced by the ship's log as in Fig.4 but the signals are allowed to be up to the maximum fin angle for ships speeds of zero to ten knots where before they would have been set to zero.

In the fault diagnostic mode, the microprocessor is used to perform a series of tests to isolate the fault condition down to a single

assembly. Obviously, if the fault lies within the microprocessor kernel, this may not allow the diagnostic programmes to run successfully. The kernel is best described as the minimum number of components necessary for the microprocessor to perform a simple task assuming that all the power supply voltages required are correct.

In this system, two modules, the Processor and ROM modules, form the microprocessor kernel. During normal operation, if a fault condition occurs, the microprocessor will send fault code information to the digital display, take corrective action by zeroing fin angle demand signals as necessary and set one of two magnetic latching relays within the Configuration and Test Module to signal the fault condition to the MCP. If the fault lies within the kernel, the above sequence is ensured due to checks made both in hardware and software on the kernel area, the only difference being that the microprocessor may not be able to send correct information to the digital display. Setting the switches to the Fault Diagnostic mode will immediately indicate if the kernel area is at fault. Then, by running through a sequence of tests in conjunction with the technical manual fault flowcharts, the offending assembly or module can be isolated.

It has been mentioned that there are two fault relays within the Configuration and Test Module. These are of the magnetic latching type that retain information even in the event of power failure. Two red light emitting diodes labelled 'FL1' and FL2' mounted on the front panel of the Configuration and Test Module indicate the state of the two relays. These relays are used to ensure that if the microprocessor malfunctions in any way, one of these relays is set and forces the microprocessor and the hardware into a known and safe state. Only by using the reset switch on the Configuration and Test Module can the latches be reset by the operator.

From Fig.5 it can be seen that the electronics is divided up into seven modules.

1) Digital Input Module - Inputs sixteen 24V level digital signals via opto-isolators. Only nine inputs are used for this system.

2) Digital Output Module - Outputs eight 24V level digital signals via line drivers. Only three outputs are used for this system.

3) Analogue Input Module - Inputs sixteen analogue signals via input buffering. All sixteen inputs are used for this system.

4) Analogue Output Module - Outputs eight analogue signals via output buffering. Only four outputs are used for this system.

5) ROM Module - Contains space for up to 8K of programme using fuse link PROMs. For this system the programme length is 3K approximately.

6) Processor Module - Contains the Texas 9900 microprocessor, crystal clock, 1K RAM and support circuits. Other features are available but are not used in this system.

7) Configuration and Test Module - Contains the following functions: 4-digit digital display, eight switches for mode and function selection, Log Failure switch, Reset switch, Internal switches for parameter selection, two fault latches, verification logic

and microprocessor watchdog & monitor.

Although these modules have spare capability, careful partitioning and layout during design has catered for redundant circuitry to be omitted from the printed wiring boards. This flexibility allows the modules to be used in varying applications, and hence costs and overheads are minimised by the larger production volume.

These seven modules are connected together to implement the block diagram shown in Fig.6.

Although conventional microprocessor techniques and circuitry are used in the modules, it is necessary to be aware of the implications brought about by Reliability, Maintainability and Safety considerations. This can be characterised into the following:-

Reliability - the design shall not cause directly or indirectly, fault conditions to occur.

Maintainability - the design, if fault conditions occur, shall provide quick and easy detection and correction.

Safety - the design, when fault conditions occur, shall be failsafe.

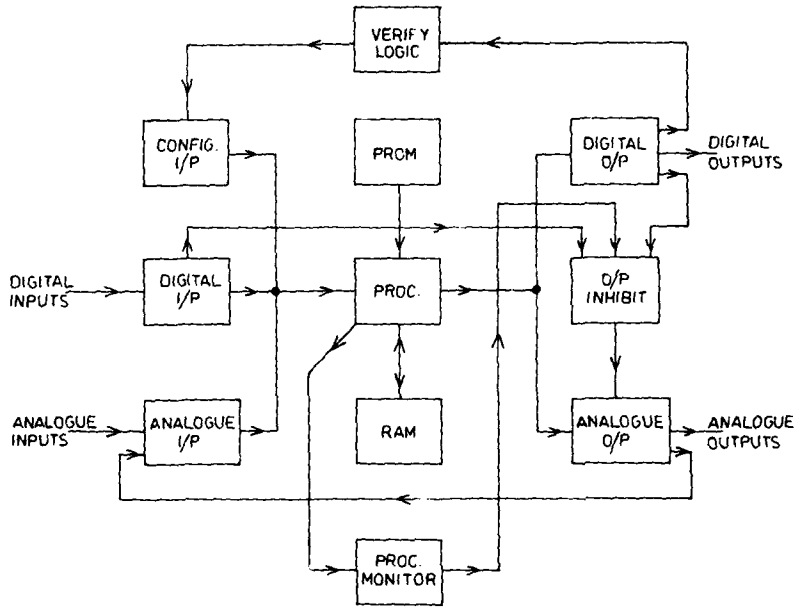

Fig.6 C.P.U. Block Diagram

This philosophy, once understood and practised, is easily implemented into any new design. This aspect therefore, is examined in the following text in relation to the block diagram shown in Fig.6.

The main problems are the detection of fault conditions and to ensure that the design fails safe. The first problem splits into two main areas:

a) Fault conditions within the microprocessor kernel that cause incorrect programme operation or stoppage.

b) Fault conditions external to the microprocessor kernel that cause the microprocessor to act on, or input or output incorrect information.

If faults cause the first condition, the microprocessor cannot be relied upon to implement the correct action and hence hardware is required. The software programme should obviously contain the usual ROM sumchecks, RAM checkerboard pattern and power supply tolerance tests as standard. The hardware required for this system is not too complex to achieve as the microprocessor is interrupt-driven at a set frequency under software control. Therefore, all that is required is a watchdog monostable that is retriggered at a specific time interval by the software programme.

However, faults that cause the second condition are more complex to cater for. Analogue inputs are checked by the software for plausibility and the inclusion of analogue wraps, i.e. taking the analogue outputs and returning them back to the analogue inputs, allows the software to check what it thinks it is sending out to what it is actually sending out, but also confirms the majority of the analogue input/output circuitry to and from the kernel. Fortunately, the digital output circuitry in this system does not need verification for two reasons:

a) Failure would not cause a hazard.

b) With built-in redundancy, failure can be deduced by other means.

Conversely, this is not the case with the digital inputs. All the inputs from switches contained on the front panel or within the Configuration and Test Module, are extremely important to the function and safety of the system. Therefore, verification logic has been required to confirm exactly, under software control, the integrity of these inputs. This proved to be very simple in terms of circuitry and even allows checks to be made for correct function of each switch. Unfortunately, it does not check that the switches were set correctly by the operator in the first place!

The analogue outputs (fin angle demand signals) are required to be set to zero when fault conditions exist as this is the called-for failsafe situation. To achieve this, the analogue outputs each have direct hardwired relay shorting circuits, driven from three separate hardware sources. One from the digital input circuitry, one from the digital output circuitry and lastly, one from the watchdog circuitry. Therefore, for any fault condition, the microprocessor should zero the analogue outputs under software control but failing this, external hardware backs up the microprocessor and software.

The software programme is approximately 3K words long and has been written on a modular concept totalling seventeen modules.

At 'Power On', the programme enters an initialisation routine where RAM is checked first followed by a sumcheck on the ROM module. Next, the power supply tolerances are verified and then the programme sets the Frame Interrupt hardware into operation. Each frame interrupt is 9 m.Secs. long and there are ten frames to a complete programme cycle. A frame contains a number of predefined modules essential to the running of the system. Each group of modules within a frame is organised such that the total execution time is less than the frame interrupt time of 9 m.Secs. When the required modules within the frame have been run, the programme returns to the Background routine where RAM, ROM and power supplies are cyclically checked. At each frame interrupt the Background routine is halted to execute the modules in the new frame. On completion, the programme drops back to the Background routine to the point where it left when the frame interrupt occurred. Upon completion of the last frame in a cycle, the software retriggers the hardware Watchdog Monostable. If at any time this Watchdog Monostable times out, then a separate hardware interrupt is generated of higher priority than a frame interrupt which forces the microprocessor into a known state. The system can then only be re-initialised by the reset switch on the Configuration and Test Module.

The cycle time for ten frames and therefore the computation rate for fresh fin angle demand information, is 90 m.Secs.

The programme instigates a number of tests during each cycle to verify correct operation of the system and these are listed below although several of them have already been mentioned.

a) RAM checkerboard

b) ROM sumcheck

c) Power supply tolerance

d) Roll implausibility

e) Speed implausibility

f) Helm implausibility

g) Tracking failure between fin angle demand and actual fin angle

h) Analogue wrap error

i) Programme Time error

j) Digital input error

k) Digital output parity error

m) Analogue to Digital end of conversion error.

Constructionally, the CPU follows standard practice for marine equipment. A fully sealed steel enclosure with rear bulkhead mounting

frame houses the electronic equipment. At the top of the enclosure a rack system holds the seven electronic modules. These are based on the Eurocard system, i.e. a 160 mm by 100 mm printed wiring board size. Each printed wiring board has an indirect connector at the rear to make the necessary connections to the backplane and is supported by its own aluminium frame and front panel to ensure it passes the shock and vibration requirements. Below the rack, an interior door holds all of the necessary fuses for the system. Behind the door are mounted two power supplies, one +24V and the other +5V & $^{+}_{-}$15V, along with the list sensor unit. At the bottom of the enclosure all the interconnections to and from the CPU are made via circular bayonet-lock connectors.

ACCELERATION SENSOR UNIT (ASU)

This unit is very straightforward when compared to the CPU. It has only two major parts, one being the angular accelerometer mentioned previously (see Fig.7). The accelerometer employs a self-supported, liquid inertia mass as the sensing medium. The liquid is captured in an annular tube, blocked by a servo controlled force transducer, which produces a DC output signal proportional to the angular acceleration. The liquid is, in turn, torque-restored by the transducer.

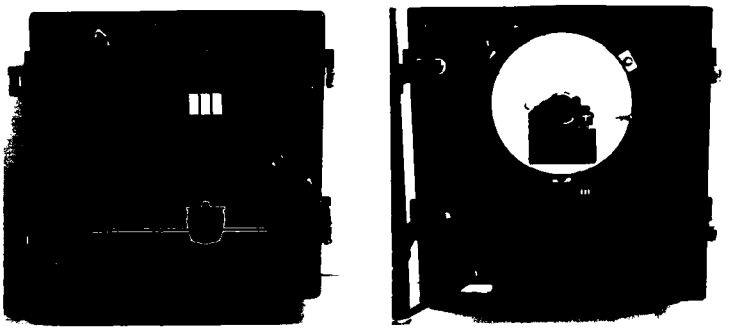

Fig.7 Exterior and Interior View of the A.S.U.

The other major part consists of a simple printed wiring board containing signal conditioning and buffering circuitry, the output of which is 20V for an acceleration of 1 radian/sec^2.

A similar form of construction to that of the CPU is used and the only design problem was to ensure that the accelerometer was rigidly mounted to the bulkhead and thus did not pick up any extraneous accelerations.

ANGLE TRANSMITTER UNIT (ATU)

The ATU is sited close to the fin shaft so that the mechanical coupling necessary for the internal transducer is accomplished. The transducer, a high reliability resistive potentiometer measures the actual fin angle and this is compared with the CPU-derived fin angle

demand, to produce an error signal. This error signal is then buffered before driving the external servo valve controlling the hydraulics. If variable delivery pumps are used, an inner servo loop can be accommodated to control the operation of the pump.

Fig.8 Exterior View of the A.T.U.

The housing for the ATU utilises an aluminium casting already used for this application on Muirhead's existing FSCS. The interior has been changed to accommodate the potentiometer and the single printed circuit wiring board.

An extra connector is provided (top right-hand Fig.8) so that a test box can be connected to either monitor the performance, or to allow the fin/hydraulic system to be exercised without powering up, or connections being made to, the CPU.

SUMMARY

The paper has described the design of a microprocessor based fin stabiliser control system which has taken one year to complete from conception to a finished prototype. This has been achieved by compliance to an initial specification defining a simple and proven concept. Only the means of implementation has been changed from an analogue to digital basis. Most of the aspects dealt with have had to be brief as many would warrant a complete paper in themselves, but it is hoped that the reader has gained an insight into some of the complex problems that confront today's system designer.

Having established a sound foundation, future development work can concentrate on implementing more advanced control functions which now have become feasible with the advent of the microprocessor.

OPTIMAL AND SUBOPTIMAL FEEDFORWARD IN AUTOMATIC TRACKKEEPING SYSTEMS

by Johan K. Zuidweg
Royal Netherlands Naval College
Den Helder, the Netherlands

ABSTRACT

The subject of this paper is the application of optimal control theory to the automatic guidance of a ship, moving at an approximately constant speed, along a pre-specified track.

If the ship is modelled as a linear system, if the stochastic disturbances are supposed to be gaussian, and if the risk to be minimized is the expectation of the sum of a sequence of quadratic loss functions, then the solution to the problem is known to be a linear controller. The control signal consists of a linear function of the (estimated) state plus a linear combination of present and future deterministic disturbances. (Stochastic disturbances are waves, wind gusts and obervation errors: deterministic disturbances are current, mean wind, and curvature of the pre-specified track.)

The resulting control system can be decomposed into two subsystems. One subsystem handles the deterministic disturbances. It is basically an open-loop system with an anticipating feedforward. In the other subsystem, which has to cope with the stochastic disturbances, feedback is essential.

The two subsystems are (ideally) non-interacting. This implies that they can be designed and evaluated separately. It is shown how this leads to increased design flexibility that can be used either to improve system performance or to simplify the system.

Results of computer simulations are presented and discussed.

1. THE GUIDANCE PROBLEM AS A LINEAR STOCHASTIC GAUSSIAN OPTIMAL REGULATOR PROBLEM WITH QUADRATIC LOSS AND QUADRATIC CONSTRAINTS

An automatic system for the guidance of a ship, proceeding at an approximately constant speed, along a pre-specified track can be based on the solution of the control problem as specified by the following points (ref. 1):

1. The ship is modelled as a linear sampled-data system, characterized by an equation of the form

$$\underline{\xi}(k+1) = \underline{\Phi}\,\underline{\xi}(k) + \underline{\Delta}\rho(k) + \underline{d}(k) + \underline{w}_1(k) \qquad (1.1)$$

where $\underline{\xi}$ is the state, $\underline{\Phi}$ is the state transition matrix, ρ is the control variable, $\underline{\Delta}$ is the control input matrix, $\underline{d} + \underline{w}_1$ is the vector of disturbances, where $\underline{w}_1$ is the zero-mean gaussian stationary stochastic part (waves, wind gusts) and $\underline{d}$ is the deterministic mean part (mean wind, path curvature). See the appendix for a further description of this model.

2. At each sampling instant k, a vector of observations $\underline{\eta}$ is obtained as described by

$$\underline{\eta}(k) = \underline{M}\,\underline{\xi}(k) + \underline{w}_2(k) \qquad (1.2)$$

where $\underline{M}$ is the observation matrix and $\underline{w}_2$ is the vector of random (zero-mean, gaussian, stationary) observational errors.

3. The non-negative definite matrix $\underline{Q}_1$ and the non-negative scalar Q_2 are given, which define the *loss functions*

$$L(k) = \underline{\xi}^T(k)\ \underline{Q}_1\ \underline{\xi}(k) + Q_2\ \rho^2(k-1) \tag{1.3}$$

The a priori expectation of the sum of their values is called the *risk* W:

$$W = E \sum_{-m}^{n} L(k) \tag{1.4}$$

4. A sequence of appropriate functions

$$\rho(k) = \rho_k\{\eta(-m),\ \eta(-m+1),\ldots.\eta(k),\ \rho(-m),\ \rho(-m+1),\ldots.\rho(k-1)\} \tag{1.5}$$

must be found so as to minimize W.

The solution to this problem can be summarized as follows (figure 1):

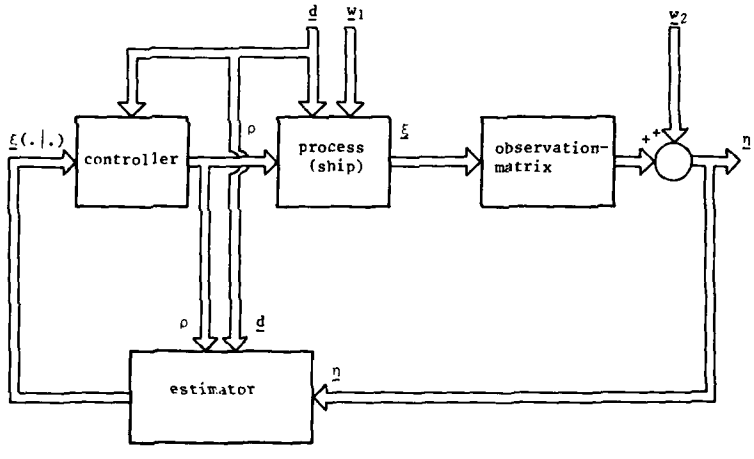

Figure 1. Structure of Basic Control System.

1. The controller consists of two distinct subsystems, the *estimator* and the *controller proper*.
2. The estimator has to find $\underline{\xi}(k|k)$, which is the expectation of $\underline{\xi}(k)$ given the information available at sampling instant k. Its operation (Kalman filter) is described by

$$\underline{\xi}(k+1|k) = \underline{\Phi}\ \underline{\xi}(k|k) + \underline{\Delta}\rho(k) + \underline{d}(k) \tag{1.6a}$$

$$\underline{\xi}(k+1|k+1) = \underline{\xi}(k+1|k) + \underline{K}(k+1)\{\underline{\eta}(k+1) - \underline{M}\,\underline{\xi}(k+1|k)\} \qquad (1.6b)$$

where K(k), k = -m, ..., n - 1 is a sequence of matrices for which a recurrent set of equations is available. In most cases, for increasing values of k, the sequence converges:

$$K(k) \to K \qquad (1.7)$$

3. The controller proper has to find $\rho(k)$, given $\underline{\xi}(k|k)$ and the present and future deterministic disturbances $\underline{d}(k)$, $\underline{d}(k+1)$, ..., $\underline{d}(n-1)$. The following result was obtained

$$\rho(k) = -\underline{C}_{\xi}(k)\,\underline{\xi}(k|k) + c_d(k) \qquad (1.8a)$$

where

$$c_d(k) = \underline{C}_d(k,k)\,\underline{d}(k) + \underline{C}_d(k,k+1)\,\underline{d}(k+1) + ... + \underline{C}_d(k,n-1)\,\underline{d}(n-1) \qquad (1.8b)$$

Sets of recurrent relations to be used for the computation of $\underline{C}_{\xi}(k)$ and $\underline{C}_d(k,\ell)$ ($k = -m, -m+1, ..., n-1$; $\ell = k, k+1, ..., n-1$) are available. In most cases, for decreasing values of k, the following convergency properties hold

$$\underline{C}_{\xi}(k) \to \underline{C}_{\xi} \qquad (1.9a)$$

$$\underline{C}_d(k,\ell) \to \underline{C}_d(\ell - k) \qquad (1.9b)$$

Therefore, if k is sufficiently far from n, we can rewrite (1.8):

$$\rho(k) = -\underline{C}_{\xi}\,\underline{\xi}(k|k) + c_d(k) \qquad (1.10a)$$

$$c_d(k) = \underline{C}_d(0)\,\underline{d}(k) + \underline{C}_d(1)\,\underline{d}(k+1) + ... \qquad (1.10b)$$

The actual problem is not to minimize W for fixed values of Q_1 and Q_2, but rather to minimize $E\{y^2(k)\}$ under the constraints

$$E\,\delta^2(k) \leq \delta^2_{max} \qquad (1.11a)$$

$$E\,\rho^2(k) \leq \rho^2_{max} \qquad (1.11b)$$

where y and δ are state variables (see appendix). This problem is solved by way of a repeated minimization of

$$E \Sigma \{y^2(k) + Q_1 \delta^2(k) + Q_2 \rho(k-1)\}$$

while Q_1 and Q_2 are varied (Lagrange multipliers), thus converting the problem to an optimization in (Q_1, Q_2)-space.

2. DECOMPOSITION OF THE CONTROL SYSTEM INTO A DETERMINISTIC FEEDFORWARD AND A STOCHASTIC FEEDBACK SYSTEM

Figure 1 shows that the track-keeping system has three inputs $\underline{d}$, $\underline{w}_1$ and $\underline{w}_2$, where $\underline{d}$ is deterministic whereas $\underline{w}_1$ and $\underline{w}_2$ are zero-mean random processes. As the system is linear, the state $\underline{\xi}$ can be thought of as a superposition of a deterministic component $\underline{\xi}'$, which is the response to $\underline{d}$, and a zero-mean random component $\underline{\xi}''$, which is the response to $\underline{w}_1$ and $\underline{w}_2$. Decomposing all variables similarly, we have:

$$\left.\begin{aligned} \underline{\xi}(k) &= \underline{\xi}'(k) + \underline{\xi}''(k) \\ \underline{\xi}(k|k) &= \underline{\xi}'(k) + \underline{\xi}''(k|k) \\ \underline{\xi}(k+1|k) &= \underline{\xi}'(k+1) + \underline{\xi}''(k+1|k) \\ \underline{\eta}(k) &= \underline{\eta}'(k) + \underline{\eta}''(k) \\ \rho(k) &= \rho'(k) + \rho''(k) \end{aligned}\right\} \qquad (2.1)$$

Equation (1.1) can now be decomposed as

$$\underline{\xi}'(k+1) = \underline{\Phi}\, \underline{\xi}'(k) + \underline{\Delta}\, \rho'(k) + \underline{d}(k) \qquad (2.2)$$

$$\underline{\xi}''(k+1) = \underline{\Phi}\, \underline{\xi}''(k) + \underline{\Delta}\, \rho''(k) + \underline{w}_1(k) \qquad (2.3)$$

For the controller we have

$$\begin{aligned} \rho'(k) &= -\underline{C}_\xi\, \underline{\xi}'(k) + c_d(k) \\ &= -\underline{C}_\xi\, \underline{\xi}'(k) + \underline{C}_d(0)\, \underline{d}(k) + \underline{C}_d(1)\, \underline{d}(k+1) + \ldots\ldots \end{aligned} \qquad (2.4)$$

$$\rho''(k) = -\underline{C}_\xi\, \underline{\xi}''(k|k) \qquad (2.5)$$

Since there is no need for estimation of the deterministic part of the state, the estimator has only to estimate the random part. The equations are

$$\underline{\xi}''(k+1|k) = \underline{\Phi}\, \underline{\xi}''(k|k) + \underline{\Delta}\, \rho''(k) \qquad (2.6a)$$

$$\underline{\xi}''(k+1|k+1) = \underline{\xi}''(k+1|k) + \underline{K}\{\underline{\eta}(k+1) - \underline{M}\, \underline{\xi}'(k+1) - \underline{M}\, \underline{\xi}''(k+1|k)\} \qquad (2.6b)$$

We remark that (2.4) could be written

$$\rho'(k) = \ldots\ldots + \underline{B}(-1)\, \underline{d}(k-1) + \underline{B}(0)\, \underline{d}(k) + \underline{B}(1)\, \underline{d}(k+1) + \ldots\ldots \qquad (2.8)$$

because $\underline{\xi}'(k)$ is a function of ....., $\underline{d}(k-1)$, $\underline{d}(k)$, $\underline{d}(k+1)$, ... This implies that, although (2.4) is in a form which suggests feedback control, the deterministic part of the system is basically an open loop system. Only the stochastic part of the system is a veritable feedback system.

The decomposition that we have introduced here is illustrated in figure 2.

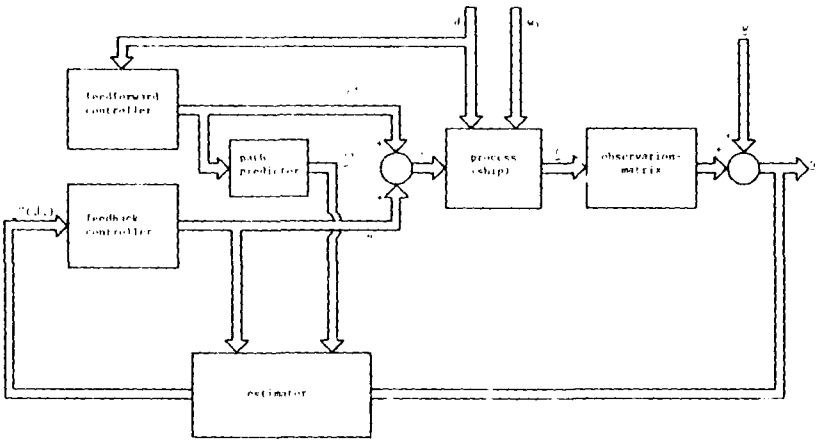

Figure 2. Structure of Decomposed Control System.

The sequence $\underline{\xi}'(k)$, $k = ..., -1, 0, 1, ...$ of the feedforward system defines the track that the ship would follow if the stochastic disturbances were absent. If $\underline{\xi}'(k) = \underline{0}$ for each k, this means that the ship's track would coincide with the pre-specified desired track. This is only possible if the latter is "feasible", i.e. it does not require rudder motions in excess of the constraints that must be put on rudder angle and rudder angular velocity. In other cases the sequence $\underline{\xi}'(k)$ defines a correction to the pre-specified path so as to replace it by a feasible or at least a more preferable one.

It is not realistic to assume that the behaviour of the ship is known exactly. This means that we have to cope with the complication of an equation error $e(k)$ in (2.2):

$$\underline{\xi}'(k+1) = \underline{\Phi}\,\underline{\xi}'(k) + \underline{\Delta o}'(k) + \underline{d}(k) + \underline{e}(k) \qquad (2.9)$$

Since the sum of (2.2) and (2.3) must be satisfied, the same equation error enters the other subsystem, where it plays the role of an additional disturbance:

$$\underline{\xi}''(k+1) = \underline{\Phi}\,\underline{\xi}''(k) + \underline{\Delta o}''(k) + \underline{w}_1(k) - \underline{e}(k) \qquad (2.10)$$

The feedback will try to reduce its influence.

3. THE SYSTEM DECOMPOSITION APPLIED

The problem formulation of section 1, where the rms of y is minimized under constraints on the rms of δ and ρ is attractive from a mathematical point of view. It is questionable, however, if the optimal system in the sense of section 1 is always the best system from the practical point of view.

We shall not try to answer the unanswerable question what really the "best" trackkeeping system is. Nevertheless we do remark that sometimes

$$\max_k |y(k)|, \quad \max_k |\delta(k)| \quad \text{and} \quad \max_k |\rho(k)|$$

are more important than the corresponding rms values and that therefore these maxima could be involved in the (sub-)optimization.

The decomposition as introduced in section 2 yields

$$E\, y^2(k) = \{y'(k)\}^2 + E\{y''(k)\}^2 \text{ for each } k \tag{3.1}$$

It is reasonable to suppose that the second term will not vary too much with respect to k. Whether or not the first term will vary much depends on the shape of the prespecified track. An extreme case is that of a track consisting of two straight lines meeting at an angle: in that case $\max_k E\, y^2(k)$ may be very large relative to the mean with respect to k of $E\, y^2(k)$, while similar observations can be made concerning δ and ρ.

From (3.1), considering the second term constant with respect to k, we may conclude

$$\max_k E\, y^2 = \max_k \{y'(k)\}^2 + E\{y''(k)\}^2 \tag{3.2}$$

while similar equations can be written for δ and ρ.

The feedback control matrix $\underline{C}_z$ occurs in (2.4) as well as in (2.5). By decomposing the control system into two separate systems, however, the controller design problem is also decomposed into two separate design problems. This makes it possible to use two different matrices, $\underline{C}'_z$ and $\underline{C}''_z$, in the two controllers:

$$\begin{aligned} \underline{\xi}'(k) &= -\underline{C}'_z\, \underline{\xi}'(k) + \underline{c}_d(k) \\ &= -\underline{C}'_z\, \underline{\xi}'(k) + \underline{C}_d(0)\, \underline{d}(k) + \underline{C}_d(1)\, \underline{d}(k+1) + \ldots . \end{aligned} \tag{3.3}$$

$$\underline{\xi}''(k) = -\underline{C}''_z\, \underline{\xi}''(k|k) \tag{3.4}$$

Now $\underline{C}'_z$ can be chosen to (sub-)optimize

$$\max_k \{y'(k)\}^2 \text{ under constraints on } \max_k \{\delta'(k)\}^2 \text{ and } \max_k \{\rho'(k)\}^2$$

while $\underline{C}''_z$ can optimize

$$E\{y''(k)\}^2 \text{ under constraints on } E\{\delta''(k)\}^2 \text{ and } E\{\rho''(k)\}^2$$

Both optimizations can be based on section 1.

An even greater freedom results if we drop the linearity of the controller. It is easy to verify that the system decomposition remains possible if

$$\underline{c}'(k) = f'_1\{\underline{\varepsilon}'(k), \underline{d}(k), \underline{d}(k+1), \ldots\} \tag{3.5a}$$

$$\text{or..} = f'_2\{\ldots \underline{d}(k-1), \underline{d}(k), \underline{d}(k+1) \ldots\} \tag{3.5b}$$

$$\underline{c}''(k) = f''\{\underline{\varepsilon}''(k)\} \tag{3.6}$$

where f'_1, f'_2 and f'' are arbitrary functions, not necessarily linear.

The possibility of non-linear control is interesting particularly for the deterministic subsystem. This is illustrated by figures 3 and 4, where the pre-specified track consists of two straight lines meeting at an angle. These figures show simple sub-optimal solutions to the problem of minimizing maximal track distance under constraints on maximal rudder angle and rudder angular velocity.

4. NUMERICAL RESULTS

In this section we present some numerical results pertinent to the following case (also considered in ref. 1). The ship is one of the Todd Sixty Series with block-coefficient 0.70 (freighter), with a length between the perpendiculars of 160.0 meters, at an average speed of 7.81 m/sec. It has in (A.2):

$$K = 0.0536 \text{ sec}^{-1}; \quad T = 56.5 \text{ sec}$$

A sampled-data description of this model was used, with the sampling period fixed at 5.65 sec.

a. Pre-Specified Track Angled

Figure 5 refers to the case where the pre-specified track consists of two straight lines meeting at an angle $\Delta\Psi$.

Curve I applies to the deterministic subsystem. It shows $\max|y'(k)|$ as a function of $|\Delta\Psi|$ under the contraints

$$|\delta'(k)| \leq 0.1 \text{ rad for each } k$$

$$|\rho'(k)| \leq 0.059 \text{ rad/sec for each } k$$

The numbers along the curve are the values of $\log Q'_2$ (it was found that Q'_1 must be $\simeq 0$ and is practically unimportant).

Curve II applies to the stochastic subsystem. For the sake of comparability the stochastic inputs jointly are "translated" into an equivalent stationary, white, gaussian noise on $\Delta\Psi$. The curve shows the rms of y" as a function of the rms of this noise input $\Delta\Psi$". The constraints are

$$\text{rms } \delta'' \leq 0.1 \text{ rad}$$

$$\text{rms } \rho'' \leq 0.059 \text{ rad/sec}$$

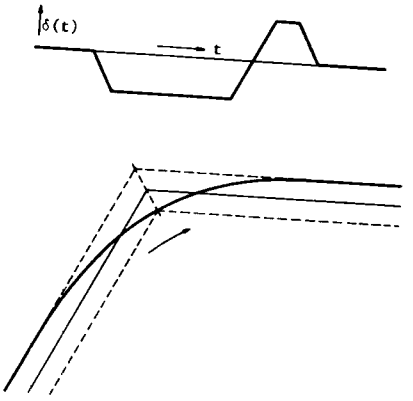

Figures 3a and b. Sub-optimal Path I.

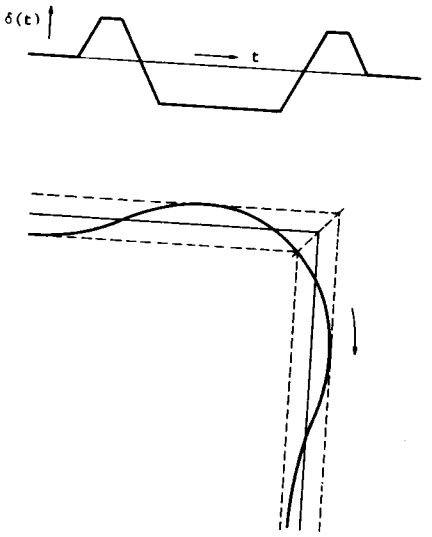

Figures 4a and b. Sub-optimal Path II.

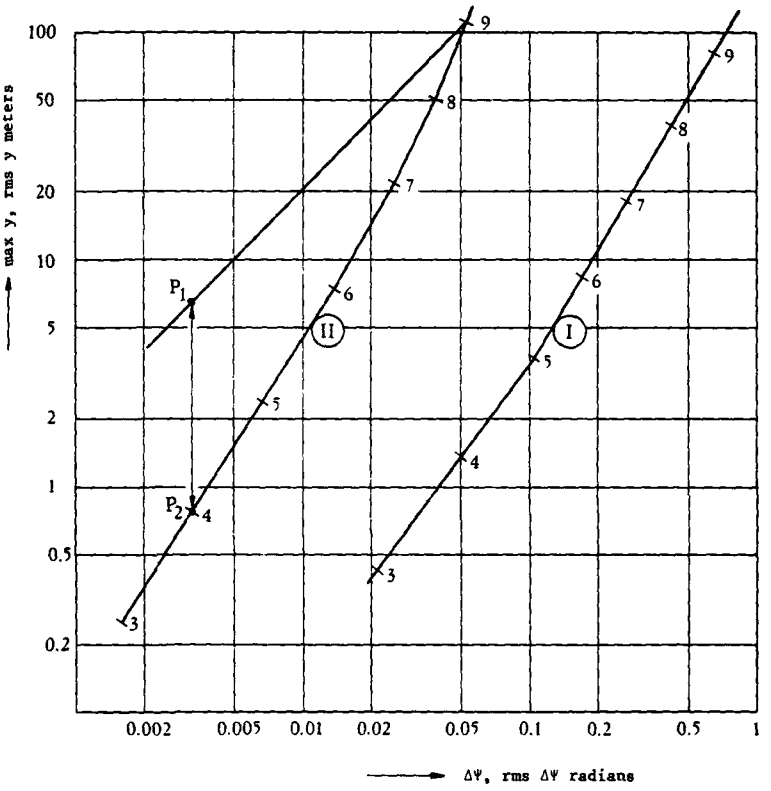

Figure 5. Pre-Specified Track Consisting of Two Straight Lines Meeting at an Angle: max y and rms y as Functions of $\Delta\psi$ and rms $\Delta\psi$, Respectively.

The numbers along the curve are the values of log Q''_2 (while $Q''_1 = 0$).

In order to demonstrate the use of separately designed deterministic and stochastic parts of the controller, let us suppose that $\Delta\Psi = 0.66$ radians while the stochastic inputs are equivalent to a $\Delta\Psi$-noise with an rms of 0.0033 radians. From curve I we conclude that for the deterministic part we must have $Q_2 = 10^9$ and that this results in a maximal track distance of 80 meters. Curve II shows that, under the same constraints on δ and $\dot{\sigma}$ and with the same Q_2, the system can handle an equivalent noise with an rms of 0.055 radians, resulting in an rms track distance of approximately 100 meters. This means that an equivalent noise with an rms of 0.0033 radians results in an rms track distance of about 6.6 meters (point P_1). If we choose $Q''_2 = 10^4$, however, then curve II shows that the rms of the stochastic part of the track distance can be reduced by a factor of 9 (point P_2). With this smaller value of Q_2, the stochastic feedback control-subsystem will be "tighter", with a higher loop gain.

b. Pre-Specified Track of Irregular Shape

In the next case to be considered the pre-specified track has an irregular shape such that the quantity $\Delta\Psi$ in (A.6) can be considered a stationary gaussian pseudo-noise. The prefix "pseudo" is used here because the controller is supposed to "know" the shape of the track in advance and to anticipate $\Delta\Psi$. Two kinds of pseudo-noise are considered: white and coloured, where for the latter we have

$$E\{y(k)\ y(k+\nu)\} = 0.95^{\nu}\ E\ y^2(k)$$
for each k and each $\nu \geq 0$

The stochastic disturbances are dealt with in the same manner as in subsection a. The constraints on δ and $\dot{\sigma}$ are also the same as in subsection a.

Results are shown in figure 6: curve I = white pseudo-noise, curve II = noise representing stochastic disturbances (the same curve as II in figure 5), curve III = coloured pseudo-noise. The numbers along the curves are log Q_2.

c. Influence of Optimization Horizon

Theoretically, the deterministic part of the controller has to take into account all future deterministic disturbances, where the "future" may extend as far as $t \to \infty$. The influence of disturbances in a remote future, however, is found to be small. Therefore we tried to find out how suboptimal the deterministic part of the controller is if it cannot look ahead beyond a limited number of sampling periods n. The results are given in figures 7 and 9.

Figure 7 refers to a pre-specified track consisting two straight lines meeting at an angle $\Delta\Psi$. It shows max y(k) as a function of $\Delta\Psi$ with n as a parameter. The constraints are the same as in subsection a. Figure 8 shows the time responses.

Figure 9 refers to an irregularly shaped pre-specified track, where $\Delta\Psi$ is considered a stationary white gaussian pseudo-noise, and where the constraints are the same as above. The rms of y is shown as a function of the rms of $\Delta\Psi$, with n as a parameter.

The results of this subsection lead to the general conclusion that as the magnitude of the deterministic disturbances is larger, the controller must anticipate them over a longer period of time.

d. Non-Linear Feedforward

In this subsection, linear and non-linear feedforward are compared. Once again, the pre-specified track consists of two straight lines meeting at an angle, and the problem is to minimize maximal track distance under the known constraints of maximal rudder angle and maximal rudder angular velocity.

More specifically, the sub-optimal track depicted in figures 3a and b, which can be realized by means of non-linear feedforward, is compared with the optimal tracks of section a, which results from optimal linear feedforward as specified in section b.

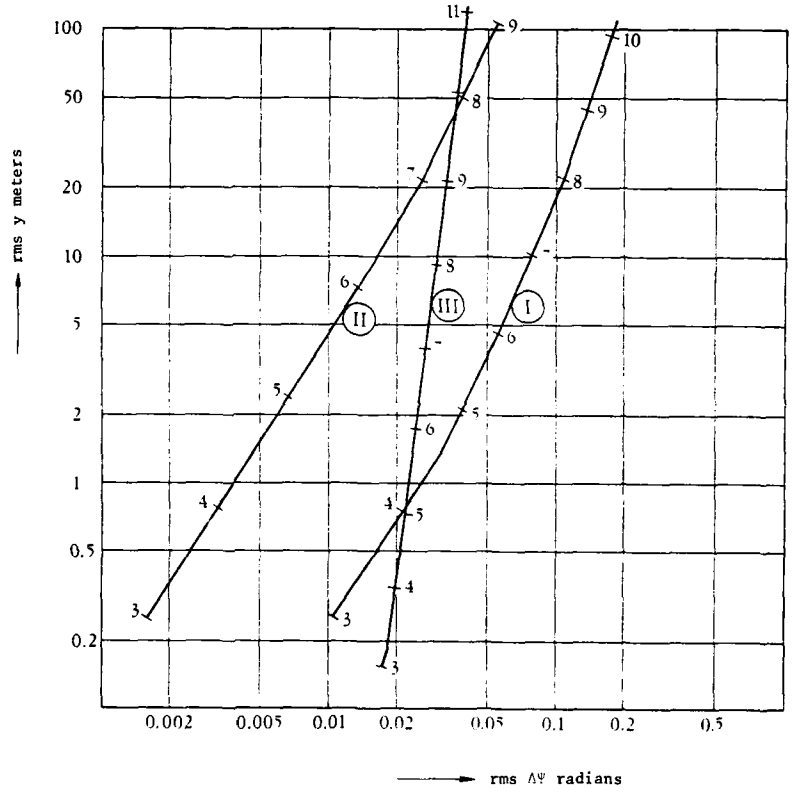

Figure 6. Pre-Specified Track of Irregular Shape: rms y as a Function of rms Δψ.

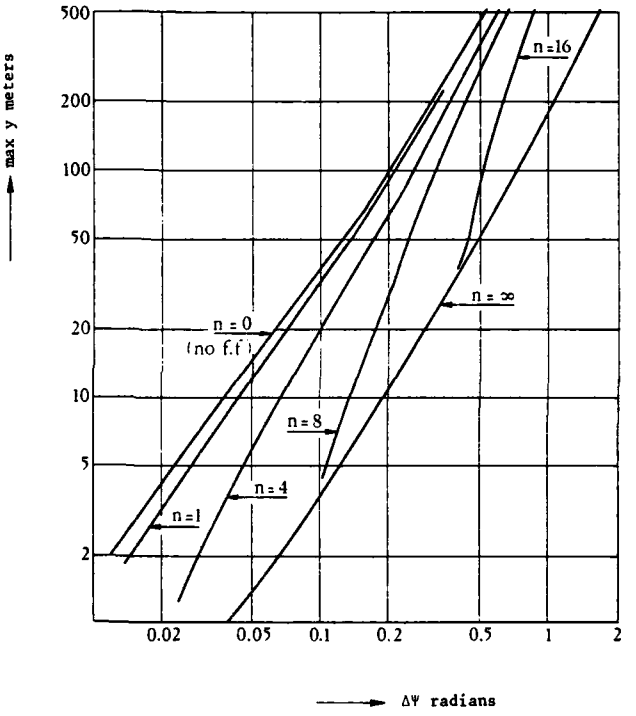

Figure 7. Optimization over n Sampling Periods: Pre-Specified Track Consisting of Two Straight Lines Meeting at an Angle.

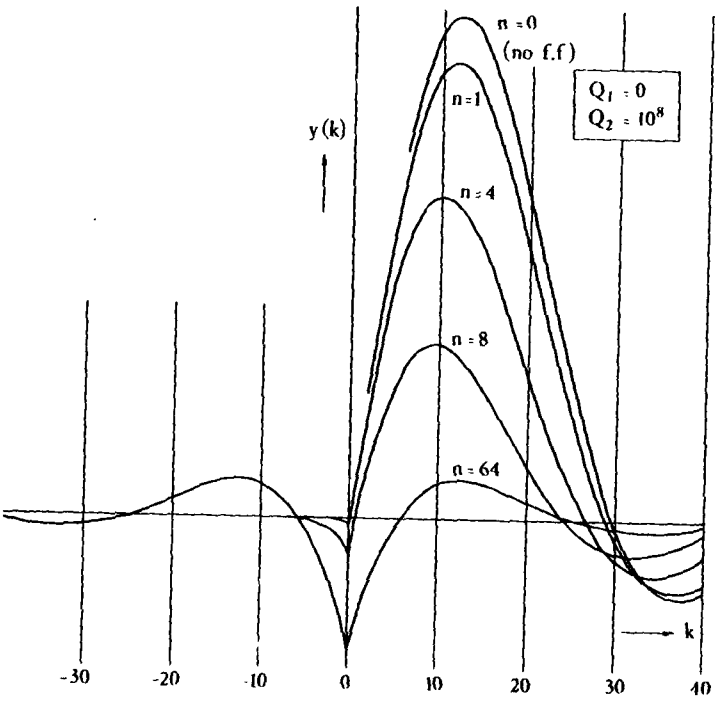

Figure 8. Optimization over n Sampling Intervals: Time Responses Near Angle (at k = 0).

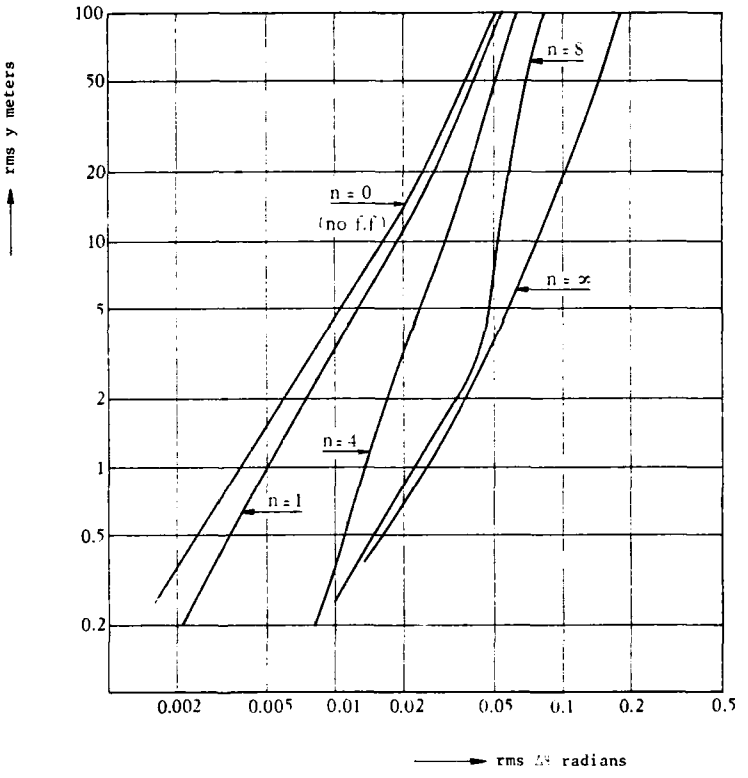

Figure 9. Optimization over n Sampling Intervals: Pre-Specified Track of Irregular Shape.

The results are given in figure 10.

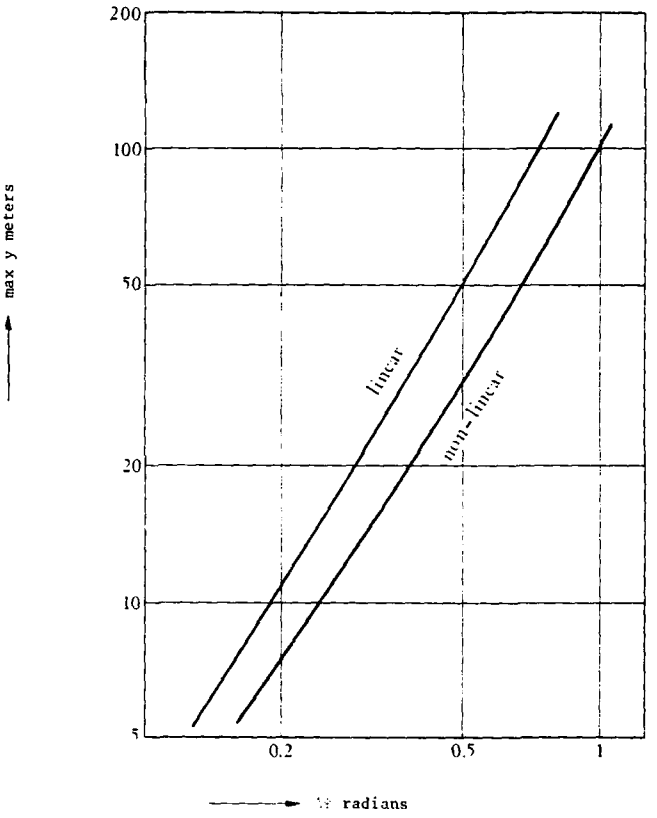

Figure 10. Non-linear vs. Linear Feedforward.

CONCLUDING REMARKS

In this paper the problem was considered of guiding a ship automatically along a pre-specified track. It was shown that the control system can be decomposed into two subsystems which can be designed separately. Numerical examples indicated that the greater design flexibility resulting from this decomposition can be used to improve the performance of the system.

The problem of automatic track-keeping with a finite optimization horizon was also considered in ref. (2). In ref. (3) algorithms are discussed which could be useful for the computation of (sub-)optimal non-linear feedforward.

In the examples the controllers were supposed to be pre-designed, i.e. the parameters were supposed to be fixed. There are no reasons, however, why such controllers could not be "self-tuning", "model-following" or adaptive in any other sense.

REFERENCES

(1) J.K. Zuidweg, "Automatic Guidance of Ships as a Control Problem." Thesis, Technical University Delft, 1970.

(2) J. Dziedzic and L. Morawski, "Algorithm of Control of Ship's Motion According to Desired Trajectory." Ship Steering Automatic Control Symposium, Genova, 1980.

(3) W. McIlroy, G. Carpenter, "Optimal Control Model Applications at CAORF." Ship Steering Automatic Control Symposium, Genova, 1980.

APPENDIX - MATHEMATICAL MODELLING OF THE GUIDED SHIP

a. Guidance Along a Straight Track: a Continuous-Data Model

For guidance at an approximately constant speed along a straight track we use the following model:

$$\frac{d}{dt}\begin{bmatrix}\delta(t)\\ r(t)\\ \Psi(t)\\ y(t)\end{bmatrix} = \begin{bmatrix}0 & 0 & 0 & 0\\ A_{21} & A_{22} & 0 & 0\\ 0 & 1 & 0 & 0\\ 0 & 0 & U & 0\end{bmatrix}\begin{bmatrix}\delta(t)\\ r(t)\\ \Psi(t)\\ y(t)\end{bmatrix} + \begin{bmatrix}1\\ 0\\ 0\\ 0\end{bmatrix} \rho(t) + \begin{bmatrix}0 & 0\\ D_{21} & D_{22}\\ 0 & 0\\ 0 & 0\end{bmatrix}\begin{bmatrix}Y_d(t)\\ N_d(t)\end{bmatrix} \tag{A.1}$$

where (see figure A.1):

$\rho(t)$ = rudder angular velocity
$\delta(t)$ = rudder angle
$r(t)$ = angular rate of yaw
$\Psi(t)$ = heading
$y(t)$ = position relative to desired track (x-axis)
U = forward speed
$Y_d(t)$ = disturbing force
$N_d(t)$ = disturbing moment

The model presented here is essentially the well-known first order Nomoto model, as usually characterized by the transfer function

$$\frac{r(s)}{\delta(s)} = \frac{K}{sT + 1} \tag{A.2}$$

Comparing (A.1) and (A.2) we find

$$K = -\frac{A_{21}}{A_{22}} \text{ and } T = -\frac{1}{A_{22}} \tag{A.3}$$

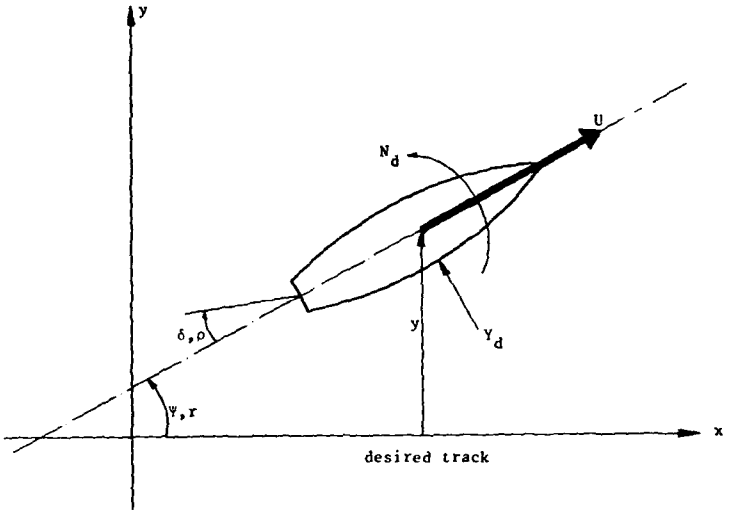

Figure A.1. Definition of Symbols.

b. Sampled-Data Form.

Let $\rho(t)$, $\delta(t)$,..... etc. be sampled synchronously, with a constant sampling period T_s. Suppose that the inputs $\rho(t)$, $Y_d(t)$ and $N_d(t)$ "enter" the system through a zero-order hold-circuit. Then (A.1) can be replaced by

$$\begin{bmatrix} \delta(k+1) \\ r(k+1) \\ \Psi(k+1) \\ y(k+1) \end{bmatrix} = \underline{\Phi} \begin{bmatrix} \delta(k) \\ r(k) \\ \Psi(k) \\ y(k) \end{bmatrix} + \underline{\Delta}\rho(k) + \underline{\Theta} \begin{bmatrix} Y_d(k) \\ N_d(k) \end{bmatrix} \qquad (A.4)$$

where

$$\underline{\Phi} = \exp \left\{ \begin{bmatrix} 0 & 0 & 0 & 0 \\ A_{21} & A_{22} & 0 & 0 \\ 0 & 1 & 0 & 0 \\ 0 & 0 & U & 0 \end{bmatrix} T_s \right\}, \text{ etc.} \qquad (A.5)$$

c. Guidance Along a Curved Track.

A curved desired track is modelled by a piecewise straight track, where the ship passes the angles at the sampling instants. Figure A.2 illustrates that the following term has to be added to the righthand side of (A.4):

$$\begin{bmatrix} 0 \\ 0 \\ 1 \\ 0 \end{bmatrix} \Psi(k+1) \qquad \text{(A.6)}$$

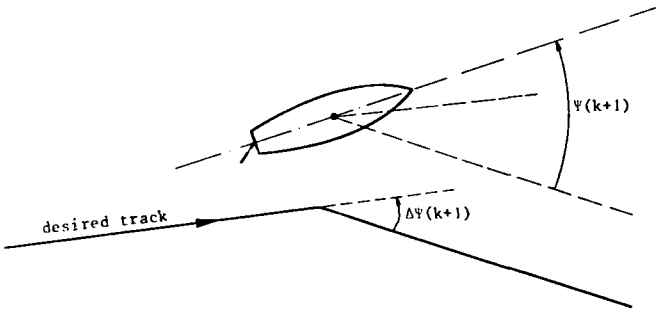

Figure A.2. Situation at Sampling Instant k+1.

SURFACE SHIP PATH CONTROL USING MULTIVARIABLE INTEGRAL CONTROL

by Hua Tu Cuong*
and Michael G. Parsons
Department of Naval Architecture and Marine Engineering
The University of Michigan

ABSTRACT

The surface ship path control problem is formulated as a multivariable, linear state variable control problem subjected to measurement noise and non-zero mean disturbances. A multivariable generalization of integral control is presented and then specialized to the surface ship path control problem. The controller provides zero steady-state error to a constant commanded set point. It is insensitive to errors in the knowledge of the system characteristics. The controller has a nonzero steady-state error to a ramp commanded set point (nonzero heading straight path). This error is established analytically which allows its calculation in advance. The effect of the error can, therefore, be eliminated by simply shifting the time at which turns are initiated. The performance of the controller in straight steaming, passing maneuvers, and turns is illustrated by digital simulations. The multivariable integral controller shows promise as an effective and practical surface ship path control concept.

INTRODUCTION

The problem of controlling surface ships along prescribed paths in restricted waters is important from operational, safety, and environmental viewpoints. In the Great Lakes system, for example, the difficulty associated with the safe movement of large bulk carriers through restricted waters such as the St. Marys River below the Soo Locks is a controlling factor in the evolution of larger, more economical vessels. The use of ships larger than the present 305 m (1000 ft) vessels may well be limited by a lack of maneuvering safety and/or excessive dredging costs. Since these larger bulk carriers would be a small, dedicated fleet, it might be practical for them to use onboard, microcomputer based automatic path controllers in the most restricted channels such as the St. Marys River. Precise, reliable, automated control might exceed the expected day-to-day performance of human operators and thus permit the use of larger, more economical vessels in more restricted channels with resulting reduced dredging costs and/or increased safety. These reduced system costs could more than offset the automatic control system costs.

In this paper, we investigate the feasibility and effectiveness of using a multivariable integral control law for the path control of a surface ship in restricted waters. This type of control would be a potential candidate for use onboard Great Lakes bulk carriers. These

---

*currently Marine Division, Westinghouse Electric Corp., Sunnyvale, CA

ships are subjected to short-term, essentially zero-mean disturbances due to passing ships, current and wind variations, waves, and bank and bottom changes. They are also subject to more long-term, non zero-mean disturbances due to current, wind, second-order wave forces, and banks. The dynamic characteristics of the ships also change significantly depending on depth-under-keel, draft, trim, and speed. Maneuvering situations can place severe demands on the helmsmen and occur often in the Great Lakes system due to the high percentage of the voyage time spent in restricted waters.

In previous work, we have investigated the feasibility and effectiveness of various control schemes for the path control of surface ships in restricted waters. Our earliest work[1] investigated the use of nonadaptive, optimal stochastic controllers for this purpose. These control systems consisted of a steady-state Kalman filter and a steady-state optimal state feedback controller. In that work, the yawing moment and lateral force disturbances acting on the ship were modeled using first-order shaping filters. These controllers were shown to provide effective control when a ship is subjected to short-term, essentially zero-mean disturbances. They could not, however, accommodate more long-term disturbances without a mean offset from the derived path. Our later work[2],[3] modeled the yawing moment and lateral force disturbances using a brownian motion approach. The Kalman filter can then effectively estimate both the essentially constant and the stochastic disturbances which are acting on the ship at any time. The controller using the brownian motion disturbance model was shown to be very effective provided the ship hydrodynamic characteristics were well known.

Since the dynamic characteristics of a ship will generally not be well known in restricted waters, our more recent work[2],[3],[4] considered the use of a gain update loop consisting of an on-line parameter estimator and a second function which recalculates the Kalman filter and controller gains using the latest estimates of the ship characteristics. A minimum variance parameter estimation scheme was utilized. This approach has shown some promise but has also shown the design concept to include seriously conflicting requirements. For the parameter estimator to be fully effective it is necessary to cause the ship to move dynamically about its desired path so that its rudder command and resulting motion histories can be used to estimate the hydrodynamic characteristics. This motion is, however, in direct conflict with the objective of precise path control. Compromise is therefore needed between the accuracy of the parameter estimates and the effectiveness of keeping the vessel on the desired track.

A preferred approach for surface ship path control in restricted waters would be a scheme which would be effective with known ship characteristics but also robust or insensitive to changes in the ship characteristics from those upon which the design was based. The multivariable integral control approach studied here has these desired characteristics. Holley and Bryson[5] recently completed a survey and evaluation of multivariable control techniques applicable to the automatic loading approach control of aircraft. This work has served as the starting point for our current work. Holley and Bryson concluded that a multivariable generalization of integral control provided effective control which allowed the zeroing of steady offsets due to essentially constant disturbances. Further, the resulting systems were insensitive to model (dynamic characteristics) errors as are present in the ship path control problem due to water depth, bank and speed changes if a nonadaptive controller is to be used. This approach may

sacrifice some performance compared with the optimal stochastic controller using brownian motion disturbance models when the ship hydrodynamic characteristics are correctly known.

This paper is presented in three principal parts. First, the surface ship path control problem is formulated as a linear multivariable control problem. Second, the multivariable integral controller is derived and then applied to the ship path control problem. The steady-state error for this controller to a ramp commanded set point is derived. Third, a multivariable integral path controller is designed for the tanker *Tokyo Maru* and its performance is evaluated using digital simulation.

PROBLEM FORMULATION

Equations of Motion

The development of the linearized, state-variable equations of motion for a surface ship moving in the horizontal plane presented here is based on the formulation by Fujino[6] and is presented in more detail in our earler work.[1] The coordinate system for the problem is shown in Fig. 1. The 0-$\xi\eta$ system is fixed in space with the desired ship path predominantly along the ξ-axis so that the prescribed lateral offset η_d could be programmed as a function of ξ. This approach is typical of many maneuvering situations where the ship is to follow a series of straight paths or leading line segments along a general direction. The G-xy system is fixed at the center of gravity of the ship. The positive sense of the drift angle β, heading angle ψ, yaw rate r, and rudder angle δ are shown. Neglecting the effects of pitch and roll, the ship motion can be described by coordinates x, y, and ψ.

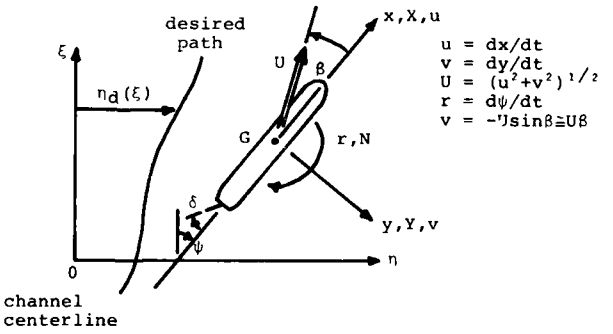

Figure 1. Coordinate System for Path Control

The exact equations of motion of the ship are integro-differential equations in which convolution integrals represent the memory ef-

fects of the fluid to previous motion.[7] An alternative formulation yields differential equations with frequency dependent coefficients. Fujino[8] has shown that for the maneuvers of interest here the frequency dependence is negligible and constant-coefficient differential equations can be utilized. This assumption becomes less and less valid as the water depth to ship draft ratio $H/T \to 1$. When the equations of motion are linearized about the nominal path, the equation in the x-coordinate decouples so that the ship motion can be expressed in terms of β, r, and η. The nondimensionalized equations of motion then become,

$$\frac{d\psi'}{dt'} = r' \quad , \tag{1}$$

$$-(m'+m_y')\frac{d\beta'}{dt'} = Y_\beta'\beta' + (-m'+Y_{\dot r}')r' + Y_{\dot\beta}'\dot\beta' + Y_\delta'\delta' + Y_\eta'\eta' + Y \quad , \tag{2}$$

$$(I_{zz}'+J_{zz}')\frac{dr'}{dt'} = N_\beta'\beta' + N_{\dot r}'r' + N_{\dot\beta}'\dot\beta' + N_\delta'\delta' + N_\eta'\eta' + N' \quad , \tag{3}$$

$$\frac{d\eta'}{dt'} = \psi' - \beta' \quad , \tag{4}$$

$$\frac{d\delta'}{dt'} = \frac{1}{T_r}(\delta_c' - \delta') \quad . \tag{5}$$

We have included a first-order model for the steering gear dynamics in order to introduce a realistic rudder time response. An external sway force Y and an external yawing moment N are included to account for disturbances which act on the ship. The terms involving Y_η' and N_η' account for bank forces and moments, respectively, when the ship is off the channel centerline. The control is the commanded rudder angle δ_c'. The unit of nondimensional time t' is the time it takes the ship to travel one ship length.

Equations [1] through [5] can be transformed into state-variable form; i.e.,

$$\frac{d}{dt'}\begin{bmatrix}\psi'\\ r'\\ \beta'\\ \eta'\\ \delta'\end{bmatrix} = \begin{bmatrix}0 & 1 & 0 & 0 & 0\\ 0 & f_{22} & f_{23} & f_{24} & f_{25}\\ 0 & f_{32} & f_{33} & f_{34} & f_{35}\\ 1 & 0 & -1 & 0 & 0\\ 0 & 0 & 0 & 0 & -1/T_r\end{bmatrix}\begin{bmatrix}\psi'\\ r'\\ \beta'\\ \eta'\\ \delta'\end{bmatrix} + \begin{bmatrix}0\\ 0\\ 0\\ 0\\ 1/T_r\end{bmatrix}\delta_c' + \begin{bmatrix}0 & 0\\ \gamma_{21} & \gamma_{22}\\ \gamma_{31} & \gamma_{32}\\ 0 & 0\\ 0 & 0\end{bmatrix}\begin{bmatrix}N'\\ Y'\end{bmatrix} , \tag{6}$$

or,

$$\dot{\underline{x}} = F\underline{x} + G\underline{u} + \Gamma\underline{w} \quad . \tag{7}$$

The coefficients of the open loop dynamics matrix f_{ij} and the disturbance distribution matrix γ_{ij} are algebraic combinations of the stability derivatives and mass and inertia terms in eq. [2] and [3]. Coefficients f_{24} and f_{34} are zero when the ship is not in a channel. The multivariable integral controller of interest here can handle disturbances with a nonzero mean. We will therefore model the disturbances as the sum of two components; i.e., an unknown but constant part $\underline{w}_s$ and an additive white noise disturbance $\underline{w}'$. Equation [7] then becomes,

$$\dot{\underline{x}} = F\underline{x} + G\underline{u} + \Gamma\underline{w}_s + \Gamma\underline{w}' \quad . \tag{8}$$

The problem thus has five states, one control, and four disturbance components. The output of the system, eq. [8], is given by,

$$\underline{y} = T\underline{x} \quad , \tag{9}$$

where T is the output selection matrix. We take the lateral offset as the output so $\underline{y}$ is just a scalar and T becomes the row vector,

$$T = [0,\ 0,\ 0,\ 1,\ 0] \quad . \tag{10}$$

For a particular example, we will utilize the data obtained by Fujino[6],[9] for a model of the 290m (951 ft) tanker *Tokyo Maru*. Fujino conducted planar motion mechanism (PMM) and oblique tow tests of the model at various water depth-to-draft ratios H/T and channel width ratios W/B. Selected characteristics for this vessel are shown in Table 1. The coefficients f_{ij} and γ_{ij} obtained for the *Tokyo Maru* at 12 knots full-scale at H/T values of 1.30, 1.89, 2.50, and ∞ without a channel and at H/T=1.89 in a W/B = 3.0 channel are given in Table 2. As shown by Fujino[6] this vessel is course unstable for the intermediate depth-to-draft ratios from about 3.0 down to 1.75 as is typical of many large vessels.

characteristic	Fujino's model	prototype
linear scale ratio, λ	145.0	-
length between perpendiculars, m	2.000	290
breadth, m	.3276	47.5
draft, m	.1103	16.0
displacement	58.4 kg	179,100 LT
block coefficient	0.8054	0.8054
rudder area	3,390.0 mm^2	71.29 m^2
propeller diameter	53.8 mm	7.80 m
P/D	0.740	0.740
expanded area ratio	0.619	0.619
number of blades	5	5

Table 1. Characteristics of *Tokyo Maru* Model and Prototype.

W/B	∞, no channel				3.0
H/T	1.30	1.89	2.50	∞	1.89
f_{22}	-1.6508	-1.7657	-1.8177	-1.9515	-2.0779
f_{23}	9.3157	5.7359	4.6112	3.1591	5.7080
f_{24}					-1.2247
f_{25}	-0.55543	-0.88074	-1.0416	-1.0410	-0.83603
Y_{21}	346.69	477.68	536.00	567.13	415.75
Y_{22}	4.8040	-5.0043	-5.8625	2.3365	-2.2292
f_{32}	0.02974	0.17199	0.23621	0.31507	0.00741
f_{33}	-1.0388	-0.52766	-0.54560	-0.63651	-0.43325
f_{34}					-0.51892
f_{35}	-0.09995	-0.15607	-0.16639	-0.16163	-0.16597
Y_{31}	11.825	21.141	21.942	16.844	30.540
Y_{32}	-19.216	-28.233	-31.490	-37.384	-26.973

key: 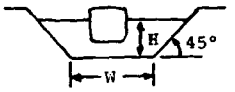

B = beam

T = draft

Table 2. Coefficients of Tokyo Maru versus H/T and W/B at F_n=0.116 (12 knots full-scale)

Measurement Selection

All of the states in the ship path control problem as formulated in eq. [8] are available for measurement. The heading ψ' can be obtained from a compass; the yaw rate r' can be obtained from a rate gyro; the drift angle $\beta' = -v'$ can be obtained from a doppler sonar; the rudder angle δ' can be obtained from the rudder stock or less accurately from the steering gear rams. The lateral offset η' must be obtained using navigation aids such as DECCA Hi-Fix or radar. In the presence of measurement "noise" and with the measurement of only selected states, the complete state vector can be estimated using a Kalman filter provided all of the states are observable with the chosen measurements.

The authors have previously shown[1] that the ship path control problem is observable with the lateral offset η'. Additional measurements improve the ability of a Kalman filter to estimate all the states and thus improve the effectiveness of an optimal state feedback controller. The drift angle β' measurement was shown to add little to the effectiveness of a ship path controller which already measures

η', r', and ψ'. With the steering gear model used here, there is little need to measure the rudder angle since the state is known exactly given any initial condition $\delta'(t_o)$ and the subsequent rudder command history $\delta'(t)$, $t > t_o$. For the controller design, it is therefore reasonable to assume a measurement vector consisting of measurements of ψ', r', and η' each contaminated by Gaussian, white noise; i.e.,

$$\underline{z} = \begin{bmatrix} 1 & 0 & 0 & 0 & 0 \\ 0 & 1 & 0 & 0 & 0 \\ 0 & 0 & 0 & 1 & 0 \end{bmatrix} \underline{x} + \begin{bmatrix} \nu_1 \\ \nu_2 \\ \nu_3 \end{bmatrix} = H\underline{x} + \underline{\nu} \quad . \tag{11}$$

The white noise power spectral density needed in our continuous system design approach can be estimated by assuming the noise to be exponentially correlated with an RMS noise level σ_j and a correlation time τ_j. The τ_j should be much faster than the time constants of the ship and less than the system sampling time for the model to be valid. The power spectral density can then be estimated by,

$$r_{jj} \cong 2(\sigma_j)^2\tau_j \quad . \tag{12}$$

To evaluate the control system effectiveness in this study, we use digital simulation with a fixed-stepsize Euler integration scheme. In these simulations, the covariance of the computer generated random measurement noise must be selected to be consistent with the design noise power spectral density. To provide equivalent state estimate error covariances, it is necessary that the simulation measurement noise variance be given by,

$$\sigma_j'^2 = \frac{r_{jj}}{\Delta t} \quad , \tag{13}$$

where Δt is the integration stepsize.[1],[10]

The reference measurement noise levels used in this work are shown in Table 3. We assume exact knowledge of the rudder angle. Åström and Källström[11] note that all sensors have dynamics with time constants less than 1 sec. and that the measurement errors are about 0.1° in ψ and 0.02°/s in r. Millers[12] uses RMS errors of 0.2° in ψ, 0.01°/s in r and 10 m. in η. Canner[13] states that DECCA Hi-Fix crosstrack errors are as low as 1 m. when the baseline is along the desired path as is done at the entrance to Europoort. Åström and Källström[11] and Byström and Källström[14] have found errors in r of less than 0.002°/s in systems identification of full-scale experiments. In view of this data, the reference levels in Table 3 were assumed. The values for r_{jj} and σ_j' are nondimensional.

measure-ment	source	RMS noise level σ_j	correla-tion time τ_j	white noise power spectral density r_{jj}	simulation noise vari-ance σ_j'
ψ'	compass	0.1°	0.1s	1.298×10^{-8}	1.611×10^{-3}
r'	rate gyro	0.001°/s	0.1s	2.860×10^{-7}	7.563×10^{-3}
η'	DECCA Hi-Fix	3m	0.1s	4.559×10^{-7}	9.549×10^{-3}

Table 3. Reference Measurement Noise Characteristics

Design Process Disturbances

While operating in restricted waters, a ship can be subjected to a wide range of disturbances. Many of these can be characterized as being short-term relative to the time constants of the ship and as having essentially a zero mean value. First-order wave forces, wind gusts, and passing ships can be included in this category. Other disturbances remain long enough relative to the time constants of the ship that they must be considered to have nonzero mean value. Second-order wave forces and the effect of a lateral current, bank, or steady wind are included in this category. For the purposes of this study, we utilize two typical or design process disturbances in digital simulations to evaluate the performance of the path controller. These design disturbances were defined in our previous work.[2]

The lateral force Y' and yawing moment N' due to a passing ship was selected as a typical short-term, essentially zero-mean disturbance. The assumed design disturbance is shown in Fig. 2. The effect

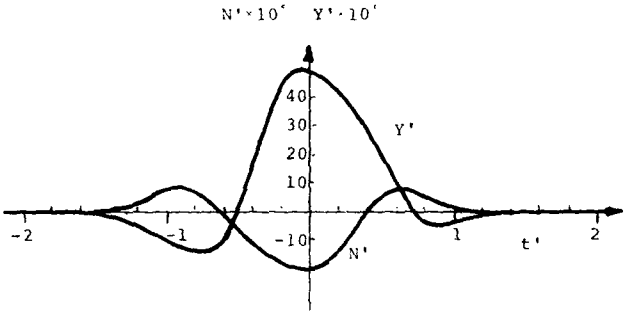

Figure 2. Design Passing Ship Disturbance

of a lateral current was selected as a typical long-term, nonzero-mean disturbance for use in our ship path controller simulations. When using the drift angle with respect to the earth in eq. [8], a steady current can be shown[2] to have the effect of applying an external lateral force and yawing moment given by,

$$Y' = Y_{\beta}' v_c' \quad , \qquad [14]$$

and,

$$N' = N_{\beta}' v_c' \quad , \qquad [15]$$

where v_c' is the non-dimensional lateral current speed. For design evaluation purposes, these equations were used to establish the lateral force and yawing moment produced by a 1 knot lateral current on the *Toyko Maru* moving at 12 knots in an intermediate water depth H/T = 1.89. This disturbance was then arbitrarily assumed to be constant for 15 ship lengths and then to reduce linearly to one half this value at 20 ship lengths. This design disturbance is shown in Fig. 3.

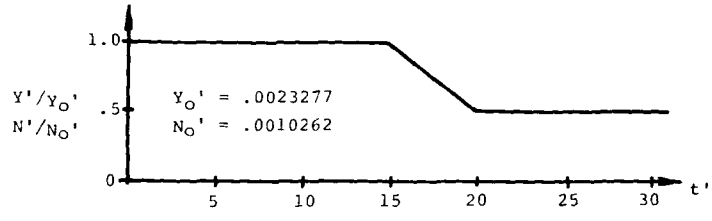

Figure 3. Design Lateral Current Disturbance

DERIVATION OF MULTIVARIABLE INTEGRAL SHIP PATH CONTROLLER

The general development follows that given by Holley and Bryson[5] but is more general in that it can accommodate a nonzero initial command without a startup transient. The development is specialized to the ship path control problem. The section closes with a derivation of the steady-state error of the controller to a ramp commanded set point.

General Derivation

The multivariable integral control law can be taken as a state variable feedback plus a feedback on a fictitious output $\underline{y}_o$; i.e.,

$$\underline{u} = C_x \underline{x} + C_y \underline{y}_o \quad . \qquad [16]$$

At this point, $\underline{y}_o$ can be defined as the difference between the desired steady-state output $\underline{y}_d$ and $\underline{y}_w$, the output due to the constant disturbance $\underline{w}_s$,

$$\underline{y}_o = \underline{y}_d - \underline{y}_w \quad . \qquad [17]$$

Substituting this expression into eq. [16], we arrive at an alternative expression for the control law;

$$\underline{u} = C_x\underline{x} + C_y(\underline{y}_d - \underline{y}_w) \quad . \tag{18}$$

The steady-state condition of the system in the presence of the constant portion of the disturbance $\underline{w}_s$ can be used to derive an expression for the feedback gain matrix C_y. In the steady-state, we have $\dot{\underline{x}}_s = 0$. We can designate the steady-state values of the state and control by the subscript s and the perturbations from these values by a prime; i.e.,

$$\begin{aligned} \underline{x} &= \underline{x}_s + \underline{x}' \quad , \\ \underline{u} &= \underline{u}_s + \underline{u}' \quad . \end{aligned} \tag{19}$$

Substituting eq. [19] into eq. [8], we obtain the following system:

$$\begin{aligned} \dot{\underline{x}}' &= F\underline{x}' + G\underline{u}' + \Gamma\underline{w}' \quad , \\ 0 &= F\underline{x}_s + G\underline{u}_s + \Gamma\underline{w}_s \quad . \end{aligned} \tag{20}$$

The steady-state solutions, if any exist, must then satisfy,

$$(F + GC_x)\underline{x}_s + GC_y\,\underline{y}_o + \Gamma\underline{w}_s = 0 \quad . \tag{21}$$

If the system (F,G) is controllable, $(F + GC_x)$ is negative definite and the steady-state output is,

$$\underline{y}_s = T\underline{x}_s = -T(F + GC_x)^{-1}(GC_y\,\underline{y}_o + \Gamma\underline{w}_s) \quad . \tag{22}$$

Defining,

$$L = -T(F + GC_x)^{-1} \quad , \tag{23}$$

this becomes,

$$\underline{y}_s = LGC_y\,\underline{y}_o + L\Gamma\underline{w}_s \quad . \tag{24}$$

If we now require that the steady-state output $\underline{y}_s$ be equal to the desired output $\underline{y}_d$, comparison of eq. [24] and eq. [17] yields,

$$\underline{y}_w = L\Gamma\underline{w}_s \quad , \tag{25}$$

and,

$$LGC_y = I \quad , \tag{26}$$

where I is the identity matrix. Equations [23] and [26] allow the calculation of the gain matrix C_y from F, G, C_x, and T.

Estimating $\underline{y}_w$. In practice $\underline{w}_s$, the nonzero bias component of the disturbance, is rarely known. Therefore both the state $\underline{x}$ and $\underline{y}_w$ are unknowns in the control law, eq. [18]. A recursive scheme can be utilized to provide an on-line estimate of $\underline{y}_w$. The linear estimator,

$$\dot{\hat{\underline{y}}}_w = K_y(\hat{\underline{y}}_w - \underline{y}_w) = -K_yL(\Gamma\underline{w}_s - \Gamma\hat{\underline{w}}_s) \quad , \tag{27}$$

where $\hat{\underline{w}}_s$ is an estimate of $\underline{w}_s$ and $\hat{\underline{y}}_w$ is an estimate of $\underline{y}_w$, can be shown[15] to be given approximately by,

$$\dot{\underline{y}}_w = - K_y L\dot{\underline{x}} - K_y(T\underline{x} - \underline{y}_d) \quad . \tag{28}$$

If we define a new state variable $\underline{v}$ by the differential equation,

$$\dot{\underline{v}} = T\underline{x} - \underline{y}_d \quad , \tag{29}$$

the new state is the integral of the output error. Substituting eq. [29] into eq. [28], we obtain the following linear estimation scheme for $\underline{y}_w$:

$$\dot{\underline{y}}_w = - K_y(L\dot{\underline{x}} + \dot{\underline{v}}) \quad . \tag{30}$$

This can be integrated to give,

$$\hat{\underline{y}}_w = - K_y(L\underline{x} + \underline{v}) + \underline{y}_c \quad , \tag{31}$$

where $\underline{y}_c$ is the constant of integration which can be obtained from the initial conditions of the system.

In eq. [27], it can be seen that if the gain matrix K_y is selected to be negative definite with eigenvalues to the left in the complex plane compared with the other closed-loop eigenvalues, this estimator will provide a rapid estimate with $\hat{\underline{y}}_w \rightarrow \underline{y}_w$. Substituting eq. [31] for $\underline{y}_w$ in the control law, eq. [18], yields,

$$\underline{u} = C_x\underline{x} + C_y\underline{y}_d + C_v(L\underline{x} + \underline{v}) - C_y\underline{y}_c \quad , \tag{32}$$

where,

$$C_v = C_y K_y \quad . \tag{33}$$

This final control law is comparable with that obtained by Holley and Bryson[5] except that they omitted the final term. This additional term resulted from the constant of integration in the integration of eq. [30]. It is necessary to allow the startup of the system with a non-zero desired output without an undesirable startup transient.

Augmented System. In equations [8], [9], and [29], the system states $\underline{x}$ and the integral error states $\underline{v}$ are only available through the noisy measurements of the states, eq. [11]. The system is also subjected to the process disturbances $\underline{w}_s$ and $\underline{w}'$. In this situation, we can estimate the states of the augmented system by the system of Kalman filters,

$$\begin{aligned} \dot{\hat{\underline{x}}} &= F\hat{\underline{x}} + G\underline{u} + K_x(\underline{z} - H\hat{\underline{x}}) \quad , \\ \dot{\hat{\underline{v}}} &= T\hat{\underline{x}} - \underline{y}_d + K_v(\underline{z} - H\hat{\underline{x}}) \quad , \end{aligned} \tag{34}$$

and then utilize these estimates in the control law,

$$\underline{u} = C_x\hat{\underline{x}} + C_y\underline{y}_d + C_v(L\hat{\underline{x}} + \hat{\underline{v}}) - C_y\underline{y}_c \quad . \tag{35}$$

From eq. [27] it can be seen that the eigenvalues of K_y will determine the dynamics of the estimate of $\underline{y}_w$ independent of $\underline{x}$. These will also be eigenvalues of the closed-loop system. The other eigenvalues will be those of the closed-loop controller ($F + GC_x$) and those of the state estimator ($F - K_xH$). The remaining Kalman filter gains K_v can be determined to produce a zero mean output error $T\underline{x} - \underline{y}_d$ even when the system is subjected to measurement noise and process disturbances. Holley and Bryson[5] show that this condition will result if,

$$(T - K_V H)(F - K_X H)\Gamma = 0 \quad . \tag{36}$$

This can be used to obtain K_V.

The complete multivariable integral controller is defined by equations [34] and [35]. The control gain C_X and state estimator gain K_X can be obtained using standard optimal control methods. The gain matrix K_V can be obtained by pole placement. The matrix C_Y is defined by eq. [26] with matrix L from eq. [23]; i.e., the solution to,

$$-T(F + GC_X)^{-1}GC_Y = I \quad . \tag{37}$$

The matrix C_V can then be obtained from eq. [33]. The matrix K_V can be obtained from eq. [36]. This control concept will produce a zero steady-state output error with respect to a constant desired output when subjected to a constant disturbance. This result is independent of errors in the knowledge of the system matrices F, G, and Γ as will be present in the ship path control problem. A schematic block diagram of the complete system is shown in Fig. 4.

Application to Ship Path Control

The general form of the multivariable integral controller can now be specialized to the surface ship path control problem as represented by equations [6], [10], and [11]. Since no assumption can be made *a priori* about a channel width B, coefficients f_{24} and f_{34} are assumed zero in this development.

Output Integral Error Estimator Gain K_V. In this problem, the output $\underline{y} = n$, the desired output $\underline{y_d} = n_d$, and the output integral error v are all scalar quantities. With three measurements, the gain K_V is then the vector of dimension three $[\tilde{k}_1, \tilde{k}_2, \tilde{k}_3]$ which drives the estimator,

$$\dot{v} = T\underline{\hat{x}} - y_d + K_V(\underline{z} - H\underline{\hat{x}}) \quad . \tag{38}$$

This gain vector can be obtained from a system of two equations produced by eq. [36]; i.e.,

$$(T - K_V H)(F - K_X H)\Gamma = 0 \quad . \tag{39}$$

The solution of these equations is a one-dimensional subspace because we have three measurements of a system which is subject to two unknown disturbances. The resulting one-dimensional solution is,

$$\begin{aligned} \tilde{k}_1 &= \frac{m_{41}m_{22} - m_{42}m_{21}}{m_{11}m_{22} - m_{12}m_{21}} (1 - \tilde{k}_3) \quad , \\ \tilde{k}_2 &= \frac{m_{11}m_{42} - m_{12}m_{41}}{m_{11}m_{22} - m_{12}m_{21}} (1 - \tilde{k}_3) \quad , \end{aligned} \tag{40}$$

where $M = [m_{ij}] = [F - K_X H]\Gamma$ and $\tilde{k}_3$ is free to be selected by the designer. This indicates that an optimization process could be utilized to determine the value of $\tilde{k}_3$ which would minimize the ITAE (integral of time multiplied by the absolute value of the error) or a similar transient response performance index.[16]

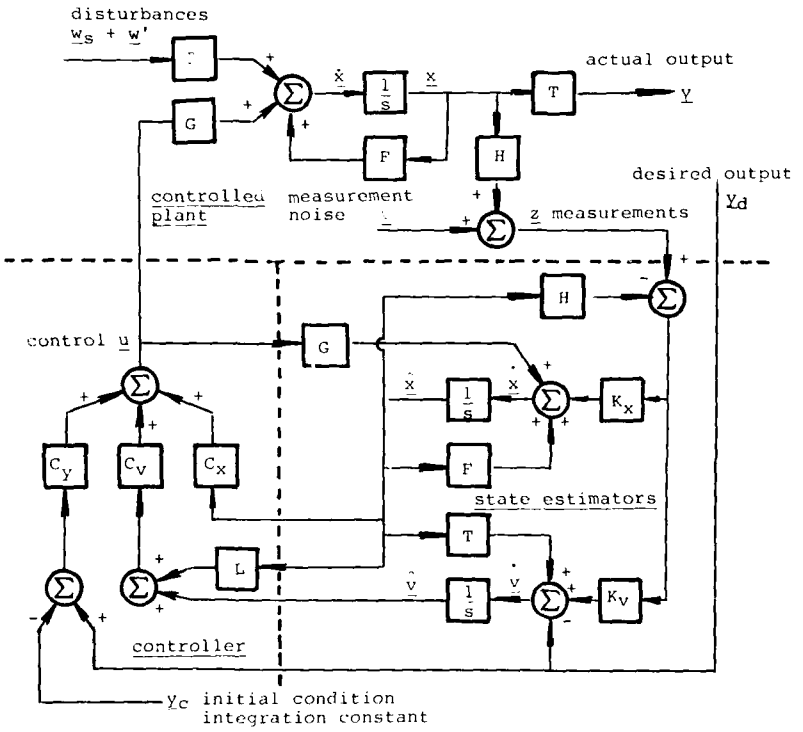

Figure 4. Schematic of Multivariable Integral Controller

In this paper, we will consider the simple special case where $\tilde{k}_3 = 1$ so that eq. [40] yields $\tilde{k}_1 = \tilde{k}_2 = 0$ and,

$$K_v = [0, 0, 1] \quad . \tag{41}$$

In this particular case, the integral error state v has the definition,

$$\dot{v} = n - n_d \quad .$$

Thus v is the integral of the difference or error between measured lateral offset and the desired lateral offset. We therefore have a proportional plus integral control as desired.

Steady-State Error to a Ramp Commanded Set Point

In most practical situations, the prescribed ship path n_d is defined by a series of straight lines or leading line segments. In general, most of these will not be parallel to the ξ-axis and thus the commanded set point $y_d = n_d$ will be a ramp function and not a constant. It is therefore of interest to study the case where the commanded set point y_d is a ramp. This corresponds to the case where the desired path is a straightline with a nonzero heading ψ_d; i.e.,

$$y_d = at' \quad , \tag{49}$$

where a is a constant. To establish the behavior of the output error of this controller when subjected to eq. [49], the closed-loop equations can be rearranged so that y_d appears as an input. The steady-state error to a ramp input can then be established.

The problem of interest here is stochastic with random measurement noise $\underline{v}$ and process disturbances $\underline{w}'$. The steady-state error can be estimated, however, by considering the deterministic case without a constant disturbance. When n_o is taken as zero, substitution of the control law yields,

$$\begin{aligned} \dot{\underline{x}} &= (F + GC_x - CG_4K_yL)\underline{x} - GC_4K_yv - GC_4y_d \quad , \\ \dot{v} &= T\underline{x} - y_d \quad , \\ y &= T'\underline{\xi} \quad , \end{aligned} \tag{50}$$

where we have defined an augmented state variable $\underline{\xi} = [\underline{x}, v]^T$ and let $T' = [0, 0, 0, 1, 0, 0]$. Equation [50] is a single-input, single-output system for which the transfer function and steady-state error can be obtained.

The steady-state error e_{ss} due to a ramp input eq. [49] can be defined as,

$$e_{ss} = \lim_{t' \to \infty} \frac{y_d(t') - y(t')}{a} \quad . \tag{51}$$

We have shown[15] that the steady-state error of eq. [50] to the ramp input eq. [49] is given by,

$$e_{ss} = \left| - \frac{C_1}{C_4} \right| \quad , \tag{52}$$

where C_1 and C_4 are elements of the state feedback gain matrix C_x. This simple result is extremely important. This indicates that even though the multivariable integral controller has a steady-state error with a ramp commanded set point, this error is bounded and known in advance. The controller can, therefore, be programmed to compensate for this error by simply changing the point at which a turn is initiated. Notice also that a control law which minimizes C_1, the feedback gain on the heading, will have a minimum steady-state error. The error can be eliminated with $C_1 = 0$.

CONTROLLER DESIGN AND EVALUATION

In this section, a multivariable integral path controller is designed for the *Tokyo Maru* using the characteristics defined in Table 2. The performance of this controller is then evaluated through a series of digital simulations.

Controller Design

The characteristics of the 290 m tanker *Tokyo Maru* are given in Tables 1 and 2. The only undefined parameter is the rudder time constant T_r which we have taken as 10 seconds. In the nondimensional form used here this becomes $T_r = 0.21287$ at $F_n = 0.116$ or 12 knots full-scale. The state feedback gain matrix C_x and the state estimation Kalman filter gain matrix K_x are taken as the optimal steady-state solutions to the Linear Quadratic Gaussian (LQG) problem,[2],[17]

$$\dot{\underline{x}} = F\underline{x} + G\underline{u} + \Gamma\underline{w} \quad , \qquad \underline{z} = H\underline{x} + \underline{v} \quad , \tag{53}$$

where $\underline{w}$ and $\underline{v}$ are vector white noise processes with power spectral density matrices Q and R, respectively. The design cost functional is defined as the expected value of the integral,

$$J = E\left[\frac{1}{2}\int_{t_o}^{t_f} (\underline{x}^T A\underline{x} + \underline{u}^T B\underline{u})dt\right] \quad , \tag{54}$$

where A and B are weighting matrices which can be initially established by the designer to reflect the relative acceptability of errors in the various states and the use of the various controls.

Matrices Q, A, and B are diagonal with the following nonzero elements:

$$q_{11} = 1.548 \times 10^{-8} \quad ,$$

$$q_{22} = 8.970 \times 10^{-8} \quad ,$$

$$a_{44} = (n_o)^{-2} = 772.5 \quad ,$$

$$a_{55} = (\delta_o)^{-2} = 131.3 \quad ,$$

$$B = b_{11} = (\delta_{co})^{-2} = 131.3 \quad .$$

The power spectral density for the process disturbance Q is based upon the passing ship disturbance shown in Fig. 2 using the root mean square values of N' and Y' between t' = -2 and t' = 1.4 and using an assumed first-order-process correlation time of one ship length for each disturbance. The nonzero diagonal terms of the A and B matrices are based on the use of a dimensional 5° of rudder when the lateral offset error becomes 10.63 m (slightly less than one-quarter beam). The diagonal terms of the measurement noise power spectral density matrix R are given in the fifth column of Table 3.

The solution to this optimal, stochastic control problem was obtained using the Michigan Terminal System (MTS) version of Bryson and

Hall's eigenvalue decomposition OPTSYS program[18]. The resulting state feedback gains C_x and the Kalman filter gains K_x are listed in Table 4. This design was developed for the characteristics of the *Toyko Maru* at the water depth to ship draft ratio H/T = 1.89, which is the least course stable depth for this ship. We have previously shown[1] that if a nonadaptive optimal, stochastic path controller is to be used, the best overall performance is obtained if the controller is designed for the ship's least course stable water depth.

controller gains C_x^T	Kalman filter gains K_x		
5.5421	4.6883	0.9507	0.0035
2.6601	20.9479	109.7887	-0.4755
6.3895	2.7730	9.0086	-8.6949
2.4252	0.1239	-0.7579	4.1275
-0.8499	0.0000	0.0000	0.0000

Table 4. Optimal Gains for *Tokyo Maru* at H/T = 1.89 and F_n = 0.116

Recall that the gain K_y can be chosen by pole placement with respect to the eigenvalues of the closed-loop system $(F + GC_x)$. We, therefore, placed K_y at the closed-loop eigenvalue furthest to the left in the complex plane giving K_y = -6.64361. This will cause the estimate of y_w (through v) to converge rapidly compared to the time response of the system. The output integral error gain K_v was taken from eq. [41]. The value of the gain C_y was obtained from eq. [43] and Table 4; i.e., $C_y = -C_4 = -2.4252$. Equation [44] then gives $C_v = -C_4K_y = 16.1121$. Finally, the steady-state error of the system to a ramp commanded set point can be evaluated numerically using eq. [52] and Table 4; i.e.,

$$e_{ss} = \left|-\frac{C_1}{C_4}\right| = \left|-\frac{5.5421}{2.4252}\right| = 2.285 \quad . \qquad [55]$$

This completes the design of the multivariable integral path controller for the *Tokyo Maru*. The performance of this design is evaluated in the series of digital simulations which follow.

Small Turn with Design Lateral Current

To illustrate the performance of the multivariable integral controller with a bias or nonzero mean disturbance, the *Tokyo Maru* was simulated to undergo a small turn while under the control of the controller designed above. In the simulation, the ship was operating at H/T = 2.50 in open water. The controller was designed for H/T = 1.89 so the ship was operating with errors in the knowledge of the ship dynamics. The simulation began with the ship in an equilibrium condition for no lateral current on the commanded straight path at n_d = 0. The ship was commanded to perform a small (2.86°) course change at t' = 10 while subjected to the "design lateral current" disturbance shown in Fig. 3. This disturbance is constant for the first 15 ship lengths, reduces linearly to half this value by 20 ship lengths, and then remains constant again after 20 ship lengths. The initial magnitude was

established to correspond to a one knot lateral current if the ship were operating in a water depth H/T = 1.89. When the simulation began, the ship and controller were in effect subjected to a step change in yawing moment and lateral force. The simulation, therefore, represents a severe startup test for the controller.

The results of this simulation are illustrated by Figures 5 and 6. Figure 5 shows the commanded and actual ship paths; Fig. 6 shows the resulting path error. The maximum path error due to the step change in the disturbance is about 43.5 m. or 0.9 beam at about t' = 3. The controller then returns the ship to the commanded path and initiates the turn at t' = 10. The ship turns smoothly and shows the expected steady-state error to the ramp commanded input. For the commanded path y_d = at = 0.05(t' -10), t' > 10 and the steady-state error e_{ss} = 2.285 from eq. [55], eq. [51] yields a steady offset error,

$$y_d - y = 2.285a = 0.1143 \quad ,$$

for this turn. This steady offset error is shown on Fig. 6. With this knowledge available in advance, the maneuver could simply be initiated 2.285 ship lengths "earlier" than shown in Fig. 5. Thus, the steady error to a ramp commanded input can be eliminated as a practical concern. The period of time-varying disturbance between t' = 15 and t' = 20 introduces a maximum crosstrack error of about 11.8 m or one-quarter beam at about t' = 20. The controller is, therefore, effective with both bias and large time-varying disturbances as might be expected from bank or current changes.

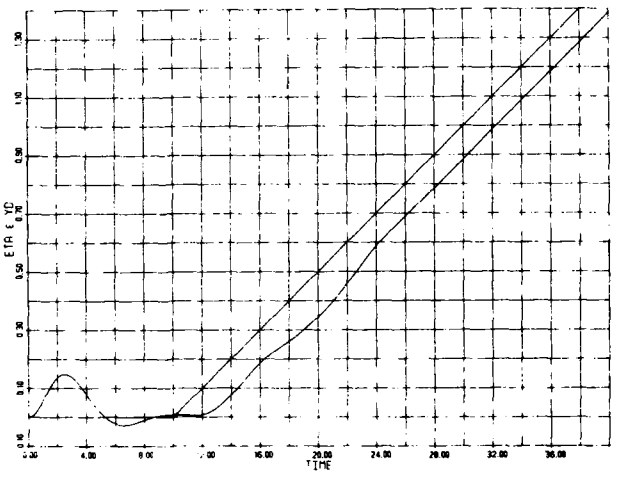

Figure 5. Commanded and Actual Ship Paths in Small Turn with Design Lateral Current

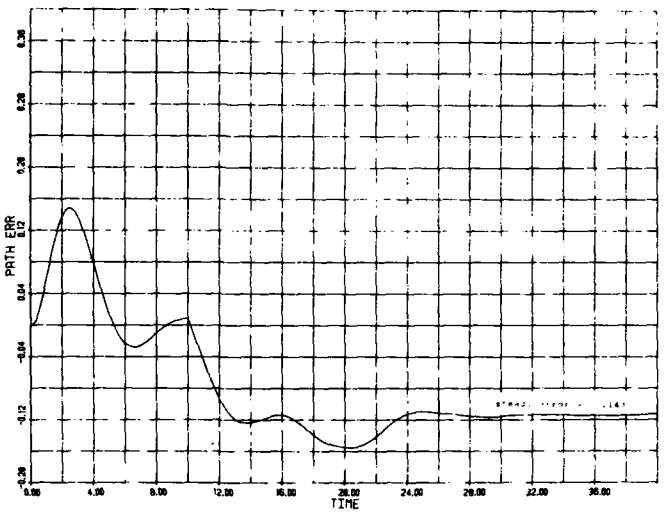

Figure 6. Path Error in Small Turn with Design Lateral Current ($\tilde{k}_3 = 1.0$)

Effect of Output Integral Error Estimator Gain K_v

As noted above, the gain matrix $K_v = [\tilde{k}_1, \tilde{k}_2, \tilde{k}_3]$ is given by a one parameter solution eq. [40] where any one gain is free to be selected by the designer. If $\tilde{k}_3 = 1$ as above, the gain matrix becomes simply $K_v = [0, 0, 1]$. If desired, an optimization process could be utilized to determine the $\tilde{k}_3$ which would minimize one of the standard transient response performance indices. To illustrate the sensitivity of the multivariable integral path controller performance to $\tilde{k}_3$, the simulation illustrated in Figures 5 and 6 was repeated for two additional cases:

Case 1: $K_v = [-341.3, -0.157, 0.1]$,

Case 2: $K_v = [3413., 0.157, 10.0]$.

The resulting path error for Case 1 is shown in Fig. 7. Comparison with Fig. 6 shows that the transient response deteriorates some from the design with $\tilde{k}_3 = 1.0$. The resulting path error for Case 2 is shown in Fig. 8. Note the greatly increased scale. The performance is much worse with $\tilde{k}_3 = 10$ and may not even be stable. The design with $\tilde{k}_3 = 1.0$ is close to an "optimum" design. Case 2 is a good example of how excessive Kalman filter gains can destabilize a system which must operate with errors in the knowledge of the system dynamics. Low values of $\tilde{k}_3$ are thus needed for a robust design.[19]

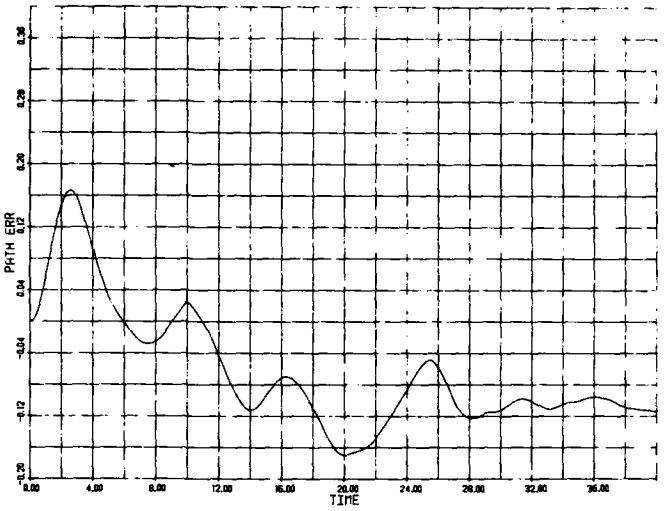

Figure 7. Path Error in Small Turn with Design Lateral Current ($\bar{k}_3 = 0.1$)

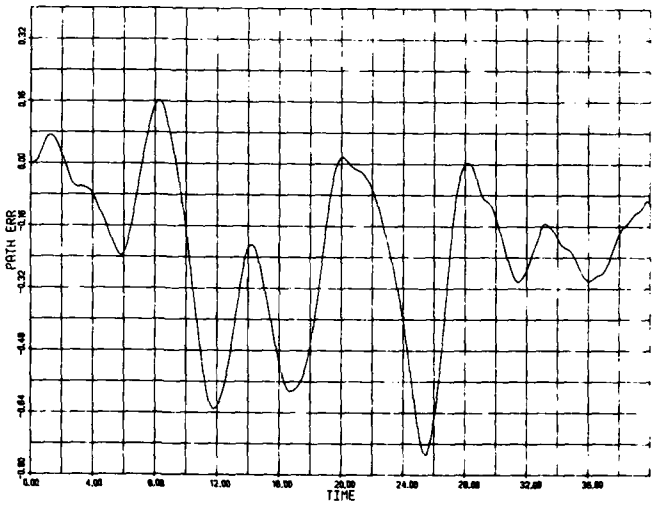

Figure 8. Path Error in Small Turn with Design Lateral Current ($\bar{k}_3 = 10.$)

Passing in a Channel

To illustrate the performance of the multivariable integral controller with a short time-varying disturbance, the *Tokyo Maru* was simulated to pass another ship in a channel while under the control of the controller designed above ($\bar{k}_3 = 1.0$). The water depth was H/T = 1.89; the channel width at the bottom was W/B = 3.0. This water depth was the design depth for the controller but channel effects were not included in the design of the controller. The channel effects ($f_{24} \neq 0$, $f_{34} \neq 0$) were included in the simulation. The ship began the maneuver on the channel centerline and was then commanded to move one beam to starboard ($n_d < 0$) between t' = 10 and t' = 11. The passing ship disturbance shown in Fig. 2 was included with the ships beam-to-beam at t' = 20. The ship was commanded to return to the channel centerline between t' = 29 and t' = 30. The commanded path thus included a series of four 9.3° turns to starboard, port, port, and starboard at t' = 10, 11, 29, and 30, respectively. A 2.285 ship length turn initiation time shift was included to account for the steady-state error of the controller for a ramp commanded set point.

The results of this simulation are illustrated in Figures 9 and 10. The desired and actual ship paths are shown in Fig. 9. The path error is very reasonable. The overshoot after each transfer is only about 4.4 m or 0.09 beam. The resulting rudder activity is shown in Fig. 10. The steady rudder angle while close to the channel boundary between t' = 11 and t' = 29 is about 25°.

St. Marys River Turns

The purpose of this simulation was to test the effectiveness of the multivariable integral controller with larger magnitude turns typical of a general transit in restricted waters. Based upon a discussion with the Captain of one of the 304.8 m (1000 ft) Great Lakes ore carriers, the series of three turns in the St. Marys River between Sand Island and Moon Island in the West Neebish Channel was selected as the prototype for this simulation. These turns were identified as some of the most difficult in the Great Lakes system for the large bulk carriers. This path is the downbound lane and is shown in Fig. 11. The second leg of this path is the "Rock Cut" which has vertical cut-stone walls. The channel at this point is roughly three beams wide for the largest ships in the system. For the purposes of the simulation reported here, only the path was utilized from the prototype. The simulation maneuver is defined in Table 5.

segment	length	heading	turn at end of segment
1	13.38	$\psi = 0$	37° turn to port
2	14.76	$\psi = -37°$	28° turn to starboard
3	13.79	$\psi = -9°$	40° turn to port
4	8.07	$\psi = -49°$	

Table 5. Simulation Maneuver Based Upon St. Marys River

Figure 9. Desired and Actual Ship Path in Passing in a Channel

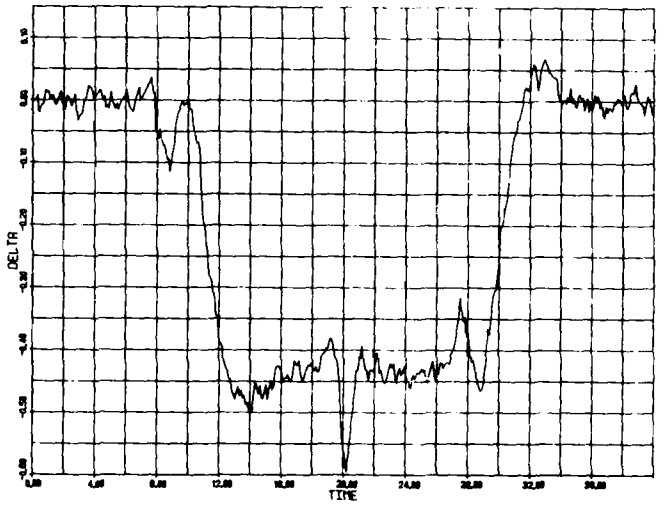

Figure 10. Rudder Angle in Passing in a Channel

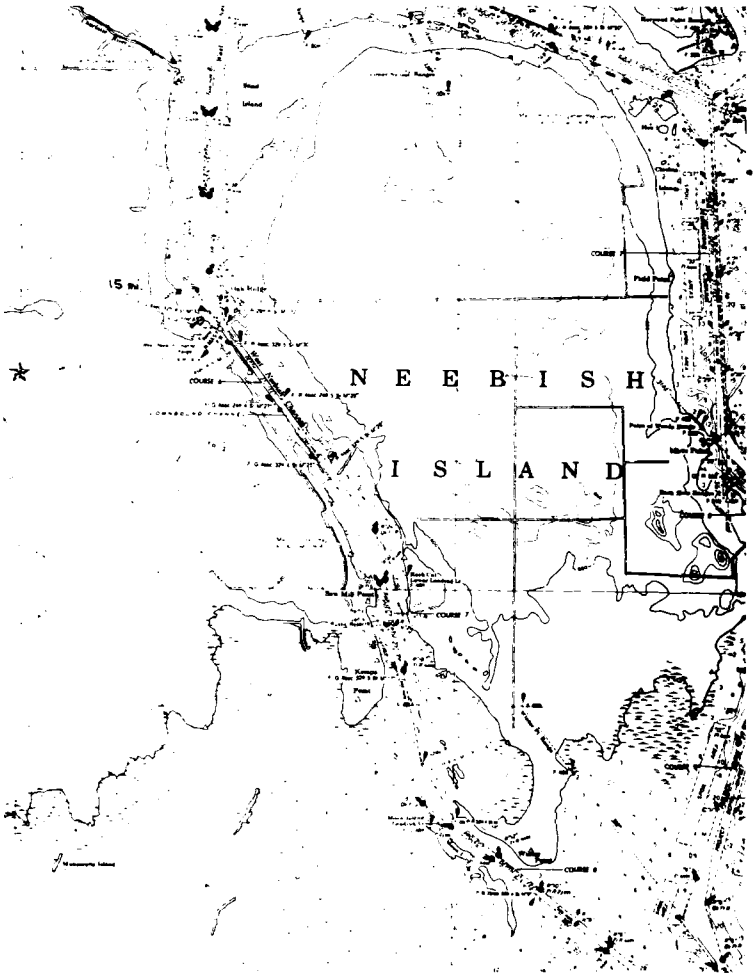

Figure 11. West Neebish Channel (from NOAA Chart 14883)

For this simulation, we continued to utilize the Tokyo Maru under the control of the controller developed above. The simulation was performed at a constant depth of H/T = 1.89. Thus, the operating and controller design depths were the same. Bank effects and current were not included in this particular simulation. The passing ship disturbance shown in Fig. 2 with the ships beam-to-beam at t' = 7 was included for test purposes even though the prototype is actually a single direction channel. The simulation was started in equilibrium on the commanded path. The results of this simulation are illustrated by Figures 12, 13 and 14. The desired and actual ship paths are shown in Fig. 12. Because of the coordinate system defined in Fig. 1, the plot of n versus t' appears as a mirror image of the actual path. The turns were initiated 2.285 ship lengths early to account for the steady-state error of the controller to a ramp commanded set point. The rudder angle in these turns is shown in Fig. 13. The maximum rudder angle at the start of the first turn is 22.7°; maximum rudder angle at the start of the third turn is 30.4°. The path error for the turns shown in Fig. 12 is shown in Fig. 14. The maximum overshoot after the first turn (t' = 15.2) is .097 which corresponds to a crosstrack overshoot of 22.5 m or .47 beam. The maximum overshoot after the second turn (t' = 29.8) is .08 which corresponds to a crosstrack overshoot of 22.9 m or .48 beam. The maximum overshoot after the third turn (t' = 43.7) is 0.13 which corresponds to a crosstrack overshoot of 24.7 m or .52 beam. Below we illustrate an approach for reducing both the overshoot and maximum rudder angles.

Cubic Turn Command

In order to reduce the path overshoot and reduce the maximum rudder angles, the commanded turn can be a smooth curve rather than a discrete change of heading as used above. To investigate the effectiveness of this approach, the first turn in the St. Marys River turns simulation described in Table 5 with the passing ship disturbance shown in Fig. 2 was repeated using a cubic turn command. For simulation convenience, however, the 37° turn was made to starboard. The desired path was as follows:

$$y_d = 0 \quad , \qquad t' < 10. \quad ,$$

$$y_d = .0086704\,(t'-10)^3 + .0056385(t'-10)^2 \quad , \qquad 10. < t' < 15.17 \quad ,$$

$$y_d = .75355\,(t' - 13.38) \quad , \qquad 15.17 < t' \quad .$$

This cubic transition path reaches the desired 37° path beginning at t' = 13.38 at t' = 15.17 with the correct 37° heading. The turn was programmed to be initiated 2.258 ship lengths early in order to eliminate the steady-state error. The rudder activity in the turn is shown in Fig. 15. The maximum rudder angle magnitude in the initation of the turn is 6.9°; the maximum rudder angle used in checking the turn is 9.5°. These values compare favorably with the 22.7° and 14.9°, respectively, shown in Fig. 13 for the first turn. The cubic turn command, therefore, provides a significant reduction in the rudder angle magnitudes used in turns made under the control of the multivariable integral controller. The path error for the 37° turn using the cubic turn command is shown in Fig. 16. Note the change in scale from the comparable Fig. 14. The maximum overshoot after the turn is .0475 at t' = 16. This corresponds to a crosstrack overshoot of 11.0 m or .23 beam compared with the 22.5 m and .47 beam, respectively, shown for the first turn in Fig. 14. The cubic turn command, therefore, provides a significant reduction in path overshoot. Figure 16 shows the possibility of

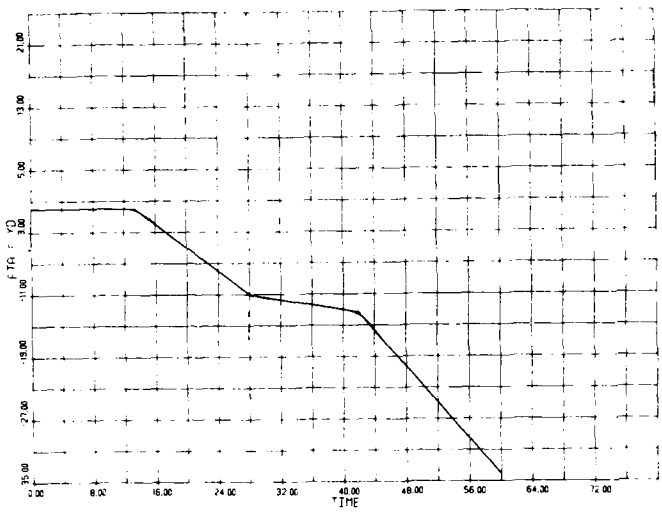

Figure 12. Desired and Actual Ship Paths in St. Marys River Turns

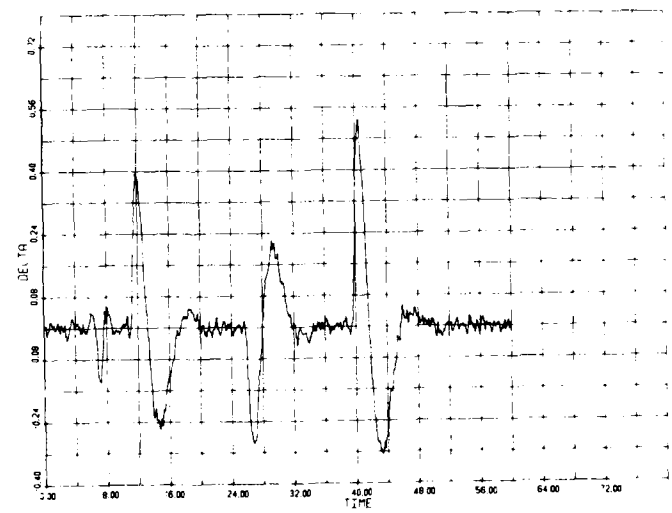

Figure 13. Rudder Angle in St. Marys River Turns

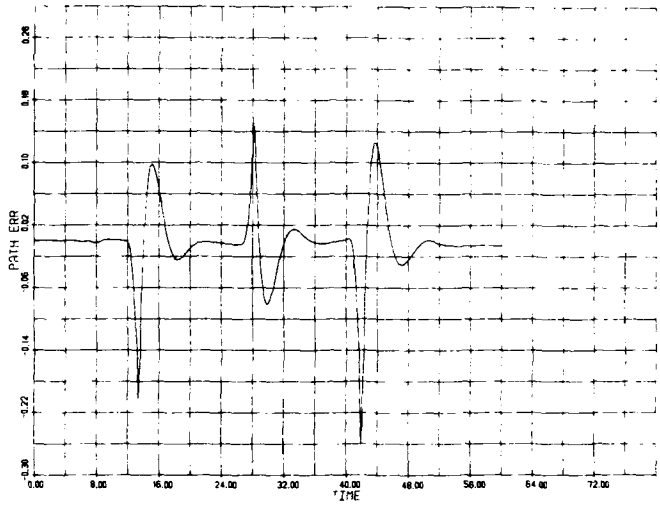

Figure 14. Path Error in St. Marys River Turns

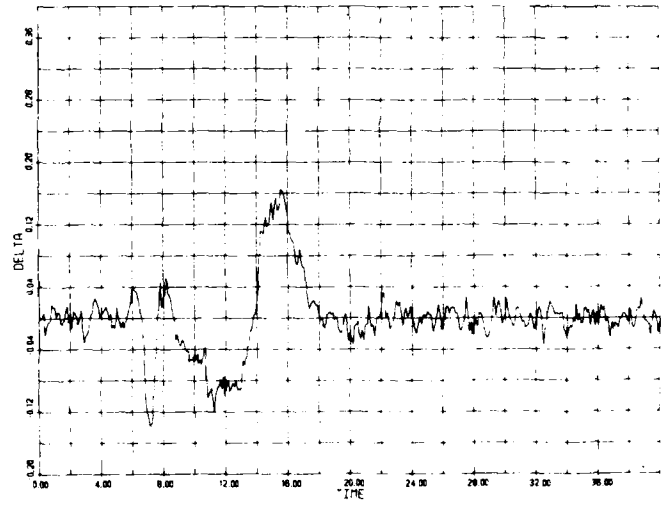

Figure 15. Rudder Angle with 37° Cubic Turn Command

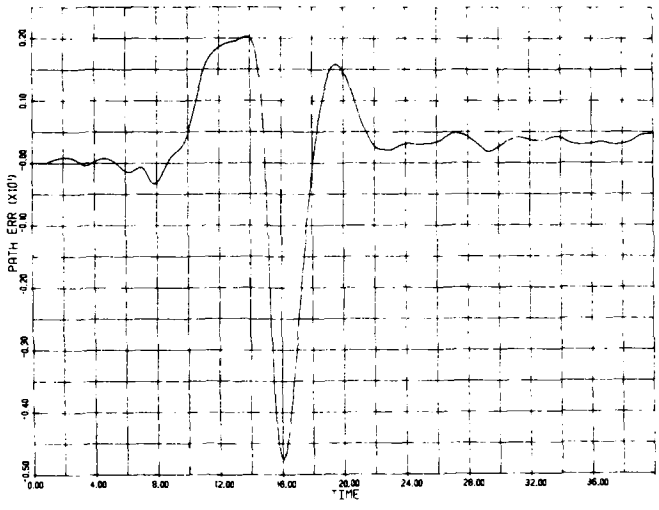

Figure 16. Path Error with 37° Cubic Turn Command

a small steady error after the turn is completed. This is less than 1 m and is most likely due to the roundoff in implementing the 2.258 shift in initiating the turn commands.

The mechanism by which the cubic turn command shown above reduces the rudder usage can be understood by considering the equations for the mean (deterministic) response of the system. If we assume the system output y exactly follows the desired path y_d and differentiate the output eq. [9], we get,

$$\dot{y}_d = T\dot{\underline{x}} = TF\underline{x} + TGu = TF\underline{x} \quad ,$$

since TG = 0 for the ship path control problem. Differentiating a second time yields,

$$\ddot{y}_d = TF^2\underline{x} + TFGu = TF^2\underline{x} \quad ,$$

since TFG = 0 for ship path control problem. Differentiating a third time yields,

$$\dddot{y}_d = TF^3\underline{x} + TF^2Gu = TF^3\underline{x} - \frac{f_{35}}{T_r}\, u \quad .$$

This expression can be solved for an inverse relationship yielding the control needed to follow the desired path exactly; i.e.,

$$u = -\frac{T_r}{f_{35}}\,(\dddot{y}_d - TF^3\underline{x}) \quad . \qquad [56]$$

Low rudder use will, therefore, result for commanded paths with small values of the third derivative $\dddot{y}_d$. The cubic turn command simulated

above completes the desired turn with a small, constant value of y_d Low rudder use will, therefore, result for commanded paths with small values of the third derivative $\dddot{y}_d$. The cubic turn command simulated above completes the desired turn with a small, constant value of $\ddot{y}_d$ and, therefore, reduces the rudder usage significantly.

CONCLUSIONS

The following are the principal conclusions based upon this work:

- The multivariable generalization of the integral controller presented here follows that of Holley and Bryson[5] except that we have obtained an additional term in the control law which results from a constant of integration. This additional term in the control law allows the controller to accommodate nonzero initial setpoint commands without a highly undesirable startup transient.

- In the specialization of this controller to ship path control, we have considered the special case where the integral error variable Kalman filter gain is $K_v = [0, 0, 1]$. The design of this gain vector contains one free variable which can be selected to optimize the transient response of the controller. The other elements of $K_v = [\tilde{k}_1, \tilde{k}_2, \tilde{k}_3]$ can then be obtained using eq. [40]. Simulations show that the transient response is sensitive to the value of $\tilde{k}_3$ and that $\tilde{k}_3 = 1.0$ is close to an optimum value.

- The multivariable integral controller has the property of zero steady-state error with a constant commanded set point when subjected to disturbances and measurement noise. In ship path control, a common situation is a nonzero heading straight path which corresponds to a ramp set point command. In this case, the multivariable integral controller has a nonzero steady-state error which can be interpreted as a time shift in the turn response. We derive a simple analytical expression for this error, eq. [52], which allows its calculation in advance. The effect of this error can then be eliminated by simply initiating the turn a fixed time earlier than would normally be expected.

- Simulation results show that the performance of the controller is excellent with a constant or ramp set point even when the ship is subjected to large time-varying disturbances and when the design is based upon incorrect knowledge of the characteristics of the ship.

- The multivariable controller provides effective control in larger magnitude turns between straight path segments as included in the St. Marys River turns maneuver defined in Table 5.

- Cubic transition set point commands can be introduced to reduce the overshoot and rudder activity in the turns. Low values of the third derivative of the commanded path offset will yield significantly reduced rudder usage.

ACKNOWLEDGEMENT

The research presented here has been supported by NOAA SEAGRANT grant no. NA-79AA-D-00093 and grant no. NA-80AA-D-0072.

REFERENCES

1. M.G. Parsons, and H.T. Cuong, "Optimal Stochastic Path Control of Surface Ships in Shallow Water," The University of Michigan, Department of Naval Architecture and Marine Engineering, Report No. 189/ONR Report ONR-CR215-249-2F, 15 Aug. 1977.

2. M.G. Parsons, and H.T. Cuong, "Adaptive Path Control of Surface Ships in Restricted Waters," The University of Michigan, Department of Naval Architecture and Marine Engineering, Report No. 211, March, 1980.

3. H.T. Cuong, "Investigation of Methods for Adaptive Path Control of Surface Ships," Ph.D. Dissertation, The University of Michigan, 1980.

4. H.T. Cuong, and M.G. Parsons, "An Adaptive Surface Ship Path Control System," Proceedings of the Workshop on Applications of Adaptive Systems Theory, Yale University, May 1981.

5. W.E. Holley, and A.E. Bryson, Jr., "Multi-Input, Multi-Output Regulator Design for Constant Disturbances and Non-Zero Set Points with Application to Automatic Landing in a Crosswind," Stanford University Report SUDAAR No. 465, Aug., 1973.

6. M. Fujino, "Maneuverability in Restricted Waters: State of the Art," The University of Michigan, Department of Naval Architecture and Marine Engineering, Report No. 184, Aug., 1976.

7. T.F. Ogilvie, "Recent Progress Toward the Understanding and Prediction of Ship Motions," Proceedings of the 5th Symposium on Naval Hydrodynamics, Bergen, Norway, Sept. 10-12, 1964, p. 3.

8. M. Fujino, "The Effect of Frequency Dependence of the Stability Derivatives on Maneuvering Motions," International Shipbuilding Progress, Vol. 22, No. 256, Dec., 1975, p. 416.

9. M. Fujino, "Experimental Studies on Ship Manoeuvrability in Restricted Waters-Part I" International Shipbuilding Progress, Vol. 15, No. 168, Aug. 1968, p. 279, and "-Part II," Vol. 17, No. 186, Feb. 1970, p. 45.

10. M.G. Parsons, and J.E. Greenblatt, "SHIPSIM/OPTSIM Simulation Program for Stationary, Linear Optimal Stochastic Control Systems," The University of Michigan, Department of Naval Architecture and Marine Engineering, Report No. 188/ONR Report ONR-CR215-249-1, 23 June 1977.

11. K.J. Åström, and C.G. Källström, "Identification of Ship-steering Dynamics," Automatica, Vol. 12, 1976, p. 9.

12. H.F. Millers, "Modern Control Theory Applied to Ship Steering," Proceedings of the IFAC/IFIP Symposium on Ship Operation Automation, Oslo, Norway, July, 1973.

13. W.H.P. Canner, "The Accuracy Requirements of Automatic Path Guidance," Proceedings of the Fourth Ship Control Systems Symposium, Den Helder, The Netherlands, p. 1-141.

14. L. Byström, and C.G. Källström, "System Identification of Linear and Nonlinear Ship Steering Dynamics," Proceedings of the Fifth

Ship Control Systems Symposium, Vol. 3, Annapolis, MD., 1978, p. J2 2-1.

15. M.G. Parsons, and H.T. Cuong, "Surface Ship Path Control using Multivariable Integral Control," Michigan SeaGrant Report MICHU-SG-81-201, Jan., 1981.

16. R.C. Dorf, Modern Control Systems, Addison-Wesley, Reading, MA, 1974, p. 111.

17. A.E. Bryson, Jr., and Y.C. Ho, Applied Optimal Control, Blaisdell, Waltham, Mass, 1969.

18. A.E. Bryson, Jr., and W.E. Hall, Jr., "Optimal Control and Filter Synthesis by Eigenvector Decomposition," Stanford University Report SUDAAR No. 436, Nov., 1971.

19. J.C. Doyle, and G. Stein, "Robustness with Observers," IEEE Transactions of Automatic Control, Vol. AC-24, No. 4, Aug., 1979, p. 607.

OPTIMAL SHIP COURSE-KEEPING DYNAMICS FOR MANUALLY TUNED PID AUTOPILOTS

by Leonard Marshall
and David R. Broome
Dept. of Mechanical Engineering
University College London
London UK

ABSTRACT

A digital computer simulation has been developed to investigate the course-keeping dynamics of a ship under PID autopilot control. A variety of environmental disturbances, defined by sea-state and direction, may be used, and the effectiveness of course-keeping control is characterised by a cost function which is a weighted integral of the ship yaw and rudder motions. Time domain responses of the ship yaw and rudder motions are stored and may be displayed on an interactive graphics terminal, so that the effects of different ships, autopilot parameter settings and disturbances can be readily observed. Maps have been obtained to show how the cost function varies with autopilot gain and derivative action, for a variety of environments, and for open-loop stable and unstable ships. A definite minimum for cost function exists, and non-optimal selection of autopilot parameters can result in considerable penalties with respect to time lost on a journey.

The effect of system non-linearities including, telemotor hysterysis and deadband, gyrocompass discretisation, rudder saturation velocity and time constant have been studied. Only the rudder rate limit is seen to significantly affect cost function.

These results infer that the autopilot should be re-tuned at various stages throughout a ships voyage, particularly when there is a change in environmental status, or a course change is implemented. This could be accomplished by providing ship personnel with an on-line cost function indication, perhaps as an additional bridge instrument. An experiment has been performed to investigate human performance in the solution of multivariable cost spaces of the type considered here. The results show that optimisation might be achieved economically by providing the human operator with qualitative information with respect to space geometry, such as the partial derivative. Furthermore, it would not appear necessary to require the operator to seek a pre-determined criterion of optimal cost to obtain satisfactory performance.

INTRODUCTION

The majority of ocean going vessels are fitted with autopilot systems based on the classical PID algorithm (Minorsky[1]). In recent years, the requirments on ship course-keeping have increased. Optimality can no longer be defined in terms of the reduction of heading errors. Conflicting specifications on the system infers that the autopilot should be varied with varying environmental conditions.

A number of workers have attempted to derive an index of optimal course-keeping in terms of a cost function. It is generally accepted that optimality requires the minimisation of long periodic yawing motions, while also taking into account the increased drag due to the rudder motions. Norrbin [2] has described this trade-off in terms of a quadratic criterion of the form:

$$\frac{\Delta R}{R} = K\bar{\psi}^2 + \lambda\bar{\delta}^2 \qquad (1)$$

where R is the drag, ΔR is the increased drag due to steering, $\bar{\psi}^2$ and $\bar{\delta}^2$ are the averages of the squared yaw and rudder angles respectively.

There is considerable doubt as to values to be assigned to the coefficients, K and λ which weight yaw and rudder. Different authors have assigned different values as a consequence of their adopted approaches. For example, Koyama [3] suggests a value $\lambda = 8$, whereas Norrbin quotes $\lambda = 0.1$. Norrbin considers losses to be due to rudder induced drag, and as such puts little emphasis on course errors per se. On the other hand, Koyama does not consider course errors to be too serious in themselves, but large rudder angles which induce high turning rates should be avoided.

Probably the major factor in this discrepancy is that Koyama explicitly takes account of the environmental disturbances, whereas Norrbin does not. Van Amerongen and Van Nauta Lemke [4] have crystallised this argument. In good weather, tight control with accurate steering infers that Norrbin's criterion would be appropriate. In bad weather, filtering and low controller gains are required to limit the bandwidth of the system. In such a case, Koyama's criterion would be appropriate.

Clarke [5] used a similar cost function in a simulation study:

$$\frac{\Delta T}{T} = \frac{1}{t^*}\int_0^{t^*} (a_0\psi^2 + a_1\dot{\psi}^2 + a_2\delta^2)\, dt \qquad (2)$$

where $\Delta T/T$ is the fractional increase in time for the ship to travel from one place to another, and t^* is the actual journey time. A similar cost function form has also been used by Van Amerongen and Van Nauta Lemke [4].

Optimality requires that we minimise the valid cost function form. The result of which should be a decrease in the rate of fuel consumption. Kallstrom and Norrbin [6] have found good correlations between cost function minimisation and fuel consumption rate in full scale trials.

Clarke [7] carried out an analog computer study of a ship being steered by a conventional autopilot in rough seas. From the results obtained, he generated a contour map of rudder against counter-rudder, clearly showing the penalties incurred by the selection of inappropriate autopilot parameter settings.

Both in automatically adaptive autopilots (see for example, Tiano [8] or Astrom and Kallstrom [9]) or in manual tuning of conventional PID autopilots, to achieve optimal course-keeping performance, it is important to ensure that the cost function, used to measure the optimality of the resultant course, is valid for the particular ship and operating conditions under consideration. In the former case the cost function, computed as the ship progresses from measurements of the ship and rudder motions, is used as part of an adaptive algorithm which changes the autopilot parameters to seek a cost function minimum. In manual tuning of the autopilot, it would be beneficial to generate an on-line cost function indication, perhaps as an additional bridge instrument, to give ships' personnel an assessment of their tuning strategy, where again a minimum cost function value is sought.

It is likely that the variation of cost function with autopilot parameters, as demonstrated by Clarke, will vary significantly with ship operating conditions, that is the environmental disturbance created by wind, waves and currents. Examination of the effects of these disturbances is difficult for both full scale

and scale model tests because the operational environment can not be easily controlled. However, several authors have performed such tests (see for example, Broome and Lambert,[10]; Van Amerongen, Goeij, Moraal, Ort and Postuma [11]).

A digital computer simulation of a ship and its operating environment has been developed to investigate the variation in cost function for different ships in a variety of sea-states. It is found that in each case, a definite minimum exists and that this value is determined by optimal tuning of the autopilot gain and derivative action. Furthermore, it is possible to assess the penalties which might be incurred for inappropriate parameter selections. As the environment is varied by say increasing the angle of incidence of the wave propogation relative to the ship's bow, the distribution of cost function variance is seen to migrate within an orthogonal, three dimensional co-ordinate system defined by the autopilot parameter settings (gain and derivative action) and absolute cost.

An on-line cost function indication, would necessarily be in discrete, numerical form. However, the bridge officer has no means of assessing whether his current tuning strategy is indeed achieving optimality. He is therefore faced with a two-variable optimisation task, with both of the input variables, autopilot proportional gain and derivative action, in discrete form, and the output, the computed cost function value, also discrete. Human performance in the optimisation of such tasks has always been assumed to be poor. Recently, Laughery and Drury [12] have shown that the contrary may be the case, and that human performance can improve upon a well tuned computer algorithm, particularly when the information flow is degraded. A computer controlled laboratory experiment has been conducted to examine the following questions.

(1) Is human performance decremented when an a priori criterion of optimum cost is not provided? This simulates very well the task of the ship's officer attempting to select optimal autopilot parameter settings for a given operational environment.

(2) Can human performance be improved by providing qualitative information with respect to cost space geometry? Such information could be provided 'cheaply' by calculating the partial derivatives of cost with respect to both autopilot parameter settings.

SHIP STEERING DYNAMICS

The main equations on which the simulation is based are presented. For a more detailed description see Broome, Keane and Marshall [13]. A block diagram of the ship and control system is given in Figure 1.

For the purposes of the simulation, the equations of motion of the ship are required in transfer function form, that is, the relationship between the demanded rudder position generated by the autopilot and the ships yaw motion.

The Rudder to Yaw Response

Nomoto [14] shows that the linear coupled equations of a ship for yaw and sway may be reduced into a single rudder to yaw response equation:

$$T_1 T_2 \dddot{\Psi} + (T_1 + T_2)\ddot{\Psi} + \dot{\Psi} = K_s\delta + K_s T_3 \dot{\delta} \qquad (3)$$

where the time constants (T_1, T_2 and T_3) and the yaw gain (K_s) are all derived from initial terms and hydrodynamic derivatives. The above model, valid only for course-keeping, is further simplified by de-coupling the ship surge equation such that surge

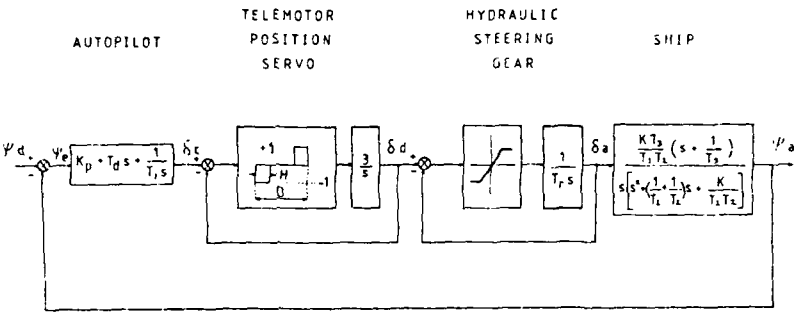

FIG 1 AUTOPILOT / SHIP BLOCK DIAGRAM

velocity is assumed to be constant.

If environmental terms are included, we obtain:

$$T_1 T_2 \dddot{\Psi} + (T_1 + T_2)\ddot{\Psi} + \dot{\Psi} = K_s \delta + K_s T_3 \dot{\delta} + K_y Y_e + K_y T_4 \dot{Y}_e + K_n N_e + K_n T_5 \dot{N}_e \qquad (4)$$

where Y_e and N_e are the sway force and yaw moment loadings due to the environment.

Steering Gear

The following model represents a hydraulic steering gear with control pumps (see Figure 1):

$$\delta_e = \delta_d - \delta_a \qquad (5)$$

A constraint is put on the maximum rudder amplitude:

$$|\delta_e| \leq \delta_{e\,max} \qquad (6)$$

The transfer function model of the steering gear is thus:

$$\frac{\delta_a(s)}{\delta_d(s)} = \frac{1}{T_r(s + 1/T_r)} \qquad (7)$$

where T_r is the rudder time constant, given by:

$$T_r = \delta_{e\,max} / \dot{\delta}_{a\,max} \qquad (8)$$

where $\dot{\delta}_{a\,max}$ is the maximum rate of rudder rotation, dependent on the number of pumps in operation at any time. It is assumed that only one pump is in operation, as might be the case on open seas, hence $\delta_{e\,max} = 6°$, and $T_r = 4\,s$.

Autopilot

In the simulation, a simple PID autopilot has been used, whose transfer function may be written as:

$$\delta_c = K_p \psi_e + T_d \dot{\psi}_e + \frac{1}{T_i} \int_0^t \psi_e \, dt \qquad (10)$$

The three coefficients of proportional gain (K_p) derivative time constant (T_d) and integral time constant (T_i) may be adjusted to vary the autopilots action, and it is their *optimal* settings that are required for any given ship and environmental condition.

The standard form of PID autopilot used on ships has been described by Bech [15], and differs from our simplified version, insofar as there are more parameters which may be varied. A comparison between the two forms is given by Broome *et al* [13], which shows that they are indeed similar.

Telemotor Position Serve

The output of the autopilot is not the direct input to the steering gear. It is subjected to non-linear factors associated with the telemotor position servo. This consists of a combined deadzone (D) and hysteresis (H) associated with the relay switching system, where:

$$H = D/4 \quad \text{and} \quad D = 1°$$

ENVIRONMENTAL DISTURBANCES

A ship is influenced by winds, currents and waves. An analysis of these phenomena has been given by Kallstrom [16] and Zuidweg [17]. In the simulation, the steady-state loadings due to wind and current have been ignored since the heading errors created by these loadings may only be countered by steady rudder deflections, and should not by 'charged' to the rudder when calculating cost function values. Stochastic wind components are also ignored as being secondary to the action of waves.

Wave Loadings Due to a Regular Sea

The sway force (Y_e) and yaw moment (N_e) loadings of Equation (4) are based on a regular sinusoidal wave pattern (Kallstrom [16]). The significant wave heights and wave periods are calculated using empirical equations based on wind speed (Price and Bishop [18]):

$$\begin{aligned} h(V_t) &= 0{\cdot}015\, V_t^2 + 1{\cdot}5 \\ T_w(V_t) &= -0{\cdot}0014\, V_t^3 + 0{\cdot}042\, V_t^2 + 5{\cdot}6 \end{aligned} \qquad (11)$$

The resultant loadings on the ship are then calculated on the basis of a regular sea model (Broome et al, [13]).

AD-A211128 (U) PROCEEDINGS OF THE SIXTH SHIP CONTROL SYSTEMS
UNCLASS. UNLTD. SYMPOSIUM HELD AT OTTAWA. ONTARIO. CANADA 6 OF 6

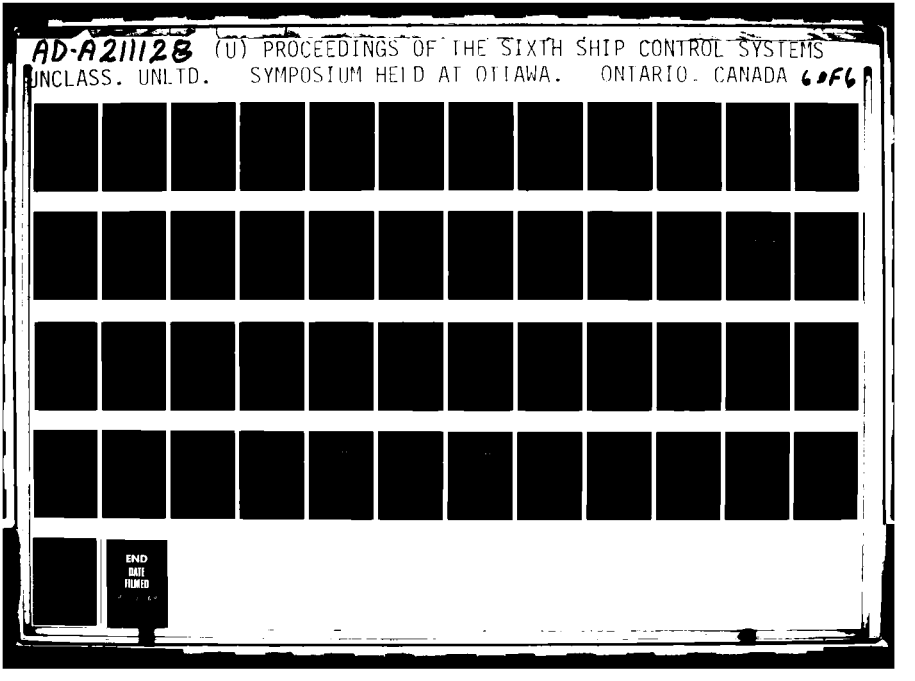

Wave Loadings Due to an Irregular Sea

Although the loadings due to each wave period are calculated on the basis of a regular sea model. It is necessary to adopt a more sopnisticated approach. Such seas do not excite the transient behaviour of the ship, and as such exhibit no variation in cost function, for a given ship and sea-state over a range of autopilot settings.

An irregular sea model can be constructed from the observed, relative frequencies of the world-wide distribution of wave periods with significant wave height (data derived from Price and Bishop). A given sea-state thus consists of a train of waves of constant period but randomly varying significant wave height, within the constraints of observed data. This simplified probabilistic representation of the sea approximate line spectra in the ITTC wave spectrum.

PROGRAM STRUCTURE

All of the programs are written in FORTRAN using RT 11 for use on a DEC PDP 11/40 with VT11 graphics support facilities. The dynamics programs run at approximately four time real time, with an iteration step size of 0.35 seconds, a trade-off between speed and accuracy. The simulation consists of four main elements.

Ship Data Files

A catalog of ship data files has been stored on disc. Each file contains all of the parametric information necessary to define a particular ship. Examples are quoted for two vessels, one of which is open-loop course-stable, the other, unstable in yaw.

Environmental Data Files

A user selectable data base, of environmental files has been stored on disc. Each defines a sea-state at a given incident angle relative to the ship's bow.

Dynamics Program

The dynamics program simulates a ship voyage in a particular sea-state, for a given set of autopilot settings. After a steady-state response has been acheived, the ship yaw and rudder motions are sampled over several cycles of yaw variation, and used to compute a cost function value. One version of the program automatically increments through a full set of autopilot parameters.

Display File Package

Another version of the program stores the time-histories of rudder and yaw activity,which form the data base for a graphics display file. This can be done for a number of ships, sea-states and autopilot settings. The displays may then be readily accessed using interactive light-pen techniques, to facilitate comparisons.

SHIP/ENVIRONMENT CODES

In the following sections, a description is given of simulated voyages of two different ships, in a variety of operational environments. To facilitate recognition, each ship and sea-state may be identified by a three-part code:

First character ; U : An unstable, 15,000 tonne containership.
S : A stable, 15,000 tonne containership.

Second character ; 1 : Sea-state 1 (Beaufort 2)
2 : Sea-state 2 (Beaufort 2-3)
3 : Sea-state 3 (Beaufort 3-4)
4 : Sea-state 4 (Beaufort 4-5)

Third character ; 45, etc: Incident angle of wave propogation relative to the bow.

DISTURBED SHIP RESPONSE

Some illustrative examples of yaw and rudder time-histories are presented for the following cases; unstable ship in quartering sea-state 3 (U:3:135). Figures (2-5) show how these quantities vary for different autopilot parameter settings. Each figure represents 1600 seconds of a ship voyage. During the first 800 seconds a cost function index of course-keeping performance has been calculated, of the form:

$$J = \frac{1}{t^*}\int_0^{t^*} (a_0 \psi_e^2 + a_1 \delta^2)\, dt \qquad (12)$$

where t^* = 800s., and the coefficients are assigned values, a_0 = 0.014 and a_1 = 0.1 as suggested by Norrbin [2]. In each case the integral time constant has been set at T_i = 200s., a moderate value. The final 800s., represents the ship response and settling to a 5 degree course change.

Figure (2) This is the standard case for major comparisons. The autopilot parameters are set at, proportional gain (K_p = 0.5) and derivative time constant (T_d = 50s.). The computed cost function value is (J = 5.8%).

Figure (3) The derivative term has been increased to (T_d = 70s.). There is a relative decrease in yaw activity and an increase in rudder amplitudes. The resultant cost function has risen slightly to (J = 6.7%).

Figure (4) The derivative term has been reduced to (T_d = 30s.). There is a relative decrease in rudder amplitude, and a remarkable increase in yaw. The cost function value has risen to (J = 17.8%). It will later be seen that for these controller settings the ship is operating very close to a stability boundary.

Figure (5) Instead of varying the derivative term, the proportional gain has been raised to (K_p = 1). There is an increase in rudder amplitude and a decrease in yaw, The cost function value of (J = 5.9%) shows that a small increase in the autopilot gain has very little effect compared with the near optimum standard setting.

For a more detailed description of yaw and rudder time-histories, including the effects of ship type, sea-state and direction of wave propogation, see Broome et al [13] and Marshall [19].

COST FUNCTION VARIATION WITH ENVIRONMENT

The stimulation has been used to automatically compute cost function values over a range of both proportional and derivative gains ($0 < K_p < 4$; $10 < T_d < 70$) such that cost function maps may be constructed in the parametric plane K_p vs T_d where contours of constant cost are drawn.

Incident Angle of Wave Propogation

Figures 6-8 illustrate the distribution of cost function for the unstable ship in sea-state 3, with different incident angles of wave propogation. Examples are given for bow seas (45°) through to quartering seas (135°).

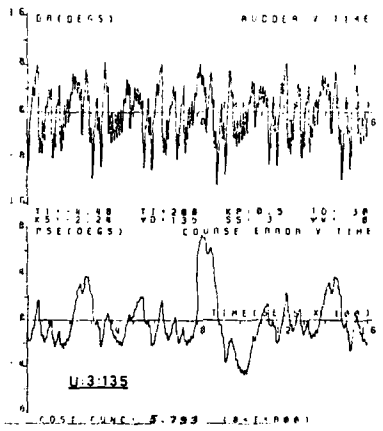

FIG 2

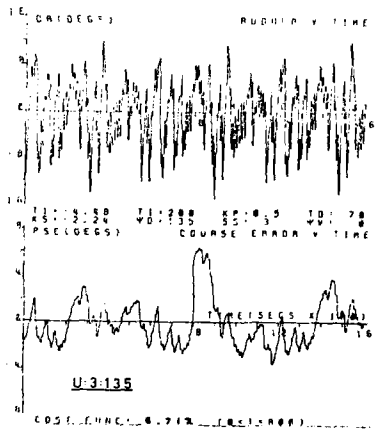

FIG 3

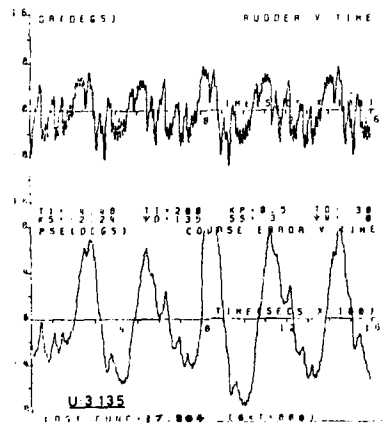

FIG 4

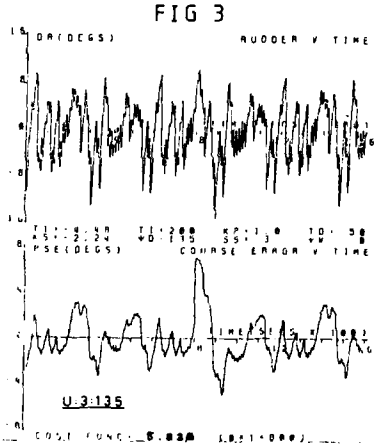

FIG 5

FIGS 2-5 RUDDER & YAW TIME HISTORIES

It can be seen that in the range 45° to 75° (Figures 6 to 8), the absolute minimum cost rises and then falls again with increasing angle. Associated with this is relative contraction and then expansion of the contours indicating that when the ship is sailing into the waves, an incident angle of 60° is worse than either 45° or 75°. It is not possible to track the locus of optimisation accurately on these maps, but inspection reveals that the autopilot parameters which define approximate optimality differ in each case.

When the seas are coming from astern (105° to 135°) the overall picture changes remarkably (Figures 9 to 11). At 105° the minimum cost rise to some 9.5% and the map begins to contract. At 120° the minimum rises to 15% and there is a further contraction of the map. For, quartering seas (135°) there is a reduction in minimum cost to some 5.5%, and a relative expansion of the map. However, the maps clearly show that it is beneficial to sail into the waves rather than to have them 'follow' the ship. This is to be expected, since in the latter case the encounter frequency between the ship and the waves is reduced, and is much nearer to the natural frequency of the ship, which creates a closed-loop resonance effect.

It will be recalled when discussing the time domain responses, for parameter settings of $K_p = 0.5$ and $T_d = 30$, the ship is indeed very close to stability boundary.

Ship Type and Sea-State

Further comparisons are made for the stable ship and different sea-states (Figures 12 and 13). The major findings are that the absolute minimum and the distribution of cost are less severe for the stable ship (Figure 12). In milder environments (sea-state 2) the absolute minimum falls very low, and the map expands to to such an extent that is difficult to define an optimal set of autopilot parameters (Figure 13).

SENSITIVITY TO SYSTEM NON-LINEARITIES

The considerable time required to produce a cost function map would be reduced if maps could be generated by a linear analysis, that is, the system could be considered as being sensibly linear. This section is concerned with comparing the effects of changing the values of various system non-linearities on the cost function contours. To avoid computing the whole cost function maps, two 'section' through the minimum point are taken as the basis for comparison as shown in Figure 14. Along one section T_d is held constant at its optimum value, and on the other K_p is constant.

Standard Cases and Variations

There are two standard cases; the course stable ship in quartering sea-state 3 (S:3:135), and the unstable ship in similar seas (U:3:135). Each run involves a change in just one of the variables from its value in one of the standard cases, given in Appendix 1.

A list of the parameter changes investigated is given in Appendix 2. The sections have been taken at the same values of T_d and K_p throughout each set of runs. As parameters change, the whole map will change, and it is likely that the two sections will not cross at the minimum value on the map. Hence, true minima are not being compared. General trends will be illustrated, and numerical values for increases and decreases only serve to show which changes are significant.

Summary of Main Results

For the unstable ship, varying the deadbandwidth (D), or the hysterysis (H) has no significant effects on cost functions (J). Similarly, assuming a linear gyro has very little effect. Varying maximum rudder rate has more effect as shown in

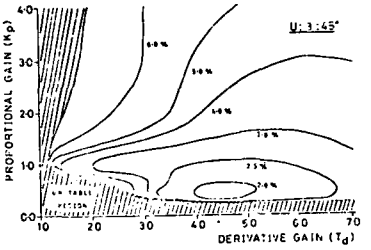

FIG 6

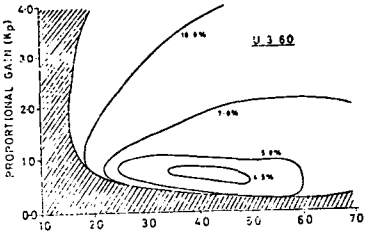

FIG 7

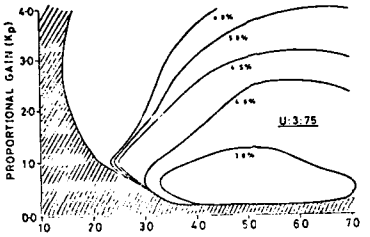

FIG 8

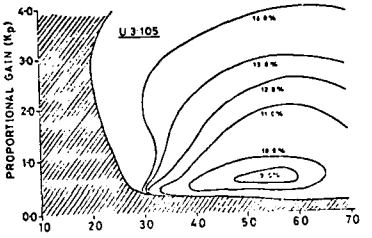

FIG 9

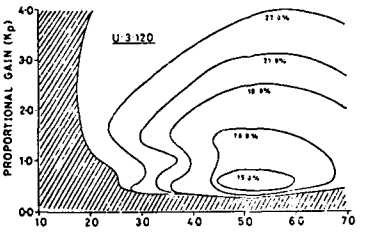

FIG 10

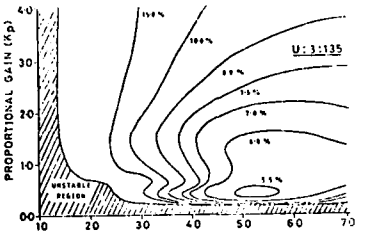

FIG 11

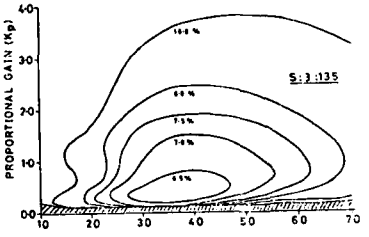

FIG 12

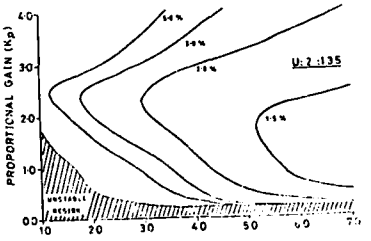

FIG 13

FIGS 6-13 COST FUNCTION MAPS

Figure 15, where the rates of 2.5°/s are superimposed on the standard 2°/s curves. A rate of 2°/s is the least maximum rate permitted by the classification societies when only one (of the two) pumps is in operation. As would be expected, the value of J decreases with increasing rudder rate.

For the maximum rate of 4°/s the minima occur at (K_p, T_d) = (0.4, 60) and (0.2, 53). The true minimum probably moves towards increasing T_d and decreasing K_p, and at (0.4, 60), J_{min} is reduced from 5.7% to 5%.

Figure 16 shows how values of J_{min} and its components vary with maximum rudder rate. There is a large change between 2°/s and 2.5/s, but much smaller changes thereafter. As might be expected, no variations in maximum permitted rudder angle for either ship makes any difference, as rudder angles remain within a maximum of about 10 degrees during any of the test conditions.

Similar results are found for the stable ship. Variations in maximum rudder rate again produces significant changes in J, as shown in Figure 17. Although the minimum rate allowed is 2°/s, a test of 1°/s shows that the deterioration due to halving the rate is much greater than the improvement due to doubling it.

It may be concluded then that the only non-linearity which will significantly affect the tuning of an autopilot for optimum course-keeping, is the rudder rate limit imposed by the hydraulic steering gear saturation flow rates.

DISCUSSION AND CONCLUSIONS

The cost function maps demonstrate clearly the necessity of re-tuning a PID autopilot if optimal course-keeping is to be achieved by ships throughout long ocean voyages. They also indicate the level of penalties which will be incurred if autopilot parameters are set away from the optimum. The required re-tuning could be done automatically using adaptive autopilots of the model reference kind, or manually, provided an on-line cost function indication could be provided, perhaps as an additional bridge instrument.

Differences of detail have been demonstrated between ships of varying open-loop stability, steering gear etc., but the main cause of large variations in the optimum cost function is the direction of the environmental disturbance. The re-tuning can be done at moderate intervals if the ship is maintained on the same course, and so has a constant incidence of prevailing seas, but the autopilot will need to be re-tuned immediately the ship's course is altered. The analysis of system non-linearities shows that the only significant non-linearity is the value of the rudder rate limit. That is,no measurable benefit will accrue by more refined engineering design of the autopilot to steering gear transmission link, as normal degrees of deadzone and hysterysis have not effect on cost function values. Similarly, the gyrocompass descretisation and maximum rudder angle non-linearities may be ignored.

The qualitative value of cost functions depend entirely on the equations of the environmental modelling, which is the main weakness in this simulation. Clarke [20] however, using a PRBS disturbance generator has demonstrated similar results. A second weakness is the assumption of horizontal plane motion only, where no account is taken of the not inconsiderable interaction between yaw, sway and roll dynamics.

In the next section, we consider how optimisation might be achieved by manual setting of the autopilot parameters.

ADAPTIVE MANUAL CONTROL

So far, we have confined our attention to mapping the variation of cost function with environmental status and ship type. Moreover, consideration has only been given

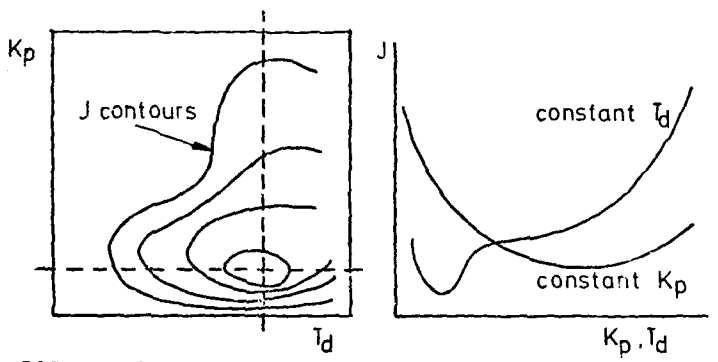

FIG 14 NON-LINEAR COMPARISONS

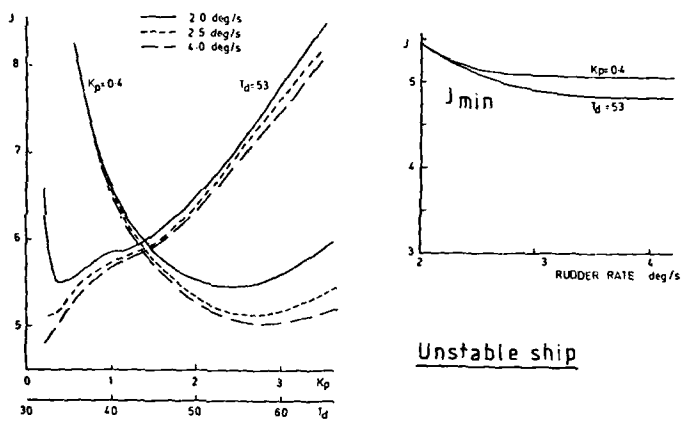

Unstable ship

FIGS 15 & 16 VARIATION IN MAX RUDDER VELOCITY

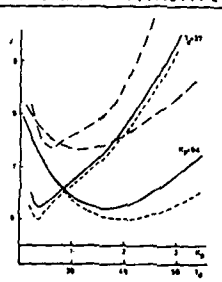

FIG 17 Stable ship

to conventional PID autopilot systems. It still remains for us to ascertain how optimal tuning parameters can be implemented for a given ship/environment scenario. It becomes necessary to focus our attention on the role of the human operator in relation to the achievment of this goal.

The Tuning Problem

Cost function (J) is a weighted function of yaw and rudder activity. For a given ship/environment scenario the value of J should be quasi-static, allowing for the stochastic processes of the sea. If the ship alters course, or the incident wave angle changes a different topological representation of cost function variation will become valid, and it will become necessary to re-tune the autopilot.

It would be a simple matter to provide the ship's officer with a discrete cost function value for a given set of autopilot tunings. Relative course-keeping performance can be determined from the cost function map. However, the geometry of the map would not be available to the operator, and under these circumstances he would have no means of assessing the appropriateness of his tuning strategy.

In terms of information processing, this is a two-variable optimisation task in which the inputs (autopilot parameters; K_p, T_d) and the output (computed cost function; J) are in discrete form. The minimisation of J is a 'hill-climbing' exercise. There is a dearth of knowledge pertaining to human performance in such tasks, despite its common occurence in many areas of process control. It has commonly been assumed that people are very bad at solving multi-variable optimisation problems. However. Laughery and Drury [12] have recently found that the strategy adopted by subjects in two-variable optimisation tasks is very similar to a well tuned computer algorithm. Furthermore, when faced with a 'noisy' data base, human performance can be more 'efficient' than that of a computer.

It would be interesting to apply these techniques to the problem of selecting optimal autopilot parameter settings. A laboratory experiment has been conducted to address the following questions.

(1) When attempting to select optimal autopilot parameter settings, the operator has no knowledge of the absolute minimum cost which might be achieved. To what extent does this affect performance compared to the case where he is given an absolute minimum cost value to aim for?

(2) Hill-climbing algorithms commonly make use of the partial derivatives ($\partial Z/\partial X$ and $\partial Z/\partial Y$ for the tuning problem) in the formulation of a steepest gradient or PARTAN search (Wilde [21]). The evaluation of any given J will incur a 'computational cost'. Would the human operator be able to make use of the qualitative derivatives in the solution of the problem (by qualitative we mean the direction of slope and not its precise value!)

THE PARTIAL DERIVATIVE AS AN AID IN PURSUIT AND COMPENSATORY MULTIVARIABLE OPTIMISATION TASKS

The Task

An analytical cost function space was created to form the basis of a computer controlled experiment, which had the following properties:

(a) Independent variables: $0 < X < 100$
$0 < Y < 100$

(b) Dependent variable $Z = f(X,Y)$

The geometry of the space is illustrated is Figure 18. The independent variables, X and Y correspond to autopilot parameters K_p and T_d arbitarily scaled to avoid Euclidean paradoxes. The function $Z = f(X,Y)$ is seen to be a set of concentric ellipsoids (the dependent variable Z corresponding to our cost variable, J). The distribution of Z above the X-Y plane was determined by a linear relationship along the major axis of the ellipse.

The orientation and eccentricity of the ellipsoidal structure were experimenter controlled, but maintained at α = 30 degrees and E = 0.8 throughout the experiment to avoid biases due to symmetry and to allow valid comparisons between conditions.

The subjects' task was to interrogate the space discretely by entering values of X and Y from a computer terminal, accurate to the nearest integer. In response to each interrogation of the stored program, the computer returned a value of the dependent variable Z. Interrogations were conducted sequentially until the minimum value of Z was obtained, at which point the experiment terminated. All subjects took part in each of four different conditions:

(1) Pursuit/Non-derivative (P): The subject was told the minimum value of Z that he was required to seek. Hence he was able to assess performance for each interrogation relative to this information. As well as discrete numerical responses, subjects were provided with a computer graphics illustration of each interrogation (see Figure 19).

(2) Compensatory/Non-derivative (C): Similar to above, except that the subject was NOT told the minimum value of Z which he was seeking. Hence, the subject had to decide for himself when he had successfully solved the problem.

(3) Pursuit/Derivative (PD): Similar to (1) except the subject was provided with qualitative information with respect to the partial derivatives, about the interrogation point. This information was displayed in the form of a flashing line pointing away from the quadrant in which the optimum could not lie (by definition in the case of a unimodal space). See Figure 19.

(4) Compensatory/Derivative (CD): Similar to (3) except the subject was not told the absolute minimum value of Z that he was seeking.

The terms pursuit and compensatory are used here to distinguish between the situation where the subject is provided with an index of performance error (pursuit) and when no such information is provided (compensatory). This is roughly analogous to the distinction adopted in manual control, and has been adopted here for convenience.

Experimental Design

Eight paid postgraduate students took part in this experiment, which took the form of a within subject repeated measures factorial design. Two subjects were assigned to each of the four conditions of a counterbalanced Latin-square. Since the subjects were acting as their own controls, it was necessary to counterbalance treatment effects and to bring each subject up to a suitable level of performance by plenty of practice on the task.

Procedure

The experiment was carefully explained to each subject for each condition, and he was then allowed plenty of practice to familarise him with the use of the computer, and the nature of the task. The experiment was performed on a DEC PDP 11/40 mini-computer with VT11 support graphics. As each experiment was controlled by the

computer, it was only necessary to record four different variables for the purposes of subsequent analyses, X,Y, Z and T the inter-interrogation time, as measured by the real time c'ock in response to keyboard commands. Each subject was told that good performance would be considered to be a trade-off between the number of interrogations, and the total time to arrive at the solution.

ANALYSIS

Optimality in solving the problem is a complex function of the operator's choice of inputs. Consequently, there is no unique measure that will reflect either adopted strategy or performance. Four measures were formulated to assess performance on the task. The rationale for their choice is described below.

(1) Number of Interrogations (N): If providing subjects with an optimisation aid, such as the partial derivative, is indeed beneficial, this should be reflected in a reduction of interrogations for this conditon.

(2) Total Solution Time (T) : Task difficulty should be reflected by the total time required to obtain a solution. Hence, for the aided condition, the task should be solved more quickly.

(3) Mean Interrogation Interval ($\bar{T}$) : This measure, defined as:

$$\bar{T} = T/N \tag{12}$$

takes account of cognitive processing effort. For example, solution aids may result in a more economical performance (smaller N and /or T) but they may require the subject to think more about his interrogation strategy. This measure provides some information with respect to input strategy.

(4) Interrogation-Time Product (NT) : The two measures, N and T are not sufficient to define optimal performance. A subject may take a long time to solve the task (large T) but interrogate the space economically (small N). Conversly, he may solve the task quickly (small T) but interrogate the space liberally (large N). This trade-off can be described by the relationship:

$$NT = N.T \tag{13}$$

This penalises not only processing time, but also the number of times the space is interrogated. The latter becomes important when there is a large 'computation cost' associated with each interrogation.

An analysis of variance (ANOVA) was performed on the above performance measures, the results of which are described below.

RESULTS

Figures 20 to 23 show the distribution of sample means in each of the four conditions, for all of the performance measures described above.

It is clear that pursuit optimisation is not superior to compensatory optimisation in any of the performance measures adopted.

Providing the operator with the partial derivative as an optimisation aid does appear to significantly improve performance.

(1) The number of interrogations (N) is less when the partial derivative is provided ($F_{1,7} = 28.74$; $p < 0.01$).

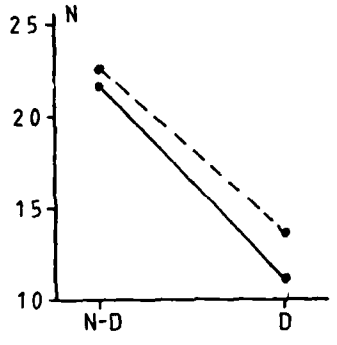

Fig 20 No of Interrogations

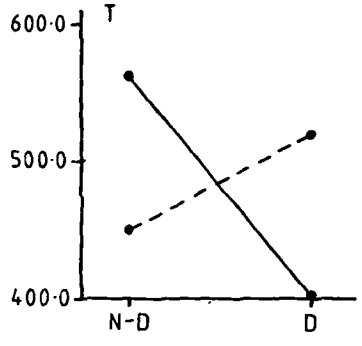

Fig 21 Total Time

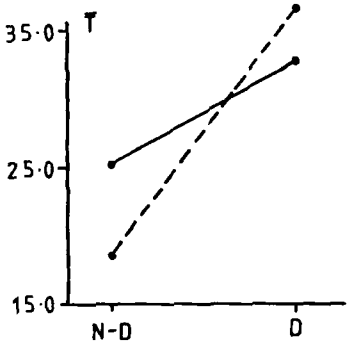

Fig 22 Mean Interrogation Time

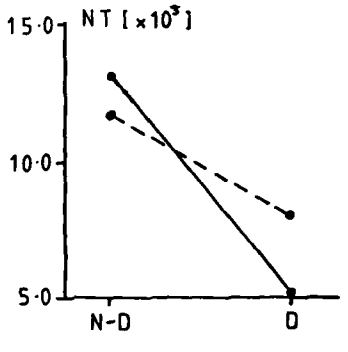

Fig 23 Interrogation-Time Product

KEY

Non-Derivative = N-D

Derivative = D

Pursuit = - - - - - - -

Compensatory = ———

FIGS 20-23 ANOVA MEANS

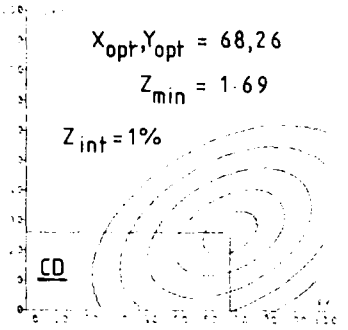

FIG 18

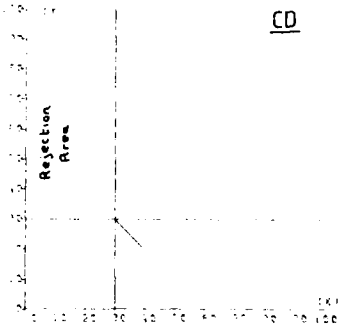

FIG 19

(2) There is no significant difference between derivative and non-derivative performance with respect to problem solving time (T). However there is a significant interraction between these conditions and the pursuit/compensatory mode. When the derivative is not provided subjects perform the pursuit task faster. When the derivative is provided, subjects solve the compensatory task faster ($F_{1,7} = 7.47$; $p < 0.05$).

(3) The mean interrogation time ($\bar{T}$) is longer when the subject is provided with the partial derivative ($F_{1,7} = 27.3$; $p < 0.01$).

(4) The interrogation-time product (NT), which weights strategy economy is less when the partial derivative is provided ($F_{1,7} = 9i$; $p < 0.05$).

DISCUSSION

It is clear that in a two-variable optimisation task of this sort, there is no advantage to be gained by providing the human operator with an a priori criterion of performance (optimum performance target). Presumably, if the input and output resolutions were more sensitive, then pursuit performance would be superior, as compensatory performance would at some stage of the process enter a final stage of diminishing returns. In the case of tuning an autopilot, resolution is determined by the sensitivity of the control potentiometers, and should not be so critical. However, the concept of diminishing returns with problem solving effort is very important. Any computed cost function value will have associated with it an error function (due to sampling and stochastic processes), and so it is only feasible to locate an optimal region of the map instead of an absolute point. Nevertheless, the finding that pursuit performance is not superior to compensatory is very encouraging since achieving optimal performance from an autopilot is a compensatory process.

Providing subjects with extra information with respect to space geometry clearly leads to an enhancement in performance. The qualitative partial derivative was chosen because it can be computed with a small amount of extra 'computational cost'. The beneficial effects of the partial derivative can be considered in terms of information reduction. It enables subjects to plan their strategies more economically because it eliminates areas of uncertainty within the space.

It is not possible to give a full analysis of human performance here, but the results clearly show that the human operator can indeed solve two-variable optimisation tasks economically when provided with simple problem solving aids.

Work is presently being carried out to determine what limits might be set on the input resolution of the autopilot in relation to the optimisation of the course-keeping problem.

REFERENCES

(1) N. Minorsky, "Directional Stability of Automatically Steered Bodies", J.A. Soc. Naval Engs., 34, 280, 1922.

(2) N.H. Norrbin, "On the Added Resistance due to Steering on a Straight Course", 13th ITTC Berlin/Hamburg, 1972.

(3) T. Koyama, "On the Optimum Automatic Steering System of Ships at Sea", J. Soc Nav. Archit. Japan, Vol. 122, 1967, p. 142.

(4) J. van Amerongen and H.R. van Nauta Lemke, "Criteria for Optimum Steering of Ships", Symp. on Ship Steering Automatic Control, Genova, Italy, June 25th, 1980.

(5) D. Clarke, Personal Communication, 7 III 1978.

(6) C.G. Kallstrom and N.H. Norribin, "Performance Criteria for Ship Autopilots: an Analysis of Shipboard Experiments". Symp. on Ship Steering Automatic Contol, Genoa, Italy, June 25th-27th, 1980.

(7) D. Clarke, "Consideration of Ship Handling in Hull Design", Proc. of the Nautical Institute Conference on Ship Handling, Plymouth Polytechnic, England, UK, Nov 24-25th, 1977.

(8) A. Tiano, "Identification and Control of the Ship Steering Process". Proc. 2nd IFAC/IFIP Symp. on Ship Operation Automation, Washington, USA 1976.

(9) K.J. Astrom and C.G. Kallstrom, "Application of System Identification Techniques to the Determination of Ship Dynamics", IFAC Symp. on Identification and Syst. Param Estimation, Delft, Holland, 1973.

(10) D.R. Broome and T.H. Lambert, "An Optimistic Function for Adaptive ships' Autopilots", 5th. Ship Control Systems Symp., Vol 3, paper J2 1-1, Annapolis, Maryland, USA, 1978.

(11) J. van Amerongen, W.F. Goeji, J.M. Moraal, J.W. Ort and A. Postuma, "Measuring the Steering Performance of Ships During Full Scale Trials and Model Tests", Symp on Ship Steering Automatic Control, Genova, Italy, June 25th-27th, 1980.

(12) K.R. Laughery, Jr. and C.G. Drury, "Human Performance and Strategy in a Two-Variable Optimisation Task", Ergonomics, Vol 22, No.12, 1979, pp 1325-1336.

(13) D.R. Broome, A.J. Keane and L. Marshall, "The Effect of Variations in Ship Operating Conditions on an Adaptive Autopilot Optimising Function", Symp., on Ship Steering Automatic Control, Genova, Italy, June 25th-27th, 1980.

(14) K. Nomoto "Simulators from the Naval Architects Point of View", Proc. of MARSIM, College of Nautical Studies, Southhampton, UK, Sept 5th-8th, 1978.

(15) M.I. Bech, "Some Guidelines to the Optimum Adjustment of Autopilots in Ships", Delft Symp. Dec. 1970.

(16) C.G Kallstrom "Identification and Adaptive Control Applied to Ship Steering", Coden: LTFD2/(TFRT-1081)-192(1979), Dept., of Automatic Control, Lund Inst. of Tech., Sweden, May 1979.

(17) J.K. Zuidweg. "Automatic Guidance of Ships as a Conrol Problem", Thesis, Technische Hogeschool, Delft, Holland, 1970.

(18) W.G. Price and R.E.D. Bishop, "Probabilistic Theory of Ship Dynamics", Chapman and Hall, 1974.

(19) L. Marshall, "A Manually Tuned Autopilot for Optimal Course Keeping in Ships", Ph.D thesis, University of London, in preparation, 1981.

(20) D. Clarke, "Development of a Cost Function for Autopilot Optimisation", Symp on Ship Steering Automatic Control, Genova, Italy, June 25th-27th, 1980.

(21) D.J. Wilde, "Optimum Seeking Methods", Prentice-Hall Inc., Englewood Cliffs N.J., USA, 1964.

APPENDIX 1

PARAMETER VALUES FOR STANDARD RUNS

Telemotor deadband width	D = 1.0°
Telemotor hysteresis	H = ±0.5°
Gyrocompass output	6 steps/degree
Maximum Rudder Angle	= 35°
Maximum Rudder Rate	= 2°/s
Rudder Time Constant	T_r = 4.0s
Length/Speed Ratio	L/U= 25

APPENDIX 2

PARAMETER VARIATIONS

Unstable Ship

Run No.

1) Standard
2) Telemotor deadband width = 0. D =0° = H
3) Low hysteresis telemotor D =1.0°, H = 0.25°
4) High hysteresis telemotor D = 1.0°, H = 0.75°
5) Large deadband width D = 2.0°, H = 1.0°
6) Linear gyrocompass output
7) Gyrocompass output; 12 steps per degree
8) Maximum rudder rate = 2.5°/s
9) " " " = 3.0°/s
10) " " " = 4.0°/s

11) Maximum rudder angle = 45°
12) " " " = 45°; Maximum rudder rate = 4°/s
13) Rudder time constant (T_r) = 1.0

" " " " = 2.0

15) " " " " = 8.0

Stable Ship

16) Standard

17) Telemotor deadband width = 0, D = 0° = H

18) Large deadband, high hysterics. D = 1.5°, H = 1.5°

19) Linear gyrocompass output

20) Gyrocompass output; 2 steps/degree

21) Maximum rudder angle = 10°

22) " " " = 20°

23) Maximum rudder rate = 1°/s

24) " " " = 3°/s

25) " " " = 4°/s

26) Rudder time constant (T_r) = 1.0

27) " " " = 2.0

28) " " " = 8.0

IDENTIFICATION AND SELF-TUNING CONTROL OF LINEAR AND NON-LINEAR SHIP MODELS

by Lt Cdr N MORT Royal Navy
Royal Naval Engineering College, UK
and D A LINKENS
University of Sheffield, UK

ABSTRACT

The generalised least squares method of parameter estimation is applied to the rudder/yaw rate dynamics of a frigate using data recorded from full-scale sea trials with PRBS rudder excitation. Rudder step response tests are also analysed using manual scale measurement techniques to determine the parameters of a simple first order linear transfer function model of the dynamics. Changes in the model parameters with ship's speed and rudder demand angle are investigated and the evidence produced indicates considerable variation in these parameters over the normal operating conditions of the ship.

The application of the self-tuning controller (STC) algorithm to the design of course- and track-keeping controllers for surface ships is also considered using digital simulation techniques. In particular, the performance of the algorithm is examined when the ship dynamics are described by the linear and non-linear models derived earlier from frigate sea trials. It is shown that the STC can be used as a digital control algorithm using limited word length ADC and DAC number representation.

1. INTRODUCTION

The dynamic behaviour of a ship at sea can be described in mathematical terms in two equivalent ways. The first approach, usually adopted by naval architects, involves equations of motion containing hydrodynamic derivatives which are derived from a Taylor series expansion of the force/moment balance equations. Engineers engaged in studies relating to the steering qualities of ships (eg autopilot design) favour an alternative input/output description often based on the transfer function between rudder angle (input) and yaw angle (output).

The parameters of these models may be determined experimentally by scale-model tests and/or full-scale sea trials. The former usually incorporates sophisticated tank and measuring facilities enabling a large number of variables to be measured. There are, however, inherent scaling problems with such a technique and full-scale trials at sea are advisable when economic considerations and ship availability are favourable.

This paper describes the application of one particular method of system identification, namely generalised least squares (1), to the determination of the linear steering dynamics of a frigate using data obtained from full-scale sea trials. Several different approaches to this parameter estimation problem have been reported in recent years. The maximum likelihood method has been used to determine

both linear (2), (3), (4), (5), (6) and non-linear (7) ship steering models. Parameters of non-linear models have also been estimated using equation error and output error methods (8), (9), (10).

The data on which the results discussed in this paper are based were recorded on board a Royal Navy frigate on passage from Plymouth to Gibraltar. The experiments consisted of applying Pseudo Random Binary Sequences (PRBS) and step change perturbations to the rudder and recording variables such as yaw rate, roll angle, log, etc. A mathematical model initially having a known structure but unknown parameters was then fitted to the PRBS experimental data using generalised least squares (GLS). The step response data were studied to identify any parameter variation/non-linear effects in a rudder angle/yaw rate model of first order when demanded rudder angle and ship's speed were varied.

The determination of the parameters of the steering dynamics of a ship can be considered to be the first step in the design of feedback controllers for course- and track-keeping. Ship steering control systems have undergone many refinements since the first designs appeared some 60 years ago (11). However, progress in the design of ship autopilots has not been as rapid as the advances in modern control theory. Conventional autopilots currently in use in many different types of ships fail to take account of variations in the ship's dynamic behaviour, due to speed, loading conditions and environmental factors such as wind, waves, water depth etc. There has thus been a growing interest in autopilots that are adaptive in nature in order to overcome these known variations. For example, both model reference techniques (12) and optimal linear quadratic controllers (13) have been examined in the context of autopilot design. More recently, the concept of "self-tuning control" (14), (15), has been investigated by a number of authors (16), (17), (18). In this paper, we use digital simulation methods to assess the performance of the self-tuning controller algorithm when the ship dynamics are described by models derived from the frigate sea trials discussed earlier.

2. GENERALISED LEAST SQUARES (GLS) IDENTIFICATION

In common with all time domain methods of system identification, the GLS approach requires a digital computer to process the input/output data records. For this particular study, use was made of an identification package, SPAID (19), developed at the Department of Control Engineering, University of Sheffield. The programs comprising the package are interactive via a graphic display terminal with user intervention to control the identification procedure. In order to make the results more meaningful, a brief summary of the GLS method is given below.

A discrete time stochastic system may be mathematically modelled by the equation:

$$y_t = z^{-k} \frac{B(z^{-1})}{A(z^{-1})} u_t + \frac{D(z^{-1})}{C(z^{-1})} \xi_t \qquad (2.1)$$

where y_t is the system output at time t

u_t is the system input at time t

ξ_t is an uncorrelated (ie white noise) sequence

z^{-1} is the backward shift operator

k is the system time delay

and A, B, C, D are polynomials of the form:

$A(z^{-1}) = 1 + a_1 z^{-1} + \ldots + a_n z^{-n}$ $\quad B(z^{-1}) = b_1 z^{-1} + b_2 z^{-2} + \ldots + b_n z^{-n}$

$C(z^{-1}) = 1 + c_1 z^{-1} + \ldots + c_n z^{-n}$ $\quad D(z^{-1}) = 1 + d_1 z^{-1} + \ldots + d_n z^{-n}$

Equation (2.1) is more conveniently written as the difference equation

$$Ay_t = z^{-k} Bu_t + \frac{AD}{C} \xi_t \qquad (2.2)$$

The least squares estimates of the process parameters (a_i, b_i) will be biased unless $ADC^{-1} = 1$, (20), and the GLS method attempts to transform the data such that the error term $e_t = ADC^{-1}\xi_t$ is reduced to an uncorrelated sequence ξ_t. The algorithm consists of the following steps:

1. Make an ordinary least squares fit to the data for the unknown parameters (a_i, b_i) in the model:

$$Ay_t = z^{-k} Bu_t + ADC^{-1} \xi_t \qquad (2.3)$$

2. Analyse the residuals

$$e_t = \hat{A}y_t - z^{-k} \hat{B}u_t \qquad (2.4)$$

(Note: The ^ symbol denotes estimated value),

and fit an autoregression

$$\hat{F}e_t = \xi_t \qquad (2.5)$$

where $\hat{F}$ approximates (ADC^{-1}).

3. Filter the process input and output with the autoregression $\hat{F}$ to produce two new sequences

$$\left.\begin{aligned} y_t^F &= \hat{F}y_t \\ u_t^F &= \hat{F}u_t \end{aligned}\right\} \qquad (2.6)$$

4. Make a new least squares fit using the filtered inputs and outputs of (2.6) and repeat the procedure from Step 2. Thus, by obtaining a least squares estimate of the process model to start the

procedure and then iterating between estimates of the noise and process parameters, unbiased estimates can be obtained from noise-corrupted data. The model which results is of the form:

$$\hat{A}(\hat{F}y_t) = z^{-k}\,\hat{B}(\hat{F}u_t) + \xi_t \qquad (2.7)$$

3. SHIP MODELS FROM PRBS TRIALS

3.1 Preliminary Data Manipulation

The recorded variables that were considered to be of most interest in this study were

(1) Demanded rudder angle ($\delta_d{}^o$),

(2) Actual rudder angle ($\delta_a{}^o$),

(3) Yaw rate ($\dot{\psi}^o/s$).

Before any SPAID analysis was carried out, the raw analogue data was successively:

(a) Amplified to increase the voltage levels.

(b) Low-pass filtered at a cut-off frequency of 0.75 Hz to remove high frequency noise.

(c) Sampled at a frequency of 5 Hz. This frequency wss chosen after consideration of the 1 second clock period of the PRBS input signal.

The PRBS trials were repeated at four different speeds of the ship and the duration of each trial was $\sim$ 20 - 30 mins. This, together with the relatively short sample period of 0.2 sec ensured a large number of data records. The graphics routines within SPAID limited the number of points to 1024 so the trials data was segmented into blocks of 1000/1024 points and one segment of data was analysed at a time.

3.2 Estimation of Parameters of Difference Equation Model

The data to be analysed first were recorded during the PRBS trial at 16 kts, for which the demanded rudder angle was set to $\pm 8^o$. Assuming that the system order is unknown, an 'a priori' model order test can be invoked within the SPAID package to give some indication of both model order and time delay. Exploratory work showed that a 3rd order model was appropriate when the input/output variables were actual rudder angle and yaw rate respectively. The parameter estimates obtained for the ARMA process model and the 10th order autoregressive noise model are given below:

Process Model Parameters	Noise Model Parameters	
$\hat{a}_1 = -1.154 \pm 0.029$	$\hat{f}_1 = -0.27$	$\hat{f}_6 = 0.108$
$\hat{a}_2 = -0.296 \pm 0.047$	$\hat{f}_2 = 0.459$	$\hat{f}_7 = -0.307$
$\hat{a}_3 = 0.459 \pm 0.029$	$\hat{f}_3 = -0.073$	$\hat{f}_8 = 0.126$
$\hat{b}_1 = -0.209 \pm 0.019$	$\hat{f}_4 = 0.164$	$\hat{f}_9 = -0.127$
$\hat{b}_2 = 0.320 \pm 0.036$	$\hat{f}_5 = -0.196$	$\hat{f}_{10} = 0.211$
$\hat{b}_3 = -0.124 \pm 0.019$	$\sigma = \pm 0.03$ for all $\hat{f}_i$	

Poles	Zeros
0.972	$0.765 \pm j0.102$
0.784	
-0.602	System Gain = -1.412

The success, or otherwise, of the estimation can be displayed graphically as shown in Fig 3.1.

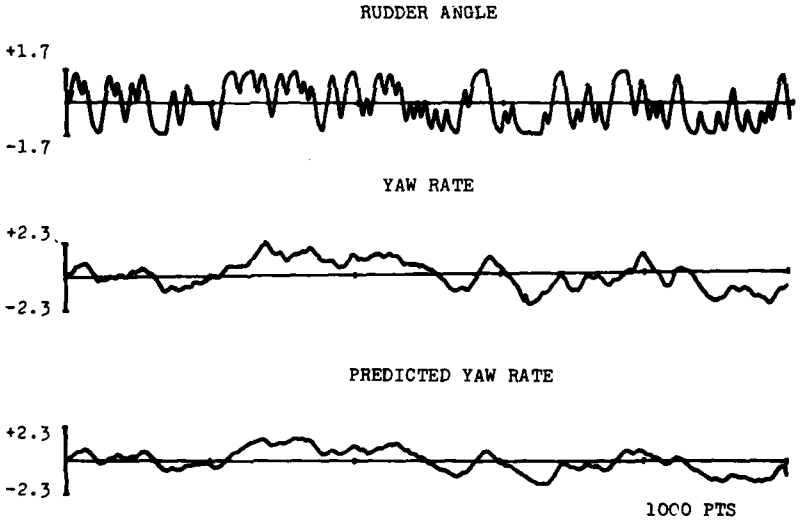

Fig 3.1 GLS Estimation Results with Third Order Model

It is reasonable to infer from these results that the process parameters have been satisfactorily estimated. The poles and zeros of the estimated pulse transfer function are given above. It is a well-known result from sampled-data theory (21) that the z-transform $z = e^{sT}$ uniquely maps the poles of the continuous transfer function $G(s)$ to corresponding poles of the pulse transfer function $G(z)$. This result does not apply to the zeros of $G(s)$ and $G(z)$. Thus the main features of the continuous time model can be deduced from an examination of the pole positions in the estimated process model. Taking each of the process model poles in turn:

(1) $\alpha_1 = 0.972 \equiv T_1 = 7.04$ sec

(2) $\alpha_2 = 0.784 \equiv T_2 = 0.82$ sec

(3) $\alpha_3 = -0.602$

The presence of a single pole on the negative real axis of the z-plane does not correspond to any single pole position in the s-plane. Åström et al (3) observed this effect in their identification work on merchant ships and attributed the position of this pole to round-off noise due to quantisation error from the ADC. This explanation can be applied in this case also since an 8-bit device was used as the ADC.

The differences in magnitude between the remaining equivalent time constant values suggest an effective step response close to that of a first order lag having a time constant of approximately 7 sec. The system gain was evaluated as -1.412 but it must be remembered that this refers to the sampled signals. When the appropriate calibration values for rudder angle (deg/volt) and yaw rate (deg/sec/volt) are included, the system gain is given by $K = -0.122$ sec^{-1}.

3.3 Effect of Ship's Speed on Estimated Parameters

During the sea trials, the tests were conducted at four different speeds viz 7, 12, 16 and 23 kts. Thus the procedures described in (3.2) can be repeated for the different speeds with a view to assessing in quantitative terms any changes in the ship dynamics with speed. The parameters obtained for 1000 data points from each test are shown in Table 3.1. The 16 kt data is repeated for comparison purposes.

Speed	a_1	a_2	a_3	b_1	b_2	b_3
7	-0.681	-0.562	0.264	-0.082	-0.013	0.037
12	-0.845	-0.742	0.646	-0.162	0.246	-0.091
16	-1.154	-0.296	0.459	-0.209	0.320	-0.124
23	-0.713	-0.016	-0.236	-0.279	0.126	0.070

Table 3.1 Variation of 3rd order model coefficients with ship's speed

The variation in the poles and zeros of the model over the same speed range is given in Table 3.2.

Speed (Kt)	Poles			Zeros	
	1	2	3	1	2
7	0.988	0.390	-0.689	0.754	-0.590
12	.856+j.105	.856-j.105	-0.868	0.641	0.877
16	0.972	0.784	-0.602	.765+j.102	.765-j.102
23	0.976	-.132+j.474	-.132-j.474	0.776	-0.325

Table 3.2 Variation of poles and zeros with ship's speed

The results relating to the various models obtained at different ship speeds are potentially the most interesting given that PRBS signals of the same amplitude are applied in each case. However, close examination of the data revealed that the amplitudes of the PRBS rudder demand signal were not constant at all the speeds considered. Notwithstanding these inconsistencies, the results do indeed suggest considerable changes in the ship's steering characteristics when the speed is increased over a significant range (eg 7 - 23 kts).

For example, from the pole positions of the estimated discrete time model, the equivalent first order lag time constant changes in the manner shown in Table 3.3.

Speed	PRBS Rudder Angle (deg)	Approximate Time Constant (sec)
7	±8	16
12	±4	N/A
16	±8	7
23	±4	8

Table 3.3 Variation in first order model time constant with speed/rudder angle from PRBS tests

The absence of an approximate time constant for the 12 kt speed condition in Table 3.3 requires some comment. The GLS estimation for this data produced a very poor data fit as is shown in Fig 3.2.

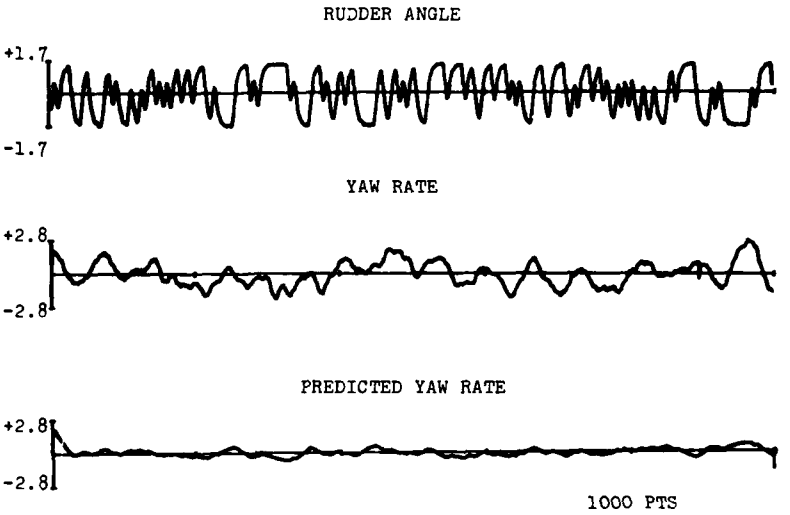

Fig 3.2 GLS Estimation for 12 kt Ship Data

An inspection of the recorded yaw rate signal shows a very definite low frequency oscillation present in the data. This oscillation does not arise directly from the stimulus provided by the rudder input; in fact, the approximate period of oscillation, 14 sec, coincides with the roll period of oscillation.

4. SHIP MODELS FROM STEP RESPONSE TRIALS

The sea trials program included rudder demand signals other than PRBS which were discussed in the preceding section. Step changes in rudder were also used at the various speeds and it was found that this form of excitation was unsuitable for parameter estimation algorithms such as GLS. This confirms the previously stated observation (20) that for satisfactory identification of the parameters of a system, the input stimulus must be "persistently exciting". Thus the primary objective of this exercise was restricted to an examination of the raw analogue data in order to identify any variations in gain K and time constant T of the simple first order (Nomoto) model

$$\frac{\dot{\psi}}{\delta_a} = \frac{K}{1 + sT} \qquad (4.1)$$

when δ_a and ship's speed are varied.

4.1 Effect of Rudder Demand on Yaw Rate Gain

The speed of the ship was set at a nominal 16 kt and measured rudder demands of $\pm 8^{\circ}$, $\pm 17^{\circ}$ and $\pm 27^{\circ}$ were successively applied. The actual recorded data is shown in Fig 4.1 (a), (b) and (c).

The variation of yaw rate with rudder angle extracted from Fig 4.1 has the non-linear characteristic shown in Fig 4.2 This non-linearity may be described in analytical terms by the cubic relation

$$\delta = a\dot{\psi} + b\dot{\psi}^3 \qquad (4.2)$$

where a, b are found from least squares curve fitting to be:

$a = 9.42 \quad b = 2.24$

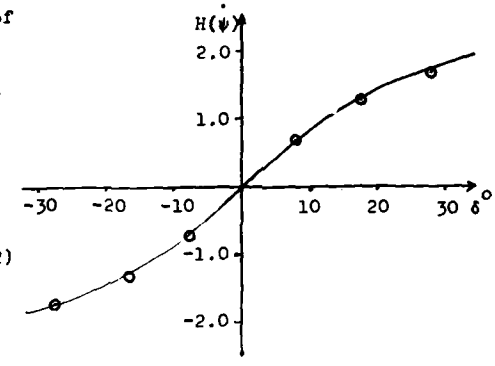

Fig 4.2 Cubic polynomial fit to $\delta - \dot{\psi}$ data

4.2 Effect of Ship's Speed on Yaw Rate Gain

Since the trials were conducted at four different ship speeds, the recorded data can be used to investigate the variation in yaw rate gain with speed. It was found that the magnitude of the rudder step demands were not consistent at each of the four speeds. Fig 4.3 (a), (b) and (c) show the step responses for the ship at 7 kt, 12 kt and 23 kt, the 16 kt case having been covered in (4.1). The measured yaw rate values can be "normalised" with respect to applied rudder angle to produce equivalent values for 8° and 16° steps over the speed range considered. The amended results are shown in Fig 4.4 where an almost linear relationship is indicated for both 8° and 16° equivalent rudder angles.

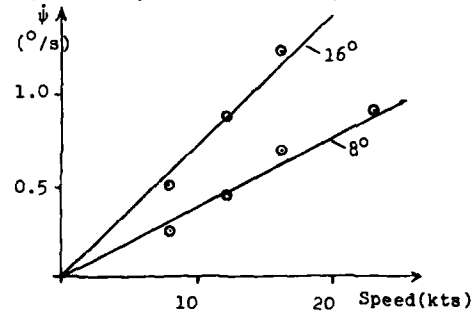

Fig 4.4 Variation of Steady State Yaw Rate with Ship's Speed

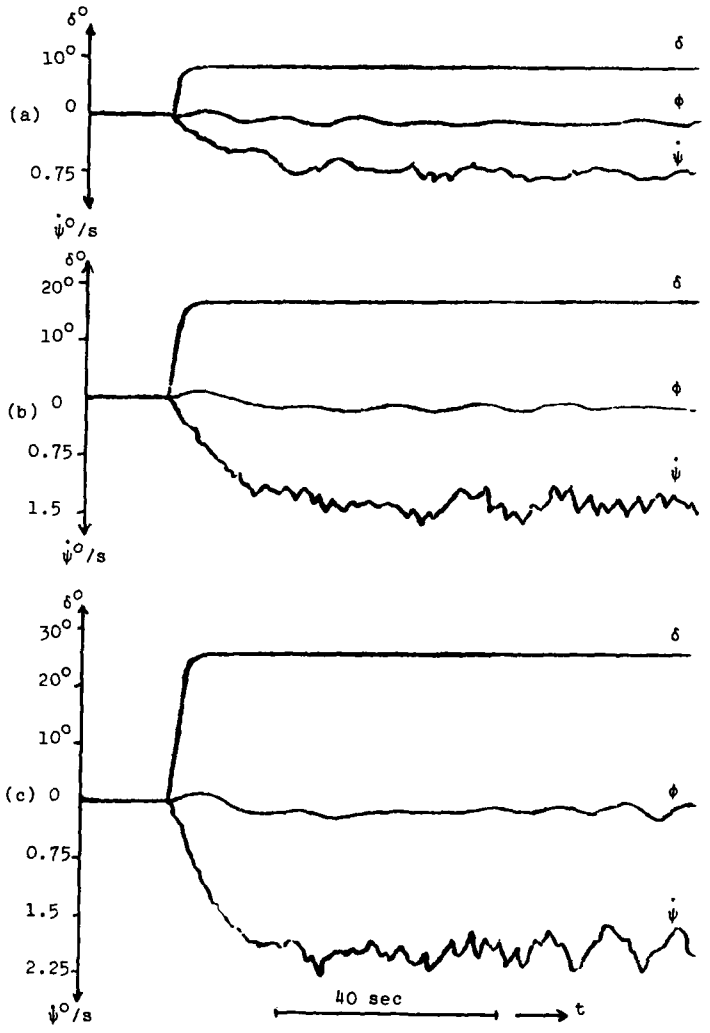

Fig 4.1 Rudder Step Response Data at 16 kt

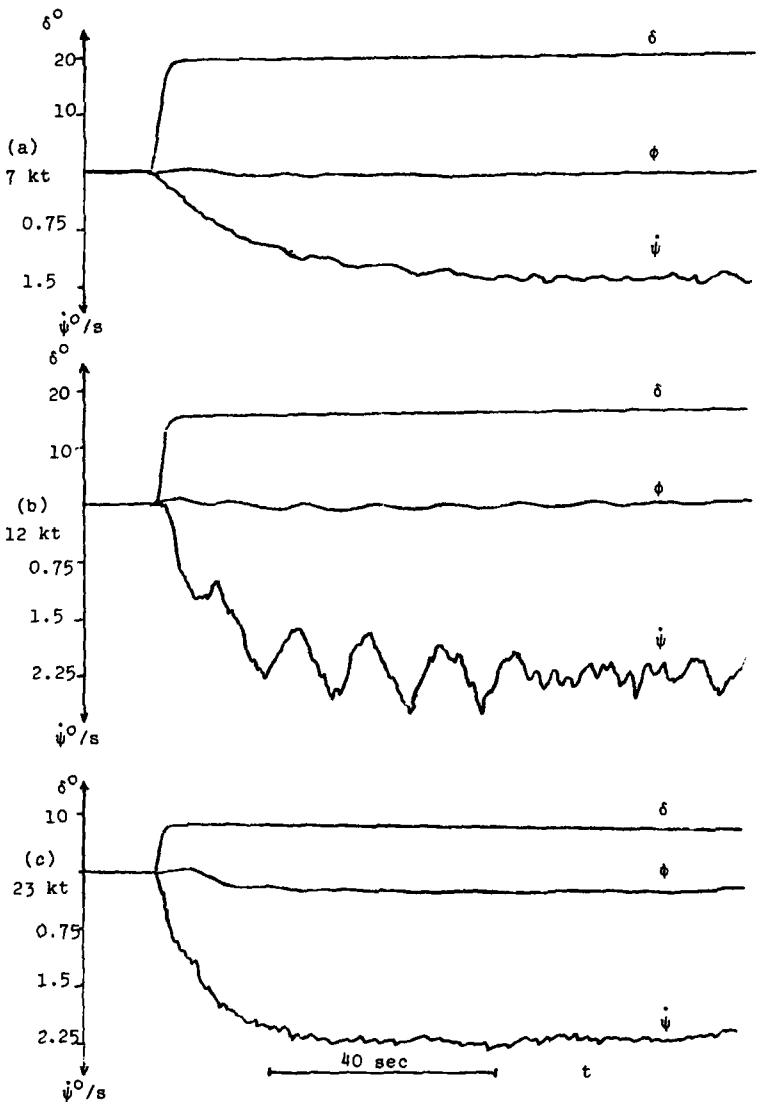

Fig 4.3 Rudder Step Response Data at different ship speeds

4.3 Variation in $\delta - \dot{\psi}$ Time Constant

In principle, the step response data can also be analysed to determine the effective time constant of the transfer function given in equation (4.1). However, accurate measurements were difficult to obtain due to the significant noise level present in the data. In qualitative terms, the results indicate that the variation of T with ship's speed is highly non-linear whereas a linear relationship is suggested between T and δ which is somewhat unexpected.

To summarise, the parameters K, T of the first order transfer function model (4.1) vary with both ship's speed and applied rudder angle. These variations as measured from simple rudder step tests are tabulated in Table 4.1 below:

Speed (kts)	δ (deg)	K (sec^{-1})	T (sec)
7	19	0.031	15.5
12	16	0.055	8.5
16	8	0.093	8.5
	17	0.078	8.0
	27	0.063	6.5
23	8	0.113	6.0

Table 4.1 Variation of K, T with speed/rudder angle

The data from the rudder step response tests provide a valuable back-up to the models derived using GLS estimation and PRBS rudder excitation. In addition to the actual rudder angle and yaw rate signals shown in Fig 4.1 and Fig 4.3, the measured roll angle (ϕ^{o}) of the ship is also included. This extra signal is useful in attempting to explain the oscillations present in the data which were noticed earlier in the PRBS tests, particularly at the 12 kt speed condition. The amplitude of the yaw rate oscillatory component is clearly directly proportional to the roll angle signal and the frequencies of the two signals are equal. There is a detectable phase shift between the two signals thus ruling out any interaction between the roll angle and yaw rate transducers which might have caused similar characteristics in both measurements. Since the ship's roll stabilisers were not operating during these particular trials, the conclusion reached is that the roll angle - yaw rate oscillations are due to the prevailing sea state.

The roll signal is also useful in recognising the presence of the rudder-to-roll angle cross-coupling which is an effect largely ignored in discussions relating to merchant ships. For a fast manoeuvrable warship, however, there is considerable interaction between the rudder/yaw and fin/roll channels leading to difficulties if feedback controllers are designed on

a single loop basis. An integrated steering/stabilisation multivariable control strategy has been proposed (22) to overcome these problems.

The rudder angle/yaw rate step test is effectively the Dieudonné Spiral Manoeuvre for stable ships and the $\delta - \dot{\psi}$ characteristic (Fig 4.2) is the spiral curve for the ship. It is interesting to note that the 3rd order polynomial gives a good fit to the data confirming the presence of non-linear effects introduced when large rudder angles are demanded. The simple linear equation relating $\dot{\psi}$ to δ can therefore be amended to include this non-linear term giving

$$\ddot{\psi} + \frac{K}{T} H(\dot{\psi}) = \frac{K}{T} \delta \qquad (4.3)$$

where $H(\dot{\psi}) = a\dot{\psi} + b\dot{\psi}^3$.

The remainder of this paper is concerned with the design of ship course control systems using the models derived above from the sea trials data. Specifically, we examine the performance of the self-tuning controller algorithm using an extension of the interactive block-oriented simulation program PSI (23).

5. APPLICATION OF THE SELF-TUNING CONTROLLER ALGORITHM TO FRIGATE DYNAMICS

5.1 The Self-Tuning Controller (STC) Algorithm

In general terms, self-tuning algorithms may be considered as 'performance-oriented' control algorithms. That is, the user specifies a desired closed-loop performance, usually in terms of the minimisation of a selected cost function, and the algorithm attempts to attain this performance despite unknown and/or slowly varying plant parameters.

The performance objective of the original 'self-tuning regulator' (14) is the minimisation of the variance of the process output ie

$$I = E\{y^2_{t+k}\} \qquad (5.1)$$

where $E\{.\}$ - expectation operator, y - system output, k - system time delay.

Two limitations in this basic algorithm are that no set point following is included and there is no penalty on control effort. These are significant points in a ship steering control system since set point following is essential if the desired course is constantly changing and excessive rudder action (control effort) should be avoided. The more general 'self-tuning controller' algorithm has been interpreted (24) to give a wide variety of performance objectives.

This algorithm has the cost function

$$I_1 = E\{(Py_{t+k} - Rw_t)^2 + Qu_t^2\} \qquad (5.2)$$

where w_t - set point, u_t - control input and P, Q, R can be polynomials or rational functions in z^{-1} (see (24)).

The optimal control law for a system with known parameters can be shown to be of the form:

$$u_t = \frac{-1}{g_0}\left\{f_0 y_t + f_1 y_{t-1} + \ldots + g_1 u_{t-1} + \ldots + h_0 w_t + h_1 w_{t-1} + \ldots\right\} \tag{5.3}$$

or $$Fy_t + Gu_t + Hw_t = 0$$

For systems whose parameters are unknown, the coefficients of the polynomials F, G and H are estimated on-line using recursive least squares.

5.2 Simulation of the STC using PSI

The simulation of the STC applied to the frigate models is achieved using an extension of the PSI continuous system simulation program. Initially, the open loop dynamics of the ship and steering system are set up using PSI blocks (see (23)). Then the user specifies particular blocks whose outputs are to be fed to the external control program at a chosen sampling interval. The external control program is written in FORTRAN and must be run from a separate terminal to the PSI simulation. This two terminal facility enhances the simulation since the open-loop ship system and digital controller (STC) are physically separate. In addition, the effects of limited word length ADC and DAC number representation can also be investigated thus creating a more meaningful simulation with respect to any future real-time implementation.

A block diagram of the feedback control system configuration is shown in Figure 5.1.

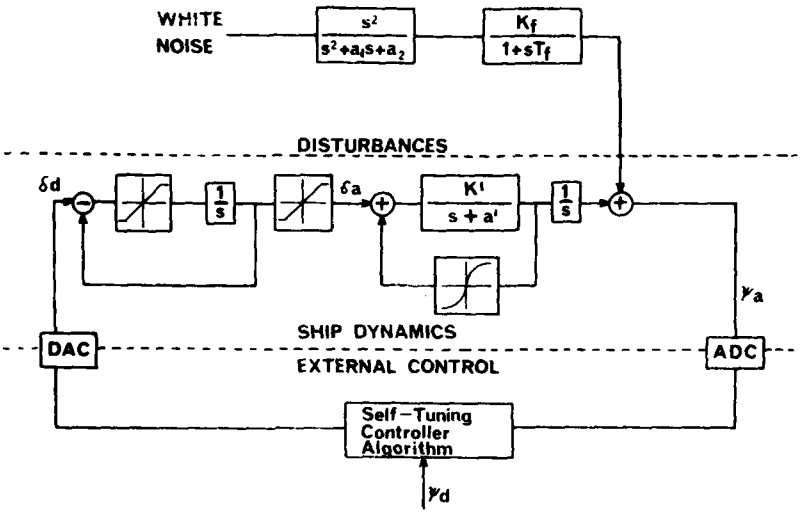

Fig 5.1 Block diagram of Ship Steering Simulation Model

Ship Dynamics - the linear and non-linear frigate models were used in the simulation with parameters corresponding to a ship's speed of 16 kt, ie $K' = 0.0107\ sec^{-2}$, $a' = 0.11\ sec^{-1}$ and $H(\dot{\psi}) = 9.42\dot{\psi} + 2.24\dot{\psi}^3$. Rudder movement was restricted to a maximum of $\pm 20^{o}$ and rate limiting of 6^{o}/sec was incorporated - this figure having been derived from measurements of the step responses.

Disturbances - The modelling of the yaw angle disturbances due to the environment (waves, wind, etc) is a complex problem. To obtain a general solution it is necessary to analyse wave motion and ship response spectra using large seakeeping program packages (25). For the purposes of this study, a 2nd order filter approximating the sea wave spectrum is cascaded with a low pass filter which converts the wave disturbances into yaw angle disturbances. The filter gain is adjusted to give a realistic yaw disturbance intensity given the particular ship hull characteristics. The bandpass centre frequency was chosen to be $\omega = 0.72$ rad/sec corresponding to a significant wave height of 3 metres.

STC Algorithm - One feature of the STC algorithm is that certain parameters have to be selected by the user at start-up. Some examples are system parameters such as model order and time delay, controller parameters such as P, Q, R weighting functions and sampling time, and estimator parameters such as exponential

weighting factor, initial estimates and initial covariance matrix. It has been argued (26) that most of these parameters are relatively easy to choose and that closed-loop control is tolerably insensitive to their values. Some parameters depend on the control design method involved and in the examples presented below the parameters chosen correspond to the STC in its original form. Specifically, the values selected were:

$P = 1.0$ $\quad Q = 1.0$ $\quad R = 1.0$

Initial covariance matrix $P_0 = 10I$ $\quad$ Sample period = 1 sec

Initial parameter estimate $\hat{\theta}_0 = [\underset{F}{0.0 \;\; 0.0} \;\; \underset{G}{0.5 \;\; 0.0} \;\; \underset{H}{-1.0 \;\; 0.0}]^*$

Estimated order of A, B, C = 2, 1, 1
Estimated time delay = 1
} System description of the form $Ay_t = z^{-k}Bu_t + C\xi_t$

Exponential weighting factor = $\beta = 0.995$

Example 1

Recursive estimation algorithms, such as those included within the STC, are susceptible to numerical problems when limited word-length hardware is used. Thus, the facility within extended PSI to simulate different word-length ADC/DAC operations enhances the designer's capability to predict the performance of the STC in real-time. The simulation of the ADC/DAC is carried out by ensuring only integer numbers are passed to the external control program with limits on the maximum integer values dependent on the number of bits in the ADC/DAC.

Fig 5.2(a) shows the response of the linear frigate model under self-tuning control when a series of 20^o course changes are demanded. The ADC/DAC word length for these responses was 12-bit and the corresponding controller parameter estimates are shown in Fig 5.2(b). If the word length of the ADC/DAC operation is now reduced to 8-bit then, for the same sequence of course changes, the estimates shown in Fig 5.2(c) are obtained. It can be seen that resolution is degraded when 8-bit conversion is used which is to be expected given the smaller range of integer number representation.

Although the 8-bit case gave only a marginally different response (not shown) to that of Fig 5.2(a), the differences apparent in the parameter estimates do indicate that consideration of the quantisation effects of the ADC/DAC process may be important. These effects would not be highlighted using conventional digital simulation methods thus giving further justification to the extended PSI approach.

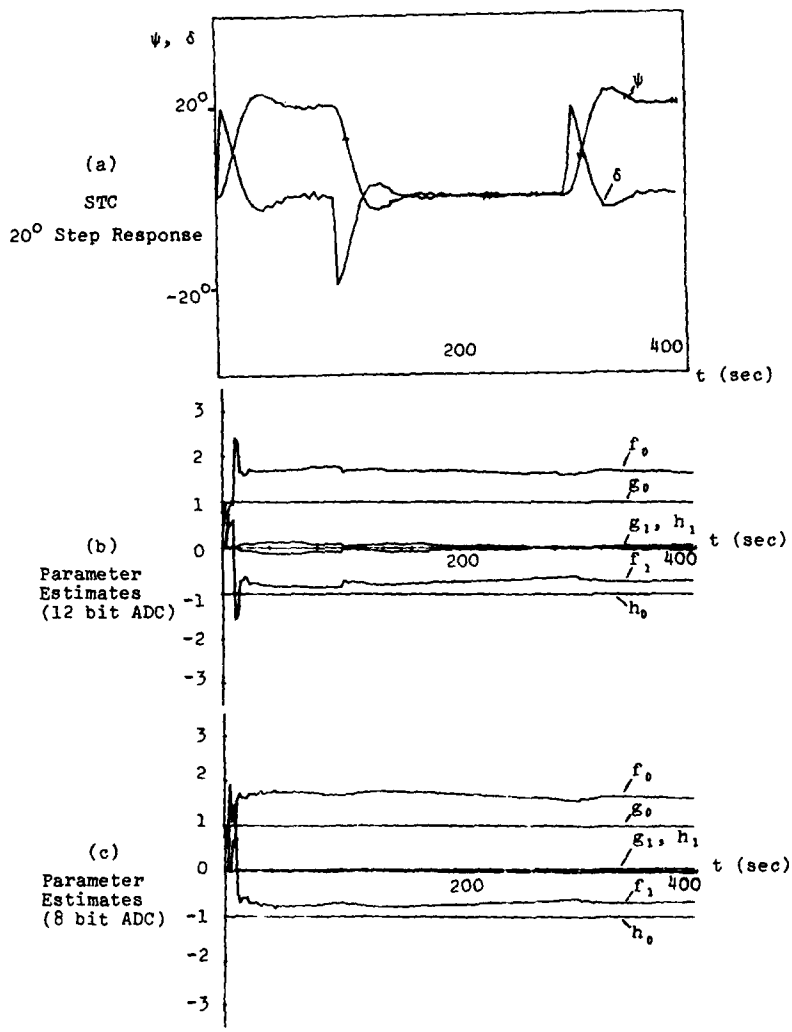

Fig 5.2 Effect of ADC/DAC Word length on STC Parameter Estimation

Example 2

Ship autopilots can be designed using analytical methods (eg root locus/frequency response compensation, linear optimal control theory) when the steering dynamics are described by linear transfer function models. However, such methods are not generally applicable when the dynamics exhibit non-linear characteristics. For non-linear systems, the design must be formulated as an optimisation problem.

This second example compares the performance of the STC with an optimised PID controller when a single course change of 20^{o} is demanded and the ship dynamics are represented by the 16 kt non-linear frigate model. The STC parameters were the same as the previous example and the coefficients of the optimised PID controller were determined by minimising an "integral of absolute error" type of performance index. The optimisation is accomplished using a hill-climbing procedure and is, in fact, invoked as a facility within PSI. The optimal values of the coefficients were found after 42 iterations to be:

$$K_p = 3.2 \qquad K_i = 0.3 \qquad K_d = 16.1$$

Fig 5.3(a) shows the response of the ship using a PID controller with these coefficients, while Fig 5.3(b) shows the response when the STC is used. The corresponding parameter estimates are shown in Fig 5.3(c).

It is interesting to note the similarity in the yaw angle responses despite the different rudder actions used by the controllers to achieve them. The PID controller remains saturated at the 20^{o} limit for approximately 10 sec during the manoeuvre whereas the STC barely reaches this maximum deflection before gradually returning to the midships position. Both responses are characterised by a small overshoot. The increased fluctuations in the parameter estimates compared with the previous example can be attributed to (i) greater resolution in the graphics routine due to a shorter final time (100 sec) and (ii) the delay of 10 sec from start up before applying the course change. During this initial period, the parameter estimator within the STC receives virtually no new information from the system and so it is not unreasonable to expect the controller parameters to take longer to "tune-in" to steady values.

6. CONCLUSIONS

The results from both the GLS parameter estimation and the rudder step responses confirm that there is significant variation in the parameters of the ship model as a function of both ship's speed and applied rudder angle. Moreover, the agreement between the results obtained by the different methods suggests that one can indeed quantify these variations with some degree of confidence. For example, given a speed change from 7 kt to 16 kt and a demanded rudder angle between 16^{o} - 19^{o}, then the gain K and time constant T of the Nomoto model (equation 4.1) change by $\approx$ 150% (increase) and $\approx$ 50% (decrease) respectively.

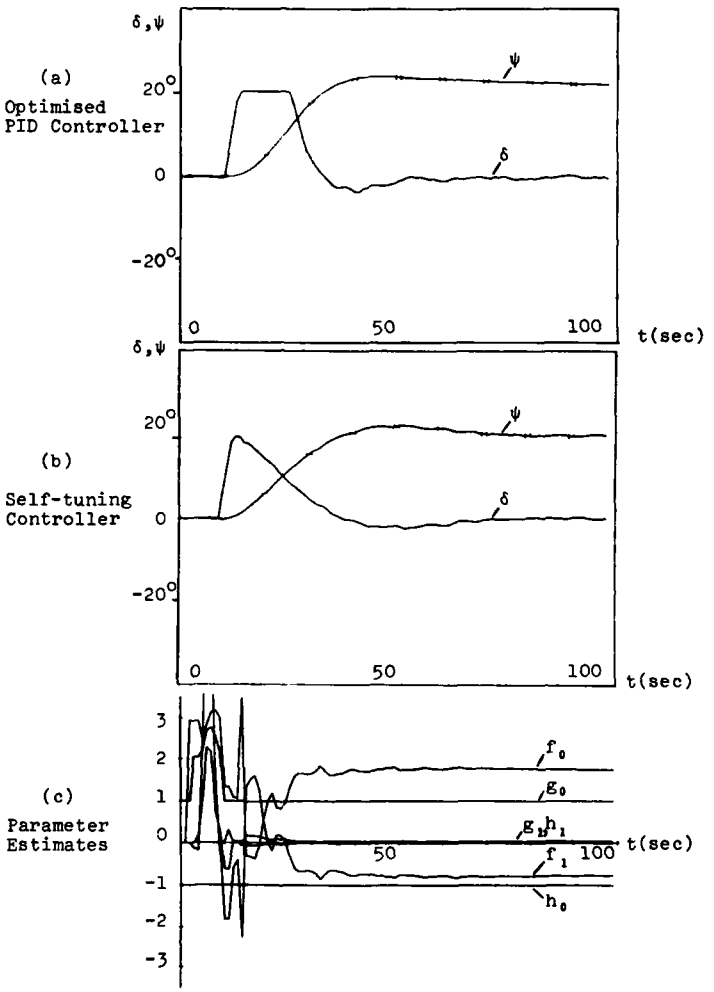

Fig 5.3 Step Responses of Non-Linear Frigate Model using Optimised PID and Self-Tuning Control

It is doubtful if further analysis of the 12 kt data using GLS would have produced better results because of the dominant low frequency oscillatory component present in all the data recorded at this speed. This phenomenon requires further investigation since any control algorithm which uses a process of identification, either implicitly or explicitly, is likely to produce an inferior performance under such conditions.

The results have shown that much valuable information regarding the rudder angle/yaw rate dynamics can be deduced from simple rudder step response tests. These tests have the advantage that they are easy to carry out and do not require the preparation necessary with PRBS excitation.

The input forcing function for all the GLS estimation results was the actual rudder angle. It has been shown (27) that difficulties occur when applying parameter estimation techniques for input/output data records when the demanded rudder angle is used as the input instead of the actual rudder angle. This is because the closed-loop rudder servo dynamics are included in the input-output model. Moreover, when the input signal is changing rapidly as with the PRBS, the rudder demand and rudder actual signals are quite different so identification methods which rely on the input signal having the properties of PRBS (eg correlation methods) could not be used with confidence.

The extended PSI simulation program has a number of advantages over other more conventional approaches to digital simulation. These have been clearly identified in this particular application where the recursive STC algorithm has been used as an autopilot design strategy.

It has been shown that the limited word-length hardware of ADC/DAC circuits can be simulated quite effectively which encourages a smoother transition from simulation design to actual implementation. This is especially important when algorithms such as the STC are used since numerical instabilities within the estimator could lead to unsatisfactory controller performance.

The second example demonstrated that the self-tuning controller compared very favourably with an optimised PID controller when the system dynamics were described by the non-linear frigate model. This is also important since the theoretical foundation of the STC algorithm assumes linear system dynamics and the results presented lend further weight to the concept of self-tuning algorithms for ship steering systems (which are clearly non-linear).

Future work in this area will involve the implementation of a microprocessor-based STC with an analogue model of the non-linear steering dynamics of a frigate. In addition, the use of a multi-variable self-tuning strategy (28), (29) should be investigated given the interaction between the rudder/yaw and fin/roll channels discussed earlier.

7. ACKNOWLEDGEMENTS

The authors wish to acknowledge the assistance and co-operation of Mr W B MARSHFIELD, Admiralty Marine Technology Establishment, Haslar who was instrumental in providing the sea trials data and Mrs L S GRAY, Department of Control Engineering, University of Sheffield, who developed the extensions to the PSI simulation program.

REFERENCES

1. D W Clarke, "Generalised Least Squares Estimation of Parameters in a Dynamic Model". IFAC Symposium on Identification in Automatic Control Systems, Prague 1967.

2. K J Åström and C G Källström, "Identification of Ship Steering Dynamics" Automatica Vol 12, No 9, 1976.

3. K J Åström, C G Källström, N H Norrbin and L Byström, "The Identification of Linear Ship Steering Dynamics using Maximum Likelihood Parameter Estimation" SSPA Report No 75, Gothenburg, Sweden, 1975.

4. A Tiano and E Volta, "Application of Identification Techniques to Ship Systems", Proc. 7th IFAC Triennial World Congress, 1978, pp 1583-1588, Helsinki.

5. J O Flower and A Towhidi, "Results from Ship Dynamic Experiments using the Maximum Likelihood Identification Technique" International Shipbuilding Progress, Vol 22, No 234, 1975.

6. K Ohtsu, M Horigome and G Kitagawa, "On the Prediction and Stochastic Control of Ship's Motion", Proc. 2nd IFAC/IFIP Symposium on Ship Operation Automation, pp 69-76, Washington, 1976.

7. L Byström and C G Källström, "System Identification of Linear and Non-Linear Ship Steering Dynamics", Proc. 5th Ship Control Systems Symposium, Vol 3, Paper J2 2-1, Annapolis, Maryland, USA, 1978.

8. P Kaplan, T P Sargent, and T R Goodman, "The Application of System Identification to the Dynamics of Naval Craft", 9th Symposium on Naval Hydrodynamics, Paris, 1972.

9. J Van Amerongen, J C Haarman, and W Verhage, "Mathematical Modelling of Ships, Proc 4th Ship Control Systems Symposium, Vol 4, pp 163-178, The Hague, 1975.

10. D Clarke, "Some Aspects of the Dynamics of Ship Steering", PhD Thesis, University of London, 1976.

11. E Sperry, "Automatic Steering", Trans. SNAME 192?.

12. J Van Amerongen and A J Udink Ten Cate, "Model Reference Adaptive Autopilots for Ships", Automatica Vol 11, pp 441-449, 1975.

13. H F Millers, "Modern Control Theory Applied to Ship Steering", Proc. 1st IFAC/IFIP Symposium on Ship Operation Automation, Oslo, 1973.

14. K J Åström and B Wittenmark, "On Self-Tuning Regulators", Automatica Vol 9, pp 185-199, 1973.

15. D W Clarke and P J Gawthrop "Self-Tuning Controller" Proc IEE, Vol 122, pp 929-934, 1975.

16. C G Kallström, K J Åström, N E Thorell, J Eriksson and L Sten. "Adaptive Autopilots for Steering of Large Tankers". Report TFRT-3145, Department of Automatic Control, Lund Institute of Technology, Sweden, 1977.

17. A Tiano, E Volta, A W Brink and T W Verbruggen, "Adaptive Control of Large Ships in Non-stationary Conditions: A Simulation Study", IIC Symposium on Ship Steering Automatic Control, Paper C2, Genoa, Italy, 1980.

18. N Mort and D A Linkens, "Self-tuning Controllers for Surface Ship Course and Track-keeping", IIC Symposium on Ship Steering Automatic Control, Paper C1, Genoa, Italy, 1980.

19. S A Billings and M J H Sterling, "SPAID - A User's Guide". Department of Control Engineering, University of Sheffield, UK.

20. P Eykhoff, "System Identification" John Wiley & Sons Ltd, 1974, p 214.

21. D P Lindorff, "Theory of Sampled Data Control Systems", New York, John Wiley & Sons Inc, 1965, p 73.

22. M G Waugh and R Whalley, "Computer-aided Design of a Ship Steering Stabilisation System", Inst MC Symposium on Dynamic Analysis of Vehicle Ride and Manoeuvring Characteristics, London, 1978.

23. P P J Van Den Bosch, "PSI - An Extended, Interactive, Block-Oriented Simulation Program". IFAC Symposium on Computer Aided Design of Control Systems. pp 223-228, Zurich, 1979.

24. P J Gawthrop, "Some Interpretations of the Self-Tuning Controller" Proc IEE, Vol 124, pp 889-894, 1977.

25. B L Hutchison and J T Bringloe, "Application of Seakeeping Analysis", Marine Technology, Vol 15, No 4, pp 416-431, Oct 1978.

26. D W Clarke,"The Theory and Applications of Self-Tuning and Adaptive Control", Peter Peregrinus (to be published).

27. N Mort, "Identification of the Linear Steering Dynamics of a Frigate using Generalised Least Squares", RNEC Control Engineering Section Report No 76, March 1981.

28. H N Koivo, "A Multivariable Self-Tuning Controller", Automatica Vol 16, pp 351-366, 1980.

29. D L Prager and P E Wellstead, "Multivariable Pole-assignment Self-Tuning Regulators", Proc IEE Vol 128, Part D, No 1, pp 9-18, Jan 1981.

LIST OF SYMPOSIUM AUTHORS, SESSION CHAIRMEN AND GUEST SPEAKERS

LIST OF SYMPOSIUM AUTHORS, SESSION CHAIRMEN AND GUEST SPEAKERS

LIST OF SYMPOSIUM AUTHORS, SESSION CHAIRMEN AND GUEST SPEAKERS

LIST OF SYMPOSIUM AUTHORS, SESSION CHAIRMEN AND GUEST SPEAKERS

LIST OF SYMPOSIUM AUTHORS, SESSION CHAIRMEN AND GUEST SPEAKERS

LIST OF SYMPOSIUM AUTHORS, SESSION CHAIRMEN AND GUEST SPEAKERS

LIST OF SYMPOSIUM AUTHORS, SESSION CHAIRMEN AND GUEST SPEAKERS

LIST OF SYMPOSIUM AUTHORS, SESSION CHAIRMEN AND GUEST SPEAKERS

LIST OF SYMPOSIUM AUTHORS, SESSION CHAIRMEN AND GUEST SPEAKERS

LIST OF SYMPOSIUM AUTHORS, SESSION CHAIRMEN AND GUEST SPEAKERS

LIST OF SYMPOSIUM AUTHORS, SESSION CHAIRMEN AND GUEST SPEAKERS

END

DATE

FILMED

16 3 89